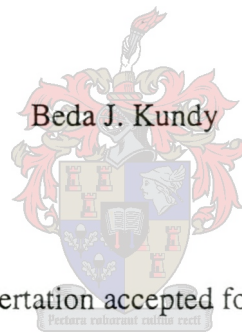


Probabilistic analytical methods for evaluating MV distribution networks
including voltage regulating devices



Beda J. Kundy

Dissertation accepted for the
Degree of Doctor of Philosophy in Engineering at
The University of Stellenbosch

Supervisor:

Prof. Ron Herman, University of Stellenbosch

November 2001

Declaration:

I, the undersigned, hereby declare that the work contained in this dissertation is my own original work and has not been previously in its entirety or in part been submitted at any university for a degree.

B.J. Kundy

November 2001

Acknowledgements

I would like to thank the following people for their contributions that enable the completion of this thesis.

- My supervisor Prof. Ron Herman for his constant encouragement and support
- Dr. Schalk W. Heunis and Dr. H.J. Beukes for supplying me some of the data
- My family for their love and patience

Accurate load models are required for the computation of load flows in MV distribution networks. Modern microprocessors in recent times enable researchers to sample and log domestic loads. The findings show that they are stochastic in nature and are best described by a beta probability distribution.

In rural areas two different load types may be present. Such loads are domestic and pump loads, the latter may be modelled as constant $P-Q$ loads. An analytical tool for computing voltage regulation on MV distribution networks for rural areas feeding the mentioned loads is therefore required. The statistical evaluation of the consumer voltages requires a description of load currents at the time of the system maximum demand. To obtain overall consumer voltages at any specified risk for the two types of the loads, the principle of superposition is adopted.

The present work deals with conventional 22kV three-phase distribution ($\Delta-\Delta$) connected networks as used by ESKOM, South Africa. As the result of the connected load, MV networks can experience poor voltage regulation. To solve the problem of voltage regulation, voltage regulators are employed. The voltage regulators considered are step-voltage regulators, capacitors and USE (Universal Semiconductor Electrification) devices. USE devices can compensate for the voltage drops of up to 35% along the MV distribution network, thus the criteria for the application of the USE devices is also investigated. The load currents are treated as signals when assessing the cost of distribution system over a period of time due to power losses. The individual load current signal is modelled by its mean and standard deviation.

The analytical work for developing general expressions of the total real and total imaginary components of branch voltage drops and line power losses in single and three-phase networks without branches are presented. To deal with beta-distributed currents on MV distribution networks, new scaling factors are evaluated at each node. These new scaling factors are derived from the distribution transformer turns ratio and the deterministic component of the statistically distributed load currents treated as constant real power loads. In the case of an individual load current signal, the transformation ratio is evaluated from the distribution transformer turns ratio and the average value of the signal treated as constant real power load.

The evaluation of the consumer voltage percentile values can be accurately evaluated up to 35% voltage drop. This is possible by the application of the expanded Taylor series, using the first three terms. The coefficients of these three terms were obtained using a search engine imbedded in the probabilistic load flow. The general expressions for evaluating the overall consumer voltages due to statistical and non-statistical loads currents are also given. These non-statistical currents may be due to constant $P-Q$ loads, line capacitance and the modeling of voltage regulators.

The Newton-Raphson algorithm is applied to perform a deterministic load flow on single-phase networks. A backward and forward sweep algorithm is applied to perform a deterministic load flow on single and three-phase systems. A new procedure for modelling step-voltage regulators in three-phase ($\Delta-\Delta$) connected networks is outlined. Specifying a transformation ratio of 1.1 and 1.15 respectively, identifies the open-delta or closed-delta configuration for three-phase networks.

The algorithms and the developed general expressions for single and three-phase networks without branches are presented in this work. A new algorithm is developed to enable the developed general expressions to be applied to practical MV distribution networks. The algorithms were tested for their accuracy by comparing the analytical results with Monte Carlo simulation and they compared well. An illustrative example to show the application of the present work on a practical MV distribution networks is presented. A criterion for the application of the USE devices is outlined.

It is anticipated that, the work presented in this thesis will be invaluable to those involved in the design of MV distribution systems in developing countries.

Akkurate lasmodelle word benodig vir drywingsvloei analises in MV distribusiestelsels. As gevolg van nuwe digitale verwerkers is dit deesdae moontlik om huishoudelike laste te monitor. Die lasdata dui daarop dat laste stochasties is en kan met behulp van die Beta verdeling beskryf word.

In landelike gebiede is daar twee tipes laste. Hulle is eendersyds huishoudelike laste en andersyds pomp-tipe laste wat as konstante P-Q laste beskou kan word. Dit is dus belangrik om toepaslike analitiese metodes te gebruik om die spanningsvalle by hierdie laste te bereken met inagnome van die las-tipes. By die statistiese berekening van die verbruiker se spanning moet 'n statistiese model van die lasstroom verskaf word op die tydstip van maksimum aanvraag. Daarna moet die prinsiep van superposissie gebruik word om die spannings by verskeie nodes by 'n gespesifiseerde vertrouensinterval te bepaal.

Hierdie proefskrif is gebaseer op konvensionele 22kV, drie fase distribusie (delta na delta) netwerke, soos deur Eskom, Suid Afrika gebruik. Hierdie stelsels ondervind dikwels nadelige spanningsvlakke en spanningsreëlaars word derhalwe aangewend. Hierdie reëlaars is gewoonlik van tap-tipe of daar kan ook gebruik gemaak word van kapasitore en ook elektroniese reëlaars soos die USE tipe toestelle. Laasgenoemde kan op LV vir spanningsvalle tot 35% kompenseer. In hierdie werk word die werkdrywing verliese in die geleiers bereken met behulp 'n seinmodel van die lasstrome. Die individuele lasstrome word by wyse van gemiddeldes en variasies beskryf.

Om die algemene algoritmes vir die berekening van die reële en imaginêre spanningsvalle, asook die verliese in enkelfase en driefase stelsels daar te stel word aanvanklik gebruik gemaak van stelsels sonder vertakkings. Om die statistiese lasbeskrywing op die laagspanningskant na die MV vlak oor te dra word van nuwe skaalfaktore gebruik gemaak. Hierdie faktore word bereken op die basis van die transformator se verhouding en die deterministiese komponent van die statistiese verspreide lasstrome, as konstante reële drywingslaste beskou.

Met die ontwikkelde metode kan die verbruiker se spanning by 'n gegewe vertrouensinterval akkuraat bereken word vir spanningsvalle tot 35%. Dit word moontlik gemaak deur die Taylor-reeks tot drie terme toe te pas. Daar moet egter gebruik gemaak word van toepaslike koëffisiënte

wat bepaal word deur 'n geprogrammeerde soektog. 'n Algemene stel vergelykings om die spanning by enige verbruiker te bereken, ongeag die topologie van die netwerk, word ook gegee.

Die Newton-Raphson metode word aangewend om die deterministiese drywingsvloei op enkelfase stelsels te bereken. A truwaartse-voorwaartse metode is gebruik om die drywingsvloei te bepaal vir driefase stelsels. 'n Nuwe prosedure is ontwikkel vir die modellering van die spanningsreëlaars in driefase, delta-delta netwerke. Deur gebruik te maak van 'n transformatorverhouding van 1.1 of 1.15 kan die oop-delta of toe-delta netwerke voorgestel word.

'n Nuwe algoritme is ontwikkel om multi-vertakkings in 'n netwerk te hanteer. Al die prosedures is deeglik met behulp van Monte Carlo simulasies getoets en die resultate is heel bevredigend. Om die metodes te illustreer word 'n gevallestudie ingesluit waar die metodes gebruik word om 'n netwerk te evalueer met en sonder die sogenaamde USE toestelle. Kriteria vir die aanwending van hierdie toerusting word voorgestel.

Daar word verwag dat die werk soos in hierdie proefskrif uiteengesit is die ontwerp van MV distribusiestelsels, veral in ontwikkelende lande, heelwat sal verbeter.

Note: The symbols in the text with the bar e.g. \bar{I} , represent phasor quantities

Chapter 2

A_o, A_1, A_2	composite real power constants
A	inverse of the partial differential of input variable in terms of X at point X_o
A^T	transpose of A
B_o, B_1, B_2	composite reactive power constants
B_{ik}^{pm}	capacitive susceptance relating node i with phase p and node k with phase m
CB	circuit breaker rating
G_{ik}^{pm}	conductance relating node i with phase p and node k with phase m
I	magnitude of the line current
P	constant real power
$(P_i^p)^{sp}$	specified real load power at node i with phase p
Q	constant reactive power
R	constant resistive load
V	voltage at the load point
$(Q_i^p)^{sp}$	specified reactive load power at node i with phase p
V_i^p	voltage magnitude at node i with phase p
V_k^m	voltage magnitude at node k with phase m
X	constant reactive load
X	state variable vector (magnitude and argument of the nodal phase-voltages)
X_o	approximated expected value of X
U	input random vector (active and reactive load phase powers)
θ_i^p	voltage phase angle at node i with phase p
$\theta_{ik}^{pm} = \theta_i^p - \theta_k^m$	
θ	load power factor angle
$\mu()$	expected value of the random vector ()
$cov()$	covariance matrix of the random vector ()
ΔV	phasor voltage drop

Chapter 3

I_k	single load current at node k
I_{kk}	the second load current at node k
R_i	branch resistance between node $i-1$ and i
X_i	branch inductive reactance between node $i-1$ and i
Z_i	branch impedance between node $i-1$ and i
α_i	load current phase angle at node i due to currents defined as I_k
α_{ii}	load current phase angle at node i due to currents defined as I_{kk}
ΔV_i	branch voltage drop between node $i-1$ and i due to currents defined as I_k
ΔV_{ii}	branch voltage drop between node $i-1$ and i due to currents defined as I_{kk}

ΔV_{ireal}	real component of the voltage drop across impedance Z_i
ΔV^2_{ireal}	square of ΔV_{ireal}
ΔV_{iimag}	imaginary component of the voltage drop across impedance Z_i
ΔV^2_{iimag}	square of ΔV_{iimag}
ΔV_{ireal_total}	total real component of the branch voltage drops at node i
ΔV_{iimag_total}	total imaginary component of the branch voltage drops at node i
$\Delta V^2_{ireal_total}$	square of ΔV_{ireal_total}
$\Delta V^2_{iimag_total}$	square of ΔV_{iimag_total}
$\Delta V^2_{ireal_total-sum}$	total sum of $\Delta V^2_{ireal_total}$ up to node i
$\Delta V^2_{iimag_total-sum}$	total sum of $\Delta V^2_{iimag_total}$ up to a node i
$\Delta * \Delta V_{ireal-sum}$	sum of the product of the real component of branch voltage drop at node i
$\Delta * \Delta V_{iimag-sum}$	sum of the product of the imaginary component of branch voltage drop at node i
$\Delta V^2_{ireal_total-sin\ gl e}$	square of the total real component of the branch voltage drop at node i with single loads
$\Delta V^2_{iimag_total-sin\ gl e}$	square of the total imaginary component of the branch voltage drop at node i with single loads
$\Delta V^2_{ireal_total-combined}$	square of the total real component of the branch voltage drop at node i with two loads
$\Delta V^2_{iimag_total-combined}$	square of the total imaginary component of the branch voltage drop at node i with two loads

Chapter 4

ba, cb, ac	identification of individual phases in the three-phase system ($\Delta - \Delta$) connected
C_b	individual consumer circuit breaker rating
C_k	shunt capacitance at node k
D_{tr}	distribution transformer turns ratio (230/22000)
f	frequency
I_{ave_statlv}	average current load due to deterministically component of the beta-distributed load currents on LV networks
I_{ave_statmv}	average current load due to deterministically component of the beta-distributed load currents on MV networks
$I_{ave_statmv,lv}$	average current load due to deterministically component of the beta-distributed load currents on MV networks converted to the LV networks
$k_{var-stat}$	variable scaling factor for beta-distributed load currents
$I_{abk}, I_{bck}, I_{cak}$	phase currents at node k for phase ba, cb and ac respectively
I_{xm}, I_{ym}, I_{zm}	current through the impedances Z_{am}, Z_{bm}, Z_{cm} respectively

$I_{xi-real}^2$	square of the real component of the current through the branch impedance Z_{ai}
$I_{xi-imag}^2$	square of the imaginary component of the current through the branch impedance Z_{ai}
$I_{yi-real}^2$	square of the real component of the current through the branch impedance Z_{bi}
$I_{yi-imag}^2$	square of the imaginary component of the current through the branch impedance Z_{bi}
$I_{zi-real}^2$	square of the real component of the current through the branch impedance Z_{ci}
$I_{zi-imag}^2$	square of the imaginary component of the current through the branch impedance Z_{ci}
I_k	statistical or non-statistical load current at node k
I_{ck}	charging current at node k
$I_{Zi-real}$	real component of the current through the branch impedance Z_i
$I_{Zi-imag}$	imaginary component of the current through the branch impedance Z_i
$I_{Zi-real}^2$	square of $I_{Zi-real}$
$I_{Zi-imag}^2$	square of $I_{Zi-imag}$
k_{var}	variable scaling factor
N	total number of connected consumers at the output of the USE device
P_{ave_statlv}	average load power due to the deterministically component of the beta-distributed load currents on LV networks
P_k	real power at iteration k
P_{i-loss}	power loss on the branch of impedance Z_i
$P_{total-loss}$	total power loss in single-phase networks
$P_{total-Aloss}$	total power loss on conductor A
$P_{total-Bloss}$	total power loss on conductor B
$P_{total-Closs}$	total power loss on conductor C
$P_{total-3loss}$	overall total power loss in three phase networks
Q_k	reactive power at iteration k
R_{ak}, R_{bk}, R_{ck}	line resistance between node $k-1$ and k for line a, b and c respectively
SF	scaling factor
$V_{bak}, V_{cbk}, V_{ack}$	phase voltages at node k for phase ba, cb and ac respectively
$V_{()}$	supply voltage for phase ()
V_k	nodal voltage at iteration k
V_k^*	conjugate of the nodal voltage at iteration k
$V_{mv-stat}^*$	conjugate of the nodal voltage on the MV distribution line due to deterministically component of the beta-distributed load currents

V_{mcon_i}	overall magnitude of the consumer voltage at node i
V_{nom_lv}	LV nominal voltage at the output of the USE device
V_{ovcon_i}	overall consumer voltage at node i
V_S	supply voltage
V_{scon_i}	magnitude of the consumer voltage due to statistical currents at node i
V_{nom_lv}	LV nominal voltage
$V^{*}_{mv-stat}$	conjugate of the nodal voltage on the MV networks due to the deterministically component of the beta-distributed load currents
X	Taylor's series parameter
X_{ak}, X_{bk}, X_{ck}	line inductive reactive between node $k-1$ and k for line a, b and c respectively
Y_{sk}	admittance at node k
Z_{ak}, Z_{bk}, Z_{ck}	line impedance between node $k-1$ and k for line a, b and c respectively
$\alpha_{abi}, \alpha_{bci}, \alpha_{cai}$	load current phase angle at node i for phase ba, cb and ac respectively
α_{vk}	voltage phase angle at node k
$\alpha_{()s-new}$	new phase angles of the statistical load currents for phase ()
$\alpha_{()s-old}$	previous phase angles of the statistical load currents for phase ()
α, β	load current statistical parameters
α_k	load current phase angle at node k
ω	angular velocity
$\Delta V_{ba-ireal}$	real component of the branch voltage drop across the impedance between node $i-1$ and i for the phase ba
$\Delta V_{ba-ireal-total}$	total real component of the branch voltage drop at node i for the phase ba
$\Delta V_{cb-ireal}$	real component of the branch voltage drop across the impedance between node $i-1$ and i for the phase cb
$\Delta V_{cb-ireal-total}$	total real component of the branch voltage drop at node i for the phase cb
$\Delta V_{ac-ireal}$	real component of the branch voltage drop across the impedance between node $i-1$ and i for the phase ac
$\Delta V_{ac-ireal-total}$	total real component of the branch voltage drop at node i for the phase ac
$\Delta V_{ba-iimag}$	imaginary component of the branch voltage drop across the impedance between node $i-1$ and i for the phase ba
$\Delta V_{ba-iimag-total}$	total imaginary component of the branch voltage drop at node i for the phase ba
$\Delta V_{cb-iimag}$	imaginary component of the branch voltage drop across the impedance between node $i-1$ and i for the phase cb
$\Delta V_{cb-iimag-total}$	total imaginary component of the branch voltage drop at node i for the phase cb

$\Delta V_{ac-iimag}$	imaginary component of the branch voltage drop across the impedance between node $i-1$ and i for the phase ac
$\Delta V_{ac-iimag-total}$	total imaginary component of the branch voltage drop at node i for the phase ac
$\Delta V^2_{ba-ireal-total-sum}$	sum of squares of the total real component of the branch voltage drop at node i for the phase ba
$\Delta V^2_{ba-iimag-total-sum}$	sum of squares of the total imaginary component of the branch voltage drop at node i for the phase ba
$\Delta * \Delta V_{ba-ireal=sum}$	real component of the sum product of the branch voltage drop for the phase ba
$\Delta * \Delta V_{ba-iimag=sum}$	imaginary component of the sum product of the branch voltage drop for the phase ba
$\Delta P_{k-mismatch}$	real power mismatch for combined load (statistical & non-statistical) at node k
$\Delta Q_{k-mismatch}$	reactive power mismatch for combined load (statistical & non-statistical) at node k
$\Delta V_{ireal-total}$	total real component of the branch voltage drop at node i due to non-statistical currents
$\Delta V_{iimag-total}$	total imaginary component of the branch voltage drop at node i due to non-statistical currents
$\Delta V^2()$	square of ()
V_{Pcon-i}	consumer voltage percentile value at node i
$\Delta V_{Preal-itotal}$	total real component of the branch voltage drop at node i due to statistical load currents
$\Delta V_{Pimag-itotal}$	total imaginary component of the branch voltage drop at node i due to statistical load currents
$\Delta V_{Treal-itotal}$	total real component of the branch voltage drop at node i due to both statistical and non-statistical currents
$\Delta V_{Timag-itotal}$	total imaginary component of the branch voltage drop at node i due to both statistical and non-statistical currents

Chapter 5

b	value equal or greater than the variable maximum value
$B()$	function of ()
CB_i	circuit breaker rating of the beta distributed load at node i
D_{tr}	distribution transformer turns ratio (230/22000)
$E[()]$	expectation of [] at node ()
$f()$	function of ()
$I_{ave-slv}$	average current load due to currents modelled as signal on LV networks
$I_{ave-smv}$	average current load due to currents modelled as signal on MV networks

$I_{ave_smv,lv}$	average current load due to current signals on MV networks converted to the LV networks
k_{var-s}	variable scaling factor due to current signals
N	number of consumers
N_{bai}	number of consumers for phase ba at node i
N_{aci}	number of consumers for phase ac at node i
N_i	number of connected consumers at node i
P_{ave_slv}	average load power due to currents modelled as signal on LV networks
$P_{s-total-loss}$	total power loss on the single-phase distribution system
R	level of risk in percent
R_i	branch resistance between node $i-1$ and i for the single-phase network
R_{ai}, R_{bi}	branch resistance between node $i-1$ and i for line A and B on the three-phase network respectively
SF_i	new scaling factor for beta-distributed load currents at node i
$SF_{bai}, SF_{cbi}, SF_{aci}$	new scaling factor for beta-distributed load currents at node i for phases ba , cb and ac respectively
tr_s	overall transformation ratio at each node on MV networks due to current signals
$V_{scon_i}^{\#}$	normalised consumer voltage at node i
$V_{scon_i}^{\#2}$	square of $V_{scon_i}^{\#}$
V_{nom_lv}	LV nominal voltage
V_{mv-s}^*	conjugate of the nodal voltage on the MV networks due to current signals
X_{ai}, X_{bi}	branch inductive reactance between node $i-1$ and i for line a and b on the three-phase network respectively
X_i	branch inductive reactance between node $i-1$ and i for the single-phase network
$Y_{bai}, Y_{cbi}, Y_{aci}$	individual current variates at node i for phase ba , cb and ac respectively
Y_k	individual current variates at node k
$\alpha_{vi}^{\#}, \beta_{vi}^{\#}$	statistical parameters of normalised consumer voltage at node i
α, β	statistical parameters of the beta-distributed function
α_k, β_k	statistical parameters of the beta-distributed load at node k
α_i	load current phase angle at node i
α_{abi}	deterministic current signal phase angle for phase ba at node i
α_{cai}	deterministic current signal phase angle for phase ac at node i

α_y	current phase angle at node y for single phase network
μ_r	r^{th} moment about origin
μ_0, σ_0^2	mean value and the variance of the data
$()^2$	square of ()
μ_{ave}	average of individual means
μ_{ave-T}	total average of individual means
$\mu_{bai-ave}$	average of consumers individual means for phase ba at node i
$\mu_{aci-ave}$	average of consumers individual means for phase ca at node i
σ_x	standard deviation of variable X
σ_{ave}^2	average of individual variance
$\sigma_{bai-ave}^2$	average of consumers individual variance for phase ba at node i
$\sigma_{aci-ave}^2$	average of consumers individual variance for phase ac at node i
ρ_{xy}	correlation coefficient between two dependent variables X and Y
ρ_{ave}	average of the correlation coefficient
$\rho_{bai-ave}$	average of consumers correlation coefficient for phase ba at node i
$\rho_{aci-ave}$	average of consumers correlation coefficient for phase ac at node i

Chapter 6

c_p, d_p	real and imaginary component of the current at node p
e_p, f_p	nodal voltage rectangular coordinate system parameters at node p
G_{pq}, B_{pq}	real and imaginary parts of the line admittance between nodes p, q
G_{pp}, B_{pp}	real and imaginary parts of the self-admittance at node p
I_{P-stat}	phasor current due to statistical load current at node p
I_i	total branch current
IMP	branch impedance in ohms per km
I_p	phasor current due to constant PQ loads at node p
I_{P-addm}	phasor current due to system shunt admittance at node p
LI	variable for a line interval in km
N_b	total number of branches connected between node k and supply
V_p	voltage at node p
Z_i	branch impedance
α_{p-stat}	statistical current phase angle at node p
$\Delta e, \Delta f$	real and reactive component to be added to the previous iterated values
$\Delta P, \Delta Q$	nodal real and reactive mismatches

Chapter 7

LI	line interval in km
NC	number of consumers at a load point in single-phase networks
$NC_{()}$	number of consumers for the phase ()
pf	power factor lagging
S	apparent power in kVA in single-phase networks
$S_{()}$	apparent power in kVA for the phase () in three-phase networks
V_{mc}	variable of evaluated consumer voltages from Monte Carlo simulation
V_{an}	variable of evaluated consumer voltages from analytical method
V_{op}	operating voltage
ΔV_{mc}	% voltage drop due to MC simulation
ΔV_{an}	% voltage drop due to analytical method

Chapter 8

$E[\mu]$	expected value of the average current traces for a group of consumers calculated for a period of time
$E[\sigma]$	expected value of the load current traces standard deviation for a group of consumers calculated for a period of time
$E[\rho]$	expected value of the correlation coefficient between all the consumers in a group
PWV	present worth value

This dissertation is dedicated to my family

CONTENTS

1	Introduction	
1.1	Nature of MV power distribution in developing countries	1.1
1.2	Existing methods of rural electrification	1.1
1.3	Voltage regulation on distribution systems	1.2
1.4	System protection	1.2
1.5	Cost assessment on distribution systems	1.3
	1.5.1 Capital	1.3
	1.5.2 Operating cost	1.3
	1.5.3 Maintenance cost	1.3
1.6	Problem identification	1.3
1.7	Objectives of this study	1.4
2	Literature review	
2.1	Introduction	2.1
2.2	Load modelling	2.1
2.3	Evaluation of the system voltage profile	2.3
	2.3.1 General	2.3
	2.3.2 Deterministic evaluation of system voltages	2.3
	2.3.3 Probabilistic evaluation of system voltages	2.4
2.4	Voltage control on distribution systems	2.7
	2.4.1 Voltage control using capacitors	2.7
	2.4.2 Voltage control by step-voltage regulators	2.8
	2.4.3 Voltage control by USE device	2.8
2.5	Evaluation of power losses in distribution systems	2.8
2.6	Summary	2.9
3	DERIVATION OF THE SYSTEM RELATED EQUATIONS	
PART 1:	Development of the branch voltage drop equations in single-phase systems	
3.1	Introduction	3.1
3.2	Development of the voltage drop equations	3.1
	3.2.1 Derivation of the real component of the branch voltage drops	3.2
	3.2.2 Derivation of the imaginary component of the branch voltage drops	3.3
	3.2.3 Derivation of the square of the total real and the total imaginary component of the branch voltage drops	3.3
	3.2.4 The product approach	3.5
	3.2.5 Dealing with a combined loading system	3.8
	3.2.5.1 The product term of the combined loading system	3.10
3.3	Summary	3.13

4 DERIVATION OF THE SYSTEM RELATED EQUATIONS**PART 2: Development of the system branch voltage drop equation in three-phase power distribution systems**

4.1	Introduction	4.1
	4.1.1 Formulation of the basic voltage-related equations	4.1
4.2	Development of the branch voltage drops in three-phase distribution systems	4.3
	4.2.1 Derivation of the real component of the branch voltage drops in three-phase distribution systems	4.4
	4.2.2 Derivation of the imaginary component of the branch voltage drops in three-phase distribution systems	4.5
	4.2.3 Derivation of the sum of squares of the real component of the branch voltage drop in three-phase distribution systems	4.7
	4.2.4 Derivation of the sum of squares of the imaginary component of the branch voltage drops	4.8
4.3	The product term of the branch voltage drops	4.9
	4.3.1 The sum product term of the real component of the branch voltage Drops	4.9
	4.3.2 The sum product term of the imaginary component of the branch voltage drops	4.11

PART 3: Development of the consumer voltage and line power loss equations on MV distribution systems

4.4	Introduction	4.12
	4.4.1 Dealing with statistically distributed load currents	4.12
	4.4.2 Evaluation of the new scaling factors	4.13
4.5	Dealing with constant P-Q loads	4.15
4.6	Dealing with charging currents due to transmission line capacitance	4.15
4.7	Determination of the consumer voltages	4.17
	4.7.1 Dealing with statistically distributed load currents	4.17
	4.7.2 Dealing with non-statistical currents	4.19
	4.7.3 Superposition of branch voltage drops	4.19
	4.7.4 Determination of the overall consumer voltages	4.21
	4.7.5 Evaluation of the consumer voltages in three-phase distribution systems	4.21
	4.7.5.1 Evaluation for the phase .	4.21
	4.7.5.2 Evaluation for the phase .	4.22
	4.7.5.2.1 Determination of the statistical load current phase angles	4.22
	4.7.5.2.2 Determination of the non-statistical phase load currents	4.23
	4.7.5.3 Evaluation for the phase .	4.23
4.8	Derivation of the system power loss related equations	4.23
	4.8.1 Evaluation of the total line power loss on single-phase distribution systems	4.23
	4.8.2 Evaluation of the total line power loss on three-phase distribution systems	4.25
4.9	Summary	4.29

5	The probabilistic approach to the evaluation of the consumer voltages and statistical evaluation of the line power losses	
5.1	Introduction	5.1
5.2	General properties of the beta distribution function	5.1
5.3	Transformation of the branch voltage drop equations	5.3
	5.3.1 Dealing with single-phase distribution systems	5.5
	5.3.1.1 The expected value of the total real and imaginary component of the branch voltage drops	5.5
	5.3.1.2 The expected value of the total square of the real component of the branch voltage drops	5.5
	5.3.1.3 The expected value of the total square of the imaginary component of the branch voltage drops	5.6
	5.3.2 Dealing with three-phase distribution systems	5.7
	5.3.2.1 The expected values of the total real component of the branch voltage drops	5.7
	5.3.2.2 The expected value of the sum of squares of the real component of the branch voltage drops	5.8
	5.3.2.3 The expected value of the sum of squares of the imaginary component of the branch voltage drops	5.9
	5.3.2.4 The expected value of the sum product term of the real component of the branch voltage drops	5.10
	5.3.2.5 The expected value of the sum product term of the imaginary component of the branch voltage drops	5.12
5.4	Determination of the consumer voltage percentile values	5.15
	5.4.2 Evaluation of the consumer voltage percentile value in single-phase MV distribution systems	5.16
	5.4.3 Evaluation of the consumer voltage percentile value in three-phase MV distribution systems	5.17
5.5	Statistical approach for the evaluation of the system power loss in MV radial distribution systems	5.17
	5.5.1 Introduction	5.17
	5.5.2 Determination of the general expression of the total line power loss in MV radial distribution systems	5.18
	5.5.3 The total line power loss in single-phase MV distribution systems	5.19
	5.5.4 The total line power loss in three-phase distribution systems	5.20
5.6	Modelling of load current as signals	5.21
	5.6.1 Correlation coefficient on the MV distribution line	5.22
	5.6.2 Evaluation of the transformation ratio due to load current signals	5.23
5.6	Summary	5.24
6	Development of the computer programs	
6.1	Introduction	6.1
6.2	Application of the Newton-Raphson algorithm	6.1
6.3	Application of the backward and forward sweep algorithm	6.4
6.4	Modeling of step-voltage regulator in three-phase delta-delta connected systems	6.6
6.4.1	Procedure adopted for modeling a step-voltage regulator	6.6
	6.4.1.1 Voltage control for the phase	6.6

6.5	Development of the universal algorithm	6.7
6.5.1	The development of the arrays for single-phase distribution systems	6.8
6.5.1.1	Development of the D-array	6.8
6.5.1.2	Development of the b-array	6.10
6.5.1.3	Development of the path-array	6.11
6.5.1.4	Development of the wx-array	6.12
6.5.1.5	Development of the x2-array	6.12
6.5.1.6	Development of the Z1-array	6.12
6.5.1.7	Development of the R1-array	6.13
6.5.1.8	Development of X1-array	6.13
6.5.2	The development of the arrays for three-phase distribution systems	6.13
6.5.3	The computer program syntax for creating arrays in single and three-phase distribution systems	6.16
6.5.3.1	The computer syntax for creating the D-array, Z1-array, R1-array and X1-array	6.17
6.5.3.2	The computer syntax for creating b-array and wx-array	6.17
6.5.3.3	The computer syntax for creating the path-array and x2-array	6.18
6.5.3.4	The computer program syntax for creating the D21-array, D32-array and D13-array	6.19
6.5.3.5	The computer syntax for formulating DD21-array and the impedance system mapping	6.20
6.5.3.6	The computer syntax for implementing line capacitance node values	6.21
6.6	Significance of the developed arrays	6.21
6.6.1	Evaluation of a single value	6.21
6.6.2	Evaluation of two or more values	6.22
6.7	Development of the probabilistic power flow program	6.22
6.8	Demonstration of the application of the universal algorithm	6.23
6.8.1	The computer program syntax for non-statistical currents	6.24
6.8.2	The computer program syntax for statistical currents	6.24
6.8.3	The computer program syntax superposition of voltage drops	6.25
6.9	Summary	6.25
7	Verification of the developed algorithms	
7.1	Introduction	7.1
7.2	Single-phase MV distribution systems	7.1
7.2.1	Comparison between calculated and simulated results for consumer voltages	7.1
7.2.2	Comparison between calculated and simulated results for system power losses in single-phase distribution systems	7.6
7.3	Three-phase MV distribution systems	7.8
7.3.1	The comparison between calculated and simulated consumer voltages	7.8
7.3.2	The comparison between calculated and simulated results for system power losses in three-phase system	7.13
7.4	Comment on the results	7.15
7.4.1	Comparison of consumer voltage percentile values	7.15
7.4.2	Comparison of total line power losses	7.16
7.5	Summary	7.16

8	Financial analysis on MV distribution systems	
8.1	Introduction	8.1
8.2	Illustrative example on existing MV distribution system	8.1
	8.2.1 Selection of parameters	8.1
	8.2.2 Approach adopted	8.2
	8.2.2.1 Analysis of a SWER network	8.2
	8.2.2.2 Analysis of a single-phase (phase-phase) network	8.2
	8.2.2.3 Analysis of a three-phase network	8.3
8.3	Criteria for the application of the USE concept	8.3
8.4	Comment on the field performance for the USE devices	8.4
8.5	Summary	8.5
9	CONCLUSION	
9.1	Introduction	9.1
9.2	Previous research work	9.1
9.2.1	Evaluation of the consumer voltages	9.1
9.2.2	Evaluation of line power losses	9.1
9.3	Contribution of present research work	9.2
9.3.1	Evaluation of the consumer voltages	9.2
9.3.2	Evaluation of line power losses	9.2
9.4	Development of the universal algorithm	9.2
9.5	Development of the computer programs	9.3
9.6	Observations	9.3
9.7	Significance of the present work	9.4
9.7.1	Development of the probability load flows	9.4
9.7.2	Modeling of step-voltage regulators on the (delta-delta) connected network	9.4
9.7.3	Derivation of a general expression of line power losses in MV distribution networks	9.4
9.7.4	Development of the universal algorithm	9.4
9.8	Future research work	9.5

References

Appendices

INTRODUCTION

1.1 Nature of MV power distribution in developing countries

Power distribution in developing countries consists of rural and semi-urban areas that are associated with high capital, operating and maintenance costs [1.1]. The electricity demand in these areas is characterised by a low annual utilisation of connected load. The combination of long distribution lines and scattered consumers is the major reason for the high cost of supplying to rural areas [1.2]. It is well known fact that, electricity is one of the main parameters on which the development of rural and suburban areas of developing countries depends.

The supply voltage to electrical consumers, particularly in rural areas, is affected by large voltage drops in the MV distribution network and by the interruption of supply due to lightning surges. In MV power distribution systems, the line impedance of the primary feeder (or backbone feeder) and lateral feeders (or spurs), is the electrical parameter which causes poor voltage regulation. In general, the magnitude of the voltage drop ΔV per unit length will depend upon the magnitude of the current and the power factor of the connected loads and can be approximated as [1.3]:

$$\Delta V = I(R \cos \alpha + X \sin \alpha) \quad (1.1)$$

where

- R is the line resistance per unit length
- X is the line inductive reactance per unit length
- I is the magnitude of the current
- α is the power factor angle

Generally, distribution networks in rural areas cover long distances of about 50km and above and it is evident that according to equation (1.1), the voltage drop can be large depending on the size of conductors. It is economically impossible to provide each and every electrical consumer on a distribution system with a constant supply voltage corresponding to the designed voltage. Compromises are required between the allowable deviation above and below the designed voltage of the equipment at which satisfactory performance can still be obtained. If the power utility companies maintained broad limits, the cost of the electrical equipments would be high because they would have to be designed to operate satisfactory at any voltage within the limits. If the limits maintained were too narrow, the cost of providing electrical power would become too high because they could use a network with a very low line impedance and/or application of voltage regulators.

Non-adherence to voltage limitations affect electrical equipment and could lead to insulation failure in case of over-voltage, while in the case of under-voltage the electrical equipment will fail to perform adequately. Equipment utilising electric motors will be damaged from both undesirable states.

1.2 Existing methods of rural electrification

Single wire earth return (SWER) distribution lines are used in South Africa due to its relative low cost for distributing electrical power in sparsely spread deep-rural communities [1.4]. In

the USA, three-phase four wire systems are employed as backbone feeders throughout the rural areas. Phase to phase and phase to neutral lines are tapped directly from the backbone. In Ireland, a typical 10kV feeder in a rural area consists of a three-phase backbone line and of single-phase spurs [1.5].

In general, the adoption of a three-phase system as a backbone seems to be the trend in most rural networks in different parts of the world. The use of single-phase (i.e. phase to neutral and phase to phase connection) and single-wire earth return (SWER) systems are facilitated by tapping from the backbone feeder. In these systems, poor voltage regulation is common [1.6]. The choice of an appropriate system topology to be adopted should be economically evaluated, reflecting the type of load to be served and the actual distances from the backbone line.

1.3 Voltage regulation on distribution systems

The major share of responsibility for providing electrical consumers with regulated voltage levels falls on the distribution system. The primary objective of system voltage control is to provide to each electrical power user, the voltage conforms to the voltage-designed limitations of the electrical equipment. For rural electrification where electrical consumers are located far from the distribution substation, the voltage control equipment is located on the primary and lateral feeders to compensate for excessive voltage drop. Where the primary feeder or lateral feeder voltage falls below the minimum permissible voltage value, the voltage control equipment will raise the voltage to within the permissible limits, preferably to the maximum value. Voltage regulators, fixed and switched capacitors [1.7] and power electronics converters known as FACTS devices [1.8] can be employed in MV power distribution systems for controlling the voltage in order to enable permissible voltage levels to electrical consumers to be attained. At the University of Stellenbosch, the USE (Universal Semiconductor Electrification) device was developed to control the voltage in the low voltage distribution system. This is a power electronics converter and it controls the voltage at a low voltage level of the electrical power network system and hence can be regarded as μ FACTS device [1.9].

1.4 System protection

The need to achieve an acceptable level of reliability, quality and safety of the electricity supply at an economic price becomes a priority to the utility company. The supply system should be designed and properly maintained in order to limit the number of faults, which might occur. One of the most important factors within the distribution networks that assist in meeting the requirements for safety, reliability and quality of supply is the protection system that is installed to clear faults and limit any damage to distribution equipment.

In order to achieve savings in the construction of distribution systems and in the particular case for rural areas, overhead construction is usually adopted. These overhead lines are susceptible to faults due to lightning and other climatic conditions, birds, falling tree branches and a variety of additional causes. But 80% of these faults are of a transient nature and in order to avoid damage, suitable and reliable protection should be installed on all circuits and electrical equipment. Manual restoration of supplies especially in rural areas after interruption is often rendered difficult due to weather conditions, rough terrain and frequently involves journeys of considerable distance. In this regard, automatic restoration of supplies should be employed in order to improve the continuity of supplies to electrical consumers [1.10].

1.5 Cost assessment on distribution systems

The evaluation of cost of the MV distribution systems falls into three categories namely capital, operating and maintenance costs.

1.5.1 Capital cost

The capital cost involves the expenses required to purchase the materials for construction and labour. Significant savings in capital expenditure can be achieved by correct design.

1.5.2 Operating cost

The conductor used for delivering electrical power has finite resistance. This resistance value will depend on the conductor size. With the passage of electric current, the power loss is proportional to the product of the square of the current and the resistance. Thus, this operating cost is a function of the system design.

1.5.3 Maintenance cost

Regular equipment maintenance is essential in order to ensure its satisfactory operation when power is delivered to consumers. This requires personnel and replacement equipment. The overall maintenance costs will depend on the topology and type of equipment employed. Equipment that uses many components for its operation or requires many moving parts will definitely cost more on the maintenance costs.

1.6 Problem identification

In the distribution of electrical power to densely populated regions in developing countries, such as those in urban areas, the present electrification techniques are being successfully implemented. But in rural areas, especially those termed as deep-rural, where there is a combination of long MV distribution lines and scattered electrical consumers, the grid connection is not feasible due to high capital costs, high operating and maintenance costs. In practice, as previously mentioned, there are four different topologies capable of distributing electrical power in MV distribution system. These are three-phase (three wire or four wire), single-phase (phase to neutral connection), single-phase (phase to phase connection) and SWER systems. Availability of a good quality of voltage supply at the electrical consumer terminals is the main objective of a utility.

In finding a solution to the voltage regulation problem and the reduction of costs in deep-rural networks, the FACTS group at the University of Stellenbosch in 1996 developed a USE device. The typical positioning of a USE device for centralized AC LV distribution network is shown in fig. 1.1.

The main objective of the USE device is to compensate for voltage-drop in the LV distribution network of up to 35% and hence enabling the reduction of cost by:

- adoption of cheap conductor material such as steel wires
- utilization of longer length of standard conductors which is not possible in current practices due to voltage constraint

Domestic loads are stochastic in nature and it was recommended in the early 90's that, the statistical description of the load current be adopted when designing reticulation networks

[1.11]. In view of this, the statistical approach to cater for statistical domestic load currents as experienced in rural area loads should be adopted. In case of fixed loads, e.g. pump loads, the deterministic approach may be adopted. For the combination of both types of loads, the overall result can be obtained by applying the principle of superposition to the two types of loads.

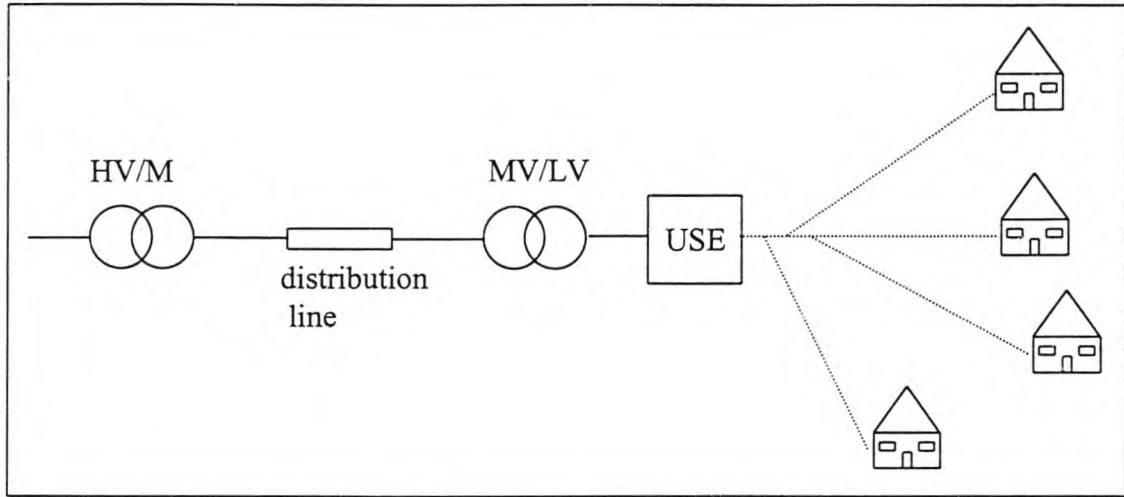


Fig. 1.1: The typical positioning of a USE device for centralized AC LV distribution network

The line power loss in MV distribution system needs to be evaluated in order to assess the operating cost for the system. The evaluation of the system power loss solely depends on how the load currents are modeled. Modeling load currents as signals is a concept developed recently [1.12]. The procedure eliminates the traditional practice of applying a load factor when the ADMD value is adopted. In this thesis, the problem of voltage regulation and system power loss in MV distribution networks, the statistical description of the load current and treating load current as signals are investigated. The underlying problem is to develop the general expressions both in single and three-phase systems that are capable of evaluating the voltage regulation and system power losses.

1.7 Objectives of this study

The objectives of the study are as follows:

- to develop the analytical tool that is capable of evaluating the voltage regulation and power loss on the conventional 22kV ESKOM distribution system. The analysis treats the load current as mentioned in section 1.6.
- incorporating step-voltage regulators and capacitors for the system voltage control
- the investigation for different line topologies as mentioned above for the viability of the USE concept for rural electrification. The areas that are involved in the study are: voltage levels, applicability of the USE devices, capital cost, operating and maintenance cost.

To achieve the above, the present work is organised to eight chapters. In chapter 2, the published literature that bears relevance to the present work is presented. In chapter 3, the general expressions for evaluating the branch voltage drops in single-phase systems are

developed. Individual and combined loads applied to a system without branches are presented. In chapter 4, the general expressions for evaluating the branch voltage drops in three-phase systems, consumer voltages and the line power losses are developed for the system without branches. In chapter 5, the probabilistic approach on the evaluation of the consumer voltages in single and three-phase system is presented. The concept of treating load current as signals is applied to evaluate the total line power losses. In chapter 6, the computer programs developed to evaluate the consumer voltages and line power losses in single and three-phase systems are discussed. In chapter 7, the developed algorithm is verified and in chapter 8, the financial analysis of MV distribution systems is presented. A case study on a conventional 22kV ESKOM distribution system and the criteria for the application of the USE concept is investigated to illustrate the application of the developed analysis tools.

LITERATURE REVIEW

2.1 Introduction

In this chapter, the published literature relating to the computation of power flows in the electric power system are reviewed. Depending on the nature of the input data, which in general depicts how the loads are modelled, the computations can be performed deterministically or probabilistically. The deterministic approach performs the steady-state simulation of the power system. With the specified set of input data, the deterministic study provides a single-valued solution. In the probabilistic approach the performance of the power system is based on the likely range of input data. If the consumer voltages fall below the permissible values, the voltage control devices such as step-voltage regulators and capacitors are employed to solve the problem of the poor voltage regulation. In this present work, the focus is on MV distribution systems and therefore the published literature material pertaining to any part of the power network system will be discussed, where it has relevance to the MV distribution system.

2.2 Load modelling

The accuracy of the computations for the power flow in electric power systems depends on how the loads are modelled. Significant research has been done and published in this area [2.1]. The load models are categorised on the basis of their applications. Despite this wide coverage of load models, their application in MV distribution network systems especially for rural electrification is inadequate. In reference [2.2], a great deal of discussion is presented regarding load modelling. The author describes three categories of load models. These are the constant $P + jQ$, the constant $R + jX$, and the constant current model. The constant $P + jQ$ model is often used in power flow load studies on transmission systems. This model assumes that the load current decreases with an increase in the voltage at a constant power factor so that the real and the reactive power are maintained constant. The author argues that, this model is useful only if the load voltage is regulated since it does not give an accurate picture of the sensitivities of most loads to voltage variations. Therefore, Brice suggests that, the constant $P + jQ$ model should not be used on distribution system studies unless the load is known to be insensitive to voltage changes. The constant $R + jX$ model assumes that the load real and reactive power varies in proportion to the square of the voltage magnitude. This model is only valid for resistance heating loads. Most loads draw real power that varies somewhat with voltage but less than what this model predicts. For example, incandescent lamp loads exhibit real power proportional to the voltage raised to the power of 1.6. Brice suggests that, the model that gives a middle ground between the extremes of the two previous models is the constant current model. This model predicts that the real and imaginary power vary in direct proportion to the voltage. While the actual load current is expected to vary somewhat with the voltage, he states that, this model is probably the best model for general use in distribution voltage studies. The idea of representing load as composite load model comprising of some portion of the load modelled as constant power, some portion modelled as constant impedance and some portion modelled as constant currents is found in reference [2.3]:

$$P = A_0 + A_1V + A_2V^2 \quad (2.1)$$

$$Q = B_0 + B_1V + B_2V^2 \quad (2.2)$$

where

V is the magnitude of the voltage at the load point

Brice [2.2] suggests that, in order to improve the load description, application of end-use models are necessary. But, this requires a considerable amount of load-research data. If data were available to support the end-use models or the composite models, better results could be obtained but at higher engineering costs. As a result of these considerations, the constant current load model at assumed unity power factor would be used in this thesis when loads are modelled at the low voltage networks. This type of load model is adequate if the voltages at the MV distribution systems are allowed to remain in the permissible values. But if voltage drop of up to 35% is to be evaluated for the application of the USE concept, then the constant current model will give pessimistic results.

Other researcher's [2.4], also put emphasis on performing the analysis of the behaviour of domestic electrical loads on the basis of valid data measurement. In achieving this goal, means of recording load data coincidentally must be realised. In order to obtain reliable load data, they applied a modern microprocessor technology, which comprises of a multi-channel microprocessor based loggers equipped with an accurate on-board time clock. This enables the monitoring of the multiple consumer load currents coincidentally at regular intervals. Results from load surveys, involving about 10 gigabytes of data are available for analysis [2.5]. Analysis to date indicates that the most appropriate statistical model for describing grouped domestic electrical loads is the beta probability density function [2.4]. Data of the 10-minute moving averages at the time of the system diversified maximum demand reveal the stochastic nature of domestic loads.

The Beta probability density function (beta pdf) used to fit the frequency of occurrence of normalised domestic loads is shown in fig. 2.1.

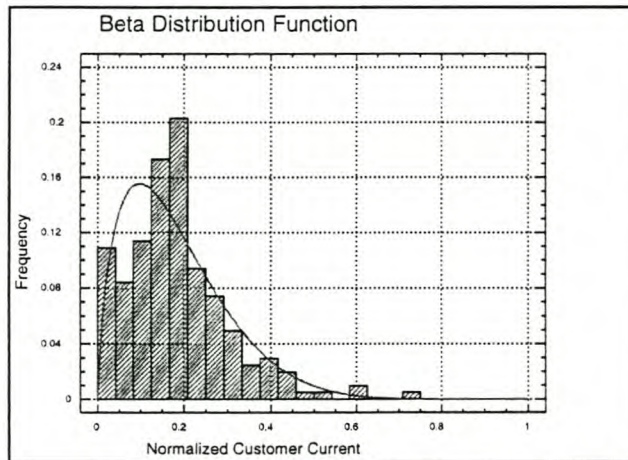


Fig. 2.1: Beta distribution function for representing domestic loads at the time of maximum demand

The essential properties of a beta pdf are as follows:

- it is bounded within the interval 0 to 1
- it can be scaled to accommodate any finite positive values
- it can represent distributions that are negatively or positively skewed

- it can represent distribution that are symmetrical

The statistical parameters of Beta pdf are α and β . The shape of the distribution is characterised by its statistical parameter values as depicted in fig. 2.2.

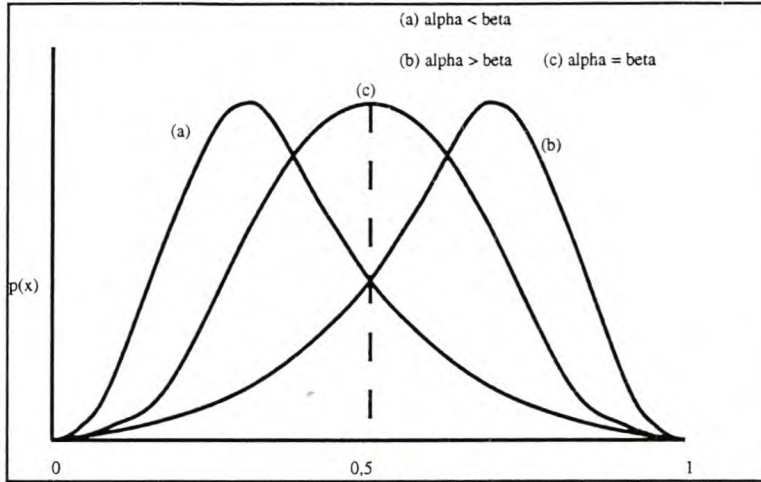


Fig. 2.2: The representation of the Beta distribution function for different statistical parameter values

The advantage of modelling the domestic load as currents is discussed in the reference [2.6]. The method considered treats the load as a stochastic current sink. As long as the application is on the low voltage part of the distribution system and the voltage statutory specifications are adhered to, the results will fall within the acceptable accuracy limits. But in MV distribution systems, the idea of adopting the current model is less accurate if the voltage drop up to 35% is to be evaluated as previously mentioned.

2.3 Evaluation of the system voltage profile

2.3.1 General

The system voltage profile can be evaluated from two different procedures as far as the loading is concerned. The procedures can be classified as deterministic or probabilistic. In the deterministic approach, the input data which is normally applied in the network equations, is known in advance or in other words is single-valued. But in probabilistic approach, the data is based on a likely range of values. It is evident that, the calculation based on a deterministic approach does not take into account the variations in consumer loading. In the case of the probabilistic load-flow, the probability distribution function or its moments of the state random vector is obtained from the given probabilistic description of the input data.

2.3.2 Deterministic evaluation of system voltages

In performing the probabilistic load-flow in this thesis, some parameters are assumed to be deterministic. Several deterministic power flow algorithms specially designed for radial distribution networks have appeared in the literature [2.7 – 2.16]. In addition to their improved numerical robustness, these techniques take full advantage of the radial structure of the networks to save computation time. There exist certain ill-conditioned cases for which the described methods may present convergence difficulties [2.9,2.10]. In reference [2.12],

the two-step procedure in which the branch currents are first computed (backward sweep) and then the bus voltages are updated (forward sweep) is shown to be computationally very efficient and can be extended to handle loops in the system. Another advantage of the algorithm is due to the fact that it can be easily programmed for the single and three-phase systems.

2.3.3 Probabilistic evaluation of system voltages

Depending on the nature of the input data, two different approaches are used in the probabilistic analysis. One approach is known as stochastic load-flow. The stochastic load flow algorithm is easily built from existing state-estimator algorithms, but the drawback of the SLF is that it handles only Gaussian nodal probabilistic density function (PDF) data. The second approach is known as the probabilistic load-flow algorithm in which the PDF of the state variables or its moments is obtained from the given probabilistic description of the input data. This type of algorithm is applicable to this present work and it is appropriate to discuss it in detail as presented by various researchers. In reference [2.17], the probabilistic power flow to the three-phase system takes into account all the uncertainties, which can affect any unbalanced power system. A simplified approach based on the linearization of the three-phase load-flow equations around an expected value region is proposed. The equations of the active power $(P_i^p)^{sp}$ and the reactive power $(Q_i^p)^{sp}$ in reference [2.17] are specified at each of the three phases as:

$$(P_i^p)^{sp} = V_i^p \sum_{k=1}^N \sum_{m=1}^3 V_k^m [G_{ik}^{pm} \cos \theta_{ik}^{pm} + B_{ik}^{pm} \sin \theta_{ik}^{pm}] \quad (2.3)$$

$$(Q_i^p)^{sp} = V_i^p \sum_{k=1}^N \sum_{m=1}^3 V_k^m [G_{ik}^{pm} \sin \theta_{ik}^{pm} - B_{ik}^{pm} \cos \theta_{ik}^{pm}] \quad (2.4)$$

The unknowns are the voltage magnitude and argument of each phase

where

- $(P_i^p)^{sp}$ is the specified real load power at node i with phase p
- $(Q_i^p)^{sp}$ is the specified reactive load power at node i with phase p
- V_i^p is the voltage magnitude at node i with phase p
- V_k^m is the voltage magnitude at node k with phase m
- G_{ik}^{pm} is the conductance relating node i with phase p and node k with phase m
- B_{ik}^{pm} is the capacitive susceptance relating node i with phase p and node k with phase m
- θ_i^p is the voltage phase angle at node i with phase p
- $\theta_{ik}^{pm} = \theta_i^p - \theta_k^m$

In this reference [2.17], the active and reactive powers are considered to be jointly normal correlated random variables. Referring to the linearized model, the statistical features of the output variables (i.e. voltage and their phase angles), the three-phase load flow equations are

linearized around an expected value region. The three-phase load flow equations given in the equation (2.3) and (2.4) can be expressed as:

$$f(X) = U \tag{2.5}$$

where

U is the input random vector (active and reactive load phase powers)

X is the state random vector (magnitude and argument of the unknown phase-voltages)

The vector $\mu(U)$ is taken to be the expected value of the input random vector U . By performing deterministic three-phase load flow using $\mu(U)$ as input data in equation (2.5), its solution is given a vector X_o such that:

$$f(X_o) = \mu(U) \tag{2.6}$$

Linearizing equation (2.5) around the point X_o it results to:

$$X \approx X_o + A\Delta U = X'_o + AU \tag{2.7}$$

where

$$A = \left[\frac{\partial f}{\partial X_{X=X_o}} \right]^{-1}$$

$$\Delta U = U - \mu(U)$$

$$X'_o = X_o - A\mu(U)$$

The elements of the random vector X in equation (2.7) are expressed as a linear combination of the random elements of the input vector U . The magnitude and the argument of the phase voltages are approximated by jointly normal correlated variables whose statistical characterization can be effected in terms of mean values and covariance matrices. The mean value $\mu(X)$ and the covariance matrix $\text{cov}(X)$ of the random vector X are given as:

$$\mu(X) \approx X_o \tag{2.8}$$

$$\text{cov}(X) = A\text{cov}(U)A^T \tag{2.9}$$

The standard deviation of the element of the random vector X is obtained from the diagonal of the covariance matrix $\text{cov}(X)$.

The procedure adopted in reference [2.17] reveals some shortcomings as follows:

- the linearization of the of the state variable is likely to cause some big errors if voltage drops of about 35% over the line should be evaluated
- the procedure is valid only when the input variables are normal distributed

In reference [2.18], the authors describe a probabilistic load-flow currently known as the Herman Beta method that is different to the one mentioned in the reference [2.17] in the approach adopted. The Herman Beta method of calculating voltage drops in LV feeders was developed for three-phase, four-wire and bi-phase topologies using the Beta pdf description for the load currents. The method uses the principle of manipulating random variables of current into voltage drop random variables. The statistical parameters of the consumer voltages are then evaluated from their first and second moments. The first and the second moments of the consumer voltages are expressed in terms of the first and the second moments of the branch voltage drops. The percentile value of the consumer voltage variable is obtained by assigning a risk level or conversely, a confidence level. The weakness of the method in reference [2.18] is the result of the successive series line sections being handled one at a time using the previous upstream result as a starting value for the next section. By applying the same risk at each section results in an overestimation of the overall risk. Another drawback is the designation of one particular phase to be the heaviest loading and treated as the reference phasor. To overcome the above-mentioned shortcomings, the original Herman Beta method was modified in reference [2.19]. Heunis et al. applied a principle of superposition to calculate the random variable for the total feeder voltage drop. The principle of superposition as known in the electric network theorems in particular reference to calculating the voltage drops in a network circuit, states as follows:

“If the voltage drop over a branch is a function of more than one voltage or current source, the voltage drop can be written as the sum of the voltage drops due to each source”.

By applying the principle of superposition, the voltage drop random variable is expressed as the sum of the random variables of each source. The authors developed general expressions for the first and the second moments of the real and imaginary components of the total voltage drop for each load current at any node of the system. By applying the principle of superposition, the individual results are summed to produce the final results. The resultant analytical procedure is summarised in Appendix 2-A.

The approach adopted in reference [2.19], proves to work well in developing the required general expressions. This is due to the fact that, the analysis is dealing with the three-phase four-wire system on the LV distribution networks where line inductive reactance and the consumer voltage phase angles are neglected. On MV distribution systems, such assumptions are not valid and therefore the analysis should take into consideration the line inductive reactance and the consumer voltage phase-angles. To apply the above algorithm in MV distribution system will prove to be a difficult task, hence an alternative approach is pursued. It should also be borne in mind that, expression (2-A11) in appendix 2-A is accurate up to a point as far as the Taylor expansion is concerned. In evaluating system voltage drop of up to 35%, the approximation will give pessimistic results. Furthermore, the algorithm cannot do the following:

- automate load currents
- automate branched systems

The automation of the load currents and handling of the branched systems automatically have to be implemented when evaluating consumer voltages and line power losses on a practical MV radial distribution system. The main reason for the total automation is due to the fact that the assumed deterministic parameters in the present work are evaluated by applying iterative procedures.

2.4 Voltage control on distribution systems

The design of MV distribution systems in densely populated areas in the developing countries, such as those in urban areas, thermal line capacity is the design constraint to be met. Such systems are generally electrically short and therefore the magnitudes of the consumer voltages are usually within the permissible values. But in rural areas, especially those termed as deep-rural where there is a combination of long MV distribution lines and scattered electrical consumers, the design criterion is no longer the line thermal but rather the voltage constraint. This is due to high voltage-drops along its longer MV distribution lines.

In finding a solution to the voltage regulation problem in MV rural distribution systems, the voltage controlling devices are employed along the distribution feeders. Such devices commonly employed are capacitors and the step-voltage regulators [2.20,2.21]. To combat the voltage regulation problem on low voltage distribution systems, the FACTS group at the University of Stellenbosch in 1996 developed a USE device. One of the main objectives of the USE device is to compensate for voltage-drop along the MV distribution networks of up to 35% with the intention of reducing MV distribution network system costs by adoption of cheap conductor material such as steel wires. The second objective is to be able to utilize longer lengths of standard conductor, which is not possible in current practices due to voltage constraint [2.22]. In this section, the published literature on voltage control devices as mentioned above is discussed.

2.4.1 Voltage control using capacitors

The approximate formula, which gives the voltage drop ∇V on one conductor, can be given as [2.23]:

$$\Delta V = I(R \cos \theta + X \sin \theta) \quad (2.10)$$

where

- I is the magnitude of the line current
- R is the line resistance
- X is the line inductive reactance
- θ is the load power factor angle

Referring to equation (2.10), the reactive part of the voltage drop, $IX \sin \theta$ has a great effect on the magnitude of the voltage drop depending on the values of X and θ . Adding a shunt capacitor to an inductive system decreases voltage drop since the in-phase drop produced across the line by capacitor current is in the opposite direction to the voltage drop produced by the load current across the inductive reactance. In essence, shunt capacitors are utilised to counteract this voltage drop by producing a fixed voltage rise across the line, which is independent of the power factor of the load.

This voltage rise is continuous so that it occurs during heavy and light loads. Depending upon the amount of capacitive reactance connected on the system, the light load voltage profile can rise to a value above the maximum permissible voltage. If capacitors are installed so that they may be switched on during heavy load periods and off at light load periods, voltage regulation can be improved.

There is a concern that, if capacitors are not properly sized and placed along the feeder, they can amplify harmonic currents and voltages due to possible resonance at one or several

harmonic frequencies. This condition could lead to potentially dangerous magnitudes of harmonic signals, causing additional stress on equipment insulation, increased capacitor failure and interference with communication systems [2.24].

2.4.2 Voltage control by step-voltage regulators

Voltage regulators referred to as step-voltage regulators are simply a tapped autotransformer that is used to raise or lower the voltage at the point of installation. The autotransformer utilises both a direct electrical connection as well as magnetic flux to transfer energy. Approximately 90 % of the energy transfer comes via the direct electrical connection when the regulator is either in the full boost or full buck mode. At nominal tap setting, nearly all the energy is transferred by direct electrical connection allowing some regulators to have higher *kVA* ratings for reduced tap settings. The rating of a regulator is determined as the product of the rated load current and the range of regulation in voltage [2.25]:

In the three-phase three-wire system, two regulators connected in open delta provide a 10 % regulation on all three phases [2.20,2.25,2.26]. But if three regulators are used in closed delta, a 15 % voltage improvement is possible [2.20,2.26]. Selection of the regulator locations does not involve any sophisticated calculations. In practice they are simply installed where the voltage falls below permissible values. Generally, the voltage regulators are not placed exactly at the point where the voltage drops to minimum permissible value, but instead slightly ahead to take care for some load growth. In theory, many regulators can be used to yield a satisfactory voltage profile. But in practice, the thermal capacity of the line and the line losses limit their number [2.20]. Modelling of the step-voltage regulator for computer programming in a system having neutral point is presented in reference [2.27].

2.4.3 Voltage control by USE device

The idea of adopting the USE concept for voltage control was conceived from the fact that the majority of the people in South Africa do not have access to electricity. Unfortunately, the majority of the people live in the rural areas where, the cost of providing power is enormous by conventional means. The Universal Semiconductor Electrification Concept (USE) employs *μFACTS* devices to compensate for extreme distribution line voltage drop at the load-end of LV systems [2.28]. It is envisaged that, the USE system can compensate for up to 35% voltage drop without affecting its rating capability [2.29]. The device works on the principle of maintaining its input power constant for different values of input voltage. Therefore, if the input voltage drops, the input current will rise. With this ability of absorbing such amounts of voltage drop enables the following:

- the use of a cheaper conductor for new distribution lines
- extension of existing distribution lines beyond the current voltage limits

Such a capability for design practices should be evaluated to ascertain the feasibility of the USE concept in rural electrification schemes.

2.5 Evaluation of power losses in distribution systems

The power loss in a distribution system forms a crucial part in estimating the cost of a system over a period of time. This cost is termed 'operating cost' due to the fact that it is present as long as power is been delivered to consumers. The power loss can be evaluated by considering the real and the imaginary components of the line current. This is the basis,

when attempting to evaluate the power loss due to load currents modelled as signal in this thesis. The treatment of load current as signals is a new concept that defines individual consumer currents over a given period of time using mean and standard deviation. The average load trace for two consecutive days as measured in Tambo community is depicted in fig. 2.3.

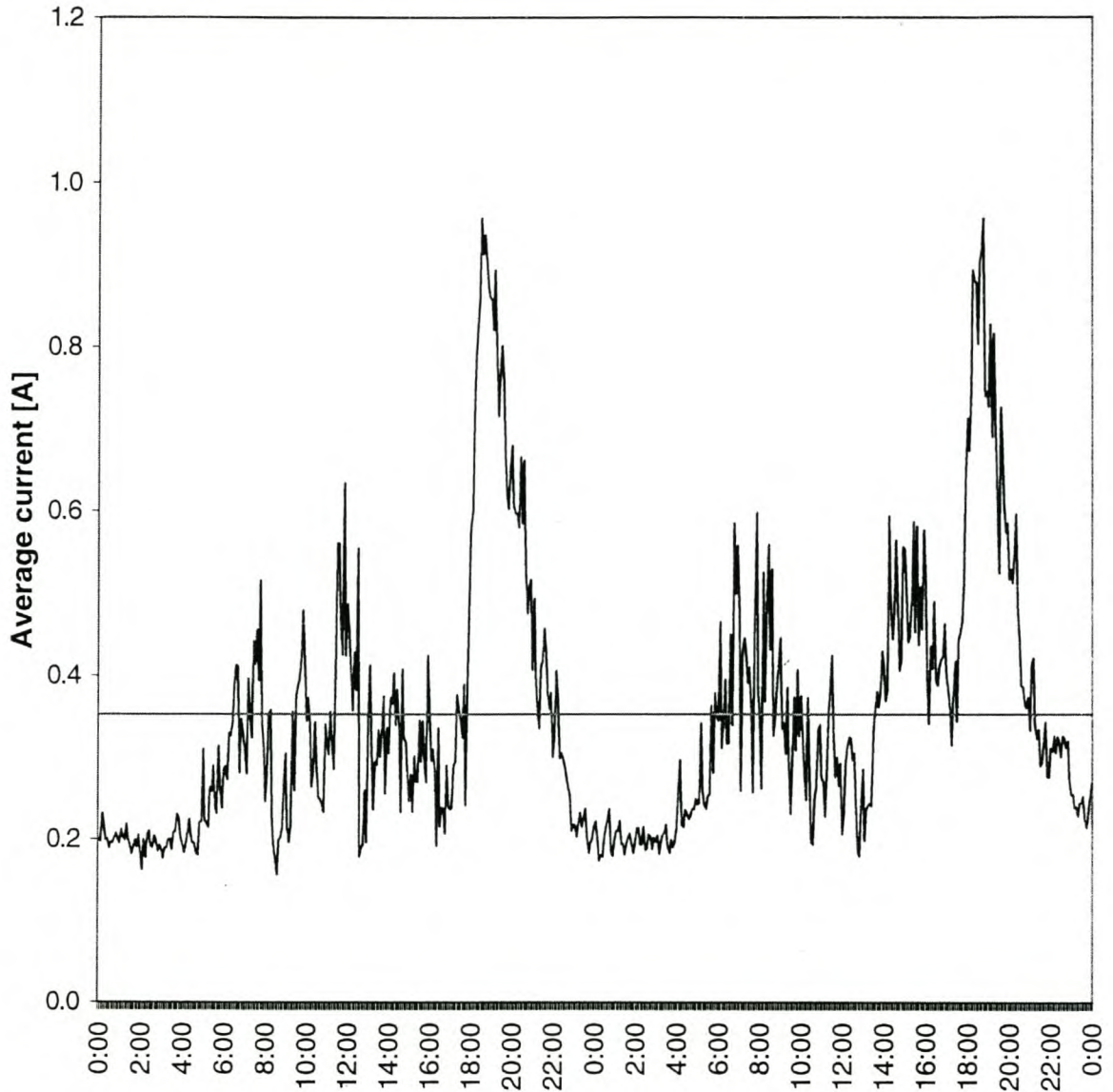


Fig. 2.3: The average load profile as measured in two consecutive days in Tambo during 1998

The trace has a mean value indicated by the horizontal line and the spread from the mean can be measured as the standard deviation of the trace. The research conducted by Heunis in South Africa reveals that, the consumer load currents treated as signals in different communities are correlated. The difference in the evaluation of line power losses due to correlated or non-correlated load currents lies in the consideration of the covariance term. This covariance term is applied to the correlated load currents.

2.6 Summary

In this chapter, some of the published literature concerning the computation of power flows in distribution networks is discussed. The critical issue is the way consumer loads are modelled. There is evidence that, domestic loads are stochastic in nature having a beta

Stellenbosch University <http://scholar.sun.ac.za>
probability density function [2.4]. The present work deals with distribution systems for supplying electricity to rural areas. Much of the anticipated loads are domestic plus some pump loads that can be modelled as constant P-Q loads. The analytical tool for computing power flows in single and three-phase distribution systems supplying domestic and pump loads is required. The approach adopted in this present work is as follows:

- beta distributed load currents are modified and the Herman beta method is applied to a new set of general expressions developed for the system without branches. The modification of the beta distributed load currents is based on the concept of modelling loads as constant P-Q loads with or without USE devices (see section 2.4.3). This type of load modelling is suitable for MV distribution systems when evaluating up to 35% voltage drop
- evaluation of the overall consumer voltages due to statistical and non-statistical currents is done using the principle of superposition
- the load currents are modelled as signals for the evaluation of the system power losses with new general expressions for systems without branches
- consumer voltage angles, current due to the modelling of voltage regulators and system line capacitance are assumed to be deterministic parameters
- development of a new algorithm applicable to practical distribution systems

The algorithms presented are a new contribution for engineering decision-making in MV distribution systems particularly those intended for rural electrification in developing countries.

CHAPTER 3

DERIVATION OF THE SYSTEM RELATED EQUATIONS

PART 1: Development of the branch voltage drop equations in single-phase systems

3.1 Introduction

The procedure adopted in the evaluation of feeder voltage drops and consumer load voltages due to statistical and non-statistical loads, with or without the application of the USE concept, is outlined. Their combined effect on the voltage profile along the MV rural distribution network can be determined by performing the superposition of the real and imaginary parts of the branch voltage drops. Statistical loads are modelled as constant currents having a beta distribution as reported in previous research on domestic consumer loads [3.1]. Non-statistical loads are modelled as constant $P-Q$ loads. Non-statistical loads are typically the pump loads to be expected in rural farm areas. The analytical work presented in this chapter deals with a radial distribution system of a short line model as depicted in fig. 3.1. The general equations to be derived from the short line model are subsequently applied to single-phase and three-phase systems of any configuration. The mathematical procedure outlining the proposed method accompanied by the formulated general equations are presented in the three parts.

3.2 Development of the voltage drop equations

The probabilistic load flow analysis is based on the determination of the first and the second moments of the real and imaginary parts of the branch voltage drops due to statistical load currents. Therefore, the development of the branch voltage drop equations is the prerequisite in order to apply probabilistic approach on the evaluation of the voltage profile along the MV radial distribution system. In order to be able to derive the required equations, the load current phasors $\bar{I}_2, \bar{I}_3, \bar{I}_4, \bar{I}_5, \dots, \bar{I}_m$ are assumed to have phase angles $\alpha_2, \alpha_3, \alpha_4, \alpha_5, \dots, \alpha_m$ respectively. A deterministic power flow program to be dealt with in a later chapter calculates these current phase angles. According to fig.3.1, the total current in a particular branch is taken to be the current entering the corresponding load node. For example, the total current $\bar{I}_{2,3T}$ through the second branch will be the sum of the load currents entering node 3 given as:

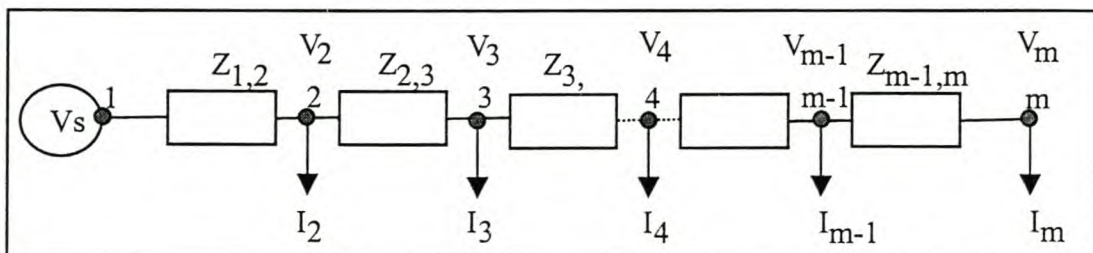


Fig. 3.1: A short line model of a MV radial power distribution system.

$$\bar{I}_{2,3T} = \bar{I}_3 + \bar{I}_4 + \bar{I}_5 + \dots + \bar{I}_{m-1} + \bar{I}_m \tag{3.1}$$

In general, the total current \bar{I}_{i-1,i_T} through any branch $i - 1, i$ can be deduced as:

$$\bar{I}_{i-1,i_T} = \sum_{k=i}^m \bar{I}_k \tag{3.2}$$

Consider branch 1, the total current through it, $\bar{I}_{1,2T}$, is given as:

$$\begin{aligned} \bar{I}_{1,2T} &= \bar{I}_2 + \bar{I}_3 + \bar{I}_4 + \dots + \bar{I}_{m-1} + \bar{I}_m \\ &= I_2 (\cos \alpha_2 + j \sin \alpha_2) + \dots + I_m (\cos \alpha_m + j \sin \alpha_m) \end{aligned} \tag{3.3}$$

The voltage drop $\Delta \bar{V}_{i-1,i}$ across the branch impedance $\bar{Z}_{i-1,i}$ will be:

$$\Delta \bar{V}_{i-1,i} = \bar{Z}_{i-1,i} \bar{I}_{i-1,i_T} \tag{3.4}$$

where

$$\bar{Z}_{i-1,i} = R_{i-1,i} + jX_{i-1,i}$$

3.2.1 Derivation of the real component of the branch voltage drops

In order to simplify the notation for the branch parameters, the following notations are adopted throughout the text:

$$\Delta \bar{V}_{i-1,i} \rightarrow \Delta \bar{V}_i$$

$$\bar{Z}_{i-1,i} \rightarrow \bar{Z}_i$$

$$R_{i-1,i} \rightarrow R_i, X_{i-1,i} \rightarrow X_i$$

$$X_{i-1,i} \rightarrow X_i$$

The general expression for the real component of the voltage drop ΔV_{ireal} across the impedance \bar{Z}_i is given as (Appendix 3-A):

$$\Delta V_{ireal} = \sum_{k=i}^m I_k (R_i \cos \alpha_k - X_i \sin \alpha_k) \tag{3.5}$$

Performing the squares of equation (3.5), it can be concluded that the general expression for the square of the real component of the voltage drop ΔV_{ireal}^2 across the impedance \bar{Z}_i can be expressed as (Appendix 3-B):

$$\begin{aligned} \Delta V^2_{ireal} = & \sum_{Z=i}^m I_Z^2 (R_i^2 \cos^2 \alpha_Z + X_i^2 \sin^2 \alpha_Z - 2R_i X_i \cos \alpha_Z \sin \alpha_Z) \\ & + 2 \sum_{k=i}^{m-1} \sum_{n=k+1}^m I_k I_n \{R_i^2 \cos \alpha_k \cos \alpha_n + X_i^2 \sin \alpha_k \sin \alpha_n - R_i X_i \sin(\alpha_k + \alpha_n)\} \end{aligned} \quad (3.6)$$

3.2.2 Derivation of the imaginary component of the branch voltage drops

The general expression for the imaginary component of the voltage drop ΔV_{iimag} across the impedance \bar{Z}_i is given as (Appendix 3-C):

$$\Delta V_{iimag} = \sum_{k=i}^m I_k (R_i \sin \alpha_k + X_i \cos \alpha_k) \quad (3.7)$$

Performing the squares of equation (3.7), it can be concluded that, the general expression for the square of the imaginary component of the voltage drop ΔV^2_{iimag} across the impedance \bar{Z}_i can be expressed as (Appendix 3-D):

$$\begin{aligned} \Delta V^2_{iimag} = & \sum_{Z=i}^m I_Z^2 (R_i^2 \sin^2 \alpha_Z + X_i^2 \cos^2 \alpha_Z + 2R_i X_i \cos \alpha_Z \sin \alpha_Z) \\ & + 2 \sum_{k=i}^{m-1} \sum_{n=k+1}^m I_k I_n \{R_i^2 \sin \alpha_k \sin \alpha_n + X_i^2 \cos \alpha_k \cos \alpha_n + R_i X_i \sin(\alpha_k + \alpha_n)\} \end{aligned} \quad (3.8)$$

3.2.3 Derivation of the square of the total real and the total imaginary component of the branch voltage drops

The consumer voltages are determined by taking the difference between the magnitude of the supply voltage V_s and the sum or the total of the branch voltage drops from the supply node to the node in question. Therefore, the total real and the total imaginary component of the branch voltage drops from the supply node with the respect to the other system nodes should be determined. By referring to equations (3.5) and (3.7), it can be stated that in general, at a node i , the total real ΔV_{ireal_total} and the total imaginary ΔV_{iimag_total} components of the branch voltage drops can be expressed as shown in equation (3.9) and (3.10) respectively.

$$\begin{aligned} \Delta V_{ireal_total} = & \sum_{y=2}^i \Delta V_{yreal} \\ = & \sum_{y=2}^i \sum_{k=y}^m I_k (R_y \cos \alpha_k - X_y \sin \alpha_k) \end{aligned} \quad (3.9)$$

$$\begin{aligned}\Delta V_{iimag_total} &= \sum_{y=2}^i \Delta V_{yimag} \\ &= \sum_{y=2}^i \sum_{k=y}^m I_k (R_y \sin \alpha_k + X_y \cos \alpha_k)\end{aligned}\quad (3.10)$$

In order to implement the probabilistic power flow to be dealt with in a later chapter, the equation (3.9) and (3.10) should be squared so that the equations for determining the first and the second moment of the consumer voltages can be obtained. The square of the total real $\Delta V_{ireal_total}^2$ and the total imaginary $\Delta V_{iimag_total}^2$ components of the branch voltage drops at node i can be expressed as (Appendix 3-E & Appendix 3-F):

$$\begin{aligned}\Delta V_{ireal_total}^2 &= \left(\sum_{y=2}^i \sum_{k=y}^m I_k (R_y \cos \alpha_k - X_y \sin \alpha_k) \right)^2 \\ &= \sum_{y=2}^i \sum_{Z=y}^m I_Z^2 (R_y^2 \cos^2 \alpha_Z + X_y^2 \sin^2 \alpha_Z - 2R_y X_y \cos \alpha_Z \sin \alpha_Z) \\ &\quad + 2 \sum_{y=2}^i \sum_{f=y+1}^i \sum_{g=f}^m I_g^2 \{ R_y R_f \cos^2 \alpha_g + X_y X_f \sin^2 \alpha_g - \cos \alpha_g \sin \alpha_g (R_y X_f - R_f X_y) \} \\ &\quad + 2 \sum_{y=2}^i \sum_{k=y}^{m-1} \sum_{n=k+1}^m I_k I_n \{ R_y^2 \cos \alpha_k \cos \alpha_n + X_y^2 \sin \alpha_k \sin \alpha_n - R_y X_y \sin(\alpha_k + \alpha_n) \} \\ &\quad + 2 \sum_{y=2}^i \sum_A^i \sum_B^{m-1} \sum_C^m I_r I_t (R_y R_p \cos \alpha_r \cos \alpha_t + X_y X_p \sin \alpha_r \sin \alpha_t \\ &\quad - R_y X_p \cos \alpha_r \sin \alpha_t - X_y R_p \sin \alpha_r \cos \alpha_t)\end{aligned}\quad (3.11)$$

$$\begin{aligned}\Delta V_{iimag_total}^2 &= \left(\sum_{y=2}^i \sum_{k=y}^m I_k (R_y \sin \alpha_k + X_y \cos \alpha_k) \right)^2 \\ &= \sum_{y=2}^i \sum_{Z=y}^m I_Z^2 (R_y^2 \sin^2 \alpha_Z + X_y^2 \cos^2 \alpha_Z + 2R_y X_y \cos \alpha_Z \sin \alpha_Z) \\ &\quad + 2 \sum_{y=2}^i \sum_{f=y+1}^i \sum_{g=f}^m I_g^2 (R_y R_f \sin^2 \alpha_g + X_y X_f \cos^2 \alpha_g + \cos \alpha_g \sin \alpha_g (R_y X_f + R_f X_y)) \\ &\quad + 2 \sum_{y=2}^i \sum_{k=y}^{m-1} \sum_{n=k+1}^m I_k I_n \{ R_y^2 \sin \alpha_k \sin \alpha_n + X_y^2 \cos \alpha_k \cos \alpha_n + R_y X_y \sin(\alpha_k + \alpha_n) \}\end{aligned}$$

$$\begin{aligned}
 &+ 2 \sum_{y=2}^i \sum_A^i \sum_B^m \sum_C^m I_r I_t (R_y R_p \sin \alpha_r \sin \alpha_t + X_y X_p \cos \alpha_r \cos \alpha_t \\
 &+ R_y X_p \sin \alpha_r \cos \alpha_t + X_y R_p \cos \alpha_r \sin \alpha_t)
 \end{aligned} \tag{3.12}$$

where A stands for $p = 2, p \neq y$
 B stands for $r = 2, r \geq y$
 C stands for $t = 2, t > r, t > y, t \geq p$

3.2.4 The product approach

The developed universal algorithm to be described later when dealing with single-phase and three-phase branched systems cannot easily adopt expression (3.11) and (3.12). Therefore, another method of determining the square of the total real and the square of the total imaginary component of the branch voltage drops, the so-called the product approach, is examined. Suppose we have an $m-1$ branched system as shown in fig. 3.2. The squares of the total real component of the branch voltage drops at the specified nodes are shown in equation (3.13).

$$\begin{aligned}
 \text{At node 2: } &(\Delta V_{2real})^2 \\
 \text{At node 3: } &(\Delta V_{2real} + \Delta V_{3real})^2 \\
 \text{At node } m: &(\Delta V_{2real} + \Delta V_{3real} + \dots + \Delta V_{m-1real} + \Delta V_{mreal})^2
 \end{aligned} \tag{3.13}$$

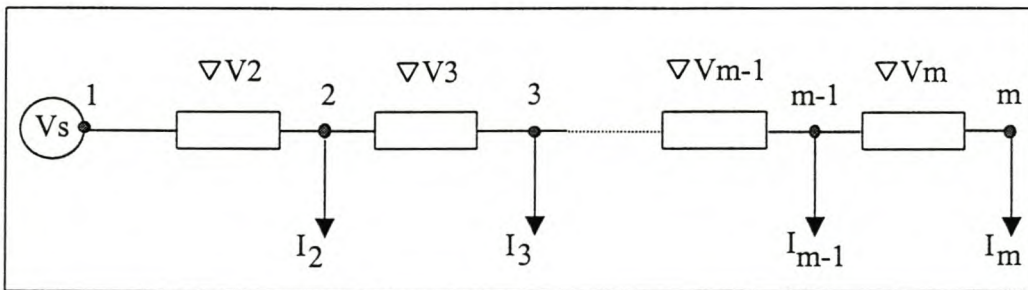


Fig. 3.2: The system for the product approach.

Expanding equation (3.13) at node m we shall have:

$$\begin{aligned}
 &(\Delta V_{2real})^2 + (\Delta V_{3real})^2 + \dots + (\Delta V_{mreal})^2 + 2\Delta V_{2real} \Delta V_{3real} \\
 &+ \dots + 2\Delta V_{2real} \Delta V_{mreal} + \dots + 2\Delta V_{m-1real} \Delta V_{mreal}
 \end{aligned} \tag{3.14}$$

For the case of the square of the total imaginary component of the branch voltage drop at node m , its expansion can be given as:

$$\begin{aligned}
 & (\Delta V_{2imag})^2 + (\Delta V_{3imag})^2 + \dots + (\Delta V_{mimag})^2 + 2\Delta V_{2imag} \Delta V_{3imag} \\
 & + \dots + 2\Delta V_{2imag} \Delta V_{mimag} + \dots + 2\Delta V_{m-1imag} \Delta V_{mimag}
 \end{aligned} \tag{3.15}$$

According to equations (3.6) and (3.8), the general expressions of the square of the real and the square of the imaginary components of the branch voltage drops across the branch of impedance \bar{Z}_i are presented. Their total value at node i is simply a summation up to node i . Therefore, the general expression for the total sum of the square of the real component of the branch voltage drops $\Delta V^2_{ireal_total-sum}$ up to node i can be expressed as:

$$\begin{aligned}
 \Delta V^2_{ireal_total-sum} &= \sum_{y=2}^i \left\{ \sum_{Z=y}^m I_Z^2 (R_y^2 \cos^2 \alpha_Z + X_y^2 \sin^2 \alpha_Z - 2R_y X_y \cos \alpha_Z \sin \alpha_Z) \right. \\
 &+ 2 \sum_{k=y}^{m-1} \sum_{n=k+1}^m I_k I_n \{ R_y^2 \cos \alpha_k \cos \alpha_n + X_y^2 \sin \alpha_k \sin \alpha_n - R_y X_y \sin(\alpha_k + \alpha_n) \}
 \end{aligned} \tag{3.16}$$

Also, the general expression for the total sum of the square of the imaginary component of the branch voltage drops $\Delta V^2_{iimag_total-sum}$ up to node i can be expressed as:

$$\begin{aligned}
 \Delta V^2_{iimag_total-sum} &= \sum_{y=2}^i \left\{ \sum_{Z=y}^m I_Z^2 (R_y^2 \sin^2 \alpha_Z + X_y^2 \cos^2 \alpha_Z + 2R_y X_y \cos \alpha_Z \sin \alpha_Z) \right. \\
 &+ 2 \sum_{k=y}^{m-1} \sum_{n=k+1}^m I_k I_n \{ R_y^2 \sin \alpha_k \sin \alpha_n + X_y^2 \cos \alpha_k \cos \alpha_n + R_y X_y \sin(\alpha_k + \alpha_n) \}
 \end{aligned} \tag{3.17}$$

The task now is to find a suitable general expression for the sum of the product of the components of the branch voltage drops as shown in equations (3.14) and (3.15).

As derived in Appendix 3-G, the sum of the product of the real component of the branch voltage drops, $\Delta^* \Delta V_{ireal-sum}$, at node i can be expressed as:

$$\begin{aligned}
 \Delta^* \Delta V_{ireal-sum} &= \sum_{t=2}^{i-1} \sum_{r=t+1}^i \sum_{k=t}^m \sum_{n=r}^m I_k I_n \{ R_t R_r \cos \alpha_k \cos \alpha_n + X_t X_r \sin \alpha_k \sin \alpha_n \\
 &\quad - R_t X_r \cos \alpha_k \sin \alpha_n - X_t R_r \sin \alpha_k \cos \alpha_n \}
 \end{aligned} \tag{3.18}$$

This can be written as:

$$\begin{aligned}
 \Delta^* \Delta V_{ireal-sum} &= \sum_{t=2}^{i-1} \sum_{r=t+1}^i \sum_{n=r}^m I_n^2 \{ R_t R_r \cos^2 \alpha_n + X_t X_r \sin^2 \alpha_n \\
 &\quad - R_t X_r \cos \alpha_n \sin \alpha_n - X_t R_r \sin \alpha_n \cos \alpha_n \}
 \end{aligned}$$

$$\begin{aligned}
 & + \sum_{t=2}^{i-1} \sum_{r=t+1}^i \sum_{k=t}^m \sum_{\substack{n=r \\ n \neq k}}^m I_k I_n \{R_t R_r \cos \alpha_k \cos \alpha_n + X_t X_r \sin \alpha_k \sin \alpha_n \\
 & - R_t X_r \cos \alpha_k \sin \alpha_n - X_t R_r \sin \alpha_k \cos \alpha_n\}
 \end{aligned} \tag{3.19}$$

Also, in Appendix 3-H, the sum of the product of the system imaginary component of the branch voltage drops $\Delta^* \Delta V_{iimag-sum}$ at node i , can be expressed as:

$$\begin{aligned}
 \Delta^* \Delta V_{iimag-sum} & = \sum_{t=2}^{i-1} \sum_{r=t+1}^i \sum_{k=t}^m \sum_{n=r}^m I_k I_n \{R_t R_r \sin \alpha_k \sin \alpha_n + X_t X_r \cos \alpha_k \cos \alpha_n \\
 & + R_t X_r \cos \alpha_n \sin \alpha_k + X_t R_r \sin \alpha_n \cos \alpha_t\}
 \end{aligned} \tag{3.20}$$

Equation (3.20) can be written as:

$$\begin{aligned}
 \Delta^* \Delta V_{iimag-sum} & = \sum_{t=2}^{i-1} \sum_{r=t+1}^i \sum_{n=r}^m I_n^2 \{R_t R_r \sin^2 \alpha_n + X_t X_r \cos^2 \alpha_n \\
 & + R_t X_r \cos \alpha_n \sin \alpha_n + X_t R_r \sin \alpha_n \cos \alpha_n\} \\
 & + \sum_{t=2}^{i-1} \sum_{r=t+1}^i \sum_{k=t}^m \sum_{\substack{n=r \\ n \neq k}}^m I_k I_n \{R_t R_r \sin \alpha_k \sin \alpha_n + X_t X_r \cos \alpha_k \cos \alpha_n \\
 & + R_t X_r \cos \alpha_n \sin \alpha_k + X_t R_r \sin \alpha_n \cos \alpha_t\}
 \end{aligned} \tag{3.21}$$

The format of equations (3.19) and (3.21) will be applied in the later chapter when the expected values of the square of the total real and the square of the total imaginary component of the branch voltage drops of single and three-phase systems are evaluated.

The square of the total real component of the branch voltage drop $\Delta V_{ireal_total_single}^2$ at node i , for single-phase systems with single loads is obtained by summing equations (3.16) and (3.18). The square of the total imaginary component of the voltage drop $\Delta V_{iimag_total_single}^2$ at node i , for single-phase systems with application of single loads is obtained by summing equation (3.17) and (3.20).

Thus, for applying the product approach:

$$\Delta V_{ireal_total_single}^2 = \sum_{y=2}^i \sum_{Z=y}^m I_Z^2 (R_y^2 \cos^2 \alpha_Z + X_y^2 \sin^2 \alpha_Z - 2R_y X_y \cos \alpha_Z \sin \alpha_Z)$$

$$\begin{aligned}
 &+ 2 \sum_{y=2}^i \sum_{k=y}^{m-1} \sum_{n=k+1}^m I_k I_n \{R_y^2 \cos \alpha_k \cos \alpha_n + X_y^2 \sin \alpha_k \sin \alpha_n - R_y X_y \sin(\alpha_k + \alpha_n)\} \\
 &+ \sum_{t=2}^{i-1} \sum_{r=t+1}^i \sum_{k=t}^m \sum_{n=r}^m I_k I_n \{R_t R_r \cos \alpha_k \cos \alpha_n + X_t X_r \sin \alpha_k \sin \alpha_n \\
 &- R_t X_r \cos \alpha_k \sin \alpha_n - X_t R_r \sin \alpha_k \cos \alpha_n\} \tag{3.22}
 \end{aligned}$$

$$\begin{aligned}
 \Delta V_{imag_total_sin\,gle}^2 &= \sum_{y=2}^i \sum_{Z=y}^m I_Z^2 (R_y^2 \sin^2 \alpha_Z + X_y^2 \cos^2 \alpha_Z + 2R_y X_y \cos \alpha_Z \sin \alpha_Z) \\
 &+ 2 \sum_{y=2}^i \sum_{k=y}^{m-1} \sum_{n=k+1}^m I_k I_n \{R_y^2 \sin \alpha_k \sin \alpha_n + X_y^2 \cos \alpha_k \cos \alpha_n + R_y X_y \sin(\alpha_k + \alpha_n)\} \\
 &+ \sum_{t=2}^{i-1} \sum_{r=t+1}^i \sum_{k=t}^m \sum_{n=r}^m I_k I_n \{R_t R_r \sin \alpha_k \sin \alpha_n + X_t X_r \cos \alpha_k \cos \alpha_n \\
 &+ R_t X_r \cos \alpha_n \sin \alpha_k + X_t R_r \sin \alpha_n \cos \alpha_k\} \tag{3.23}
 \end{aligned}$$

3.2.5 Dealing with a combined loading system

In the preceding sections, only one load is considered at each node. With a combined load, the general equations of the real and the imaginary component of the voltage drops to be derived in single-phase system will facilitate the development of the general equations in three-phase system through extrapolation. In this section the product approach, as illustrated in section 3.2.4, is used to determining the square term of total real and the total imaginary components of the branch voltage drops.

Consider the case where two loads are connected at each node as shown in fig. 3.3.

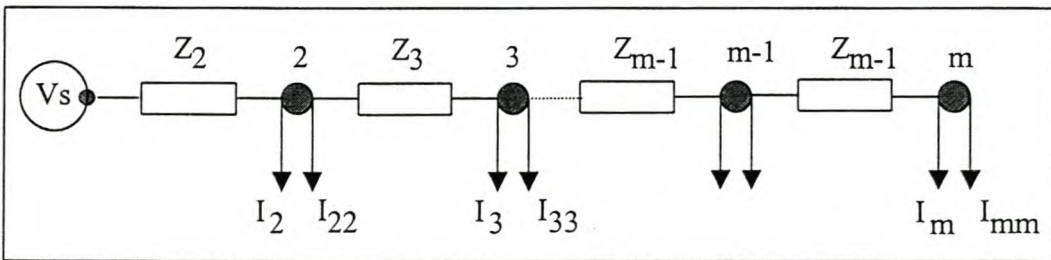


Fig. 3.3: A short line model of an MV radial distribution system connected to two loads at each node.

Consider that the branch voltage drops $\Delta \bar{V}_2, \Delta \bar{V}_3, \dots, \Delta \bar{V}_m$ across the impedances $\bar{Z}_2, \bar{Z}_3, \dots, \bar{Z}_m$ are due to load currents $\bar{I}_2, \bar{I}_3, \dots, \bar{I}_m$ having load phase angles $\alpha_2, \alpha_3, \dots, \alpha_m$ respectively.

Similarly, the branch voltage drops $\Delta\bar{V}_{22}, \Delta\bar{V}_{33}, \dots, \Delta\bar{V}_{mm}$ across the impedances $\bar{Z}_2, \bar{Z}_3, \dots, \bar{Z}_m$ are due to load currents $\bar{I}_{22}, \bar{I}_{33}, \dots, \bar{I}_{mm}$ having phase angles $\alpha_{22}, \alpha_{33}, \dots, \alpha_{mm}$ respectively.

Referring to equations (3.5) and (3.7), the general expressions of the total real $\Delta V_{ireal-total-rwo}$ and the total imaginary $\Delta V_{iimag-total-rwo}$ components of the branch voltage drops due to combined loading at node i as depicted in fig. 3.3, are:

$$\Delta V_{ireal-total-rwo} = \sum_{y=2}^i \left[\sum_{k=y}^m I_k (R_y \cos \alpha_k - X_y \sin \alpha_k) + \sum_{kk=y}^m I_{kk} (R_y \cos \alpha_{kk} - X_y \sin \alpha_{kk}) \right] \quad (3.24)$$

$$\Delta V_{iimag-total-rwo} = \sum_{y=2}^i \left[\sum_{k=y}^m I_k (R_y \sin \alpha_k + X_y \cos \alpha_k) + \sum_{kk=y}^m I_{kk} (R_y \sin \alpha_{kk} + X_y \cos \alpha_{kk}) \right] \quad (3.25)$$

Next, consider the square of the imaginary component of the voltage drop across the first branch as given in fig. 3.3, which in this case will be $(\Delta V_{2imag} + \Delta V_{22imag})^2$.

The imaginary component of the branch voltage drop will be:

$$\begin{aligned} \Delta V_{2imag} &= I_2 (R_2 \sin \alpha_2 + X_2 \cos \alpha_2) + I_3 (R_2 \sin \alpha_3 + X_2 \cos \alpha_3) \\ &+ I_4 (R_2 \sin \alpha_4 + X_2 \cos \alpha_4) + \dots + I_m (R_2 \sin \alpha_m + X_2 \cos \alpha_m) \end{aligned} \quad (3.26)$$

$$\begin{aligned} \Delta V_{22imag} &= I_{22} (R_2 \sin \alpha_{22} + X_2 \cos \alpha_{22}) + I_{33} (R_2 \sin \alpha_{33} + X_2 \cos \alpha_{33}) \\ &+ I_{44} (R_2 \sin \alpha_{44} + X_2 \cos \alpha_{44}) + \dots + I_{mm} (R_2 \sin \alpha_{mm} + X_2 \cos \alpha_{mm}) \end{aligned} \quad (3.27)$$

As derived in Appendix 3-I and Appendix 3-J, the sum of the squares of the total imaginary and total real components of the branch voltage drops at node i can be expressed as:

$$\begin{aligned} \Delta V_{iimag_total_sum}^2 &= \sum_{y=2}^i \sum_{Z=y}^m I_z^2 (R_y^2 \sin^2 \alpha_z + X_y^2 \cos^2 \alpha_z + 2R_y X_y \sin \alpha_z \cos \alpha_z) \\ &+ \sum_{y=2}^i \sum_{ZZ=y}^m I_{ZZ}^2 (R_y^2 \sin^2 \alpha_{ZZ} + X_y^2 \cos^2 \alpha_{ZZ} + 2R_y X_y \sin \alpha_{ZZ} \cos \alpha_{ZZ}) \\ &+ 2 \sum_{y=2}^i \sum_{k=y}^{m-1} \sum_{n=k+1}^m I_k I_n (R_y^2 \sin \alpha_k \sin \alpha_n + X_y^2 \cos \alpha_k \cos \alpha_n + R_y X_y \sin(\alpha_k + \alpha_n)) \\ &+ 2 \sum_{y=2}^i \sum_{kk=y}^{m-1} \sum_{nn=kk+1}^m I_{kk} I_{nn} (R_y^2 \sin \alpha_{kk} \sin \alpha_{nn} + X_y^2 \cos \alpha_{kk} \cos \alpha_{nn} + R_y X_y \sin(\alpha_{kk} + \alpha_{nn})) \end{aligned}$$

$$+ 2 \sum_{y=2}^i \sum_{k=y}^m \sum_{nn=y}^m I_k I_{nn} (R_y^2 \sin \alpha_k \sin \alpha_{nn} + X_y^2 \cos \alpha_k \cos \alpha_{nn} + R_y X_y \sin(\alpha_k + \alpha_{nn}))] \quad (3.28)$$

$$\begin{aligned} \Delta V_{ireal_total_sum}^2 &= \sum_{y=2}^i \sum_{Z=y}^m I^2 Z (R_y^2 \cos^2 \alpha_Z + X_y^2 \sin^2 \alpha_Z - 2R_y X_y \cos \alpha_Z \sin \alpha_Z) \\ &+ \sum_{y=2}^i \sum_{ZZ=y}^m I_{ZZ}^2 (R_y^2 \cos^2 \alpha_{ZZ} + X_y^2 \sin^2 \alpha_{ZZ} - 2R_y X_y \cos \alpha_{ZZ} \sin \alpha_{ZZ}) \\ &+ 2 \sum_{y=2}^i \sum_{k=y}^{m-1} \sum_{nn=k+1}^m I_k I_n \{R_y^2 \cos \alpha_k \cos \alpha_n + X_y^2 \sin \alpha_k \sin \alpha_n - R_y X_y \sin(\alpha_k + \alpha_n)\} \\ &+ 2 \sum_{y=2}^i \sum_{kk=y}^{m-1} \sum_{nn=kk+1}^m I_{kk} I_{nn} \{R_y^2 \cos \alpha_{kk} \cos \alpha_{nn} + X_y^2 \sin \alpha_{kk} \sin \alpha_{nn} - R_y X_y \sin(\alpha_{kk} + \alpha_{nn})\} \\ &+ 2 \sum_{y=2}^i \sum_{k=y}^m \sum_{nn=y}^m I_k I_{nn} \{R_y^2 \cos \alpha_k \cos \alpha_{nn} + X_y^2 \sin \alpha_k \sin \alpha_{nn} - R_y X_y \sin(\alpha_k + \alpha_{nn})\} \end{aligned} \quad (3.29)$$

3.2.5.1 The product term of the combined loading system

Referring to fig. 3.3, consider the product of first and the second branch voltage drops i.e. $(\Delta \bar{V}_2 + \Delta \bar{V}_{22}) * (\Delta \bar{V}_3 + \Delta \bar{V}_{33})$.

The real component of the branch voltage drops $(\Delta V_2 + \Delta V_{22})_{real}$ and $(\Delta V_3 + \Delta V_{33})_{real}$ can be given as:

$$\begin{aligned} (\Delta V_2 + \Delta V_{22})_{real} &= I_2 (R_2 \cos \alpha_2 - X_2 \sin \alpha_2) + \dots + I_m (R_2 \cos \alpha_m - X_2 \sin \alpha_m) \\ &+ I_{22} (R_2 \cos \alpha_{22} - X_2 \sin \alpha_{22}) + \dots + I_{mm} (R_2 \cos \alpha_{mm} - X_2 \sin \alpha_{mm}) \end{aligned} \quad (3.30)$$

$$\begin{aligned} (\Delta V_3 + \Delta V_{33})_{real} &= I_3 (R_3 \cos \alpha_3 - X_3 \sin \alpha_3) + \dots + I_m (R_3 \cos \alpha_m - X_3 \sin \alpha_m) \\ &+ I_{33} (R_3 \cos \alpha_{33} - X_3 \sin \alpha_{33}) + \dots + I_{mm} (R_3 \cos \alpha_{mm} - X_3 \sin \alpha_{mm}) \end{aligned} \quad (3.31)$$

In Appendix 3-K, it is shown that, the general expression of the real component of the sum product of the branch voltage drops $\Delta * \Delta V_{ireal_sum}$ at load node i due to a combined load is:

$$\begin{aligned} \Delta * \Delta V_{ireal_sum} &= \sum_{t=2}^{i-1} \sum_{r=t+1}^i \sum_{k=t}^m \sum_{n=r}^m I_k I_n \{R_t R_r \cos \alpha_k \cos \alpha_n + X_t X_r \sin \alpha_k \sin \alpha_n \\ &- R_t X_r \cos \alpha_k \sin \alpha_n - X_t R_r \sin \alpha_k \cos \alpha_n\} \end{aligned}$$

$$\begin{aligned}
 & + \sum_{t=2}^{i-1} \sum_{r=t+1}^i \sum_{kk=t}^m \sum_{nn=r}^m I_{kk} I_{nn} \{ R_t R_r \cos \alpha_{kk} \cos \alpha_{nn} + X_t X_r \sin \alpha_{kk} \sin \alpha_{nn} \\
 & - R_t X_r \cos \alpha_{kk} \sin \alpha_{nn} - X_t R_r \sin \alpha_{kk} \cos \alpha_{nn} \} \\
 & + \sum_{t=2}^{i-1} \sum_{r=t+1}^i \sum_{k=t}^m \sum_{nn=r}^m I_k I_{nn} \{ R_t R_r \cos \alpha_k \cos \alpha_{nn} + X_t X_r \sin \alpha_k \sin \alpha_{nn} \\
 & - R_t X_r \cos \alpha_k \sin \alpha_{nn} - X_t R_r \sin \alpha_k \cos \alpha_{nn} \} \\
 & + \sum_{t=2}^{i-1} \sum_{r=t+1}^i \sum_{kk=t}^m \sum_{n=r}^m I_{kk} I_n \{ R_t R_r \cos \alpha_{kk} \cos \alpha_n + X_t X_r \sin \alpha_{kk} \sin \alpha_n \\
 & - R_t X_r \cos \alpha_{kk} \sin \alpha_n - X_t R_r \sin \alpha_{kk} \cos \alpha_n \} \tag{3.32}
 \end{aligned}$$

In Appendix 3-L, it is shown that, the general expression of the imaginary component of the sum product of the branch voltage drops $\Delta^* \Delta V_{imag-sum}$ at load node i due to a combined load is:

$$\begin{aligned}
 \Delta^* \Delta V_{imag-sum} & = \sum_{t=2}^{i-1} \sum_{r=t+1}^i \sum_{k=t}^m \sum_{n=r}^m I_k I_n \{ R_t R_r \sin \alpha_k \sin \alpha_n + X_t X_r \cos \alpha_k \cos \alpha_n \\
 & + R_t X_r \cos \alpha_n \sin \alpha_k + X_t R_r \sin \alpha_n \cos \alpha_t \} \\
 & + \sum_{t=2}^{i-1} \sum_{r=t+1}^i \sum_{kk=t}^m \sum_{nn=r}^m I_{kk} I_{nn} \{ R_t R_r \sin \alpha_{kk} \sin \alpha_{nn} + X_t X_r \cos \alpha_{kk} \cos \alpha_{nn} \\
 & + R_t X_r \sin \alpha_{kk} \cos \alpha_{nn} + X_t R_r \cos \alpha_{kk} \sin \alpha_{nn} \} \\
 & + \sum_{t=2}^{i-1} \sum_{r=t+1}^i \sum_{k=t}^m \sum_{nn=r}^m I_k I_{nn} \{ R_t R_r \sin \alpha_k \sin \alpha_{nn} + X_t X_r \cos \alpha_k \cos \alpha_{nn} \\
 & + R_t X_r \sin \alpha_k \cos \alpha_{nn} + X_t R_r \cos \alpha_k \sin \alpha_{nn} \} \\
 & + \sum_{t=2}^{i-1} \sum_{r=t+1}^i \sum_{kk=t}^m \sum_{n=r}^m I_{kk} I_n \{ R_t R_r \sin \alpha_{kk} \sin \alpha_n + X_t X_r \cos \alpha_{kk} \cos \alpha_n \\
 & + R_t X_r \sin \alpha_{kk} \cos \alpha_n + X_t R_r \cos \alpha_{kk} \sin \alpha_n \} \tag{3.33}
 \end{aligned}$$

The square of the total real component of the branch voltage drop $\Delta V_{ireal_total_combined}^2$ at node i , for single-phase systems with two loads at each node is obtained by summing equations (3.29)

and (3.32). The square of the total imaginary component of the voltage drop, $\Delta V^2_{imag_total_combined}$, at node i for single-phase systems with two loads at each node is obtained by summing equations (3.28) and (3.33).

Thus, for the product approach:

$$\begin{aligned}
 \Delta V^2_{ireal_total_combined} &= \sum_{y=2}^i \sum_{Z=y}^m I^2_Z (R_y^2 \cos^2 \alpha_Z + X_y^2 \sin^2 \alpha_Z - 2R_y X_y \cos \alpha_Z \sin \alpha_Z) \\
 &+ \sum_{y=2}^i \sum_{ZZ=y}^m I^2_{ZZ} (R_y^2 \cos^2 \alpha_{ZZ} + X_y^2 \sin^2 \alpha_{ZZ} - 2R_y X_y \cos \alpha_{ZZ} \sin \alpha_{ZZ}) \\
 &+ 2 \sum_{y=2}^i \sum_{k=y}^{m-1} \sum_{n=k+1}^m I_k I_n \{R_y^2 \cos \alpha_k \cos \alpha_n + X_y^2 \sin \alpha_k \sin \alpha_n - R_y X_y \sin(\alpha_k + \alpha_n)\} \\
 &+ 2 \sum_{y=2}^i \sum_{kk=y}^{m-1} \sum_{nn=kk+1}^m I_{kk} I_{nn} \{R_y^2 \cos \alpha_{kk} \cos \alpha_{nn} + X_y^2 \sin \alpha_{kk} \sin \alpha_{nn} - R_y X_y \sin(\alpha_{kk} + \alpha_{nn})\} \\
 &+ 2 \sum_{y=2}^i \sum_{k=y}^m \sum_{nn=y}^m I_k I_{nn} \{R_y^2 \cos \alpha_k \cos \alpha_{nn} + X_y^2 \sin \alpha_k \sin \alpha_{nn} - R_y X_y \sin(\alpha_k + \alpha_{nn})\} \\
 &+ \sum_{t=2}^{i-1} \sum_{r=t+1}^i \sum_{k=t}^m \sum_{n=r}^m I_k I_n \{R_t R_r \cos \alpha_k \cos \alpha_n + X_t X_r \sin \alpha_k \sin \alpha_n \\
 &- R_t X_r \cos \alpha_k \sin \alpha_n - X_t R_r \sin \alpha_k \cos \alpha_n\} \\
 &+ \sum_{t=2}^{i-1} \sum_{r=t+1}^i \sum_{kk=t}^m \sum_{nn=r}^m I_{kk} I_{nn} \{R_t R_r \cos \alpha_{kk} \cos \alpha_{nn} + X_t X_r \sin \alpha_{kk} \sin \alpha_{nn} \\
 &- R_t X_r \cos \alpha_{kk} \sin \alpha_{nn} - X_t R_r \sin \alpha_{kk} \cos \alpha_{nn}\} \\
 &+ \sum_{t=2}^{i-1} \sum_{r=t+1}^i \sum_{k=t}^m \sum_{nn=r}^m I_k I_{nn} \{R_t R_r \cos \alpha_k \cos \alpha_{nn} + X_t X_r \sin \alpha_k \sin \alpha_{nn} \\
 &- R_t X_r \cos \alpha_k \sin \alpha_{nn} - X_t R_r \sin \alpha_k \cos \alpha_{nn}\} \\
 &+ \sum_{t=2}^{i-1} \sum_{r=t+1}^i \sum_{kk=t}^m \sum_{n=r}^m I_{kk} I_n \{R_t R_r \cos \alpha_{kk} \cos \alpha_n + X_t X_r \sin \alpha_{kk} \sin \alpha_n \\
 &- R_t X_r \cos \alpha_{kk} \sin \alpha_n - X_t R_r \sin \alpha_{kk} \cos \alpha_n\}
 \end{aligned} \tag{3.34}$$

$$\begin{aligned}
 \Delta V^2_{iimag_total_combined} &= \sum_{y=2}^i \sum_{Z=y}^m I^2_Z (R_y^2 \sin^2 \alpha_Z + X_y^2 \cos^2 \alpha_Z + 2R_y X_y \sin \alpha_Z \cos \alpha_Z) \\
 &+ \sum_{y=2}^i \sum_{ZZ=y}^m I_{ZZ}^2 (R_y^2 \sin^2 \alpha_{ZZ} + X_y^2 \cos^2 \alpha_{ZZ} + 2R_y X_y \sin \alpha_{ZZ} \cos \alpha_{ZZ}) \\
 &+ 2 \sum_{y=2}^i \sum_{k=y}^{m-1} \sum_{n=k+1}^m I_k I_n (R_y^2 \sin \alpha_k \sin \alpha_n + X_y^2 \cos \alpha_k \cos \alpha_n + R_y X_y \sin(\alpha_k + \alpha_n)) \\
 &+ 2 \sum_{y=2}^i \sum_{kk=y}^{m-1} \sum_{nn=kk+1}^m I_{kk} I_{nn} (R_y^2 \sin \alpha_{kk} \sin \alpha_{nn} + X_y^2 \cos \alpha_{kk} \cos \alpha_{nn} + R_y X_y \sin(\alpha_{kk} + \alpha_{nn})) \\
 &+ 2 \sum_{y=2}^i \sum_{k=y}^m \sum_{nn=y}^m I_k I_{nn} (R_y^2 \sin \alpha_k \sin \alpha_{nn} + X_y^2 \cos \alpha_k \cos \alpha_{nn} + R_y X_y \sin(\alpha_k + \alpha_{nn})) \\
 &+ \sum_{t=2}^{i-1} \sum_{r=t+1}^i \sum_{k=t}^m \sum_{n=r}^m I_k I_n \{R_t R_r \sin \alpha_k \sin \alpha_n + X_t X_r \cos \alpha_k \cos \alpha_n \\
 &+ R_t X_r \cos \alpha_n \sin \alpha_k + X_t R_r \sin \alpha_n \cos \alpha_t\} \\
 &+ \sum_{t=2}^{i-1} \sum_{r=t+1}^i \sum_{kk=t}^m \sum_{nn=r}^m I_{kk} I_{nn} \{R_t R_r \sin \alpha_{kk} \sin \alpha_{nn} + X_t X_r \cos \alpha_{kk} \cos \alpha_{nn} \\
 &+ R_t X_r \sin \alpha_{kk} \cos \alpha_{nn} + X_t R_r \cos_{kk} \sin \alpha_{nn}\} \\
 &+ \sum_{t=2}^{i-1} \sum_{r=t+1}^i \sum_{k=t}^m \sum_{nn=r}^m I_k I_{nn} \{R_t R_r \sin \alpha_k \sin \alpha_{nn} + X_t X_r \cos \alpha_k \cos \alpha_{nn} \\
 &+ R_t X_r \sin \alpha_k \cos \alpha_{nn} + X_t R_r \cos_k \sin \alpha_{nn}\} \\
 &+ \sum_{t=2}^{i-1} \sum_{r=t+1}^i \sum_{kk=t}^m \sum_{n=r}^m I_{kk} I_n \{R_t R_r \sin \alpha_{kk} \sin \alpha_n + X_t X_r \cos \alpha_{kk} \cos \alpha_n \\
 &+ R_t X_r \sin \alpha_{kk} \cos \alpha_n + X_t R_r \cos_{kk} \sin \alpha_n\}
 \end{aligned} \tag{3.35}$$

3.3 Summary

In this chapter, the general expressions for the square total of the real and imaginary components of the branch voltage drops at any node of the single-phase system with single and combined loads are derived. It is apparent that, if the branch voltage drop is related to two load currents at each node, the square of the total real and the total imaginary components of the branch voltage

drops become a bit cumbersome. But on MV three-phase three-wire distribution systems ($\Delta - \Delta$) connection, three different currents are involved in the determination of the system branch voltage drops. This will be developed in the next chapter. The developed general expressions for combined loading in this chapter will enable the general expression for the total real and the total imaginary component of the branch voltage drops at any node for the three-phase system to be developed through extrapolation.

CHAPTER 4

DERIVATION OF THE SYSTEM RELATED EQUATIONS

PART 2: Development of the system branch voltage drop equations in three-phase power distribution systems

4.1 Introduction

In chapter 3, the general expressions of the total real and total imaginary components of the branch voltage drops based on a one-line diagram are presented. In order to apply these general expressions to a three-phase three-wire system ($\Delta - \Delta$) connection, the individual three phases should have phase voltages equal to line-to-line system voltage. The general expression of the component of the system branch voltage drops will be developed through extrapolation as cited in chapter 3 section 3.3. To develop the system voltage-related equations, it will be appropriate to consider only one load point with individual phase loads in delta connection.

4.1.1 Formulation of the basic voltage-related equations

Three single-phase loads are connected between phases of a three-phase system as shown in fig. 4.1.

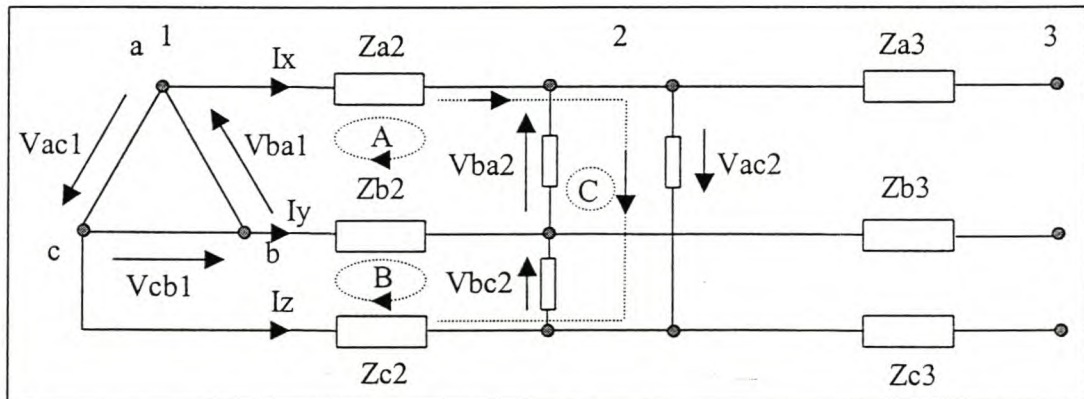


Fig. 4.1: Transformed three single-phase loads connected at node 2.

At node 1 in fig. 4.1, the three phases are identified as phase ba , cb and ac with designated phase voltage \vec{V}_{ba1} , \vec{V}_{cb1} and \vec{V}_{ac1} respectively. The phase voltage notation as applies to the principle of voltage phasors convention, manifest the following:

- point a is at higher potential than point b
- point b is at higher potential than point c
- point c is at higher potential than point a
- the direction of the system line to line voltages is from the lower potential to higher potential
- the direction of the phase currents are from the higher potential to lower potential

Therefore, according to the above, the phase currents are designated as \bar{I}_{ab} , \bar{I}_{bc} and \bar{I}_{ca} for phase ba , cb and ac respectively. By treating the supply phase voltage \bar{V}_{ba1} to be the reference phasor, it follows that:

$$\begin{aligned}\bar{V}_{ba1} &= V_{ba1} \angle 0^\circ \\ \bar{V}_{cb1} &= V_{cb1} \angle 240^\circ \\ \bar{V}_{ac1} &= V_{ac1} \angle 120^\circ\end{aligned}\tag{4.1}$$

The voltage related equations are developed by considering the three loops A , B and C . Assume that currents \bar{I}_x , \bar{I}_y and \bar{I}_z are flowing in the line conductors as shown in fig. 4.1. By applying Kirchoff's voltage law around loop A ,

$$-\bar{V}_{ba1} + \bar{I}_x \cdot \bar{Z}_{a2} + \bar{V}_{ba2} - \bar{I}_y \cdot \bar{Z}_{b2} = 0\tag{4.2}$$

$$\bar{V}_{ba2} = \bar{V}_{ba1} - \bar{I}_x \cdot \bar{Z}_{a2} + \bar{I}_y \cdot \bar{Z}_{b2}$$

$$\text{But } \bar{I}_x = \bar{I}_{ab2} - \bar{I}_{ca2} \text{ and } \bar{I}_y = \bar{I}_{bc2} - \bar{I}_{ab2}\tag{4.3}$$

Therefore,

$$\begin{aligned}\bar{V}_{ba2} &= \bar{V}_{ba1} + \bar{Z}_{b2}(\bar{I}_{bc2} - \bar{I}_{ab2}) - \bar{Z}_{a2}(\bar{I}_{ab2} - \bar{I}_{ca2}) \\ &= \bar{V}_{ba1} - \bar{I}_{ab2}(\bar{Z}_{a2} + \bar{Z}_{b2}) + \bar{I}_{bc2} \cdot \bar{Z}_{b2} + \bar{I}_{ca2} \cdot \bar{Z}_{a2}\end{aligned}\tag{4.4}$$

By applying Kirchoff's voltage law around loop B ,

$$-\bar{V}_{cb1} + \bar{I}_y \cdot \bar{Z}_{b2} + \bar{V}_{bc2} - \bar{I}_z \cdot \bar{Z}_{c2} = 0$$

$$\bar{V}_{bc2} = \bar{V}_{cb1} + \bar{I}_y \cdot \bar{Z}_{b2} - \bar{I}_z \cdot \bar{Z}_{c2}\tag{4.5}$$

$$\text{But } \bar{I}_z = \bar{I}_{ca2} - \bar{I}_{bc2}\tag{4.6}$$

Therefore,

$$\begin{aligned}\bar{V}_{bc2} &= \bar{V}_{cb1} + \bar{Z}_{b2}(\bar{I}_{bc2} - \bar{I}_{ab2}) - \bar{Z}_{c2}(\bar{I}_{ca2} - \bar{I}_{bc2}) \\ &= \bar{V}_{cb1} + \bar{I}_{ab2} \cdot \bar{Z}_{b2} - \bar{I}_{bc2}(\bar{Z}_{b2} + \bar{Z}_{c2}) + \bar{I}_{ca2} \cdot \bar{Z}_{c2}\end{aligned}\tag{4.7}$$

By applying Kirchoff's voltage law around loop C ,

$$-\bar{V}_{ac1} + \bar{I}_z \cdot \bar{Z}_{c2} + \bar{V}_{ac2} - \bar{I}_x \cdot \bar{Z}_{a2} = 0 \quad (4.8)$$

$$\bar{V}_{ac2} = \bar{V}_{ac1} - \bar{I}_z \cdot \bar{Z}_{c2} + \bar{I}_x \cdot \bar{Z}_{a2} \quad (4.9)$$

Therefore,

$$\begin{aligned} \bar{V}_{ac2} &= \bar{V}_{ac1} - \bar{Z}_{c2}(\bar{I}_{ca2} - \bar{I}_{bc2}) - \bar{Z}_{a2}(\bar{I}_{ab2} - \bar{I}_{ca2}) \\ &= \bar{V}_{ac1} + \bar{I}_{ab2} \cdot \bar{Z}_{a2} + \bar{I}_{bc2} \cdot \bar{Z}_{c2} - \bar{I}_{ca2}(\bar{Z}_{a2} + \bar{Z}_{c2}) \end{aligned} \quad (4.10)$$

Referring to equation (4.4), (4.7) and (4.10), the branch voltage drops $\Delta\bar{V}_{ba2}$, $\Delta\bar{V}_{cb2}$ and $\Delta\bar{V}_{ac2}$ for phase ba , cb and ac respectively, can be expressed as:

$$\Delta\bar{V}_{ba2} = \bar{I}_{ab2}(\bar{Z}_{a2} + \bar{Z}_{b2}) - \bar{I}_{bc2} \cdot \bar{Z}_{b2} - \bar{I}_{ca2} \cdot \bar{Z}_{a2} \quad (4.11)$$

$$\Delta\bar{V}_{cb2} = \bar{I}_{bc2}(\bar{Z}_{b2} + \bar{Z}_{c2}) - \bar{I}_{ab2} \cdot \bar{Z}_{b2} - \bar{I}_{ca2} \cdot \bar{Z}_{c2} \quad (4.12)$$

$$\Delta\bar{V}_{ac2} = \bar{I}_{ca2}(\bar{Z}_{a2} + \bar{Z}_{c2}) - \bar{I}_{ab2} \cdot \bar{Z}_{a2} - \bar{I}_{bc2} \cdot \bar{Z}_{c2} \quad (4.13)$$

It also implies that, if the phase current through node m are \bar{I}_{abm} , \bar{I}_{bcm} and \bar{I}_{cam} , the voltage phase voltage \bar{V}_{bam} , \bar{V}_{cbm} and \bar{V}_{acm} at node m can be expressed in a matrix form as:

$$\begin{bmatrix} \bar{V}_{bam} \\ \bar{V}_{cbm} \\ \bar{V}_{acm} \end{bmatrix} = \begin{bmatrix} \bar{V}_{bam-1} \\ \bar{V}_{cbm-1} \\ \bar{V}_{acm-1} \end{bmatrix} - \begin{bmatrix} \bar{Z}_{am} + \bar{Z}_{bm} & \dots & -\bar{Z}_{bm} & \dots & -\bar{Z}_{am} \\ -\bar{Z}_{bm} & \dots & \bar{Z}_{bm} + \bar{Z}_{cm} & \dots & -\bar{Z}_{cm} \\ -\bar{Z}_{am} & \dots & -\bar{Z}_{cm} & \dots & \bar{Z}_{am} + \bar{Z}_{cm} \end{bmatrix} \begin{bmatrix} \bar{I}_{abm} \\ \bar{I}_{bcm} \\ \bar{I}_{cam} \end{bmatrix} \quad (4.14)$$

4.2 Development of the branch voltage drops in three-phase distribution systems

The branch voltage drops of a three-phase system are developed by virtue of extrapolation of the equations derived for combined load in a single-phase system. For the three-phase system, the branch voltage drop equations are presented in equation (4.11), (4.12) and (4.13). In the following section (4.2.1) and (4.2.2), the real and imaginary component of the branch voltage drop of a three-phase distribution system is presented. As mentioned above, the resulting equations are obtained through the extrapolation of the equations developed previously for single-phase systems.

The three-phase radial distribution system adopted for the development of the branch voltage drop is depicted in fig. 4.1. The load current phasors for phase ba are designated as $\bar{I}_{ab2}, \bar{I}_{ab3}, \bar{I}_{ab4}, \bar{I}_{ab5}, \dots, \bar{I}_{abm}$ with phase angles $\alpha_{ab2}, \alpha_{ab3}, \alpha_{ab4}, \alpha_{ab5}, \dots, \alpha_{abm}$ respectively. The load current phasors for phase cb are designated as $\bar{I}_{bc2}, \bar{I}_{bc3}, \bar{I}_{bc4}, \bar{I}_{bc5}, \dots, \bar{I}_{bcm}$ with phase angles $\alpha_{bc2}, \alpha_{bc3}, \alpha_{bc4}, \alpha_{bc5}, \dots, \alpha_{bcm}$

respectively. The load current phasors for phase ac are designated as $\bar{I}_{ca2}, \bar{I}_{ca3}, \bar{I}_{ca4}, \bar{I}_{ca5}, \dots, \bar{I}_{cam}$ with phase angles $\alpha_{ca2}, \alpha_{ca3}, \alpha_{ca4}, \alpha_{ca5}, \dots, \alpha_{cam}$ respectively. The deterministic load flow computer program described in chapter 7 is applied to determine the phase angles of the load currents.

4.2.1 Derivation of the real component of the branch voltage drops in three-phase distribution systems

In this section, the development of the real component of branch voltage drops for the phase ba , cb and ac is considered. By referring to equation (3.24) and equation (4.11), (4.12), (4.13), the general expression of the real component of the branch voltage drops for the individual phases can be derived. Therefore, the general expression of the real component of the branch voltage drops for phase ba , $\Delta V_{ba-ireal}$ across the impedance between node $i-1$ and i can be given as:

$$\Delta V_{ba-ireal} = \sum_{k=i}^m [I_{abk} \{ (R_{ak} + R_{bk}) \cdot \cos \alpha_{abk} - (X_{ak} + X_{bk}) \cdot \sin \alpha_{abk} \} - I_{bck} (R_{bk} \cdot \cos \alpha_{bck} - X_{bk} \cdot \sin \alpha_{bck}) - I_{cak} (R_{ak} \cdot \cos \alpha_{cak} - X_{ak} \cdot \sin \alpha_{cak})] \quad (4.15)$$

As pointed previously in chapter 3, the total real component of the branch voltage drop at any node of the system is of interest. Therefore, the total real component of the branch voltage drop $\Delta V_{ba-ireal-total}$ at any node i , can be expressed as:

$$\Delta V_{ba-ireal-total} = \sum_{y=2}^i \Delta V_{ba-yreal} = \sum_{y=2}^i [\sum_{k=y}^m [I_{abk} \{ (R_{ak} + R_{bk}) \cdot \cos \alpha_{abk} - (X_{ak} + X_{bk}) \cdot \sin \alpha_{abk} \} - I_{bck} (R_{bk} \cdot \cos \alpha_{bck} - X_{bk} \cdot \sin \alpha_{bck}) - I_{cak} (R_{ak} \cdot \cos \alpha_{cak} - X_{ak} \cdot \sin \alpha_{cak})]] \quad (4.16)$$

The general expression of the real component of the branch voltage drops for phase cb , $\Delta V_{cb-ireal}$ across the impedance between nodes $i-1$ and i can be given as:

$$\Delta V_{cb-ireal} = \sum_{k=i}^m [I_{bck} \{ (R_{bk} + R_{ck}) \cdot \cos \alpha_{bck} - (X_{bk} + X_{ck}) \cdot \sin \alpha_{bck} \} - I_{abk} (R_{bk} \cdot \cos \alpha_{abk} - X_{bk} \cdot \sin \alpha_{abk}) - I_{cak} (R_{ck} \cdot \cos \alpha_{cak} - X_{ck} \cdot \sin \alpha_{cak})] \quad (4.17)$$

In the case of phase cb , the total real component of the branch voltage drops $\Delta V_{cb-ireal-total}$ at any node i , can be expressed as:

$$\begin{aligned}
 \Delta V_{cb-ireal-total} &= \sum_{y=2}^i \Delta V_{cb-yreal} \\
 &= \sum_{y=2}^i \left[\sum_{k=y}^m [I_{bck} \{ (R_{bk} + R_{ck}) \cdot \cos \alpha_{bck} - (X_{bk} + X_{ck}) \cdot \sin \alpha_{bck} \} \right. \\
 &\quad \left. - I_{abk} (R_{bk} \cdot \cos \alpha_{abk} - X_{bk} \cdot \sin \alpha_{abk}) - I_{cak} (R_{ck} \cdot \cos \alpha_{cak} - X_{ck} \cdot \sin \alpha_{cak}) \right] \quad (4.18)
 \end{aligned}$$

The general expression for the real component of the voltage drops for phase ac , $\Delta V_{ac-ireal}$ across the impedance between nodes $i-1$ and i can be given as:

$$\begin{aligned}
 \Delta V_{ac-ireal} &= \sum_{k=i}^m [I_{cak} \{ (R_{ak} + R_{ck}) \cdot \cos \alpha_{cak} - (X_{ak} + X_{ck}) \cdot \sin \alpha_{cak} \} \\
 &\quad - I_{abk} (R_{ak} \cdot \cos \alpha_{abk} - X_{ak} \cdot \sin \alpha_{abk}) - I_{bck} (R_{ck} \cdot \cos \alpha_{bck} - X_{ck} \cdot \sin \alpha_{bck})] \quad (4.19)
 \end{aligned}$$

Therefore, the total real component of the branch voltage drops $\Delta V_{ac-ireal-total}$ at any node i , for phase ac can be expressed as:

$$\begin{aligned}
 \Delta V_{ac-ireal-total} &= \sum_{y=2}^i \Delta V_{ac-yreal} \\
 &= \sum_{y=2}^i \left[\sum_{k=y}^m [I_{cak} \{ (R_{ak} + R_{ck}) \cdot \cos \alpha_{cak} - (X_{ak} + X_{ck}) \cdot \sin \alpha_{cak} \} \right. \\
 &\quad \left. - I_{abk} (R_{ak} \cdot \cos \alpha_{abk} - X_{ak} \cdot \sin \alpha_{abk}) - I_{bck} (R_{ck} \cdot \cos \alpha_{bck} - X_{ck} \cdot \sin \alpha_{bck}) \right] \quad (4.20)
 \end{aligned}$$

4.2.2 Derivation of the imaginary component of the branch voltage drops in three-phase distribution systems

In this section, the development of the imaginary component of branch voltage drops for the phase ba , cb and ac is considered. By referring to equation (3.25) and (4.11), (4.12), (4.13), the general expression of the real component of the branch voltage drops for phase ba , $\Delta V_{ba-iimag}$ across the impedance between node $i-1$ and i can be given as:

$$\begin{aligned}
 \Delta V_{ba-iimag} &= \sum_{k=i}^m [I_{abk} \{ (R_{ak} + R_{bk}) \cdot \sin \alpha_{abk} + (X_{ak} + X_{bk}) \cdot \cos \alpha_{abk} \} \\
 &\quad - I_{bck} (R_{bk} \cdot \sin \alpha_{bck} + X_{bk} \cdot \cos \alpha_{bck}) - I_{cak} (R_{ak} \cdot \sin \alpha_{cak} + X_{ak} \cdot \cos \alpha_{cak})] \quad (4.21)
 \end{aligned}$$

As pointed previously in chapter 3, the total imaginary component of the branch voltage drop at any node of the system is of interest. Therefore, the total imaginary component of the branch voltage drop $\Delta V_{ba-iimag-total}$ at any node i , can be expressed as:

$$\begin{aligned}\Delta V_{ba-iimag-total} &= \sum_{y=2}^i \Delta V_{ba-yimag} \\ &= \sum_{y=2}^i \left[\sum_{k=y}^m [I_{abk} \{ (R_{ak} + R_{bk}) \cdot \sin \alpha_{abk} + (X_{ak} + X_{bk}) \cdot \cos \alpha_{abk} \} \right. \\ &\quad \left. - I_{bck} (R_{bk} \cdot \sin \alpha_{bck} + X_{bk} \cdot \cos \alpha_{bck}) - I_{cak} (R_{ak} \cdot \sin \alpha_{cak} + X_{ak} \cdot \cos \alpha_{cak}) \right]\end{aligned}\quad (4.22)$$

The general expression of the imaginary component of the branch voltage drops for phase cb , $\Delta V_{cb-iimag}$ across the impedance between nodes $i-1$ and i can be given as:

$$\begin{aligned}\Delta V_{cb-iimag} &= \sum_{k=i}^m [I_{bck} \{ (R_{bk} + R_{ck}) \cdot \sin \alpha_{bck} + (X_{bk} + X_{ck}) \cdot \cos \alpha_{bck} \} \\ &\quad - I_{abk} (R_{bk} \cdot \sin \alpha_{abk} + X_{bk} \cdot \cos \alpha_{abk}) - I_{cak} (R_{ck} \cdot \sin \alpha_{cak} + X_{ck} \cdot \cos \alpha_{cak})]\end{aligned}\quad (4.23)$$

In the case of phase cb , the total imaginary component of the branch voltage drops $\Delta V_{cb-iimag-total}$ at any node i , can be expressed as:

$$\begin{aligned}\Delta V_{cb-iimag-total} &= \sum_{y=2}^i \Delta V_{cb-yimag} \\ &= \sum_{y=2}^i \left[\sum_{k=y}^m [I_{bck} \{ (R_{bk} + R_{ck}) \cdot \sin \alpha_{bck} + (X_{bk} + X_{ck}) \cdot \cos \alpha_{bck} \} \right. \\ &\quad \left. - I_{abk} (R_{bk} \cdot \sin \alpha_{abk} + X_{bk} \cdot \cos \alpha_{abk}) - I_{cak} (R_{ck} \cdot \sin \alpha_{cak} + X_{ck} \cdot \cos \alpha_{cak}) \right]\end{aligned}\quad (4.24)$$

The general expression for the imaginary component of the voltage drops for phase ac , $\Delta V_{ac-iimag}$ across the impedance between nodes $i-1$ and i can be given as:

$$\begin{aligned}\Delta V_{ac-iimag} &= \sum_{k=i}^m [I_{cak} \{ (R_{ak} + R_{ck}) \cdot \sin \alpha_{cak} + (X_{ak} + X_{ck}) \cdot \cos \alpha_{cak} \} \\ &\quad - I_{abk} (R_{ak} \cdot \sin \alpha_{abk} + X_{ak} \cdot \cos \alpha_{abk}) - I_{bck} (R_{ck} \cdot \sin \alpha_{bck} + X_{ck} \cdot \cos \alpha_{bck})]\end{aligned}\quad (4.25)$$

Therefore, the total imaginary component of the branch voltage drops $\Delta V_{ac-iimag-total}$ at any node i for phase ac , can be expressed as:

$$\begin{aligned}
 \Delta V_{ac-iimag-total} &= \sum_{y=2}^i \Delta V_{ac-yimag} \\
 &= \sum_{y=2}^i \left[\sum_{k=y}^m [I_{cak} \{ (R_{ak} + R_{ck}) \cdot \sin \alpha_{cak} + (X_{ak} + X_{ck}) \cdot \cos \alpha_{cak} \} \right. \\
 &\quad \left. - I_{abk} (R_{ak} \cdot \sin \alpha_{abk} + X_{ak} \cdot \cos \alpha_{abk}) - I_{bck} (R_{ck} \cdot \sin \alpha_{bck} + X_{ck} \cdot \cos \alpha_{bck}) \right] \quad (4.26)
 \end{aligned}$$

4.2.3 Derivation of the sum of squares of the real component of the branch voltage drop in three-phase distribution systems

It is evident that, the procedure will become very cumbersome, when attempting to derive the general expression for the sum of squares of the total real component of the branch voltage drops for the three individual phases.

In this respect, an extrapolation technique is applied to the result obtained when dealing with combined loading as presented in equation (3.29). By examining equation (3.24) and (3.29) as related to figure 3.3, and equation (4.16), (4.18) and (4.20) as related to figure 4.1, extrapolation procedure is possible. The logic adopted is as follows: If $(a+b)^2 = a^2 + b^2 + ab + ba$, then $(a+b+c)^2$ can be deduced from observing the pattern of $(a+b)^2$. After extrapolation, the required general expressions are as follows:

For the phase ba , the sum of squares of the total real component of the branch voltage drops $\Delta V^2_{ba_ireal-total-sum}$ at node i , can be given as:

$$\begin{aligned}
 \Delta V^2_{ba_ireal-total-sum} &= \sum_{y=2}^i \sum_{Z=y}^m [I^2_{abZ} \{ (R_{ay} + R_{by})^2 \cdot \cos^2 \alpha_{abZ} + (X_{ay} + X_{by})^2 \cdot \sin^2 \alpha_{abZ} \\
 &\quad - 2 \cdot (R_{ay} + R_{by}) \cdot (X_{ay} + X_{by}) \cdot \cos \alpha_{abZ} \cdot \sin \alpha_{abZ} \} \\
 &\quad + I^2_{bcZ} (R_{by}^2 \cdot \cos^2 \alpha_{bcZ} + X_{by}^2 \cdot \sin^2 \alpha_{bcZ} - 2 \cdot R_{by} \cdot X_{by} \cdot \cos \alpha_{bcZ} \cdot \sin \alpha_{bcZ}) \\
 &\quad + I^2_{caZ} (R_{ay}^2 \cdot \cos^2 \alpha_{caZ} + X_{ay}^2 \cdot \sin^2 \alpha_{caZ} - 2 \cdot R_{ay} \cdot X_{ay} \cdot \cos \alpha_{caZ} \cdot \sin \alpha_{caZ})] \\
 &\quad + 2 \sum_{y=2}^i \sum_{k=y}^{m-1} \sum_{n=k+1}^m [I_{abk} I_{abn} \{ (R_{ay} + R_{by})^2 \cdot \cos \alpha_{abk} \cos \alpha_{abn} + (X_{ay} + X_{by})^2 \sin \alpha_{abk} \sin \alpha_{abn} \\
 &\quad - (R_{ay} + R_{by}) \cdot (X_{ay} + X_{by}) \cdot \sin(\alpha_{abk} + \alpha_{abn}) \} \\
 &\quad + I_{bck} I_{bcn} \{ R_{by}^2 \cos \alpha_{bck} \cos \alpha_{bcn} + X_{by}^2 \sin \alpha_{bck} \sin \alpha_{bcn} - R_{by} \cdot X_{by} \cdot \sin(\alpha_{bck} + \alpha_{bcn}) \}
 \end{aligned}$$

$$\begin{aligned}
 &+ I_{cak} I_{can} \{ R_{ay}^2 \cos \alpha_{cak} \cos \alpha_{can} + X_{ay}^2 \sin \alpha_{cak} \sin \alpha_{can} - R_{ay} \cdot X_{ay} \cdot \sin(\alpha_{cak} + \alpha_{can}) \} \\
 &+ 2 \sum_{y=2}^i \sum_{k=y}^m \sum_{n=y}^m [I_{abk} I_{bcn} \{ (R_{ay} + R_{by}) \cdot (-R_{by}) \cdot \cos \alpha_{abk} \cos \alpha_{bcn} \\
 &+ (X_{ay} + X_{by}) \cdot (-X_{by}) \cdot \sin \alpha_{abk} \sin \alpha_{bcn} \\
 &- (R_{ay} + R_{by}) \cdot (-X_{by}) \cdot \cos \alpha_{abk} \cdot \sin \alpha_{bcn} - (X_{ay} + X_{by}) \cdot (-R_{by}) \cdot \sin \alpha_{abk} \cdot \cos \alpha_{bcn} \} \\
 &+ I_{abk} I_{can} \{ (R_{ay} + R_{by}) \cdot (-R_{ay}) \cdot \cos \alpha_{abk} \cos \alpha_{can} + (X_{ay} + X_{by}) \cdot (-X_{ay}) \cdot \sin \alpha_{abk} \sin \alpha_{can} \\
 &- (R_{ay} + R_{by}) \cdot (-X_{ay}) \cdot \cos \alpha_{abk} \cdot \sin \alpha_{can} - (X_{ay} + X_{by}) \cdot (-R_{ay}) \cdot \sin \alpha_{abk} \cdot \cos \alpha_{can} \} \\
 &+ I_{bck} I_{can} \{ R_{by} \cdot R_{ay} \cdot \cos \alpha_{bck} \cos \alpha_{can} + X_{by} \cdot X_{ay} \cdot \sin \alpha_{bck} \sin \alpha_{can} \\
 &- R_{by} \cdot X_{ay} \cdot \cos \alpha_{bck} \cdot \sin \alpha_{can} - X_{by} \cdot R_{ay} \cdot \sin \alpha_{bck} \cdot \cos \alpha_{can} \}] \quad (4.27)
 \end{aligned}$$

Similar expressions may be deduced for phases cb and ac .

4.2.4 Derivation of the sum of squares of the imaginary component of the branch voltage drops

In order to derive the sum of squares of the total imaginary component of the branch voltage drops for the three individual phases ba , cb and ac of a three-phase system, the same procedure is adopted as explained in section 4.2.3.

The extrapolation technique is applied to the result obtained when dealing with combined loading as presented in equation (3.28). By examining equation (3.25) and (3.28) as related to figure 3.3, and equation (4.22), (4.24) and (4.26) as related to figure 4.1, the extrapolation is possible. After extrapolation, the required general expressions are as follows:

For the phase ba , the sum of squares of the total imaginary component of the branch voltage drops $\Delta V^2_{ba_iimag-total-sum}$ at node i , can be given as:

$$\begin{aligned}
 \Delta V^2_{ba_iimag-total-sum} &= \sum_{y=2}^i \sum_{Z=y}^m [I^2_{abZ} \{ (R_{ay} + R_{by})^2 \cdot \sin^2 \alpha_{abZ} + (X_{ay} + X_{by})^2 \cdot \cos^2 \alpha_{abZ} \\
 &+ 2 \cdot (R_{ay} + R_{by}) \cdot (X_{ay} + X_{by}) \cdot \cos \alpha_{abZ} \cdot \sin \alpha_{abZ} \} \\
 &+ I^2_{bcZ} (R_{by}^2 \cdot \sin^2 \alpha_{bcZ} + X_{by}^2 \cdot \cos^2 \alpha_{bcZ} + 2 \cdot R_{by} \cdot X_{by} \cdot \cos \alpha_{bcZ} \cdot \sin \alpha_{bcZ})
 \end{aligned}$$

$$\begin{aligned}
 & + I_{caZ}^2 (R_{ay}^2 \cdot \sin^2 \alpha_{caZ} + X_{ay}^2 \cdot \cos^2 \alpha_{caZ} + 2 \cdot R_{ay} \cdot X_{ay} \cdot \cos \alpha_{caZ} \cdot \sin \alpha_{caZ}) \\
 & + 2 \sum_{y=2}^i \sum_{k=y}^{m-1} \sum_{n=k+1}^m [I_{abk} I_{abn} \{ (R_{ay} + R_{by})^2 \cdot \sin \alpha_{abk} \sin \alpha_{abn} + (X_{ay} + X_{by})^2 \cos \alpha_{abk} \cos \alpha_{abn} \\
 & + (R_{ay} + R_{by}) \cdot (X_{ay} + X_{by}) \cdot \sin(\alpha_{abk} + \alpha_{abn}) \} \\
 & + I_{bck} I_{bcn} \{ R_{by}^2 \sin \alpha_{bck} \sin \alpha_{bcn} + X_{by}^2 \cos \alpha_{bck} \cos \alpha_{bcn} + R_{by} \cdot X_{by} \cdot \sin(\alpha_{bck} + \alpha_{bcn}) \} \\
 & + I_{cak} I_{can} \{ R_{ay}^2 \sin \alpha_{cak} \sin \alpha_{can} + X_{ay}^2 \cos \alpha_{cak} \cos \alpha_{can} + R_{ay} \cdot X_{ay} \cdot \sin(\alpha_{cak} + \alpha_{can}) \} \\
 & + 2 \sum_{y=2}^i \sum_{k=y}^m \sum_{n=y}^m [I_{abk} I_{bcn} \{ (R_{ay} + R_{by}) \cdot (-R_{by}) \cdot \sin \alpha_{abk} \sin \alpha_{bcn} \\
 & + (X_{ay} + X_{by}) \cdot (-X_{by}) \cdot \cos \alpha_{abk} \cos \alpha_{bcn} \\
 & + (R_{ay} + R_{by}) \cdot (-X_{by}) \cdot \sin \alpha_{abk} \cdot \cos \alpha_{bcn} + (X_{ay} + X_{by}) \cdot (-R_{by}) \cdot \cos \alpha_{abk} \cdot \sin \alpha_{bcn} \} \\
 & + I_{abk} I_{can} \{ (R_{ay} + R_{by}) \cdot (-R_{ay}) \cdot \sin \alpha_{abk} \sin \alpha_{can} \\
 & + (X_{ay} + X_{by}) \cdot (-X_{ay}) \cdot \cos \alpha_{abk} \cos \alpha_{can} \\
 & + (R_{ay} + R_{by}) \cdot (-X_{ay}) \cdot \sin \alpha_{abk} \cdot \cos \alpha_{can} + (X_{ay} + X_{by}) \cdot (-R_{ay}) \cdot \cos \alpha_{abk} \cdot \sin \alpha_{can} \} \\
 & + I_{bck} I_{can} \{ R_{by} \cdot R_{ay} \cdot \sin \alpha_{bck} \sin \alpha_{can} + X_{by} \cdot X_{ay} \cdot \cos \alpha_{bck} \cos \alpha_{can} \\
 & + R_{by} \cdot X_{ay} \cdot \sin \alpha_{bck} \cdot \cos \alpha_{can} + X_{by} \cdot R_{ay} \cdot \cos \alpha_{bck} \cdot \sin \alpha_{can} \}] \tag{4.28}
 \end{aligned}$$

Similar expressions may be deduced for phases cb and ac .

4.3 The product term of the branch voltage drops

According to section 3.2.5.1, and in reference to Appendix 3-K and 3-L, the general expressions of the real and the imaginary component of the sum product of the branch voltage drops due to combined loading of a single-phase radial distribution system are presented. The expressions derived for the real and imaginary component of the sum product of the branch voltage drops at any load point i , as shown in equation (3.32) and equation (3.33) respectively, are to be extrapolated when dealing with a three-phase scenario.

4.3.1 The sum product term of the real component of the branch voltage drops

The general expressions of the real component of the sum product of the branch voltage drops at any load point i , for the phase ba , cb and ac of the three-phase distribution system can be extrapolated from equation (3.32). Therefore, at any load point i , the real component of the sum product of the branch voltage drops $\Delta^* \Delta V_{ba_ireal-sum}$ for phase ba , can be expressed as:

$$\begin{aligned}
 \Delta^* \Delta V_{ba_ireal-sum} &= \sum_{t=2}^{i-1} \sum_{r=t+1}^i \sum_{k=t}^m \sum_{n=r}^m I_{abk} I_{abn} \{ (R_{at} + R_{bt}) \cdot (R_{ar} + R_{br}) \cos \alpha_{abk} \cos \alpha_{abn} \\
 &+ (X_{at} + X_{bt}) \cdot (X_{ar} + X_{br}) \sin \alpha_{abk} \sin \alpha_{abn} \\
 &- (R_{at} + R_{bt}) \cdot (X_{ar} + X_{br}) \cos \alpha_{abk} \sin \alpha_{abn} - (X_{at} + X_{bt}) \cdot (R_{ar} + R_{br}) \sin \alpha_{abk} \cos \alpha_{abn} \} \\
 &+ \sum_{t=2}^{i-1} \sum_{r=t+1}^i \sum_{k=t}^m \sum_{n=r}^m I_{bck} I_{bcn} \{ R_{bt} R_{br} \cos \alpha_{bck} \cos \alpha_{bcn} + X_{bt} X_{br} \sin \alpha_{bck} \sin \alpha_{bcn} \\
 &- R_{bt} X_{br} \cos \alpha_{bck} \sin \alpha_{bcn} - X_{bt} R_{br} \sin \alpha_{bck} \cos \alpha_{bcn} \} \\
 &+ \sum_{t=2}^{i-1} \sum_{r=t+1}^i \sum_{k=t}^m \sum_{n=r}^m I_{cak} I_{can} \{ R_{at} R_{ar} \cos \alpha_{cak} \cos \alpha_{can} + X_{at} X_{ar} \sin \alpha_{cak} \sin \alpha_{can} \\
 &- R_{at} X_{ar} \cos \alpha_{cak} \sin \alpha_{can} - X_{at} R_{ar} \sin \alpha_{cak} \cos \alpha_{can} \} \\
 &+ \sum_{t=2}^{i-1} \sum_{r=t+1}^i \sum_{k=t}^m \sum_{n=r}^m I_{abk} I_{bcn} \{ (R_{at} + R_{bt}) \cdot (-R_{br}) \cos \alpha_{abk} \cos \alpha_{bcn} \\
 &+ (X_{at} + X_{bt}) \cdot (-X_{br}) \sin \alpha_{abk} \sin \alpha_{bcn} \\
 &- (R_{at} + R_{bt}) \cdot (-X_{br}) \cos \alpha_{abk} \sin \alpha_{bcn} - (X_{at} + X_{bt}) \cdot (-R_{br}) \sin \alpha_{abk} \cos \alpha_{bcn} \} \\
 &+ \sum_{t=2}^{i-1} \sum_{r=t+1}^i \sum_{k=t}^m \sum_{n=r}^m I_{bck} I_{abn} \{ (-R_{bt}) \cdot (R_{ar} + R_{br}) \cos \alpha_{bck} \cos \alpha_{abn} \\
 &+ (-X_{bt}) \cdot (X_{ar} + X_{br}) \sin \alpha_{bck} \sin \alpha_{abn} \\
 &- (-R_{bt}) \cdot (X_{ar} + X_{br}) \cos \alpha_{bck} \sin \alpha_{abn} - (-X_{bt}) \cdot (R_{ar} + R_{br}) \sin \alpha_{bck} \cos \alpha_{abn} \} \\
 &+ \sum_{t=2}^{i-1} \sum_{r=t+1}^i \sum_{k=t}^m \sum_{n=r}^m I_{abk} I_{can} \{ (R_{at} + R_{bt}) \cdot (-R_{ar}) \cos \alpha_{abk} \cos \alpha_{can}
 \end{aligned}$$

$$\begin{aligned}
 & + (X_{at} + X_{bt}) \cdot (-X_{ar}) \sin \alpha_{abk} \sin \alpha_{can} \\
 & - (R_{at} + R_{bt}) \cdot (-X_{ar}) \cos \alpha_{abk} \sin \alpha_{can} - (X_{at} + X_{bt}) \cdot (-R_{ar}) \sin \alpha_{abk} \cos \alpha_{can} \} \\
 & + \sum_{t=2}^{i-1} \sum_{r=t+1}^i \sum_{k=t}^m \sum_{n=r}^m I_{cak} I_{abn} \{ (-R_{at}) \cdot (R_{ar} + R_{br}) \cos \alpha_{cak} \cos \alpha_{abn} \\
 & + (-X_{at}) \cdot (X_{ar} + X_{br}) \sin \alpha_{cak} \sin \alpha_{abn} \\
 & - (-R_{at}) \cdot (X_{ar} + X_{br}) \cos \alpha_{cak} \sin \alpha_{abn} - (-X_{at}) \cdot (R_{ar} + R_{br}) \sin \alpha_{cak} \cos \alpha_{abn} \} \quad (4.29)
 \end{aligned}$$

Similar expressions may be deduced for phases cb and ac .

4.3.2 The sum product term of the imaginary component of the branch voltage drops

The general expressions of the imaginary component of the sum product of the branch voltage drops at any load point i , for phase ba , cb and ac of the three-phase distribution system can be extrapolated from equation (3.33). Therefore, at any load point i , the real component of the sum product of the branch voltage drops $\Delta^* \Delta V_{ba_iimag-sum}$ for phase ba , can be expressed as:

$$\begin{aligned}
 \Delta^* \Delta V_{ba_iimag-sum} & = \sum_{t=2}^{i-1} \sum_{r=t+1}^i \sum_{k=t}^m \sum_{n=r}^m I_{abk} I_{abn} \{ (R_{at} + R_{bt}) \cdot (R_{ar} + R_{br}) \sin \alpha_{abk} \sin \alpha_{abn} \\
 & + (X_{at} + X_{bt}) \cdot (X_{ar} + X_{br}) \cos \alpha_{abk} \cos \alpha_{abn} \\
 & + (R_{at} + R_{bt}) \cdot (X_{ar} + X_{br}) \sin \alpha_{abk} \cos \alpha_{abn} + (X_{at} + X_{bt}) \cdot (R_{ar} + R_{br}) \cos \alpha_{abk} \sin \alpha_{abn} \} \\
 & + \sum_{t=2}^{i-1} \sum_{r=t+1}^i \sum_{k=t}^m \sum_{n=r}^m I_{bck} I_{bcn} \{ R_{bt} R_{br} \sin \alpha_{bck} \sin \alpha_{bcn} + X_{bt} X_{br} \cos \alpha_{bck} \cos \alpha_{bcn} \\
 & + R_{bt} X_{br} \sin \alpha_{bck} \cos \alpha_{bcn} + X_{bt} R_{br} \cos \alpha_{bck} \sin \alpha_{bcn} \} \\
 & + \sum_{t=2}^{i-1} \sum_{r=t+1}^i \sum_{k=t}^m \sum_{n=r}^m I_{cak} I_{can} \{ R_{at} R_{ar} \sin \alpha_{cak} \sin \alpha_{can} + X_{at} X_{ar} \cos \alpha_{cak} \cos \alpha_{can} \\
 & + R_{at} X_{ar} \sin \alpha_{cak} \cos \alpha_{can} + X_{at} R_{ar} \cos \alpha_{cak} \sin \alpha_{can} \} \\
 & + \sum_{t=2}^{i-1} \sum_{r=t+1}^i \sum_{k=t}^m \sum_{n=r}^m I_{abk} I_{bcn} \{ (R_{at} + R_{bt}) \cdot (-R_{br}) \sin \alpha_{abk} \sin \alpha_{bcn} \\
 & + (X_{at} + X_{bt}) \cdot (-X_{br}) \cos \alpha_{abk} \cos \alpha_{bcn}
 \end{aligned}$$

$$\begin{aligned}
 & + (R_{at} + R_{bt}).(-X_{br}) \sin \alpha_{abk} \cos \alpha_{bcn} + (X_{at} + X_{bt}).(-R_{br}) \cos \alpha_{abk} \sin \alpha_{bcn} \} \\
 & + \sum_{t=2}^{i-1} \sum_{r=t+1}^i \sum_{k=t}^m \sum_{n=r}^m I_{bck} I_{abn} \{ (-R_{bt}).(R_{ar} + R_{br}) \sin \alpha_{bck} \sin \alpha_{abn} \\
 & + (-X_{bt}).(X_{ar} + X_{br}) \cos \alpha_{bck} \cos \alpha_{abn} \\
 & + (-R_{bt}).(X_{ar} + X_{br}) \sin \alpha_{bck} \cos \alpha_{abn} + (-X_{bt}).(R_{ar} + R_{br}) \cos \alpha_{bck} \sin \alpha_{abn} \} \\
 & + \sum_{t=2}^{i-1} \sum_{r=t+1}^i \sum_{k=t}^m \sum_{n=r}^m I_{abk} I_{can} \{ (R_{at} + R_{bt}).(-R_{ar}) \sin \alpha_{abk} \sin \alpha_{can} \\
 & + (X_{at} + X_{bt}).(-X_{ar}) \cos \alpha_{abk} \cos \alpha_{can} \\
 & + (R_{at} + R_{bt}).(-X_{ar}) \sin \alpha_{abk} \cos \alpha_{can} + (X_{at} + X_{bt}).(-R_{ar}) \cos \alpha_{abk} \sin \alpha_{can} \} \\
 & + \sum_{t=2}^{i-1} \sum_{r=t+1}^i \sum_{k=t}^m \sum_{n=r}^m I_{cak} I_{abn} \{ (-R_{at}).(R_{ar} + R_{br}) \sin \alpha_{cak} \sin \alpha_{abn} \\
 & + (-X_{at}).(X_{ar} + X_{br}) \cos \alpha_{cak} \cos \alpha_{abn} \\
 & + (-R_{at}).(X_{ar} + X_{br}) \sin \alpha_{cak} \cos \alpha_{abn} + (-X_{at}).(R_{ar} + R_{br}) \cos \alpha_{cak} \sin \alpha_{abn} \}
 \end{aligned} \tag{4.30}$$

Similar expressions may be deduced for phases *cb* and *ac*.

Note: The square of the total real component of the branch voltage drop of each phase at any node, will be the summation of the sum of the squares of the total real component of the branch voltage drop and the sum product of the branch voltage drop. The same description applies also to the total square of the imaginary components.

PART 3: Development of the consumer voltage and line power loss equations on MV distribution systems

4.4 Introduction

The present work deals with two type of loading as mentioned in the preceding chapters. These are constant P-Q loads and statistically distributed current loads at unity power factor having a beta distribution function. If the network is treated as a medium length line model, the charging currents should be taken into consideration.

4.4.1 Dealing with statistically distributed load currents

The domestic loads are modelled as constant current at unity power factor [4.1]. The USE device operates on a principle of maintaining its input power equal to its output power [4.2]. The

probabilistic load flow for the statistical load currents depends largely on the appropriate scaling factor used for different beta distributed load types. In practice, the scaling factors can conveniently be chosen as the circuit-breaker size of the customers [4.3]. This enables the determination of the beta distribution statistical parameters α and β of the load currents at the low voltage side. The present work deals with MV distribution systems. To maintain the same statistical parameters at the MV level, new scaling factors should be determined. The proof of this statement is illustrated in appendix 4-A. To evaluate new scaling factors for the statistical load currents modelled as constant current at unity power factor as discussed in chapter 2 with or without the application of USE devices, the procedure indicated in section 4.4.2 is adopted

4.4.2 Evaluation of the new scaling factors

The evaluation of the new scaling factors is based on the assumption that at the output of the USE device, the average load power due to the deterministic component of beta-distributed load currents is maintained constantly in order to justify the application of a constant load current model as mentioned in chapter 2. The phase voltage at the LV network is assumed constant and equal to a nominal voltage.

The average load power P_{ave_statlv} at the output of the USE device feeding a load consuming an average current I_{ave_statlv} at a nominal voltage V_{nom_lv} and unity power factor is evaluated as:

$$P_{ave_statlv} = V_{nom_lv} \cdot I_{ave_statlv} \quad (4.31)$$

The average current I_{ave_statlv} is determined as [4.1]:

$$I_{ave_statlv} = C_b N \left(\frac{\alpha}{\alpha + \beta} \right) \quad (4.32)$$

where

C_b is the circuit breaker rating

N is the total number of connected consumers

Using equations (4.31) and (4.32), the average power P_{ave_statlv} can be expressed as:

$$P_{ave_statlv} = C_b \left(\frac{\alpha}{\alpha + \beta} \right) N \cdot V_{nom_lv} \quad (4.33)$$

The average load current \bar{I}_{ave_statmv} at each node on the MV distribution system is iteratively evaluated as:

$$\bar{I}_{ave_statmv} = \frac{P_{ave_statlv}}{\bar{V}_{mv-stat}^*} \quad (4.34)$$

where

$\bar{V}_{mv-stat}^*$ is the conjugate of the nodal voltage on the MV distribution line

The variable scaling factor $k_{var-stat}$ at each node point is evaluated as:

$$k_{var-stat} = \frac{I_{ave_statmv,lv}}{I_{ave_statlv}} \quad (4.35)$$

where

$I_{ave_statmv,lv}$ is the I_{ave_statmv} value converted to the low voltage side

The overall scaling factor SF at each load point taking into account the variable scaling factor $k_{var-stat}$, the circuit breaker scaling factor C_b and the distribution transformer turns ratio D_{tr} is evaluated as:

$$SF = k_{var-stat} C_b D_{tr} \quad (4.36)$$

Note that the overall scaling factor SF is different at each node due to the fact that the variable scaling factor $k_{var-stat}$ will take different values at different load points along the MV distribution system due to the different voltage levels.

In the deterministic load flow employing the Newton-Raphson algorithm described in a later chapter, the statistical load currents are treated as real power loads. Therefore, at each iteration, the statistical load current at node k can be expressed as:

$$\begin{aligned} P_k &= V_k I_k \\ Q_k &= 0 \end{aligned} \quad (4.37)$$

But for the backward and forward sweep algorithm, the statistical load current \bar{I}_k at node k is iteratively evaluated as:

$$\begin{aligned} \bar{I}_k &= \frac{P_k}{V_k^*} \\ \text{OR} & \\ \bar{I}_k &= \frac{P_k (\cos \alpha_{vk} + j \sin \alpha_{vk})}{V_k} \end{aligned} \quad (4.38)$$

where

α_{vk} is the voltage phase angle at node k

NOTE: According to the derivation in this section, if the constant power load model is used, the USE device does not have influence on load parameters

4.5 Dealing with constant P-Q loads

Non-statistical loads are modelled as constant $P-Q$ loads. These loads are shown on a one-line diagram as depicted in fig. 4.2. For the backward and forward sweep algorithm as mentioned in a later chapter, the load current \bar{I}_k at node k due to the constant $P-Q$ loads is evaluated by employing iterative procedure based on the equation (4.39).

$$\bar{I}_k = (P_k - jQ_k) / \bar{V}_k^* \tag{4.39}$$

In the case of the NR-algorithm, the calculation of the power mismatch for combined load [4.4] i.e. statistical plus constant $P-Q$ loads, $\Delta P_{k_mismatch}$ and $\Delta Q_{k_mismatch}$ at node k , is governed by the expression (4.40).

$$\Delta P_{k_mismatch} = P_{k_specified} - P_{k_calculated} \tag{4.40}$$

$$\Delta Q_{k_mismatch} = Q_{k_specified} - Q_{k_calculated}$$

where

$$P_{k_specified} = -P_k$$

$$Q_{k_specified} = -Q_k$$

$$P_{k_calculated} \text{ and } Q_{k_calculated} \text{ \{see equation (6.5) and (6.6)\}}$$

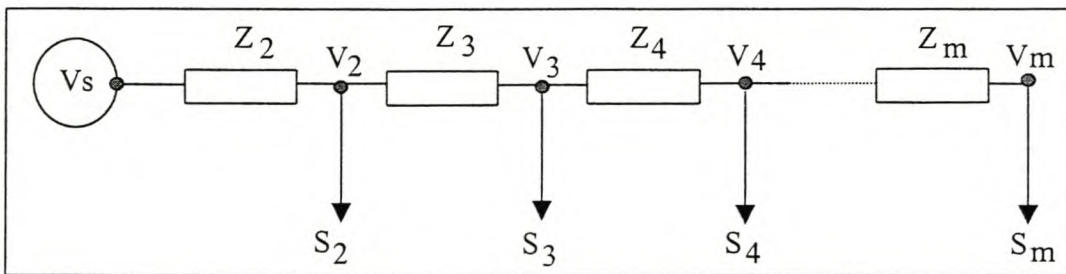


Fig. 4.2: One line diagram with constant P & Q loads.

4.6 Dealing with charging currents due to transmission line capacitance

For power lines less than 80km long, the effect of capacitance can be slight and is often neglected [4.5]. But distribution lines for rural electrification traverse long distances that are more than 80 km and hence the capacitance of the line should be taken into account.

The charging currents due to the line capacitance are shown on the one line diagram shown in fig. 4.3. Suppose the consumer voltages $\bar{V}_2, \bar{V}_3, \bar{V}_4, \bar{V}_5, \dots, \bar{V}_m$ are assumed to have phase angles $\alpha_{v_2}, \alpha_{v_3}, \alpha_{v_4}, \alpha_{v_5}, \dots, \alpha_{v_m}$ respectively. It follows that, the charging currents $\bar{I}_{c_2}, \bar{I}_{c_3}, \bar{I}_{c_4}, \dots, \bar{I}_{c_m}$ will have phase angles $\alpha_{v_2} + 90, \alpha_{v_3} + 90, + \dots + \alpha_{v_m} + 90$ respectively. In other words, the charging currents can be represented in the rectangular co-ordinate system as:

$$\begin{aligned} \bar{I}_{c_2} &= I_{c_2} [\cos(90 + \alpha_{v_2}) + j \sin(90 + \alpha_{v_2})] \\ \bar{I}_{c_3} &= I_{c_3} [\cos(90 + \alpha_{v_3}) + j \sin(90 + \alpha_{v_3})] \\ &\vdots \\ \bar{I}_{c_m} &= I_{c_m} [\cos(90 + \alpha_{v_m}) + j \sin(90 + \alpha_{v_m})] \end{aligned} \tag{4.41}$$

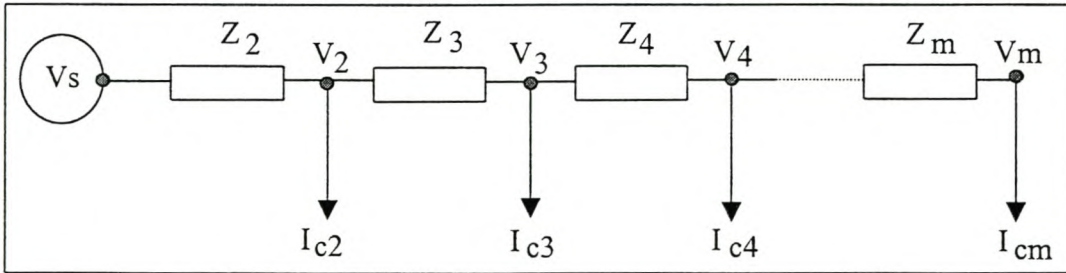


Fig. 4.3: One line diagram with charging currents.

From which, the current \bar{I}_{c_2} can be expressed as:

$$\begin{aligned} \bar{I}_{c_2} &= I_{c_2} [\cos(90 + \alpha_{v_2}) + j \sin(90 + \alpha_{v_2})] \\ &= I_{c_2} [\cos 90 \cos \alpha_{v_2} - \sin 90 \sin \alpha_{v_2} + j \sin 90 \cos \alpha_{v_2} + \cos 90 \sin \alpha_{v_2}] \\ &= I_{c_2} (-\sin \alpha_{v_2} + j \cos \alpha_{v_2}) \\ &= V_2 \omega C_2 (-\sin \alpha_{v_2} + j \cos \alpha_{v_2}) \end{aligned}$$

In general, the charging current \bar{I}_{c_k} at each node k can be expressed as:

$$\bar{I}_{c_k} = V_k \omega C_k (-\sin \alpha_{v_k} + j \cos \alpha_{v_k}) \tag{4.42}$$

where

V_k is the absolute value of the consumer voltage at node k
 α_{vk} is the angle of the voltage phasor at node k
 C_k is the shunt capacitance at node k
 $\omega = 2\pi f$

In the deterministic load flow employing the Newton-Raphson algorithm as described in a later chapter, the charging currents are represented as shunt admittance. These admittance's are incorporated in the Y-bus [4.4]. The admittance at node k is calculated as:

$$\bar{Y}_{sk} = j2\pi f C_k \quad (4.43)$$

In case of the backward and forward sweep algorithm, the charging currents are iteratively calculated by the expression shown in equation (4.42).

4.7 Determination of the consumer voltages

The consumer voltages are determined by the principle of superposition. The currents flowing in the system are due to statistical and non-statistical currents. The consumer voltage phase angles are evaluated due to the effect of the combination of the statistical and non-statistical average currents. In other words, the consumer voltage phase angles are obtained deterministically. The consumer voltages due to statistical load currents are beta distributed and their percentile values are determined by considering 1st and 2nd moments of the distribution. In evaluating the consumer voltages, three stages are involved. These stages are discussed in section (4.7.1), (4.7.2) and (4.7.3).

4.7.1 Dealing with statistically distributed load currents

As cited in section 3.2.3, the consumer voltages at any node of the MV distribution system are obtained by subtracting the corresponding total branch voltage drops from the supply source V_S . Therefore, the magnitude of the consumer voltage V_{scon_i} at node i can be expressed as:

$$\begin{aligned} V_{scon_i} &= \left\{ (V_S - \Delta V_{ireal_total})^2 + (\Delta V_{iimag_total})^2 \right\}^{\frac{1}{2}} \\ &= V_S \left\{ 1 - 2 \frac{\Delta V_{ireal_total}}{V_S} + \frac{\Delta V_{ireal_total}^2}{V_S^2} + \frac{\Delta V_{iimag_total}^2}{V_S^2} \right\}^{\frac{1}{2}} \end{aligned} \quad (4.44)$$

where

ΔV_{ireal_total} is the total real component of the branch voltage drop at node i
 ΔV_{iimag_total} is the total imaginary component of the voltage drop at node i

In previous research [4.1], the method using Taylor's expansion was used to express equation (4.44) in such a way that the first statistical moment of the consumer voltage V_{scon_i} may be determined. The Taylor series is described as:

$$(1 + X)^{\frac{1}{2}} = 1 + \frac{1}{2}X - \frac{1}{8}X^2 + \frac{1}{16}X^3 \dots\dots\dots -1 < X < 1 \quad (4.45)$$

If equation (4.44) is normalised, the parameter X in equation (4.45) can be given as:

$$X = -\frac{2\Delta V_{ireal_total}}{V_S} + \frac{\Delta V^2_{ireal_total}}{V_S^2} + \frac{\Delta V^2_{iimag_total}}{V_S^2} \quad (4.46)$$

The terms $1 + \frac{1}{2}X - \frac{1}{8}X^2 + \frac{1}{16}X^3$ will be considered in the Taylor's expansion. As derived in appendix 4-B, the final result of the consumer voltage V_{scon_i} at node i after discarding powers greater than 2, is approximated as:

$$V_{scon_i} \approx V_S \left\{ 1 - \frac{\Delta V_{ireal_total}}{V_S} + 0.5 \frac{\Delta V^2_{iimag_total}}{V_S^2} + 0.5 \frac{\Delta V_{real_total} \Delta V^2_{iimag_total}}{V_S^3} + 0.5 \frac{\Delta V^2_{ireal_total} \Delta V^2_{iimag_total}}{V_S^4} \right\} \quad (4.47)$$

Application of USE devices allows MV networks to operate with voltage drops of the order of 35%. In order to improve the accuracy of expression (4.47), the coefficients for the last three terms were evaluated with the aid of a search engine that was imbedded in the probabilistic load flow program. Preliminary sample networks with or without feeder voltage regulators were investigated to determine the possible ranges of the individual coefficients. The search engine estimates the coefficients based on results from Monte Carlo simulations. The upper and lower values were used. From the preliminary results a possible range of coefficients were established to satisfy all pertinent system electrical parameters. Finally, a typical one-line diagram network was applied. In order to include both the real and the reactive parts of the system voltage drops, the line resistance were made equal to the line reactance and Monte Carlo simulations were performed. These results were used as initial values for the search engine to estimate the final coefficients. The coefficients were applied to different network systems; both single and three-phase systems and the results are presented in a later chapter. Therefore, the consumer voltage at node i can be expressed as:

$$V_{scon_i} = V_S \left\{ 1 - \frac{\Delta V_{ireal_total}}{V_S} + 0.501 \frac{\Delta V^2_{iimag_total}}{V_S^2} + 0.448 \frac{\Delta V_{real_total} \Delta V^2_{iimag_total}}{V_S^3} + 0.829 \frac{\Delta V^2_{ireal_total} \Delta V^2_{iimag_total}}{V_S^4} \right\} \quad (4.48)$$

The square of the consumer voltage $V^2_{scon_i}$ is obtained by squaring equation (4.44).

$$\begin{aligned}
 V^2_{scon_i} &= (V_S - \Delta V_{ireal_total})^2 + (\Delta V_{iimag_total})^2 \\
 &= V_S^2 - 2V_S \Delta V_{ireal_total} + \Delta V_{ireal_total}^2 + \Delta V_{iimag_total}^2
 \end{aligned} \tag{4.49}$$

The first and second moments of the distribution of V_{scon_i} , can be determined using equation (4.48) and (4.49) respectively. This will eventually facilitate the evaluation of the consumer voltage statistical parameters so that, the percentile values can be obtained.

4.7.2 Dealing with non-statistical currents

The total real and the total imaginary components of the branch voltage drops due to non-statistical currents cannot be accurately determined by applying equations (3.9) and (3.10) respectively. The problem arises when voltage regulation is effected by means of capacitor control or by step-voltage regulators as discussed in chapter 2. This is due to the fact that, it is difficult to ensure the correct evaluation of the node current phase angles. To circumvent this problem when dealing with non-statistical currents, the total nodal phasor currents are applied directly without resorting to the evaluation of their phase angles. The procedure adopted in this present work is illustrated in one line diagram depicted in fig. 4.4.

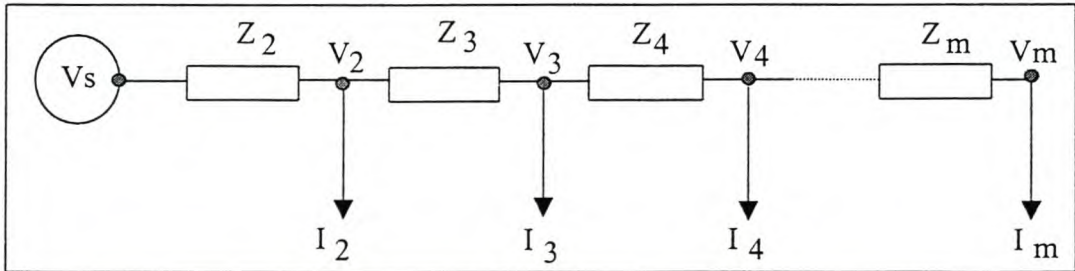


Fig. 4.4: One line diagram for the determination of the total component of the branch voltage drops due to non-statistical node currents

The currents shown in fig. 4.4 are the phasor sum of all non-statistical currents at a particular node. This could be due to currents resulting from the voltage regulators (i.e. step-voltage regulators or capacitors), constant P-Q loads and line capacitance. In the derivation of appendix 4-C, the total real $\Delta V_{real-itotal}$ and the total imaginary $\Delta V_{imag-itotal}$ components of the branch voltage drops at node i can be expressed as:

$$\Delta V_{real-itotal} = \text{real} \left\{ \sum_{k=2}^i \sum_{n=k}^m \bar{Z}_k \bar{I}_n \right\} \tag{4.50}$$

$$\Delta V_{imag-itotal} = \text{imaginary} \left\{ \sum_{k=2}^i \sum_{n=k}^m \bar{Z}_k \bar{I}_n \right\} \tag{4.51}$$

4.7.3 Superposition of branch voltage drops

The statistical load currents determine the percentile values of the consumer voltages. These values should be converted to phasors so that the total real and the total imaginary component of the branch voltage drops can be evaluated. This is achieved by retrieving the calculated consumer voltage angles solved by iterative procedure imbedded in the deterministic computer program to be dealt with in a later chapter. The consumer voltage angles that are deterministically evaluated are applied at any specified risk. In a later chapter, the above statement is validated by the results that were obtained from the Monte Carlo simulation. In the course of evaluating the consumer voltages for different system parameters some definite results were observed that were very interesting compared to those obtained from Monte Carlo simulations on the regard to the system voltage angles. The results reveal the following:

- the voltage angles are valid if line capacitance is neglected and the voltage regulation is not done through the application of capacitors
- if voltage regulation is done using capacitors or line capacitance is not neglected, the deterministic voltage angles prior to the inclusion of voltage regulating capacitors or line capacitance should be used in the probabilistic load flow as well as when the percentile values at any risk are to be converted to phasors
- for non-statistical currents, their phasors at any system condition are valid, this includes currents due to constant $P-Q$ loads, line capacitance and voltage regulators (step-voltage regulators or capacitors)

The consumer voltage percentile values V_{Pcon_i} can be converted into phasors using equation (4.52).

$$\bar{V}_{Pcon_i} = V_{Pcon_i}(\cos \alpha_i + j \sin \alpha_i) \quad (4.52)$$

where

α_i is the consumer voltage angle at node i

The total real ΔV_{Preal_itotal} and the total imaginary ΔV_{Pimag_itotal} component of the branch voltage drops at node i due to statistical load currents are calculated as indicated in equation (4.53) and (4.54).

$$\Delta V_{Preal_itotal} = \sum_{k=2}^i \text{real}(\bar{V}_{Pcon_k-1} - \bar{V}_{Pcon_k}) \quad (4.53)$$

$$\Delta V_{Pimag_itotal} = \sum_{k=2}^i \text{imaginary}(\bar{V}_{Pcon_k-1} - \bar{V}_{Pcon_k}) \quad (4.54)$$

where

\bar{V}_{Pcon_i} is the supply voltage V_S

The total real and the total imaginary component of the branch voltage drops at node i due to both the statistical and non-statistical load currents can be obtained by summing their real and imaginary components respectively as shown in equation (4.55) and (4.56).

$$\Delta V_{Treal_itotal} = \Delta V_{real_itotal} + \Delta V_{Prreal_itotal} \quad (4.55)$$

$$\Delta V_{Timag_itotal} = \Delta V_{imag_itotal} + \Delta V_{Pimag_itotal} \quad (4.56)$$

4.7.4 Determination of the overall consumer voltages

The overall consumer phasor voltage \bar{V}_{ovcon_i} at node i , due to statistical and non-statistical loads is determined as expressed in equation (4.57).

$$\bar{V}_{ovcon_i} = V_S - \Delta V_{Treal_itotal} + j\Delta V_{Timag_itotal} \quad (4.57)$$

Therefore, the magnitude of the consumer voltage V_{mcon_i} at node i , is determined as shown in equation (4.58).

$$V_{mcon_i} = \{(V_S - \Delta V_{Treal-itotal})^2 + \Delta V_{Timag-itotal}^2\}^{\frac{1}{2}} \quad (4.58)$$

The determination of the consumer voltages due to statistical and non-statistical currents is based on a one-line diagram scenario. This means that, only single-phase systems are applicable. In section 4.7.5, the concept is extended to deal with the three-phase network applications.

4.7.5 Evaluation of the consumer voltages in three-phase distribution systems

The three individual phases in three-phase system are described in section 4.1.1. The phase currents, as demonstrated in this chapter, are determined by taking into consideration the phase difference between the supply phase voltages as explained in section 4.1.1. The total real and the total imaginary components of the branch voltage drops at any node of the system (without branches) as well as their squares were developed previously in this chapter. In order to apply expressions (4.48)-(4.58) for the individual phases ba , cb and ac in three-phase systems, the approach adopted in this present work is developed in section 4.7.5.1, 4.7.5.2 and 4.7.5.3. The underlying principle is to treat the phase in consideration as the reference phasor in order to make the calculations possible, otherwise it can become impossible when attempting to evaluate the statistical parameters of the consumer voltages due to statistical load currents which will be dealt with in chapter 5.

4.7.5.1 Evaluation for the phase ba

The supply voltage \bar{V}_{ba} for the phase ba is treated as the reference phasor, therefore, the supply phase voltages can be expressed as:

$$\begin{aligned}\bar{V}_{ba} &= V_{ba} \angle 0^\circ \\ \bar{V}_{cb} &= V_{cb} \angle 240^\circ \\ \bar{V}_{ac} &= V_{ac} \angle 120^\circ\end{aligned}\tag{4.59}$$

The phase currents and the total real and the total imaginary components of the branch voltage drops at each node for phases ba , cb and ac are evaluated directly in this particular case. When the other phases cb and ac are treated as the reference phasors, some manipulation is required to obtain accurate results. It should be understood that, the deterministic power flow program, treats the supply system phase voltages as presented in equation (4.59).

4.7.5.2 Evaluation for the phase cb

The supply phase voltage \bar{V}_{cb} for the phase cb is treated as the reference phasor, therefore, the other phases should be shifted by 120° in the anti-clockwise direction as referred to expression (4.59). In doing so, the supply phase voltages can be expressed as:

$$\begin{aligned}\bar{V}_{cb} &= V_{cb} \angle 0^\circ \\ \bar{V}_{ba} &= V_{ba} \angle 120^\circ \\ \bar{V}_{ac} &= V_{ac} \angle 240^\circ\end{aligned}\tag{4.60}$$

The consumer phase voltage angles at each node that are evaluated by the deterministic load flow should also be shifted in the same manner as described in the expression (4.60). In this regard, the angle of the phase currents should also be shifted accordingly. For statistical currents, it can be implemented without difficulty. But as explained in section 4.7.2, the determination of the phase angles for non-statistical currents can sometimes pose some difficulties. By applying the magnitude of the consumer voltages evaluated at each node by the deterministic load flow that is based on expression (4.59), the phase current phasors at each node due to non-statistical currents are evaluated based on the new system of the phase voltages described in this section.

4.7.5.2.1 Determination of the statistical load current phase angles

The calculation in the probabilistic load flow utilises the phase angles of the statistical currents. These angles are the same as the consumer phase voltage angles. Therefore, the new phase angles of the statistical load currents for different phases are determined as:

$$\alpha_{cbs-new} = \alpha_{cbs-old} + 120^{\circ}$$

$$\alpha_{bas-new} = \alpha_{bas-old} + 120^{\circ} \tag{4.61}$$

$$\alpha_{acs-new} = \alpha_{acs-old} + 120^{\circ}$$

4.7.5.2 Determination of the non-statistical phase load currents

The mathematical procedure adopted in this present work to evaluate the non-statistical phase currents when the supply phase voltage \bar{V}_{cb} is treated as the reference phasor is as follows:

- the deterministic phase voltage magnitudes at each node are converted into phasors by adopting the new system phase angles as explained in section 4.7.5.2
- the phase load currents at each node are evaluated as previously presented in this chapter based on the deterministic phase voltage phasors described above.

4.7.5.3 Evaluation for the phase *ac*

In this case, the supply phase voltage \bar{V}_{ac} for the phase *ac* is treated as the reference phasor, it follows that, other phases should be shifted by 240° in the anti-clockwise direction as referred to expression (4.59). In doing so, the resulting supply phase voltages will be:

$$\bar{V}_{ac} = V_{ac} \angle 0^{\circ}$$

$$\bar{V}_{ba} = V_{ba} \angle 240^{\circ} \tag{4.62}$$

$$\bar{V}_{cb} = V_{cb} \angle 120^{\circ}$$

The consumer phase voltage angles at each node that are evaluated by the deterministic load flow should also be shifted in the same manner as described in the expression (4.62). The rest of the discussion presented in section 4.7.5.2, 4.7.5.2.1 and 4.7.5.2.2 is also applicable in this section respectively.

4.8 Derivation of the system power loss related equations

The product between the line resistance and the square of the line current determines the system line power losses. Since the line currents in MV distribution systems are to be treated as phasors, the square of the branch current can be determined as the sum of the squares of its real and imaginary components. This will enable application of statistical loads in evaluation of line power losses later. The general expressions of the total power loss in single and three-phase systems on a radial system without branches are determined in the section 4.8.1 and 4.8.2. This will enable the development of the general expression for the total power loss in single and three-phase systems that are due to the load currents modelled as signals.

4.8.1 Evaluation of the total line power loss on single-phase distribution systems

The general expressions of the squares of the real and imaginary component of the branch currents are determined based on fig. 4.5. The line currents that are responsible for the line power losses over any part of the system are the phasor sum of the load currents for that section.

The current \bar{I}_{Z_2} through the branch impedance Z_2 is given as:

$$\begin{aligned} \bar{I}_{Z_2} &= \bar{I}_2 + \bar{I}_3 + \bar{I}_4 + \bar{I}_5 + \dots + \bar{I}_{m-1} + \bar{I}_m \\ &= I_2(\cos \alpha_2 + j \sin \alpha_2) + I_3(\cos \alpha_3 + j \sin \alpha_3) + \dots + I_m(\cos \alpha_m + j \sin \alpha_m) \end{aligned} \quad (4.63)$$

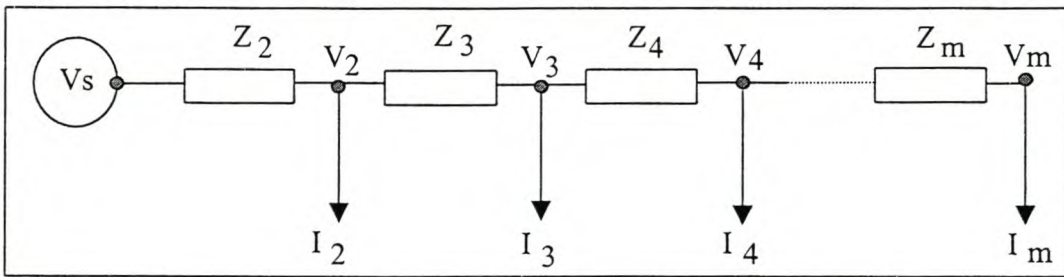


Fig. 4.5: One line diagram for the formulation of the general expression of the total line power losses

The real component I_{Z_2-real} and imaginary component I_{Z_2-imag} of the current I_{Z_2} can be expressed as:

$$I_{Z_2-real} = I_2 \cos \alpha_2 + I_3 \cos \alpha_3 + I_4 \cos \alpha_4 + \dots + I_{m-1} \cos \alpha_{m-1} + I_m \cos \alpha_m \quad (4.64)$$

$$I_{Z_2-imag} = I_2 \sin \alpha_2 + I_3 \sin \alpha_3 + I_4 \sin \alpha_4 + \dots + I_{m-1} \sin \alpha_{m-1} + I_m \sin \alpha_m \quad (4.65)$$

If other branches are considered, it will become apparent that, the general expression of the real I_{Z_i-real} and imaginary I_{Z_i-imag} components of the current through the branch impedance \bar{Z}_i can be given as:

$$I_{Z_i-real} = \sum_{k=i}^m I_k \cos \alpha_k \quad (4.66)$$

$$I_{Z_i-imag} = \sum_{k=i}^m I_k \sin \alpha_k \quad (4.67)$$

The above general expressions are closely related to the real and imaginary component of the branch voltage drops shown in equation (3.5) and (3.7) respectively. Examining the above-mentioned equations, the general expression of the real and imaginary component of the branch

current can be obtained by setting R_i and X_i to a value of one and zero respectively. This procedure will be adopted in determining the general expressions of the squares of the real and imaginary component of the branch currents in single-phase and three-phase systems.

For the single-phase system, the general expression of the square of the real component $I^2_{Zi-real}$ through the branch impedance \bar{Z}_i in fig. 4.5, can be determined by referring to equation (3.6) and by setting R_i and X_i to a value of one and zero respectively. Therefore, the result will be:

$$I^2_{Zi-real} = \sum_{y=i}^m I_y^2 \cos^2 \alpha_y + 2 \sum_{k=i}^{m-1} \sum_{n=k+1}^m I_k I_n \cos \alpha_k \cos \alpha_n \quad (4.68)$$

The general expression of the square of the imaginary component $I^2_{Zi-imag}$ through the branch impedance \bar{Z}_i in fig. 4.5 can also be determined by referring to equation (3.8) and by setting R_i and X_i to a value of one and zero respectively. Therefore, the result will be:

$$I^2_{Zi-imag} = \sum_{y=i}^m I_y^2 \sin^2 \alpha_y + 2 \sum_{k=i}^{m-1} \sum_{n=k+1}^m I_k I_n \sin \alpha_k \sin \alpha_n \quad (4.69)$$

The general expression of the branch power loss P_{i-loss} on the branch of impedance \bar{Z}_i can be expressed as:

$$\begin{aligned} P_{i-loss} &= R_i (I^2_{Zi-real} + I^2_{Zi-imag}) \\ &= R_i \left\{ \sum_{y=i}^m I_y^2 \cos^2 \alpha_y + 2 \sum_{k=i}^{m-1} \sum_{n=k+1}^m I_k I_n \cos \alpha_k \cos \alpha_n + \sum_{y=i}^m I_y^2 \sin^2 \alpha_y \right. \\ &\quad \left. + 2 \sum_{k=i}^{m-1} \sum_{n=k+1}^m I_k I_n \sin \alpha_k \sin \alpha_n \right\} \end{aligned} \quad (4.70)$$

The total power loss $P_{total-loss}$ is the summation of all the branch power losses and is given as:

$$\begin{aligned} P_{total-loss} &= \sum_{i=2}^m P_{i-loss} \\ &= \sum_{i=2}^m \left[R_i \left\{ \sum_{y=i}^m I_y^2 \cos^2 \alpha_y + 2 \sum_{k=i}^{m-1} \sum_{n=k+1}^m I_k I_n \cos \alpha_k \cos \alpha_n + \sum_{y=i}^m I_y^2 \sin^2 \alpha_y \right. \right. \\ &\quad \left. \left. + 2 \sum_{k=i}^{m-1} \sum_{n=k+1}^m I_k I_n \sin \alpha_k \sin \alpha_n \right\} \right] \end{aligned} \quad (4.71)$$

4.8.2 Evaluation of the total line power loss on three-phase distribution systems

The three-phase radial distribution system adopted for the development of the general expression of the total line power loss is depicted in fig. 4.6. The phases are designated as previously described in section 4.1.1.

For a balanced three-phase system and by treating the phase current \bar{I}_{abi} to be the reference phasor at node i , it follows that:

$$\bar{I}_{abi} = I_{abi} \angle 0^\circ$$

$$\bar{I}_{bci} = I_{bci} \angle 240^\circ \tag{4.72}$$

$$\bar{I}_{cai} = I_{cai} \angle 120^\circ$$

The current through the impedance \bar{Z}_{ai} , \bar{Z}_{bi} and \bar{Z}_{ci} are designated as \bar{I}_{xi} , \bar{I}_{yi} and \bar{I}_{zi} respectively.

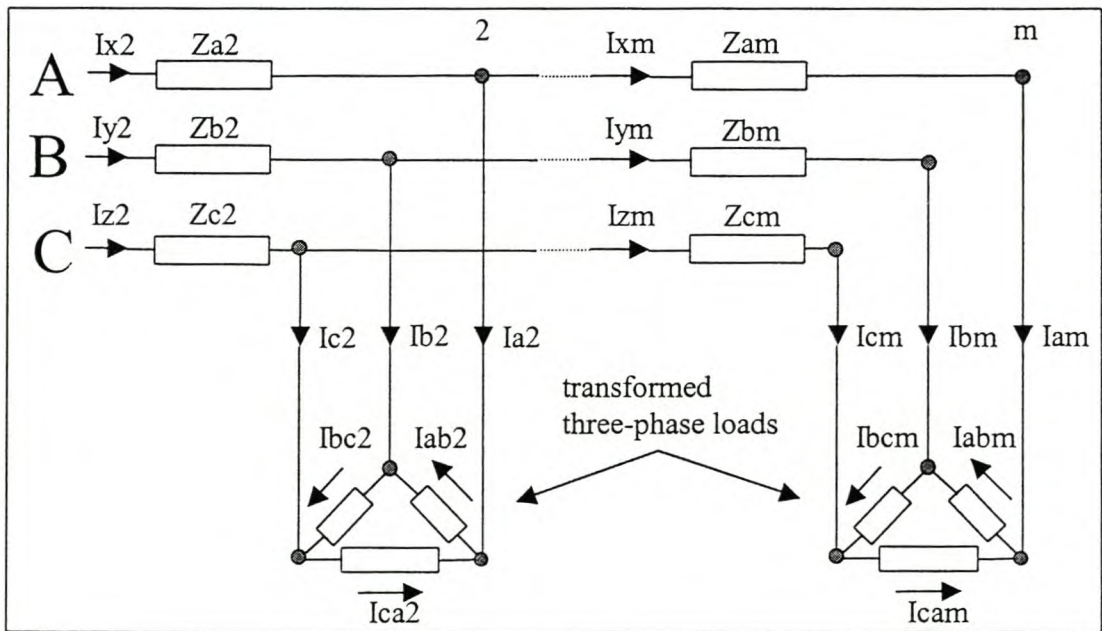


Fig. 4.6: The diagram for the formulation of the general expression of the total line power losses in three-phase systems.

Note: In this section the conductor A refer to all line conductors that are physically connected to the line identified as A in fig. 4.6. The same applies to the conductor B and C .

According to the above definitions, the line current through the impedance \bar{Z}_{am} , \bar{Z}_{bm} and \bar{Z}_{cm} as shown in fig. 4.6, can be described as:

$$\bar{I}_{xm} = \bar{I}_{am} = \bar{I}_{abm} - \bar{I}_{cam} \quad (4.73)$$

$$\bar{I}_{ym} = \bar{I}_{bm} = \bar{I}_{bcm} - \bar{I}_{abm} \quad (4.74)$$

$$\bar{I}_{zm} = \bar{I}_{cm} = \bar{I}_{cam} - \bar{I}_{bcm} \quad (4.75)$$

By referring to equation (4.73), (4.74) and (4.75), the line currents through the impedance \bar{Z}_{ai} , \bar{Z}_{bi} and \bar{Z}_{ci} can be given as:

$$\bar{I}_{xi} = \sum_{k=i}^m (\bar{I}_{abk} - \bar{I}_{cak}) \quad (4.76)$$

$$\bar{I}_{yi} = \sum_{k=i}^m (\bar{I}_{bck} - \bar{I}_{abk}) \quad (4.77)$$

$$\bar{I}_{zm} = \sum_{k=i}^m (\bar{I}_{cak} - \bar{I}_{bck}) \quad (4.78)$$

The general expression of the total power loss for each line conductor at a given instant or over a period of time can be evaluated as cited in section 4.8.1. As described above, the branch currents are due to a combination of two-phase currents. Therefore, a general expression of the sum of the squares of the real and imaginary component of the branch voltage drops of equation (3.6) and (3.8) can be applied to individual currents. Equation (3.28) and (3.29) can be referred so that the general expression of the product term of the two currents can be determined. Note that equation (3.28) and (3.29) deals with the summation up to a node of interest whereas in this case the general expression over the branch of the system is of interest.

For the conductor A in the three-phase system shown in fig. 4.6, the general expression of the square of the real component $I^2_{xi-real}$ and imaginary component $I^2_{xi-imag}$ through the branch impedance \bar{Z}_{ai} , can be determined by referring to equation (4.76). By setting R_i and X_i in equation (3.6) and (3.8) to a value of one and zero respectively for each phase current and equation (3.29) and (3.28) for their product, the result will be:

$$\begin{aligned} I^2_{xi-real} = & \sum_{y=i}^m I^2_{aby} \cos^2 \alpha_{aby} + 2 \sum_{k=i}^{m-1} \sum_{n=k+1}^m I_{abk} I_{abn} \cos \alpha_{abk} \cos \alpha_{abn} \\ & + \sum_{y=i}^m I^2_{cay} \cos^2 \alpha_{cay} + 2 \sum_{k=i}^{m-1} \sum_{n=k+1}^m I_{cak} I_{can} \cos \alpha_{cak} \cos \alpha_{can} - 2 \sum_{k=i}^m \sum_{n=i}^m I_{abk} I_{can} \cos \alpha_{abk} \cos \alpha_{can} \end{aligned} \quad (4.79)$$

$$I^2_{xi-imag} = \sum_{y=i}^m I^2_{aby} \sin^2 \alpha_{aby} + 2 \sum_{k=i}^{m-1} \sum_{n=k+1}^m I_{abk} I_{abn} \sin \alpha_{abk} \sin \alpha_{abn}$$

$$+ \sum_{y=i}^m I_{cay}^2 \sin^2 \alpha_{cay} + 2 \sum_{k=i}^{m-1} \sum_{n=k+1}^m I_{cak} I_{can} \sin \alpha_{cak} \sin \alpha_{can} - 2 \sum_{k=i}^m \sum_{n=i}^m I_{abk} I_{can} \sin \alpha_{abk} \sin \alpha_{can} \quad (4.80)$$

For the conductor B in the three-phase system shown in fig. 4.6, the general expression of the square of the real component $I_{xi-real}^2$ and imaginary component $I_{xi-imag}^2$ through the branch impedance \bar{Z}_{bi} , can be determined by referring to equation (4.77). By setting R_i and X_i in equation (3.6) and (3.8) to a value of one and zero respectively for each phase current and equation (3.29) and (3.28) for their product, the result will be:

$$I_{yi-real}^2 = \sum_{y=i}^m I_{bcy}^2 \cos^2 \alpha_{bcy} + 2 \sum_{k=i}^{m-1} \sum_{n=k+1}^m I_{bck} I_{bcn} \cos \alpha_{bck} \cos \alpha_{bcn} \\ + \sum_{y=i}^m I_{aby}^2 \cos^2 \alpha_{aby} + 2 \sum_{k=i}^{m-1} \sum_{n=k+1}^m I_{abk} I_{abn} \cos \alpha_{abk} \cos \alpha_{abn} - 2 \sum_{k=i}^m \sum_{n=i}^m I_{bck} I_{abn} \cos \alpha_{bck} \cos \alpha_{abn} \quad (4.81)$$

$$I_{yi-imag}^2 = \sum_{y=i}^m I_{bcy}^2 \sin^2 \alpha_{bcy} + 2 \sum_{k=i}^{m-1} \sum_{n=k+1}^m I_{bck} I_{bcn} \sin \alpha_{bck} \sin \alpha_{bcn} \\ + \sum_{y=i}^m I_{aby}^2 \sin^2 \alpha_{aby} + 2 \sum_{k=i}^{m-1} \sum_{n=k+1}^m I_{abk} I_{abn} \sin \alpha_{abk} \sin \alpha_{abn} - 2 \sum_{k=i}^m \sum_{n=i}^m I_{bck} I_{abn} \sin \alpha_{bck} \sin \alpha_{abn} \quad (4.82)$$

In the case of the conductor C the general expression of the square of the real component $I_{xi-real}^2$ and imaginary component $I_{xi-imag}^2$ through the branch impedance \bar{Z}_{ci} , can be determined by referring to equation (4.78). By setting R_i and X_i in equation (3.6) and (3.8) to a value of one and zero respectively for each phase current and equation (3.29) and (3.28) for their product, the result will be:

$$I_{zi-real}^2 = \sum_{y=i}^m I_{cay}^2 \cos^2 \alpha_{cay} + 2 \sum_{k=i}^{m-1} \sum_{n=k+1}^m I_{cak} I_{can} \cos \alpha_{cak} \cos \alpha_{can} \\ + \sum_{y=i}^m I_{bcy}^2 \cos^2 \alpha_{bcy} + 2 \sum_{k=i}^{m-1} \sum_{n=k+1}^m I_{bck} I_{bcn} \cos \alpha_{bck} \cos \alpha_{bcn} - 2 \sum_{k=i}^m \sum_{n=i}^m I_{cak} I_{bcn} \cos \alpha_{cak} \cos \alpha_{bcn} \quad (4.83)$$

$$I_{zi-imag}^2 = \sum_{y=i}^m I_{cay}^2 \sin^2 \alpha_{cay} + 2 \sum_{k=i}^{m-1} \sum_{n=k+1}^m I_{cak} I_{can} \sin \alpha_{cak} \sin \alpha_{can}$$

$$+ \sum_{y=i}^m I_{bcy}^2 \sin^2 \alpha_{bcy} + 2 \sum_{k=i}^{m-1} \sum_{n=k+1}^m I_{bck} I_{bcn} \sin \alpha_{bck} \sin \alpha_{bcn} - 2 \sum_{k=i}^m \sum_{n=i}^m I_{cak} I_{bcn} \sin \alpha_{cak} \sin \alpha_{bcn} \quad (4.84)$$

The total power loss $P_{total-Aloss}$, $P_{total-Bloss}$ and $P_{total-Closs}$ on conductor A, B and C respectively, can be expressed as:

$$P_{total-Aloss} = \sum_{k=2}^m R_{ak} (I_{xk-real}^2 + I_{xk-imaginary}^2) \quad (4.85)$$

$$P_{total-Bloss} = \sum_{k=2}^m R_{bk} (I_{yk-real}^2 + I_{yk-imaginary}^2) \quad (4.86)$$

$$P_{total-Closs} = \sum_{k=2}^m R_{ck} (I_{zk-real}^2 + I_{zk-imaginary}^2) \quad (4.87)$$

The overall total power loss on the three-phase system $P_{total-3loss}$ will be the summation of the total powers on conductor A, B and C. Therefore, it can be expressed as:

$$P_{total-3loss} = P_{total-Aloss} + P_{total-Bloss} + P_{total-Closs}$$

$$= \sum_{k=2}^m \{ R_{ak} (I_{xk-real}^2 + I_{xk-imag}^2) + R_{bk} (I_{yk-real}^2 + I_{yk-imag}^2) + R_{ck} (I_{zk-real}^2 + I_{zk-imag}^2) \} \quad (4.88)$$

Equation (4.88) can be interpreted as the instantaneous total power at a given instant or the average total power over a certain period depending on how the currents are defined. In this thesis, the currents are modelled as signals and hence the average total power over a certain period can be evaluated. For example, if the currents repeat the same pattern after each week, then, the cost of the energy on a feeder for a whole year can be evaluated as:

$$Feeder\ cost(Rands) / year = P_{total-3loss} (kW) \frac{52.143 weeks}{1 week} 24hr \times tariff (Rands / kW - hr) \quad (4.89)$$

4.9 Summary

The general expressions for the total real and total imaginary component of the branch voltage drops for each phase of the three-phase system, 3 wire ($\nabla - \nabla$) connections are presented as well as their squares. Also, the general expressions of the nodal currents, nodal admittance, consumer voltages and the total line power losses in distribution systems are presented.

CHAPTER 5

THE PROBABILISTIC APPROACH TO THE EVALUATION OF THE CONSUMER VOLTAGES AND STATISTICAL EVALUATION OF THE LINE POWER LOSSES

5.1 Introduction

The general expression of the consumer voltages due to statistical load currents in single and three-phase MV radial distribution systems are discussed in chapter 4. Extensive research in the application of beta distributed load currents, has shown that a beta-distributed set of currents produce beta distributed set of consumer voltages [5.1,5.2,5.3]. In this chapter, the statistical parameters of the beta-distributed consumer voltages in single and three-phase systems are determined. These statistical parameters will facilitate the evaluation of the consumer voltage percentile values at any confidence level or a given level of risk. The statistical evaluation of the total power losses due to load currents modelled as signal in single and three-phase MV radial distribution systems are also dealt in this chapter based on the general expression of the power losses developed in chapter 4.

5.2 General properties of the beta distribution function

The beta probability density function $f(x)$ is described as:

$$f(x) = \frac{x^{\alpha-1} \cdot (1-x)^{\beta-1}}{B(\alpha, \beta)} \quad (5.1)$$

given the condition: $0 \leq x \leq 1$ and $\alpha > 0$ and $\beta > 0$

and

$$B(\alpha, \beta) = \int_0^1 x^{\alpha-1} \cdot (1-x)^{\beta-1} du \quad (5.2)$$

The moments of the beta distribution function as described in equations (5.1) and (5.2) are expressed by its statistical parameters, α and β . The r^{th} moment about the origin can be expressed as [5.4]:

$$\mu_r = \frac{\alpha^{[r]}}{(\alpha + \beta)^{[r]}} \quad (5.3)$$

where

r is an integer

$p^{[r]} = p(p+1)\dots\dots(p+r-1)$ is the ascending factorial

The first moment of the distribution about the origin or the mean value μ_o is expressed as:

$$\mu_o = \frac{\alpha}{(\alpha + \beta)} \tag{5.4}$$

The variance σ_o^2 is given by:

$$\sigma_o^2 = \frac{\alpha\beta}{(\alpha + \beta)^2(\alpha + \beta + 1)} \tag{5.5}$$

In accordance with equation (5.1), the random variable x should lie between 0 and 1. It is evident that, the values of μ_o and σ_o of equation (5.4) and (5.5) will refer to the data, which fall within the range of zero to 1. If the beta function is to be fitted to observations on a positive random variable whose maximum value is greater than 1, then, the data should be scaled by a certain factor b . The magnitude of b must be equal to, or greater than the maximum value of the variables in the data set [5.5].

The mean of the original data distribution will be:

$$\mu = b \cdot \frac{\alpha}{(\alpha + \beta)} \tag{5.6}$$

Its variance will be:

$$\sigma^2 = b^2 \cdot \frac{\alpha\beta}{(\alpha + \beta)^2(\alpha + \beta + 1)} \tag{5.7}$$

In practice the values of μ , σ and b are used to determine estimates of α and β . By rewriting α and β in terms of the original data μ , σ and b , the result will be

$$\alpha = \frac{\mu(b\mu - \mu^2 - \sigma^2)}{b\sigma^2} \tag{5.8}$$

$$\beta = \frac{(b - \mu)(b\mu - \mu^2 - \sigma^2)}{b\sigma^2} \tag{5.9}$$

In statistics, if $Y_1, Y_2, Y_3, \dots, Y_k$ are independent variables and are identically distributed according to a distribution having parameters α and β , it follows that the expected value is:

$$E[Y_1 \cdot Y_2 \cdot Y_3 \cdot \dots \cdot Y_k] = E[Y_1] \cdot E[Y_2] \cdot E[Y_3] \cdot \dots \cdot E[Y_k] \tag{5.10}$$

According to expressions (5.3), (5.4), and (5.10), the expected values for the variable Y_i , the product of two variables $Y_i.Y_j$ and variable squared Y_i^2 can be expressed as:

$$E[Y_i] = \frac{\alpha}{\alpha + \beta} \tag{5.11}$$

$$E[Y_i.Y_j] = \frac{\alpha^2}{(\alpha + \beta)^2} \tag{5.12}$$

$$E[Y_i^2] = \frac{\alpha(\alpha + 1)}{(\alpha + \beta)(\alpha + \beta + 1)} \tag{5.13}$$

The properties given by equations (5.11), (5.12) and (5.13), are later used to evaluate the first moment and the second moment of the total real and the total imaginary component of the branch voltage drops. These values will be used to determine the first and the second moments of the consumer voltages and hence, the evaluation of their statistical parameters. By applying a built in function BETAINV in *MATLAB* software package, the percentile value of consumer voltages at specified level of risk can be determined.

5.3 Transformation of the branch voltage drop equations

The general expressions of the total real and the total imaginary component of the branch voltage drops together with their squares for single-phase and three-phase radial distribution systems are presented in chapters 3 and 4. The general expression of the consumer voltage at each node is presented in chapter 4. As stated above, the consumer voltage percentile values due to statistical load currents can be determined if the first and the second moments of the total real and the total imaginary component of the branch voltage drops are known. Therefore, the task at hand is to transform the derived expressions of the total real and the total imaginary components of the branch voltage drops into their first and second moments.

Before attempting to derive the first and the second moment general expressions for the total real and the total component of the branch voltage drops, it is a prerequisite to know in advance, the first and second moments of the statistical load currents flowing in the typical branch as depicted in fig. 5.1.

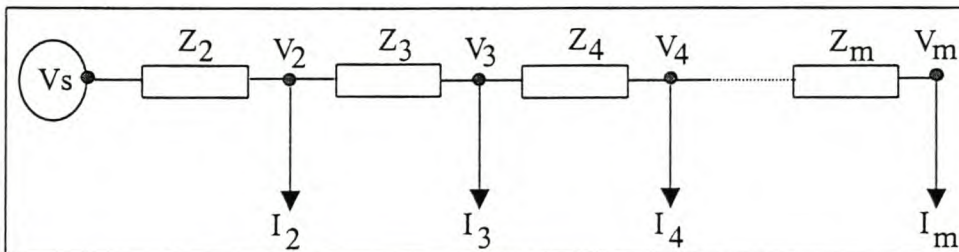


Fig. 5.1: One line diagram for statistical load currents

Suppose each load current has N_i electrical consumers. Therefore at node 2, the current I_2 can be expressed as [5.5]:

$$I_2 = CB_2(Y_1 + Y_2 + Y_3 + Y_4 + Y_5 + Y_6 + \dots + Y_{N_2}) \tag{5.14}$$

where

Y^s are the individual current variates
 CB_2 is the scaling factor or circuit breaker rating

If all Y^s are independent and are identically distributed with parameters α_2 and β_2 , it follows that according to equation (5.11), the expected value of the current I_2 , $E[I_2]$ will be:

$$E[I_2] = CB_2 \cdot N_2 \cdot E[Y] = CB_2 N_2 \left(\frac{\alpha_2}{\alpha_2 + \beta_2} \right) \tag{5.15}$$

According to equation (3.6) and (3.8), the square term of the load currents as well as the product of two load currents is present. Let us consider again node 2 of fig. 5.1, and consider the square of the current I_2 as expressed in equation (5.14). It can be shown that:

$$\begin{aligned} I_2^2 &= \{CB_2(Y_1 + Y_2 + Y_3 + Y_4 + Y_5 + Y_6 + \dots + Y_{N_2})\}^2 \\ &= CB_2^2(Y_1^2 + Y_2^2 + Y_3^2 + Y_4^2 + Y_5^2 + Y_6^2 + \dots + Y_{N_2}^2 + 2Y_1Y_2 + 2Y_1Y_3 + \dots + 2Y_1Y_{N_2} \\ &\quad + 2Y_2Y_3 + 2Y_2Y_4 + \dots + 2Y_2Y_{N_2} + \dots + 2Y_{N_2-1}Y_{N_2}) \end{aligned} \tag{5.16}$$

By referring to equation (5.12) and (5.13), the expected value of the expression (5.16), $E[I_2^2]$ can be written as:

$$\begin{aligned} E[I_2^2] &= CB_2^2 \{N_2 \cdot E[Y^2] + N_2(N_2 - 1) \cdot E[Y] \cdot E[Y]\} \\ &= CB_2^2 \left\{ N_2 \frac{\alpha_2(\alpha_2 + 1)}{(\alpha_2 + \beta_2)(\alpha_2 + \beta_2 + 1)} + N_2(N_2 - 1) \frac{\alpha_2^2}{(\alpha_2^2 + \beta_2^2)} \right\} \end{aligned} \tag{5.17}$$

For the product of two load currents I_k and I_n due to N_k and N_n consumers that are not identically distributed, their expected value $E[I_k I_n]$ can be expressed as:

$$\begin{aligned} E[I_k I_n] &= CB_k CB_n E[Y_k] E[Y_n] N_k N_n \\ &= CB_k CB_n N_k N_n \left(\frac{\alpha_k}{\alpha_k + \beta_k} \right) \left(\frac{\alpha_n}{\alpha_n + \beta_n} \right) \end{aligned} \tag{5.18}$$

The scaling factor CB is valid only on the LV side of the distribution transformer. At the MV distribution line, new scaling factors should be determined. The new scaling factor SF as described in section 4.4.2 should be applied in the analysis.

5.3.1 Dealing with single-phase distribution systems

The transformation of the equations in single-phase systems will be considered in section 5.3.1.1, 5.3.1.2 and 5.3.1.3. If the voltage-profile is different at all nodes on the MV radial distribution systems, the scaling factor SF at each node will be different even if the individual current variates are identically distributed and scaled by the same scaling factor CB. In this present work, different statistical parameters for the statistical load currents are considered, and therefore, the scaling factor and the expected values for the statistical load currents are treated as variables.

5.3.1.1 The expected value of the total real and imaginary component of the branch voltage drops

In view of expression (5.15), the expected value of the total real $E[\Delta V_{ireal_total}]$ and the total imaginary $E[\Delta V_{iimag_total}]$ component of the branch voltage drops of equation (3.9) and (3.10) respectively at node i , can be given as:

$$E[\Delta V_{ireal_total}] = \sum_{y=2}^i \sum_{k=y}^m \{SF_k E[Y_k] N_k (R_y \cos \alpha_k - X_y \sin \alpha_k)\} \quad (5.19)$$

$$E[\Delta V_{iimag_total}] = \sum_{y=2}^i \sum_{k=y}^m \{SF_k E[Y_k] N_k (R_y \sin \alpha_k + X_y \cos \alpha_k)\} \quad (5.20)$$

5.3.1.2 The expected value of the total square of the real component of the branch voltage drops

According to expressions (5.17) and (5.18), the expected value of the square of the total real component of the branch voltage drops at node i , $E[\Delta V^2_{ireal_total_single}]$ of equation (3.22) can be expressed as:

$$E[\Delta V^2_{ireal_total_single}] =$$

$$\sum_{y=2}^i \sum_{Z=y}^m \{SF^2_Z E[Y^2_Z] N_Z (R_y^2 \cos^2 \alpha_Z + X_y^2 \sin^2 \alpha_Z - 2R_y X_y \cos \alpha_Z \sin \alpha_Z)\}$$

$$+ \sum_{y=2}^i \sum_{Z=y}^m \{SF^2_Z E[Y_Z] E[Y_Z] N_Z (N_Z - 1) [R_y^2 \cos^2 \alpha_Z + X_y^2 \sin^2 \alpha_Z - 2R_y X_y \cos \alpha_Z \sin \alpha_Z]\}$$

$$\begin{aligned}
 & + \sum_{y=2}^i \sum_{k=y}^{m-1} \sum_{n=k+1}^m 2SF_k SF_n E[Y_k] E[Y_n] N_k N_n \{R_y^2 \cos \alpha_k \cos \alpha_n + X_y^2 \sin \alpha_k \sin \alpha_n - R_y X_y \sin(\alpha_k + \alpha_n)\} \\
 & + \sum_{t=2}^{i-1} \sum_{r=t+1}^i \sum_{n=r}^m \{SF_n^2 E[Y_n^2] N_n (R_t R_r \cos^2 \alpha_n + X_t X_r \sin^2 \alpha_n \\
 & - R_t X_r \cos \alpha_n \sin \alpha_n - X_t R_r \sin \alpha_n \cos \alpha_n)\} \\
 & + \sum_{t=2}^{i-1} \sum_{r=t+1}^i \sum_{n=r}^m [SF_n^2 E[Y_n] E[Y_n] N_n (N_n - 1) \{R_t R_r \cos^2 \alpha_n + X_t X_r \sin^2 \alpha_n \\
 & - R_t X_r \cos \alpha_n \sin \alpha_n - X_t R_r \sin \alpha_n \cos \alpha_n\}] \\
 & \sum_{t=2}^{i-1} \sum_{r=t+1}^i \sum_{k=t}^m \sum_{\substack{n=r \\ n \neq k}}^m [SF_k SF_n E[Y_k] E[Y_n] N_k N_n (R_t R_r \cos \alpha_k \cos \alpha_n + X_t X_r \sin \alpha_k \sin \alpha_n \\
 & - R_t X_r \cos \alpha_k \sin \alpha_n - X_t R_r \sin \alpha_k \cos \alpha_n)] \tag{5.21}
 \end{aligned}$$

5.3.1.3 The expected value of the total square of the imaginary component of the branch voltage drops

According to expressions (5.17) and (5.18), the expected value of the square of the total imaginary component of the branch voltage drops at node i , $E[\Delta V^2_{imag_total_single}]$ of equation (3.23) can be expressed as:

$$\begin{aligned}
 E[\Delta V^2_{imag_total_single}] = & \\
 & \sum_{y=2}^i \sum_{Z=y}^m \{SF_Z^2 E[Y_Z^2] N_Z (R_y^2 \sin^2 \alpha_Z + X_y^2 \cos^2 \alpha_Z + 2R_y X_y \cos \alpha_Z \sin \alpha_Z)\} \\
 & + \sum_{y=2}^i \sum_{Z=y}^m [SF_Z^2 E[Y_Z] E[Y_Z] N_Z (N_Z - 1) \{R_y^2 \sin^2 \alpha_Z + X_y^2 \cos^2 \alpha_Z + 2R_y X_y \cos \alpha_Z \sin \alpha_Z\}] \\
 & + \sum_{y=2}^i \sum_{k=y}^{m-1} \sum_{n=k+1}^m 2SF_k SF_n E[Y_k] E[Y_n] N_k N_n \{R_y^2 \sin \alpha_k \sin \alpha_n + X_y^2 \cos \alpha_k \cos \alpha_n + R_y X_y \sin(\alpha_k + \alpha_n)\} \\
 & + \sum_{t=2}^{i-1} \sum_{r=t+1}^i \sum_{n=r}^m \{SF_n^2 E[Y_n^2] N_n (R_t R_r \sin^2 \alpha_n + X_t X_r \cos^2 \alpha_n \\
 & + R_t X_r \cos \alpha_n \sin \alpha_n + X_t R_r \sin \alpha_n \cos \alpha_n)\}
 \end{aligned}$$

$$\begin{aligned}
 & + \sum_{t=2}^{i-1} \sum_{r=t+1}^i \sum_{n=r}^m [SF_n^2 E[Y_n] E[Y_n] N_n (N_n - 1) \{R_t R_r \sin^2 \alpha_n + X_t X_r \cos^2 \alpha_n \\
 & + R_t X_r \cos \alpha_n \sin \alpha_n + X_t R_r \sin \alpha_n \cos \alpha_n \}] \\
 & \sum_{t=2}^{i-1} \sum_{r=t+1}^i \sum_{\substack{k=t \\ n \neq k}}^m \sum_{n=r}^m [SF_k SF_n E[Y_k] E[Y_n] N_k N_n (R_t R_r \sin \alpha_k \sin \alpha_n + X_t X_r \cos \alpha_k \cos \alpha_n \\
 & + R_t X_r \cos \alpha_n \sin \alpha_k + X_t R_r \sin \alpha_n \cos \alpha_k)] \tag{5.22}
 \end{aligned}$$

5.3.2 Dealing with three-phase distribution systems

The transformation of the equations in three-phase systems will be considered in the coming sub-sections. If the three-phase system is feeding unbalanced three-phase loads, the voltage profile on each phase will be different. Therefore, each phase should be presented by its own scaling factor at the MV distribution line in order to take care of any system loading.

5.3.2.1 The expected values of the total real component of the branch voltage drops

In this sub-section, the expected value of the total real component of branch voltage drops for phase ba , cb and ac are presented. In view of expression (5.15), the expected value of the total real component of the branch voltage drop for the phase ba at node i , $E[\Delta V_{ba-ireal-total}]$, of equation (4.16) can be expressed as:

$$\begin{aligned}
 E[\Delta V_{ba-ireal-total}] = & \\
 & \sum_{y=2}^i \sum_{k=y}^m [SF_{bak} E[Y_{bak}] N_{bak} \{(R_{ak} + R_{bk}) \cos \alpha_{abk} - (X_{ak} + X_{bk}) \sin \alpha_{abk}\}] \\
 & - \sum_{y=2}^i \sum_{k=y}^m \{SF_{cbk} E[Y_{cbk}] N_{cbk} (R_{bk} \cos \alpha_{bck} - X_{bk} \sin \alpha_{bck})\} \\
 & - \sum_{y=2}^i \sum_{k=y}^m \{SF_{ack} E[Y_{ack}] N_{ack} (R_{ak} \cos \alpha_{cak} - X_{ak} \sin \alpha_{cak})\} \tag{5.23}
 \end{aligned}$$

Similar expressions may be deduced for phases cb and ac .

5.3.2.2 The expected value of the sum of squares of the real component of the branch voltage drops

According to expressions (5.17) and (5.18), the expected value of the sum of squares of the total real component of the branch voltage drops at node i for the phase ba , $E[\Delta V^2_{ba_ireal-total-sum}]$ of equation (4.27) can be given as:

$$\begin{aligned}
 E[\Delta V^2_{ba_ireal-total-sum}] &= \sum_{y=2}^i \sum_{Z=y}^m [SF^2_{baZ} E[Y^2_{baZ}] N_{baZ} \{(R_{ay} + R_{by})^2 \cos^2 \alpha_{abZ} \\
 &+ (X_{ay} + X_{by})^2 \sin^2 \alpha_{abZ} - 2(R_{ay} + R_{by})(X_{ay} + X_{by}) \cos \alpha_{abZ} \sin \alpha_{abZ}\} \\
 &+ SF^2_{baZ} E[Y_{baZ}]^2 N_{baZ} (N_{baZ} - 1) \{(R_{ay} + R_{by})^2 \cos^2 \alpha_{abZ} + (X_{ay} + X_{by})^2 \sin^2 \alpha_{abZ} \\
 &- 2(R_{ay} + R_{by})(X_{ay} + X_{by}) \cos \alpha_{abZ} \sin \alpha_{abZ}\} \\
 &+ SF^2_{cbZ} N_{cbZ} \{E[Y^2_{cbZ}] (R_{by}^2 \cos^2 \alpha_{bcZ} + X_{by}^2 \sin^2 \alpha_{bcZ} - 2R_{by} X_{by} \cos \alpha_{bcZ} \sin \alpha_{bcZ}) \\
 &+ E[Y_{cbZ}]^2 (N_{cbZ} - 1) (R_{by}^2 \cos^2 \alpha_{bcZ} + X_{by}^2 \sin^2 \alpha_{bcZ} - 2R_{by} X_{by} \cos \alpha_{bcZ} \sin \alpha_{bcZ})\} \\
 &+ SF^2_{acZ} N_{acZ} \{E[Y^2_{acZ}] (R_{ay}^2 \cos^2 \alpha_{caZ} + X_{ay}^2 \sin^2 \alpha_{caZ} - 2R_{ay} X_{ay} \cos \alpha_{caZ} \sin \alpha_{caZ}) \\
 &+ E[Y_{acZ}]^2 (N_{acZ} - 1) (R_{ay}^2 \cos^2 \alpha_{caZ} + X_{ay}^2 \sin^2 \alpha_{caZ} - 2R_{ay} X_{ay} \cos \alpha_{caZ} \sin \alpha_{caZ})\}] \\
 &+ \sum_{y=2}^i \sum_{k=y}^{m-1} \sum_{n=k+1}^m [2SF_{bak} SF_{ban} E[Y_{bak}] E[Y_{ban}] N_{bak} N_{ban} \{(R_{ay} + R_{by})^2 \cos \alpha_{abk} \cos \alpha_{abn} \\
 &+ (X_{ay} + X_{by})^2 \sin \alpha_{abk} \sin \alpha_{abn} - (R_{ay} + R_{by})(X_{ay} + X_{by}) \sin(\alpha_{abk} + \alpha_{abn})\} \\
 &+ 2SF_{cbk} SF_{cbn} E[Y_{cbk}] E[Y_{cbn}] N_{cbk} N_{cbn} \{R_{by}^2 \cos \alpha_{bck} \cos \alpha_{bcn} + X_{by}^2 \sin \alpha_{bck} \sin \alpha_{bcn} \\
 &- R_{by} X_{by} \sin(\alpha_{bck} + \alpha_{bcn})\} \\
 &+ 2SF_{ack} SF_{acn} E[Y_{ack}] E[Y_{acn}] N_{ack} N_{acn} \{R_{ay}^2 \cos \alpha_{cak} \cos \alpha_{can} + X_{ay}^2 \sin \alpha_{cak} \sin \alpha_{can} \\
 &- R_{ay} X_{ay} \sin(\alpha_{cak} + \alpha_{can})\}] \\
 &+ \sum_{y=2}^i \sum_{k=y}^m \sum_{n=y}^m [2SF_{bak} SF_{cbn} E[Y_{bak}] E[Y_{cbn}] N_{bak} N_{cbn} \{(R_{ay} + R_{by})(-R_{by}) \cos \alpha_{abk} \cos \alpha_{bcn}
 \end{aligned}$$

$$\begin{aligned}
 & + (X_{ay} + X_{by})(-X_{by}) \sin \alpha_{abk} \sin \alpha_{bcn} \\
 & - (R_{ay} + R_{by})(-X_{by}) \cos \alpha_{abk} \sin \alpha_{bcn} - (X_{ay} + X_{by})(-R_{by}) \sin \alpha_{abk} \cos \alpha_{bcn} \} \\
 & + 2SF_{bak}SF_{acn}E[Y_{bak}]E[Y_{acn}]N_{bak}N_{acn} \{(R_{ay} + R_{by})(-R_{ay}) \cos \alpha_{abk} \cos \alpha_{can} \\
 & + (X_{ay} + X_{by})(-X_{ay}) \sin \alpha_{abk} \sin \alpha_{can} \\
 & - (R_{ay} + R_{by})(-X_{ay}) \cos \alpha_{abk} \sin \alpha_{can} - (X_{ay} + X_{by})(-R_{ay}) \sin \alpha_{abk} \cos \alpha_{can} \} \\
 & + 2SF_{cbk}SF_{acn}E[Y_{cbk}]E[Y_{acn}]N_{cbk}N_{acn} \{R_{by}R_{ay} \cos \alpha_{bck} \cos \alpha_{can} \\
 & + X_{by}X_{ay} \sin \alpha_{bck} \sin \alpha_{can} - R_{by}X_{ay} \cos \alpha_{bck} \sin \alpha_{can} - X_{by}R_{ay} \sin \alpha_{bck} \cos \alpha_{can} \} \quad (5.24)
 \end{aligned}$$

Similar expressions may be deduced for phases cb and ac .

5.3.2.3 The expected value of the sum of squares of the imaginary component of the branch voltage drops

According to expressions (5.17) and (5.18), the expected value of the sum of squares of the total imaginary component of the branch voltage drops at node i for the phase ba , $E[\Delta V^2_{ba_iimag-total-sum}]$ of equation (4.28) can be given as:

$$\begin{aligned}
 E[\Delta V^2_{ba_iimag-total-sum}] & = \sum_{y=2}^i \sum_{Z=y}^m [SF^2_{baZ} E[Y^2_{baZ}] N_{baZ} \{(R_{ay} + R_{by})^2 \sin^2 \alpha_{abZ} \\
 & + (X_{ay} + X_{by})^2 \cos^2 \alpha_{abZ} + 2(R_{ay} + R_{by})(X_{ay} + X_{by}) \cos \alpha_{abZ} \sin \alpha_{abZ} \} \\
 & + SF^2_{baZ} E[Y_{baZ}]^2 N_{baZ} (N_{baZ} - 1) \{(R_{ay} + R_{by})^2 \sin^2 \alpha_{abZ} + (X_{ay} + X_{by})^2 \cos^2 \alpha_{abZ} \\
 & + 2(R_{ay} + R_{by})(X_{ay} + X_{by}) \cos \alpha_{abZ} \sin \alpha_{abZ} \} \\
 & + SF^2_{cbZ} N_{cbZ} \{E[Y^2_{cbZ}] (R_{by}^2 \sin^2 \alpha_{bcZ} + X_{by}^2 \cos^2 \alpha_{bcZ} + 2R_{by}X_{by} \cos \alpha_{bcZ} \sin \alpha_{bcZ}) \\
 & + E[Y_{cbZ}]^2 (N_{cbZ} - 1) (R_{by}^2 \sin^2 \alpha_{bcZ} + X_{by}^2 \cos^2 \alpha_{bcZ} + 2R_{by}X_{by} \cos \alpha_{bcZ} \sin \alpha_{bcZ}) \} \\
 & + SF^2_{acZ} N_{acZ} \{E[Y^2_{acZ}] (R_{ay}^2 \sin^2 \alpha_{caZ} + X_{ay}^2 \cos^2 \alpha_{caZ} + 2R_{ay}X_{ay} \cos \alpha_{caZ} \sin \alpha_{caZ}) \\
 & + E[Y_{acZ}]^2 (N_{acZ} - 1) (R_{ay}^2 \sin^2 \alpha_{caZ} + X_{ay}^2 \cos^2 \alpha_{caZ} + 2R_{ay}X_{ay} \cos \alpha_{caZ} \sin \alpha_{caZ}) \} \}
 \end{aligned}$$

$$\begin{aligned}
 & + \sum_{y=2}^i \sum_{k=y}^{m-1} \sum_{n=k+1}^m [2SF_{bak} SF_{ban} E[Y_{bak}] E[Y_{ban}] N_{bak} N_{ban} \{(R_{ay} + R_{by})^2 \sin \alpha_{abk} \sin \alpha_{abn} \\
 & + (X_{ay} + X_{by})^2 \cos \alpha_{abk} \cos \alpha_{abn} + (R_{ay} + R_{by})(X_{ay} + X_{by}) \sin(\alpha_{abk} + \alpha_{abn})\} \\
 & + 2SF_{cbk} SF_{cbn} E[Y_{cbk}] E[Y_{cbn}] N_{cbk} N_{cbn} \{R_{by}^2 \sin \alpha_{bck} \sin \alpha_{bcn} + X_{by}^2 \cos \alpha_{bck} \cos \alpha_{bcn} \\
 & + R_{by} X_{by} \sin(\alpha_{bck} + \alpha_{bcn})\} \\
 & + 2SF_{ack} SF_{acn} E[Y_{ack}] E[Y_{acn}] N_{ack} N_{acn} \{R_{ay}^2 \sin \alpha_{cak} \sin \alpha_{can} + X_{ay}^2 \cos \alpha_{cak} \cos \alpha_{can} \\
 & + R_{ay} X_{ay} \sin(\alpha_{cak} + \alpha_{can})\}] \\
 & + \sum_{y=2}^i \sum_{k=y}^m \sum_{n=y}^m [2SF_{bak} SF_{cbn} E[Y_{bak}] E[Y_{cbn}] N_{bak} N_{cbn} \{(R_{ay} + R_{by})(-R_{by}) \sin \alpha_{abk} \sin \alpha_{bcn} \\
 & + (X_{ay} + X_{by})(-X_{by}) \cos \alpha_{abk} \cos \alpha_{bcn} \\
 & + (R_{ay} + R_{by})(-X_{by}) \sin \alpha_{abk} \cos \alpha_{bcn} + (X_{ay} + X_{by})(-R_{by}) \cos \alpha_{abk} \sin \alpha_{bcn}\} \\
 & + 2SF_{bak} SF_{acn} E[Y_{bak}] E[Y_{acn}] N_{bak} N_{acn} \{(R_{ay} + R_{by})(-R_{ay}) \sin \alpha_{abk} \sin \alpha_{can} \\
 & + (X_{ay} + X_{by})(-X_{ay}) \cos \alpha_{abk} \cos \alpha_{can} \\
 & + (R_{ay} + R_{by})(-X_{ay}) \sin \alpha_{abk} \cos \alpha_{can} + (X_{ay} + X_{by})(-R_{ay}) \cos \alpha_{abk} \sin \alpha_{can}\} \\
 & + 2SF_{cbk} SF_{acn} E[Y_{cbk}] E[Y_{acn}] N_{cbk} N_{acn} \{R_{by} R_{ay} \sin \alpha_{bck} \sin \alpha_{can} \\
 & + X_{by} X_{ay} \cos \alpha_{bck} \cos \alpha_{can} + R_{by} X_{ay} \sin \alpha_{bck} \cos \alpha_{can} + X_{by} R_{ay} \cos \alpha_{bck} \sin \alpha_{can}\}] \quad (5.25)
 \end{aligned}$$

Similar expressions may be deduced for phases cb and ac .

5.3.2.4 The expected value of the sum product term of the real component of the branch voltage drops

According to expressions (5.17) and (5.18), at node i , the expected value of the real component of the sum product of the branch voltage drops for phase ba , $E[\Delta^* \Delta V_{ba_ireal-sum}]$ of equation (4.29) can be expressed as:

$$E[\Delta^* \Delta V_{ba_ireal-sum}] = \sum_{t=2}^{i-1} \sum_{r=t+1}^i \sum_{n=r}^m SF_{ban}^2 E[Y_{ban}^2] N_{ban} \{(R_{at} + R_{bt})(R_{ar} + R_{br}) \cos^2 \alpha_{abn}$$

$$\begin{aligned}
 & + (X_{at} + X_{bt})(X_{ar} + X_{br}) \sin^2 \alpha_{abn} \\
 & - (R_{at} + R_{bt})(X_{ar} + X_{br}) \cos \alpha_{abn} \sin \alpha_{abn} - (X_{at} + X_{bt})(R_{ar} + R_{br}) \sin \alpha_{abn} \cos \alpha_{abn} \} \\
 & + \sum_{t=2}^{i-1} \sum_{r=t+1}^i \sum_{n=r}^m SF_{ban}^2 E[Y_{ban}]^2 N_{ban} (N_{ban} - 1) \{ (R_{at} + R_{bt})(R_{ar} + R_{br}) \cos^2 \alpha_{abn} \\
 & + (X_{at} + X_{bt})(X_{ar} + X_{br}) \sin^2 \alpha_{abn} \\
 & - (R_{at} + R_{bt})(X_{ar} + X_{br}) \cos \alpha_{abn} \sin \alpha_{abn} - (X_{at} + X_{bt})(R_{ar} + R_{br}) \sin \alpha_{abn} \cos \alpha_{abn} \} \\
 & + \sum_{t=2}^{i-1} \sum_{r=t+1}^i \sum_{\substack{k=t \\ n \neq k}}^m \sum_{n=r}^m SF_{bak} SF_{ban} E[Y_{bak}] E[Y_{ban}] N_{bak} N_{ban} (R_{at} R_{ar} \cos \alpha_{abk} \cos \alpha_{abn} \\
 & + X_{at} X_{ar} \sin \alpha_{abk} \sin \alpha_{abn} - R_{at} X_{ar} \cos \alpha_{abk} \sin \alpha_{abn} - X_{at} R_{ar} \sin \alpha_{abk} \cos \alpha_{abn}) \\
 & + \sum_{t=2}^{i-1} \sum_{r=t+1}^i \sum_{n=r}^m SF_{cbn}^2 E[Y_{cbn}]^2 N_{cbn} \{ R_{bt} R_{br} \cos^2 \alpha_{bcn} + X_{bt} X_{br} \sin^2 \alpha_{bcn} \\
 & - R_{bt} X_{br} \cos \alpha_{bcn} \sin \alpha_{bcn} - X_{bt} R_{br} \sin \alpha_{bcn} \cos \alpha_{bcn} \} \\
 & + \sum_{t=2}^{i-1} \sum_{r=t+1}^i \sum_{n=r}^m SF_{cbn}^2 E[Y_{cbn}]^2 N_{cbn} (N_{cbn} - 1) \{ R_{bt} R_{br} \cos^2 \alpha_{bcn} + X_{bt} X_{br} \sin^2 \alpha_{bcn} \\
 & - R_{bt} X_{br} \cos \alpha_{bcn} \sin \alpha_{bcn} - X_{bt} R_{br} \sin \alpha_{bcn} \cos \alpha_{bcn} \} \\
 & + \sum_{t=2}^{i-1} \sum_{r=t+1}^i \sum_{\substack{k=t \\ n \neq k}}^m \sum_{n=r}^m SF_{cbk} SF_{cbn} E[Y_{cbk}] E[Y_{cbn}] N_{cbk} N_{cbn} \{ R_{bt} R_{br} \cos \alpha_{bck} \cos \alpha_{bcn} \\
 & + X_{bt} X_{br} \sin \alpha_{bck} \sin \alpha_{bcn} - R_{bt} X_{br} \cos \alpha_{bck} \sin \alpha_{bcn} - X_{bt} R_{br} \sin \alpha_{bck} \cos \alpha_{bcn} \} \\
 & + \sum_{t=2}^{i-1} \sum_{r=t+1}^i \sum_{n=r}^m SF_{acn}^2 E[Y_{acn}]^2 N_{acn} \{ R_{at} R_{ar} \cos^2 \alpha_{can} + X_{at} X_{ar} \sin^2 \alpha_{can} \\
 & - R_{at} X_{ar} \cos \alpha_{can} \sin \alpha_{can} - X_{at} R_{ar} \sin \alpha_{can} \cos \alpha_{can} \} \\
 & + \sum_{t=2}^{i-1} \sum_{r=t+1}^i \sum_{n=r}^m SF_{acn}^2 E[Y_{acn}]^2 N_{acn} (N_{acn} - 1) \{ R_{at} R_{ar} \cos^2 \alpha_{can} + X_{at} X_{ar} \sin^2 \alpha_{can} \\
 & - R_{at} X_{ar} \cos \alpha_{can} \sin \alpha_{can} - X_{at} R_{ar} \sin \alpha_{can} \cos \alpha_{can} \}
 \end{aligned}$$

$$\begin{aligned}
 & + \sum_{t=2}^{i-1} \sum_{r=t+1}^i \sum_{k=t}^m \sum_{\substack{n=r \\ n \neq k}}^m SF_{ack} SF_{acn} E[Y_{ack}] E[Y_{acn}] N_{ack} N_{acn} \{R_{at} R_{ar} \cos \alpha_{cak} \cos \alpha_{can} \\
 & + X_{at} X_{ar} \sin \alpha_{cak} \sin \alpha_{can} - R_{at} X_{ar} \cos \alpha_{cak} \sin \alpha_{can} - X_{at} R_{ar} \sin \alpha_{cak} \cos \alpha_{can}\} \\
 & + \sum_{t=2}^{i-1} \sum_{r=t+1}^i \sum_{k=t}^m \sum_{n=r}^m SF_{bak} SF_{cbn} E[Y_{bak}] E[Y_{cbn}] N_{bak} N_{cbn} \{(R_{at} + R_{bt})(-R_{br}) \cos \alpha_{abk} \cos \alpha_{bcn} \\
 & + (X_{at} + X_{bt})(-X_{br}) \sin \alpha_{abk} \sin \alpha_{bcn} \\
 & - (R_{at} + R_{bt})(-X_{br}) \cos \alpha_{abk} \sin \alpha_{bcn} - (X_{at} + X_{bt})(-R_{br}) \sin \alpha_{abk} \cos \alpha_{bcn}\} \\
 & + \sum_{t=2}^{i-1} \sum_{r=t+1}^i \sum_{k=t}^m \sum_{n=r}^m SF_{cbk} SF_{bak} E[Y_{cbk}] E[Y_{bak}] N_{cbk} N_{ban} \{(-R_{bt})(R_{ar} + R_{br}) \cos \alpha_{bck} \cos \alpha_{abn} \\
 & + (-X_{bt})(X_{ar} + X_{br}) \sin \alpha_{bck} \sin \alpha_{abn} \\
 & - (-R_{bt})(X_{ar} + X_{br}) \cos \alpha_{bck} \sin \alpha_{abn} - (-X_{bt})(R_{ar} + R_{br}) \sin \alpha_{bck} \cos \alpha_{abn}\} \\
 & + \sum_{t=2}^{i-1} \sum_{r=t+1}^i \sum_{k=t}^m \sum_{n=r}^m SF_{bak} SF_{acn} E[Y_{bak}] E[Y_{acn}] N_{bak} N_{acn} \{(R_{at} + R_{bt})(-R_{ar}) \cos \alpha_{abk} \cos \alpha_{can} \\
 & + (X_{at} + X_{bt})(-X_{ar}) \sin \alpha_{abk} \sin \alpha_{can} \\
 & - (R_{at} + R_{bt})(-X_{ar}) \cos \alpha_{abk} \sin \alpha_{can} - (X_{at} + X_{bt})(-R_{ar}) \sin \alpha_{abk} \cos \alpha_{can}\} \\
 & + \sum_{t=2}^{i-1} \sum_{r=t+1}^i \sum_{k=t}^m \sum_{n=r}^m SF_{ack} SF_{ban} E[Y_{ack}] E[Y_{ban}] N_{ack} N_{ban} \{(-R_{at})(R_{ar} + R_{br}) \cos \alpha_{cak} \cos \alpha_{abn} \\
 & + (-X_{at})(X_{ar} + X_{br}) \sin \alpha_{cak} \sin \alpha_{abn} \\
 & - (-R_{at})(X_{ar} + X_{br}) \cos \alpha_{cak} \sin \alpha_{abn} - (-X_{at})(R_{ar} + R_{br}) \sin \alpha_{cak} \cos \alpha_{abn}\} \tag{5.26}
 \end{aligned}$$

Similar expressions may be deduced for phases cb and ac .

5.3.2.5 The expected value of the sum product term of the imaginary component of the branch voltage drops

According to expressions (5.17) and (5.18), at node i , the expected value of the imaginary component of the sum product of the branch voltage drops for the phase ba , $E[\Delta^* \Delta V_{ba_iimag-sum}]$ of equation (4.30) can be expressed as:

$$\begin{aligned}
 E[\Delta * \Delta V_{ba_iimag-sum}] &= \sum_{t=2}^{i-1} \sum_{r=t+1}^i \sum_{n=r}^m SF^2_{ban} E[Y^2_{ban}] N_{ban} \{ (R_{at} + R_{bt})(R_{ar} + R_{br}) \sin^2 \alpha_{abn} \\
 &+ (X_{at} + X_{bt})(X_{ar} + X_{br}) \cos^2 \alpha_{abn} \\
 &+ (R_{at} + R_{bt})(X_{ar} + X_{br}) \sin \alpha_{abn} \cos \alpha_{abn} + (X_{at} + X_{bt})(R_{ar} + R_{br}) \cos \alpha_{abn} \sin \alpha_{abn} \} \\
 &+ \sum_{t=2}^{i-1} \sum_{r=t+1}^i \sum_{n=r}^m SF^2_{ban} E[Y_{ban}]^2 N_{ban} (N_{ban} - 1) \{ (R_{at} + R_{bt})(R_{ar} + R_{br}) \sin^2 \alpha_{abn} \\
 &+ (X_{at} + X_{bt})(X_{ar} + X_{br}) \cos^2 \alpha_{abn} \\
 &+ (R_{at} + R_{bt})(X_{ar} + X_{br}) \sin \alpha_{abn} \cos \alpha_{abn} + (X_{at} + X_{bt})(R_{ar} + R_{br}) \cos \alpha_{abn} \sin \alpha_{abn} \} \\
 &+ \sum_{t=2}^{i-1} \sum_{r=t+1}^i \sum_{k=t}^m \sum_{\substack{n=r \\ n \neq k}}^m SF_{bak} SF_{ban} E[Y_{bak}] E[Y_{ban}] N_{bak} N_{ban} (R_{at} R_{ar} \sin \alpha_{abk} \sin \alpha_{abn} \\
 &+ X_{at} X_{ar} \cos \alpha_{abk} \cos \alpha_{abn} + R_{at} X_{ar} \sin \alpha_{abk} \cos \alpha_{abn} + X_{at} R_{ar} \cos \alpha_{abk} \sin \alpha_{abn}) \\
 &+ \sum_{t=2}^{i-1} \sum_{r=t+1}^i \sum_{n=r}^m SF^2_{cbn} E[Y^2_{cbn}] N_{cbn} \{ R_{bt} R_{br} \sin^2 \alpha_{bcn} + X_{bt} X_{br} \cos^2 \alpha_{bcn} \\
 &+ R_{bt} X_{br} \sin \alpha_{bcn} \cos \alpha_{bcn} + X_{bt} R_{br} \cos \alpha_{bcn} \sin \alpha_{bcn} \} \\
 &+ \sum_{t=2}^{i-1} \sum_{r=t+1}^i \sum_{n=r}^m SF^2_{cbn} E[Y_{cbn}]^2 N_{cbn} (N_{cbn} - 1) \{ R_{bt} R_{br} \sin^2 \alpha_{bcn} + X_{bt} X_{br} \cos^2 \alpha_{bcn} \\
 &+ R_{bt} X_{br} \sin \alpha_{bcn} \cos \alpha_{bcn} + X_{bt} R_{br} \cos \alpha_{bcn} \sin \alpha_{bcn} \} \\
 &+ \sum_{t=2}^{i-1} \sum_{r=t+1}^i \sum_{k=t}^m \sum_{\substack{n=r \\ n \neq k}}^m SF_{cbk} SF_{cbn} E[Y_{cbk}] E[Y_{cbn}] N_{cbk} N_{cbn} \{ R_{bt} R_{br} \sin \alpha_{bck} \sin \alpha_{bcn} \\
 &+ X_{bt} X_{br} \cos \alpha_{bck} \cos \alpha_{bcn} + R_{bt} X_{br} \sin \alpha_{bck} \cos \alpha_{bcn} + X_{bt} R_{br} \cos \alpha_{bck} \sin \alpha_{bcn} \} \\
 &+ \sum_{t=2}^{i-1} \sum_{r=t+1}^i \sum_{n=r}^m SF^2_{acn} E[Y^2_{acn}] N_{acn} \{ R_{at} R_{ar} \sin^2 \alpha_{can} + X_{at} X_{ar} \cos^2 \alpha_{can} \\
 &+ R_{at} X_{ar} \sin \alpha_{can} \cos \alpha_{can} + X_{at} R_{ar} \cos \alpha_{can} \sin \alpha_{can} \} \\
 &+ \sum_{t=2}^{i-1} \sum_{r=t+1}^i \sum_{n=r}^m SF^2_{acn} E[Y_{acn}]^2 N_{acn} (N_{acn} - 1) \{ R_{at} R_{ar} \sin^2 \alpha_{can} + X_{at} X_{ar} \cos^2 \alpha_{can}
 \end{aligned}$$

$$\begin{aligned}
 & + R_{at} X_{ar} \sin \alpha_{can} \cos \alpha_{can} + X_{at} R_{ar} \cos \alpha_{can} \sin \alpha_{can} \} \\
 & + \sum_{t=2}^{i-1} \sum_{r=t+1}^i \sum_{k=t}^m \sum_{\substack{n=r \\ n \neq k}}^m SF_{ack} SF_{acn} E[Y_{ack}] E[Y_{acn}] N_{ack} N_{acn} \{ R_{at} R_{ar} \sin \alpha_{cak} \sin \alpha_{can} \\
 & + X_{at} X_{ar} \cos \alpha_{cak} \cos \alpha_{can} + R_{at} X_{ar} \sin \alpha_{cak} \cos \alpha_{can} + X_{at} R_{ar} \cos \alpha_{cak} \sin \alpha_{can} \} \\
 & + \sum_{t=2}^{i-1} \sum_{r=t+1}^i \sum_{k=t}^m \sum_{n=r}^m SF_{bak} SF_{cbn} E[Y_{bak}] E[Y_{cbn}] N_{bak} N_{cbn} \{ (R_{at} + R_{bt}) (-R_{br}) \sin \alpha_{abk} \sin \alpha_{bcn} \\
 & + (X_{at} + X_{bt}) (-X_{br}) \cos \alpha_{abk} \cos \alpha_{bcn} \\
 & + (R_{at} + R_{bt}) (-X_{br}) \sin \alpha_{abk} \cos \alpha_{bcn} + (X_{at} + X_{bt}) (-R_{br}) \cos \alpha_{abk} \sin \alpha_{bcn} \} \\
 & + \sum_{t=2}^{i-1} \sum_{r=t+1}^i \sum_{k=t}^m \sum_{n=r}^m SF_{cbk} SF_{bak} E[Y_{cbk}] E[Y_{bak}] N_{cbk} N_{ban} \{ (-R_{bt}) (R_{ar} + R_{br}) \sin \alpha_{bck} \sin \alpha_{abn} \\
 & + (-X_{bt}) (X_{ar} + X_{br}) \cos \alpha_{bck} \cos \alpha_{abn} \\
 & + (-R_{bt}) (X_{ar} + X_{br}) \sin \alpha_{bck} \cos \alpha_{abn} + (-X_{bt}) (R_{ar} + R_{br}) \cos \alpha_{bck} \sin \alpha_{abn} \} \\
 & + \sum_{t=2}^{i-1} \sum_{r=t+1}^i \sum_{k=t}^m \sum_{n=r}^m SF_{bak} SF_{acn} E[Y_{bak}] E[Y_{acn}] N_{bak} N_{acn} \{ (R_{at} + R_{bt}) (-R_{ar}) \sin \alpha_{abk} \sin \alpha_{can} \\
 & + (X_{at} + X_{bt}) (-X_{ar}) \cos \alpha_{abk} \cos \alpha_{can} \\
 & + (R_{at} + R_{bt}) (-X_{ar}) \sin \alpha_{abk} \cos \alpha_{can} + (X_{at} + X_{bt}) (-R_{ar}) \cos \alpha_{abk} \sin \alpha_{can} \} \\
 & + \sum_{t=2}^{i-1} \sum_{r=t+1}^i \sum_{k=t}^m \sum_{n=r}^m SF_{ack} SF_{ban} E[Y_{ack}] E[Y_{ban}] N_{ack} N_{ban} \{ (-R_{at}) (R_{ar} + R_{br}) \sin \alpha_{cak} \sin \alpha_{abn} \\
 & + (-X_{at}) (X_{ar} + X_{br}) \cos \alpha_{cak} \cos \alpha_{abn} \\
 & + (-R_{at}) (X_{ar} + X_{br}) \sin \alpha_{cak} \cos \alpha_{abn} + (-X_{at}) (R_{ar} + R_{br}) \cos \alpha_{cak} \sin \alpha_{abn} \}
 \end{aligned} \tag{5.27}$$

Similar expressions may be deduced for phases cb and ac .

Note: The expected value of the square of the total real component of the branch voltage drop for each phase at any node, will be the summation of the expected value of the sum of the squares of the total real and the sum product term of the real component of the

branch voltage drops. The same description applies also to the expected value of the total square of the imaginary component at each node for individual phases.

5.4 Determination of the consumer voltage percentile values

As mentioned previously, it is already demonstrated that, the beta distributed load currents produce consumer voltages that have beta distribution function. The general expression of the first and second moment of the consumer voltage distribution V_{scon_i} at node i , can be determined by finding the expected values of equation (4.48) and (4.49) respectively. When dealing with a beta distribution function, the magnitude of the random variable should lie in the interval (0,1) and is associated with positive statistical parameters $\alpha_v^\#$ and $\beta_v^\#$. Due to these conditions, the consumer voltage random variable V_{scon_i} at node i , should be scaled or normalised in order to satisfy the magnitude criteria and at the same time rendering positive statistical parameters $\alpha_{vi}^\#$ and $\beta_{vi}^\#$. The scaling factor adopted in this present work is the MV nominal voltage or the operating voltage V_S . Therefore, the normalised consumer voltage $V^\#_{scon_i}$ can be expressed as:

$$V^\#_{scon_i} = \frac{V_{scon_i}}{V_S} \quad (5.28)$$

Referring to equation (5.11), the expected value of the normalised consumer voltage $E[V^\#_{scon_i}]$ can be expressed as:

$$E[V^\#_{scon_i}] = E\left[\frac{V_{scon_i}}{V_S}\right] = \frac{\alpha_{vi}^\#}{\alpha_{vi}^\# + \beta_{vi}^\#} \quad (5.29)$$

It follows that according to equation (5.13), the 2nd moment of the scaled consumer voltage $E[V^{\#2}_{scon_i}]$ can be expressed as:

$$E[V^{\#2}_{scon_i}] = E\left[\frac{V^2_{scon_i}}{V_S^2}\right] = \frac{\alpha_{vi}^\#(\alpha_{vi}^\# + \beta_{vi}^\#)}{(\alpha_{vi}^\# + \beta_{vi}^\#)(\alpha_{vi}^\# + \beta_{vi}^\# + 1)} \quad (5.30)$$

According to reference [5.5], the statistical parameters $\alpha_{vi}^\#$ and $\beta_{vi}^\#$ of the scaled consumer voltage at node i , can be expressed as:

$$\alpha_{vi}^\# = \frac{E[V^{\#2}_{scon_i}] - E[V^\#_{scon_i}]^2}{E[V^\#_{scon_i}] - E[V^\#_{scon_i}]^2} \quad (5.31)$$

$$\beta_{vi}^{\#} = \frac{\alpha_{vi}^{\#}}{E[V_{scon_i}^{\#}]} - \alpha_{vi}^{\#} \quad (5.32)$$

From equation (4.48), the expected value of the normalised consumer voltage $E[V_{scon_i}^{\#}]$ at node i , can be expressed as:

$$\begin{aligned} E[V_{scon_i}^{\#}] = & 1 - \frac{E[\Delta V_{ireal_total}]}{V_S} + 0.501 \frac{E[\Delta V_{iimag_total}^2]}{V_S^2} \\ & + 0.448 \frac{E[\Delta V_{ireal_total}]E[\Delta V_{iimag_total}^2]}{V_S^3} + 0.829 \frac{E[\Delta V_{ireal_total}^2]E[\Delta V_{iimag_total}^2]}{V_S^4} \end{aligned} \quad (5.33)$$

Also, from equation (4.49), the second moment of the normalised consumer voltage $E[V_{scon_i}^{\#2}]$ at node i , can be expressed as:

$$E[V_{scon_i}^{\#2}] = 1 - 2 \frac{E[\Delta V_{ireal_total}]}{V_S} + \frac{E[\Delta V_{ireal_total}^2]}{V_S^2} + \frac{E[\Delta V_{iimag_total}^2]}{V_S^2} \quad (5.34)$$

When the probabilistic approach is used for consumer voltage calculations, a range of values is obtained. By assigning a confidence level or alternatively a level of risk in percent, a percentile voltage value or a single voltage value for design purposes can be extracted from the voltage probabilistic density function. By substituting equation (5.33) and (5.34) in equation (5.31) and (5.32), the statistical parameters of the normalised consumer voltage $\alpha_{vi}^{\#}$ and $\beta_{vi}^{\#}$ at node i can be evaluated. The percentile value of the consumer voltage $V_{scon_i}^{\#}$ at node i can be obtained by applying a built in function BETAINV in MATLAB software package at a specified level of risk R as:

$$V_{scon_i}^{\#} = BETAINV(R, \alpha_{vi}^{\#}, \beta_{vi}^{\#}) \quad (5.35)$$

Finally, the actual consumer voltage V_{scon_i} at node i at a specified level of risk is calculated through rescaling the consumer voltage $V_{scon_i}^{\#}$ of equation (5.28). Therefore, it can be expressed as:

$$V_{scon_i} = V_{scon_i}^{\#} * V_S \quad (5.36)$$

Note: The BETAINV is common to the other software packages e.g. MS Excel etc.

5.4.2 Evaluation of the consumer voltage percentile value in single-phase MV distribution systems

The first moment of the total real component of the branch voltage drops and the second moment of the total real and the total imaginary component of the branch voltage drops to be

applied in equation (5.33) and (5.34) are presented in equation (5.19), (5.21) and (5.22). By applying these expressions, the statistical parameters of the normalised consumer voltages can be evaluated using equation (5.31) and (5.32) and hence the percentile value of the consumer voltages are finally calculated using equation (5.35) and (5.36).

5.4.3 Evaluation of the consumer voltage percentile value in three-phase MV distribution systems

In three-phase MV distribution systems, the consumer voltage percentile value for the individual phases at each node is done separately. The information contained in section 5.4.1 is applicable for the individual three phases. The first moment of the total real component of the branch voltage drops and the second moment of the total real and the total imaginary component of the branch voltage drop for the individual phases *ba*, *cb* and *ac* should be applied accordingly as previously derived in this chapter.

5.5 Statistical approach for the evaluation of the system power loss in MV radial distribution systems

5.5.1 Introduction

In evaluating the losses in MV radial distribution systems, the concept of treating individual consumer load current as signals in time is applied [5.6]. The reason one uses the signal approach is that losses are usually evaluated over a period of time, for example annual losses whereas voltage drop can be calculated for a particular time slot. The current signal in a given time has a distribution with mean and standard deviation. Furthermore, the individual signals are correlated to each other. The survey conducted in various sites in South Africa confirms the correlation between load currents in domestic consumers [5.6]. In statistics, correlation coefficient can be used to assess the degree of linear dependence between two individual load currents. The determination of the technical loss on a feeder over a period of time is possible by applying the following property of independent random variables [5.7]:

$$E[X^2] = E[X]^2 + V[X] \quad (5.37)$$

$$E[X.Y] = E[X].E[Y] \quad (5.38)$$

where

$E[X^2]$	is the second moment around the origin of the random variable X
$E[X]^2$	is the square of the average value of the random variable X
$V[X]$	is the variance of the random variable X
$E[X.Y]$	is the average value of the product of the random variables X and Y
$E[X]$	is the average value of the random variable X
$E[Y]$	is the average value of the random variable Y

This concept of treating the load currents as signals was developed by Heunis [5.6] and he describes the expected value of the two dependent variables X and Y as:

$$E[XY] = E[X].E[Y] + \rho_{xy}\sigma_x\sigma_y \quad (5.39)$$

where

- ρ_{xy} is the correlation coefficient between two dependent variables X and Y
- σ_x is the standard deviation of variable X
- σ_y is the standard deviation of the variable Y

By applying the equation (5.39) to the data set obtained from NRS LR project [5.8], the analytical results did not compare well with the Monte Carlo simulation results. If equation (5.38) is applied, the analytical results compare well with the Monte Carlo simulation results. This could be due to the value of the average correlation coefficient used. The correlation coefficient used in this present work was obtained from the reference [5.6]. The value of 0.04 applied may be is higher compared to the value of the load data. If expression (5.39) is to be used, the covariance term can be easily accommodated in the general expression of the line losses due to current signals.

The total line loss in MV radial distribution systems can assume a range of probable values due to the number of feeders and the different consumers that might be connected to them. It will be shown later that the spread of the loss distribution is not significant. In the coming sections, the general expressions of the average total line losses on single and three-phase MV radial distribution systems without branches due to load current modelled as signals are derived.

5.5.2 Determination of the general expression of the total line power loss in MV radial distribution systems

As stated in chapter 4, the product of the line resistance and the magnitude of the line current squared determine the line power loss. If the current I_{k_signal} of a consumer k is modelled as a current signal having a mean value μ_k and mean standard deviation σ_k , then for N consumers, the average total μ_{av-T} and the standard deviation total σ_T are defined as [5.6]:

$$\mu_{av-T} = \sum_{k=1}^N \mu_k \quad (5.40)$$

$$\sigma_T = \left\{ \sum_{k=1}^N \sigma_k^2 + \sum_{k=1}^N \sum_{\substack{m=1 \\ k \neq m}}^N \rho_{km} \cdot \sigma_k \sigma_m \right\}^{\frac{1}{2}} \quad (5.41)$$

OR

$$\sigma_T^2 = \sum_{k=1}^N \sigma_k^2 + \sum_{k=1}^N \sum_{\substack{m=1 \\ k \neq m}}^N \rho_{km} \cdot \sigma_k \sigma_m \quad (5.42)$$

where

ρ_{km} is the correlation coefficient between consumer k and consumer m

Based on equation (5.40) and (5.42), if the average of individual means is μ_{ave} , the average of individual variance is σ^2_{ave} and average of the correlation coefficient is ρ_{ave} , then the total average of individual means μ_{ave-T} and the total average of individual variance σ^2_{ave-T} at a specific load point can be expressed in terms of N consumers as:

$$\mu_{ave-T} = N\mu_{ave} \quad (5.43)$$

$$\mu^2_{ave-T} = N^2\mu^2_{ave} \quad (5.44)$$

$$\sigma^2_{ave-T} = N\sigma^2_{ave} + N(N-1)\sigma^2_{ave}\rho_{ave} \quad (5.45)$$

Suppose a line current I_L is due to N consumers, then, the average line power loss P_{loss-1} on a section of resistance R can be calculated as:

$$\begin{aligned} P_{loss-1} &= E[R.I^2_L] = R(\mu^2_{ave-T} + \sigma^2_{ave-T}) \\ &= R\{N^2\mu^2_{ave} + N\sigma^2_{ave} + N(N-1)\sigma^2_{ave}\rho_{ave}\} \end{aligned} \quad (5.46)$$

From equation (5.38) and (5.43), the average line power loss P_{loss-2} due to the product of two currents I_1 and I_2 from N_1 and N_2 consumers respectively on a section of resistance R , can be expressed as:

$$\begin{aligned} P_{loss-2} &= E[R.I_1.I_2] = R.E[I_1]E[I_2] \\ &= RN_1\mu_{ave}N_2\mu_{ave} = RN_1N_2\mu^2_{ave} \end{aligned} \quad (5.47)$$

Equation (5.46) and (5.47) will be applied to transform equations developed in chapter 4 section 4.8.1 and 4.8.2 so that total line power losses in single-phase and three-phase MV radial distribution systems due to the load currents modelled as signals can be evaluated.

5.5.3 The total line power loss in single-phase MV distribution systems

By applying equation (5.46) and (5.47), the general expression of the total power loss $P_{s-total-loss}$ of equation (4.71) on the single-phase distribution systems due to the load currents modelled as signals at each load point, can be expressed as:

$$P_{s-total-loss} = \sum_{i=2}^m [R_i \sum_{y=i}^m \{N^2_y \mu^2_{y-ave} + N_y \sigma^2_{y-ave} + N(N-1)\sigma^2_{y-ave}\rho_{y-ave}\} \cos^2 \alpha_y]$$

$$\begin{aligned}
 &+ R_i \sum_{y=i}^m \{N_y^2 \mu_{y-ave}^2 + N_y \sigma_{y-ave}^2 + N(N-1) \sigma_{y-ave}^2 \rho_{y-ave}\} \sin^2 \alpha_y \\
 &+ 2R_i \sum_{k=i}^{m-1} \sum_{n=k+1}^m N_k N_n \mu_{k-ave} \mu_{n-ave} (\cos \alpha_k \cos \alpha_n + \sin \alpha_k \sin \alpha_n) \quad (5.48)
 \end{aligned}$$

where

R_i	is the line resistance at branch i
N_i	is the number of consumers at node i
μ_{i-ave}	is the average of consumers individual means at node i
σ_{i-ave}^2	is the average of consumers individual variance at node i
ρ_{i-ave}	is the average of consumers correlation coefficient at node i
α_i	is the deterministic current phase angle at node i

5.5.4 The total line power loss in three-phase distribution systems

By applying equation (5.46) and (5.47) to the three-phase distribution system as depicted in fig.4.6, the general expression of the total power loss on each line conductor can be evaluated.

For the line conductor A , the general expression of the total power loss $P_{total-Aloss}$ as given in equation (4.85) due to the load currents modelled as signals at each load point, can be expressed as:

$$\begin{aligned}
 P_{total-Aloss} &= \sum_{i=2}^m \sum_{y=i}^m R_{ai} \{N_{bay}^2 \mu_{bay-ave}^2 + N_{bay} \sigma_{bay-ave}^2 + N_{bay} (N_{bay} - 1) \sigma_{bay-ave}^2 \rho_{bay-ave}\} \cos^2 \alpha_{aby} \\
 &+ \sum_{i=2}^m \sum_{y=i}^m R_{ai} \{N_{bay}^2 \mu_{bay-ave}^2 + N_{bay} \sigma_{bay-ave}^2 + N_{bay} (N_{bay} - 1) \sigma_{bay-ave}^2 \rho_{bay-ave}\} \sin^2 \alpha_{aby} \\
 &+ \sum_{i=2}^m \sum_{y=i}^m R_{ai} \{N_{acy}^2 \mu_{acy-ave}^2 + N_{acy} \sigma_{acy-ave}^2 + N_{acy} (N_{acy} - 1) \sigma_{acy-ave}^2 \rho_{acy-ave}\} \cos^2 \alpha_{cay} \\
 &+ \sum_{i=2}^m \sum_{y=i}^m R_{ai} \{N_{acy}^2 \mu_{acy-ave}^2 + N_{acy} \sigma_{acy-ave}^2 + N_{acy} (N_{acy} - 1) \sigma_{acy-ave}^2 \rho_{acy-ave}\} \sin^2 \alpha_{cay} \\
 &+ \sum_{i=2}^m \sum_{k=i}^{m-1} \sum_{n=k+1}^m 2R_{ai} N_{bak} N_{ban} \mu_{bak-ave} \mu_{ban-ave} (\cos \alpha_{abk} \cos \alpha_{abn} + \sin \alpha_{abk} \sin \alpha_{abn}) \\
 &+ \sum_{i=2}^m \sum_{k=i}^{m-1} \sum_{n=k+1}^m 2R_{ai} N_{ack} N_{acn} \mu_{ack-ave} \mu_{acn-ave} (\cos \alpha_{cak} \cos \alpha_{can} + \sin \alpha_{cak} \sin \alpha_{can})
 \end{aligned}$$

$$-\sum_{i=2}^m \sum_{k=i}^m \sum_{n=i}^m 2R_{ai} N_{bak} N_{acn} \mu_{bak-ave} \mu_{acn-ave} (\cos \alpha_{abk} \cos \alpha_{can} + \sin \alpha_{abk} \sin \alpha_{can}) \quad (5.49)$$

where

R_{ai}	is the line resistance at branch i for line conductor A
N_{bai}	is the number of consumers for phase ba at node i
N_{aci}	is the number of consumers for phase ac at node i
$\mu_{bai-ave}$	is the average of consumers individual means for phase ba at node i
$\mu_{aci-ave}$	is the average of consumers individual means for phase ac at node i
$\sigma^2_{bai-ave}$	is the average of consumers individual variance for phase ba at node i
$\sigma^2_{aci-ave}$	is the average of consumers individual variance for phase ac at node i
$\rho_{bai-ave}$	is the average of consumers correlation coefficient for phase ba at node i
$\rho_{aci-ave}$	is the average of consumers correlation coefficient for phase ac at node i
α_{abi}	is the deterministic current phase angle for phase ba at node i
α_{cai}	is the deterministic current phase angle for phase ac at node i

Similar expressions may be derived for lines B and C .

The overall total power loss $P_{total-3loss}$ will be the summation of the total powers on line conductor A, B and C. Therefore, it can be given as:

$$P_{total-3loss} = P_{total-Aloss} + P_{total-Bloss} + P_{total-Closs} \quad (5.50)$$

5.6 Modelling of load current as signals

The concept adopted in chapter 4 regarding the determination of the overall scaling factor for the statistical load currents is revisited in this section. The variation of the load currents resulting from the voltage profiles along the MV distribution line is evaluated by the usual deterministic power flow analysis of distribution systems using $P-Q$ loads.

The values of the average of individual means μ_{ave} and the average of individual variance σ^2_{ave} as applied previously in section 5.5.3 and 5.5.4 should be average values referred to the MV side of the distribution transformers. In appendix 4-A, the relationship between the mean and standard deviation for the two scenarios with arbitrary values is shown. This requires that, the transformation ratio at each node on the MV distribution line must be calculated on the basis of the average value of the load currents. The procedure to determine the transformation ratio is the same as described in chapter 4, section 4.4.2 and is presented in section 5.6.2. The only difference is the way the average load currents are defined.

5.6.1 Correlation coefficient on the MV distribution line

The correlation coefficient of the loads determined from the previous research [5.6], is the value to be applied at the load side. The present work is pursued on the MV distribution systems. Therefore, it is also necessary to determine the relationship of the correlation coefficient that exists between the data that has been transformed. The relationship in terms of the mean value and the standard deviation is already dealt with in section 5.6.

The correlation coefficient r can be estimated from the data set as [5.9]:

$$r = \frac{\sum (x - \bar{x})(y - \bar{y})}{\{\sum (x - \bar{x})^2 \sum (y - \bar{y})^2\}^{\frac{1}{2}}} \quad (5.51)$$

where

$x - \bar{x}$ is the deviation of each x from the mean \bar{x}
 $y - \bar{y}$ is the deviation of each y from the mean \bar{y}

If the transformation ratio is denoted as n , the new correlation of coefficient denoted r_{new} can be expressed as (see appendix 4-A):

$$\begin{aligned} r_{new} &= \frac{\sum n(x - \bar{x})n(y - \bar{y})}{\{\sum n^2(x - \bar{x})^2 n^2(y - \bar{y})^2\}^{\frac{1}{2}}} \\ &= \frac{\sum (x - \bar{x})(y - \bar{y})}{\{\sum (x - \bar{x})^2 (y - \bar{y})^2\}^{\frac{1}{2}}} \end{aligned} \quad (5.52)$$

According to equations (5.51) and (5.52), the two correlation coefficients are the same. Therefore the correlation coefficient evaluated at the LV level is applicable at the MV distribution level. The correlation coefficient used in this present work was obtained from the reference [5.6]. Heunis determines the correlation coefficient by suggesting the following relationship when N is sufficiently large:

$$E[\sigma^2_n] \approx \frac{N * E[\sigma^2_1] + N(N-1)E[\sigma_1]^2 * E[\rho]}{N^2} \quad (5.53)$$

where

$E[\sigma^2_n]$ is the expected value of the variance of the average current trace of N consumers
 $E[\sigma_1]$ is the expected value of the individual consumer standard deviation
 $E[\sigma^2_1]$ is the expected value of the individual consumer variance
 $E[\rho]$ is the average correlation coefficient term

5.6.2 Evaluation of the transformation ratio due to load current signals

In order to evaluate the transformation ratio due to load current signals, the supply voltage at the LV networks is assumed equal to the nominal voltage. Therefore, at each distribution transformer point, the average load power P_{ave_slv} due to load current signals at a nominal voltage V_{nom_lv} is evaluated as:

$$P_{ave_slv} = V_{nom_lv} \cdot I_{ave_slv} \quad (5.54)$$

The average current I_{ave_slv} as applied in equation (5.54) is defined as the average of individual means designated previously as μ_{ave} .

Therefore, the average load power P_{ave_slv} due to N consumers can be expressed as:

$$P_{ave_slv} = \mu_{ave} \cdot N \cdot V_{nom_lv} \quad (5.55)$$

The average load current \bar{I}_{ave_smv} at each node on the MV distribution system is iteratively evaluated as:

$$\bar{I}_{ave_smv} = \frac{P_{ave_slv}}{\bar{V}_{mv-s}^*} \quad (5.56)$$

where

\bar{V}_{mv-s}^* is the conjugate of the nodal voltage on the MV distribution line due to signal currents

The variable scaling factor k_{var-s} at each node point is evaluated as:

$$k_{var-s} = \frac{I_{ave_smv,lv}}{I_{ave_slv}} \quad (5.57)$$

where

$I_{ave_smv,lv}$ is the I_{ave_smv} value converted to the low voltage side

The overall transformation ratio tr_s at each load point taking into account the variable scaling factor k_{var-s} and the distribution transformer turns ratio D_{tr} is evaluated as:

$$tr_s = k_{var-s} \cdot D_{tr} \quad (5.58)$$

Note that the transformation ratio tr_s at each node can be different due to the fact that the variable scaling factor k_{var-s} can take different values at different load points along the MV distribution system due to the different voltage levels that can be experienced.

5.7 Summary

In this chapter, the general expressions of the first and the second moments of the real and imaginary component of the branch voltage drops at each node in single and three-phase radial distribution systems were derived. These enable the evaluation of the percentile value of the consumer voltages at a specified level of risk as discussed in this chapter. Also presented are the general expressions of the total technical line losses due to load currents modelled as signals in single and three-phase radial distribution systems. It should be understood that, these general expressions are derived from the distribution system without branches. But in practice, the MV radial distribution system consists of many branches. In order to perform the probabilistic load flow based on the general expressions presented in this chapter, a new algorithm will be developed in the next chapter.

DEVELOPMENT OF THE COMPUTER PROGRAMS

6.1 Introduction

The computer program is written in Matlab. Due to the manipulation involved in performing the probabilistic load flow as described by the general expressions developed in chapter 5, it is necessary to formulate an algorithm that can estimate the consumer voltage percentile values and power losses in MV branched distribution systems. To perform the probabilistic load flow due to the statistical load currents and the load currents modelled as signals, the load current phase angles must be determined deterministically. Therefore, the main objective of the deterministic load flow as described in this chapter, is to determine the load current phase angles so that the equations derived in chapter 5 can be implemented. If constant P-Q loads are to be taken into consideration, the combination of the two types of loads should be applied in determining the load phase angles for statistical and the non-statistical load currents. In this work, two power flow algorithms are employed namely, the NR- algorithm and the backward and forward sweep algorithm. The Newton-Raphson algorithm is employed to perform a deterministic load flow for single-phase power distribution systems. The backward and forward sweep algorithm is employed to perform deterministic power load flow for single and three-phase distribution systems. As cited in chapter 2, step-voltage regulators and capacitors are employed to perform the feeder voltage control in single-phase and three-phase MV distribution systems. The algorithms to cater for the application of the feeder voltage regulators are incorporated in the Newton-Raphson and back and forward sweep algorithms. In three-phase systems the algorithm is tailored in such a way that three different line topologies can be evaluated. These line topologies are three-phase, single phase (phase-phase connection) and SWER systems. The NR-algorithm and back and forward sweep algorithms are compared for their rate of convergence when dealing with the combination of statistical and non-statistical load currents in single-phase MV radial distribution systems.

6.2 Application of the Newton-Raphson algorithm

The N-R algorithm is employed to perform a deterministic power flow in single-phase MV radial distribution systems. The algorithm as applied in this work, initially assumes a voltage value of 1 per unit for all nodal voltages including the slack node, which is treated as node 1 with phase angle equal to zero.

The statistical load currents, constant P-Q loads and the effect of capacitive currents that include currents due to line capacitance and the capacitors for feeder voltage regulation are treated as previously indicated in chapter 4. In the case of the feeder voltage control by step-voltage regulator whose turns ratio is 1: t with the admittance Y in p.u. to the tapping side, its electrical modelling between node i and j of the network system is shown in fig. 6.1. The electrical modelling of the step-voltage regulator is incorporated in the Y-bus of the single-phase systems to formulate a new system Y-bus as shown in the reference [6.1].

For single-phase power distribution systems, the set of equations expressing the relationship between the changes in real and reactive powers and the component of nodal voltages in rectangular co-ordinate systems at various nodes can be represented in matrix form [6.2] as shown in equation (6.1).

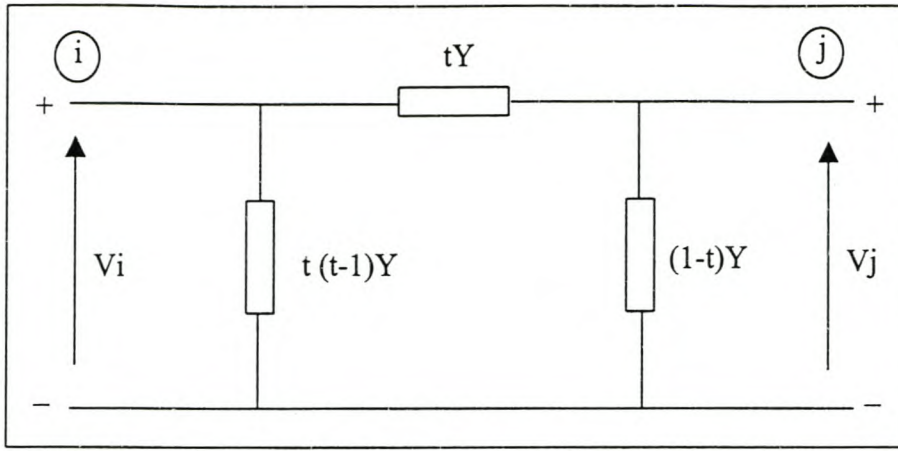


Fig. 6.1: The electrical modelling of a step-voltage regulator between node i and j of the system

$$\begin{bmatrix} \frac{\nabla P}{\nabla Q} \end{bmatrix} = \begin{bmatrix} J_1 & J_2 \\ J_3 & J_4 \end{bmatrix} \begin{bmatrix} \frac{\nabla e}{\nabla f} \end{bmatrix} \quad (6.1)$$

where

∇P is the nodal real power mismatches

∇Q is the nodal reactive power mismatches

∇e is the real component of the nodal voltages to be added to the previous iterated values

∇f is the reactive component of the nodal voltages to be added to the previous iterated values

$J_1 - J_4$ are the jacobian matrices whose elements are derived from the nodal power equations

At a particular nodal point p , the nodal voltage \bar{V}_p expressed in rectangular coordinate system, the real ∇P_p and the reactive ∇Q_p power mismatches are given as:

$$\bar{V}_p = e_p + jf_p \quad (6.2)$$

$$\nabla P_p = -P_{p-scheduled} - P_{p-calculated} \quad (6.3)$$

$$\nabla Q_p = -Q_{p-scheduled} - Q_{p-calculated} \quad (6.4)$$

The calculated real $P_{p-calculated}$ and the calculated imaginary $Q_{p-calculated}$ part of the power at node p are expressed as:

$$P_{p-calculated} = \sum_{q=1}^n \{e_p(e_q G_{pq} + f_q B_{pq}) + f_p(f_q G_{pq} - e_q B_{pq})\} \quad (6.5)$$

$$Q_{p\text{-calculated}} = \sum_{q=1}^n \{f_p(e_q G_{pq} + f_q B_{pq}) - e_p(f_q G_{pq} - e_q B_{pq})\} \quad (6.6)$$

where

G_{pq}, B_{pq} are the real and imaginary parts of the line admittance between nodes p, q
 G_{pp}, B_{pp} are the real and imaginary parts of the self-admittance at node p

The elements of the jacobian $J_1 - J_4$ are given as shown in equations (6.7)- (6.14).

For jacobian J_1 , the off diagonal and the diagonal elements are given in equation (6.7) and (6.8) respectively.

$$\frac{\partial P_p}{\partial e_q} = e_p G_{pq} - f_p B_{pq} \quad q \neq p \quad (6.7)$$

$$\frac{\partial P_p}{\partial e_p} = e_p G_{pp} - f_p B_{pp} + c_p \quad (6.8)$$

For jacobian J_2 , the off diagonal and the diagonal elements are given in equation (6.9) and (6.10) respectively.

$$\frac{\partial P_p}{\partial f_q} = e_p B_{pq} + f_p G_{pq} \quad q \neq p \quad (6.9)$$

$$\frac{\partial P_p}{\partial f_p} = e_p B_{pp} + f_p G_{pp} + d_p \quad (6.10)$$

For jacobian J_3 , the off diagonal and the diagonal elements are given in equation (6.11) and (6.12) respectively.

$$\frac{\partial Q_p}{\partial e_q} = e_p B_{pq} + f_p G_{pq} \quad q \neq p \quad (6.11)$$

$$\frac{\partial Q_p}{\partial e_p} = e_p B_{pp} + f_p G_{pp} - d_p \quad (6.12)$$

For jacobian J_4 , the off diagonal and the diagonal elements are given in equation (6.13) and (6.14) respectively.

$$\frac{\partial Q_p}{\partial f_q} = -e_p G_{pq} + f_p G_{pq} \quad q \neq p \quad (6.13)$$

$$\frac{\partial Q_p}{\partial f_p} = -e_p G_{pp} + f_p G_{pp} + c_p \quad (6.14)$$

where

$$c_p = e_p G_{pp} + f_p B_{pp} + \sum_{\substack{q=1 \\ q \neq p}}^n (e_q G_{pq} + f_q B_{pq}) \text{ is the real component of the current at node } p$$

$$d_p = f_p G_{pp} - e_p B_{pp} + \sum_{\substack{q=1 \\ q \neq p}}^n (f_q G_{pq} - e_q B_{pq}) \text{ is the imaginary component of the current at}$$

node p

After convergence of the algorithm, the phasor node currents at node p due to statistical currents \bar{I}_{p-stat} , due to the constant PQ loads \bar{I}_p , and due to the system shunt admittance \bar{I}_{p-addm} are evaluated as:

$$\bar{I}_{p-stat} = \frac{P_{p-stat}}{\bar{V}_p^*} \quad (6.15)$$

$$\bar{I}_p = \frac{P_p - jQ_p}{\bar{V}_p^*} \quad (6.16)$$

$$\bar{I}_{p-addm} = \bar{V}_p \bar{Y}_p \quad (6.17)$$

where

Y_p is the shunt admittance due to application of voltage regulators and/or line capacitive currents

\bar{V}_p^* is the conjugate voltage at node p

According to equation (6.15), the statistical current phase angle at node p , α_{p-stat} can be evaluated as:

$$\alpha_{p-stat} = \arctan \left\{ \frac{\text{imaginary}(\bar{I}_{p-stat})}{\text{real}(\bar{I}_{p-stat})} \right\} \quad (6.18)$$

The non-statistical phasor current at node p is obtained by summing equation (6.16) and (6.17) and its phase angle is not evaluated as previously discussed in chapter 4.

6.3 Application of the backward and forward sweep algorithm

The backward and forward sweep procedure is adopted to solve for the nodal voltages and currents for single-phase and three-phase distribution systems. The solution technique is the same as the one mentioned in reference [6.3], but uses a different approach. The approach adopted in this reference is based on the line section model that describes the voltage and current relationship across the terminals of a line section. The solution method adopts successive iteration of two steps, called the backward and the forward sweep, which iteratively update the system branch currents and node voltages. However, in this present work the approach is based on the line section(s) connecting the node point in consideration

and the supply node point. To illustrate the process, consider the one line diagram shown in fig. 6.2.

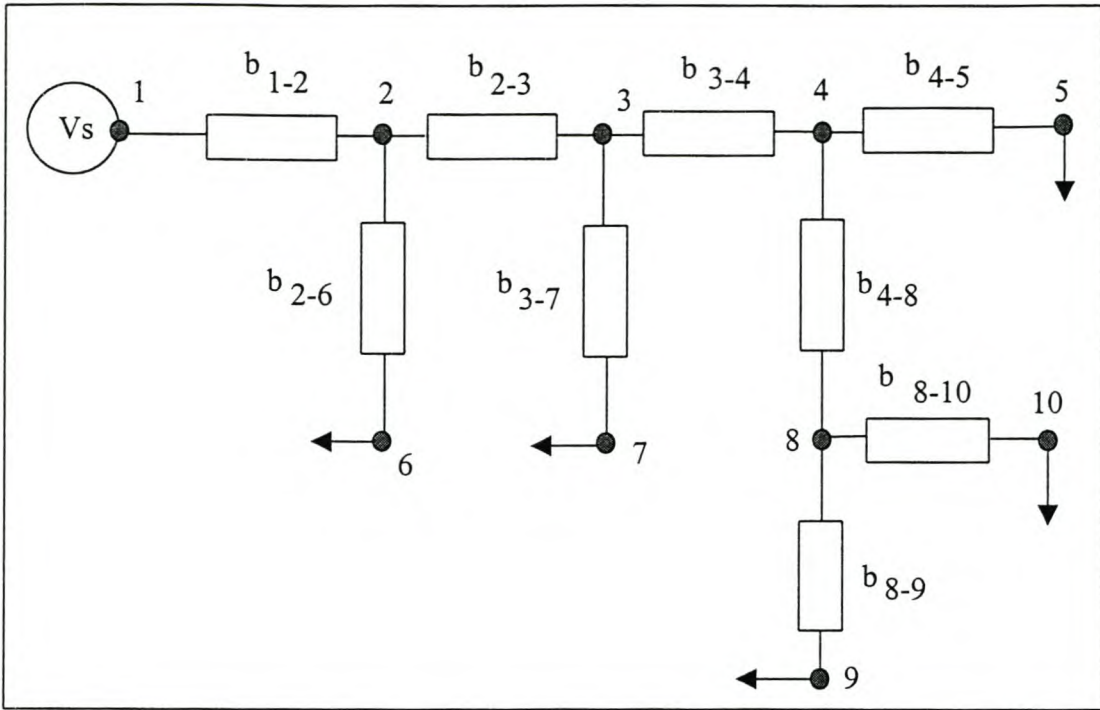


Fig. 6.2: One line diagram for the MV branched radial power distribution system

The forward and backward update procedures as applied in this present work are as follows:

Backward Sweep: Node current update

Applying the updated node voltages, $V_k, k = 2, \dots, 10$, the node currents are then updated as mentioned in chapter 4. It should be understood that, the node currents exist either due to statistical or non-statistical loads or both. If voltage regulators are present, their node currents take part in the solution. The line charging currents can also be included at each node due to the fact that, MV rural power distribution systems are sometimes longer than 80km and should be represented as a medium line model.

Forward Sweep:

Knowing the updated node currents, the node voltages are then updated. This is achieved by tracking all the branch currents in the system due to the node currents by the aid of the developed universal algorithm as described in section 6.5. Given the branch currents, the node voltages are calculated as:

$$\bar{V}_k = V_s - \sum_{i=1}^{N_b} (\bar{I}_i \bar{Z}_i) \quad k = 2, \dots, 10 \quad (6.19)$$

where

V_s is the supply voltage

N_b is the total number of branches connected between node k and the supply node

\bar{I}_i is the total phasor branch current

\bar{Z}_i is the branch impedance

According to equation 6.19, during the forward sweep, the total phasor voltage drop between the supply node and the node k is used to update the node voltages \bar{V}_k . If the voltage at node 9 is of interest, then the total number of branches N_b will be equal to five namely: $b_{8-9}, b_{4-8}, b_{3-4}, b_{2-3}$ and b_{1-2} as shown from fig. 6.2.

6.4 Modelling of step-voltage regulator in three-phase delta-delta connected systems

The step-voltage regulator model described in section 6.2 can easily be accommodated in single and three-phase star-connected systems. Due to the type of loads to be connected to the three-phase backbone feeder, which is delta-delta connected as shown in fig. 6.4, the three-phase star connected system model cannot be realised. But, the model presented in section 6.2, can also be applied in the three-phase delta-delta connected systems. In section 6.4.1, the procedure adopted in this present work is illustrated.

6.4.1 Procedure adopted for modelling a step-voltage regulator

In this present work, the procedure adopted focuses on individual phases. Therefore, if the voltage control is to be considered for the phase ba , the step-voltage regulator model as described in section 6.2 will be applicable only to phase ba , the other phases cb and ac are treated normally. In the case of the phase cb , the step-voltage regulator model will be applicable only to phase cb , the other phases ba and ac are treated normally. The above statement is also applicable to phase ac . In order to implement the above-mentioned procedure, two different line network impedances are required. The two-system network line impedance should be able to represent the new node arrangement for the network system after introduction of the artificial nodes due to the application of the step-voltage regulators.

6.4.1.1 Voltage control for the phase ba

The procedure to be adopted for phase ba is as follows:

- 1) determine the deterministic system voltages and currents without voltage regulators for the phase cb and ac . The statistical current phase angles for phases cb and ac are applied in step 6 when evaluating the consumer voltage percentile values for the phase ba . The non-statistical currents for phases cb and ac are applied in step 7 when evaluating the total real and the total imaginary component of the branch voltage drops at each node for phase ba
- 2) apply the voltage regulator model to phase ba only as described in section 6.2. The network system for phases cb and ac should be modified accordingly
- 3) evaluate the deterministic system voltages and currents for phase ba based on the following:
 - network system parameters for phase ba are obtained in step 2 above
 - network system parameters for other phases cb and ac are obtained in step 2 above

- 4) determine the scaling factors and the phase angles for statistical currents as explained in chapter 4 for the phase *ba* based on the values obtained in step 3
- 5) determine the scaling factors and the phase angles for statistical currents as explained in chapter 4 for phases *cb* and *ac* based on the values obtained in step 1 but applying the network system obtained in step 2
- 6) evaluate the consumer voltage percentile values due to statistical load currents for the phase *ba* utilising the general expressions developed in chapter 5
- 7) determine the total real and the total imaginary component of the branch voltage drops at each node as given by the consumer phasor voltage percentile values for the phase *ba* as discussed in chapter 4
- 8) determine the total real and the total imaginary component of the branch voltage drops due to non-statistical currents for phases *cb* and *ac* based on the results obtained in step 1 but applying the network system obtained in step 2
- 9) evaluate the overall consumer voltages by applying the principle of superposition for the phase *ba* as described in chapter 4.

When dealing with other phases *cb* and *ac*, the procedure adopted for the phase *ba* is applied to the individual phases by following the logic described in this section. The modelling of the step-voltage regulator described in this section can be applied when two single-phase regulators are connected in the open delta or three single-phase regulators connected in delta-closed configuration as mentioned in chapter 2 are used.

6.5 Development of the universal algorithm

The consumer voltages on the MV distribution network systems are evaluated resulting from both statistical and non-statistical loads. The general expressions for the first and the second moments of the real and imaginary component of the system branch voltage drops were developed on the basis of the non-branched network system as stipulated in chapter 5. These enable the determination of the first and the second moments of the consumer voltages with their statistical parameters. Also, in the same chapter 5, the general expressions for the total line power losses in MV distribution network systems were developed based on non-branched network systems. These general expressions are applied to develop the probabilistic power load flow that will be discussed later. Due to the complexity involved in solving the probabilistic power load flow for branched systems, the so-called universal algorithm was developed to enable the above-mentioned general expressions to be translated into a branched system scenario. Therefore, the universal algorithm can be applied to estimate the consumer voltages and line power losses in single and three-phase radial distribution systems of any configuration based on the general expressions developed in chapters 3, 4 and 5.

The universal algorithm creates four main arrays as follows:

- array describing the path from any node to the supply node, this path contains all the branches connected between the node point in question and the supply node
- array describing the individual load currents through any branch of the system

- array containing the total number of paths (i.e. total number of connected branches) from any node of the system to the supply node
- array containing the total number of load currents through any branch of the system

With the aid of the four main arrays, at each node point i , the computer program can apply the general expressions developed in chapters 3, 4 and 5 for any type of distribution network. In other words, any type of the network is treated as if it is not a branched system. This is possible by tracking the entire load currents flowing through the system branches between the node point i in question and the supply node. In order to check for the accuracy of the entire algorithm, the equations describing the total real and the total imaginary component of the branch voltage drops are incorporated. The idea is to compare the square of the equations responsible for the first moment determination of the total real and the total imaginary component of the branch voltage drops to the ones for determining the second moment at each node point. If the programming is accurate, the two should be exactly equal.

This chapter describes the concept adopted, which is very flexible in the sense that any electrical parameter of interest on the power distribution network can be calculated without difficulty. The computer program, upon reading the input data, automatically creates the above-mentioned four main arrays as well as others. For the single-phase system, there will be a total number of 8 arrays. These arrays are: D-array, R1-array, X1-array, Z1-array, b-array, wx-array, x2-array and path-array. However, when dealing with three-phase systems, there will be a total of 17 arrays. These arrays are D-array, D21-array, D32-array, D13-array, R1-array, R2-array, R3-array, X1-array, X2-array, X3-array, Z1-array, Z2-array, Z3-array, b-array, wx-array, x2-array and the path-array. The number of arrays required can be reduced if the programmer wants to work with the impedance array only. Each of the above-mentioned arrays is described in this chapter.

6.5.1 The development of the arrays for single-phase distribution systems

The computer program formulates the arrays automatically. The input data should accurately be supplied and the format is provided in the section 6.5.1.1

6.5.1.1 Development of the D-array

The most vital array is the so-called D-array. This is the array that describes the entire distribution power network. The process is applied to the system shown in fig. 6.3 to show the appearance of the D-array. This will entirely depend on how the line-input data are defined. The format for the line input data is given below.

The length of the line in km is given as variable m . If the network system has equal line length intervals of LI km, the line input data to be supplied should be as follows:

$$m(1,2)=LI; m(2,11)= LI; m(2,3)= LI; m(3,4)= LI ; m(3,7)= LI ; m(4,5)= LI ; m(4,6)= LI ; m(7,9)= LI ; m(7,10)= LI ; m(7,8)= LI ; m(8,12)= LI ; m(8,13)= LI ;$$

With this input data, the D-array will be formulated automatically by the program and will appear as shown in table 6.1. The second row of the D-array represents all the nodes of the system. In the computer program, the load node is identified in terms of the column number of the D-array. The total number of columns represents the total number of the branches and

their identification. The D-array adequately represents the one line diagram depicted in fig. 6.3. The interesting thing to note is the last number 13 appearing in the column number 12, that is one value less. This will always be the case, if the numbering of the nodes is done in a proper way.

Table 6.1: The D-array as formulated from the input data

1	2	2	3	3	4	4	7	7	7	8	8
2	3	11	4	7	5	6	8	9	10	12	13

In order for the computer program to perform as expected, the numbering of the nodes in

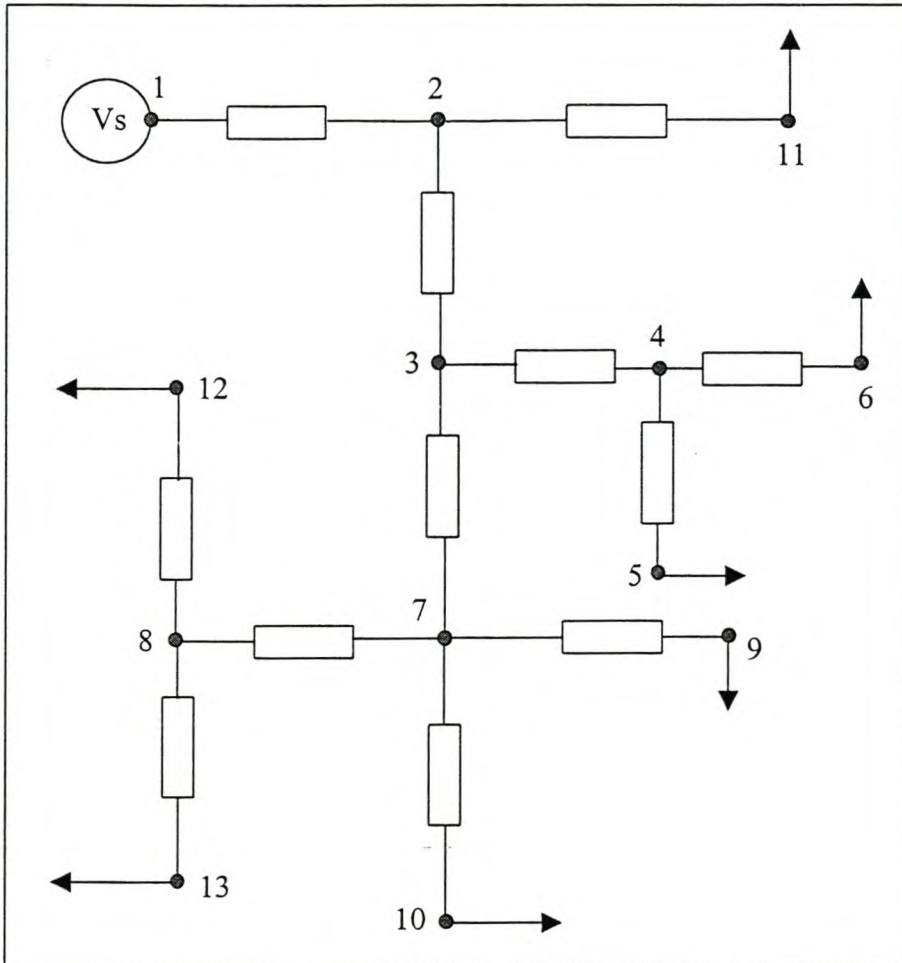


Fig. 6.3: One line diagram to illustrate the appearance of the D-array

single-phase systems should adhere to the following specification:

- number 1 is assigned to the supply node
- jumping of the numeric sequence order is not allowed
- naming of the nodes should follow the direction of the current flow, that means, the current must flow always from the smaller number towards the bigger number as can be seen in fig. 6.3

- the last node number must be connected to the node that is the biggest compared to other nodes that are connected

The D-array is applied extensively in the probabilistic power load flow and backward and forward sweep algorithm. But in the Newton-Raphson algorithm, another type of D-array is employed to enable the implementation of the algorithm from the data supplied by the D-array. In this present work this array is called the DD21-array.

When examining the second row of the D-array, the system nodes do not appear in the numeric sequence order. The DD21-array has nodes in its second row that appear in the numeric sequence order. A certain technique is devised to achieve its formulation based on the information contained in the D-array. After formulation of the DD21-array, the system impedance should also be transformed to match the information contained in the DD21-array. The process is given a name: system impedance mapping. The computer syntax for formulating DD21-array and the system impedance mapping is shown in section 6.5.3.5. The appearance of DD21-array based on the D-array shown in table 6.1 is given in table 6.2.

Table 6.2: The DD21-array as formulated from the D-array

1	2	2	3	3	5	5	6	6	6	9	9
2	3	4	5	6	7	8	9	10	11	12	13

The main objective of the DD21-array and the system impedance mapping, as employed in the NR-algorithm, is to assist in the formulation of the Y-bus for any number of step-voltage regulators that may be required for voltage control. The numeric sequence order of the DD21-array in its second row is utilised to create the power column matrix and the voltage column matrix. After the convergence of the algorithm, the results are assigned to the actual nodes of the network system.

The relationship between the D-array and DD21-array can easily be understood from the computer syntax provided. When examining the two arrays in respect to their column numbers, it shows that:

- the load node in the second row of the DD21-array which substitute the node number in the D-array will appear in its first row at the column number where the node number substituted appears in the first row of the D-array
- if the load node substituted in the D-array does not appear in the first row of the D-array, then, the load node in the second row of the DD21-array will not appear in its first row

The node parameters should be assigned to the new node arrangement (e.g. line capacitance, constant $P-Q$ loads etc.). After the convergence of the NR-algorithm, required node parameter values are assigned to the actual nodes. The computer syntax for implementing line capacitance node values is shown in section 6.5.3.6.

6.5.1.2 Development of the b-array

The b-array records the load currents through any branch of the system. The column number of the D-array identifies the system branch. For example, consider branch 3-7 which is identified in column number 5 in the D-array. According to fig. 6.3, the load currents through this branch are 7, 8, 9, 10, 12 and 13. These currents appear in the 5th row of the b-

array as shown in table 6.3. Thus, the information regarding the load currents through a branch, identified by column number Q5 in the D-array will appear in the Q5th row of the b-array.

Table 6.3: The b-array as formulated from the input data.

3	11	4	7	5	6	8	9	10	12	13	2
4	7	5	6	8	9	10	12	13	3	0	0
11	0	0	0	0	0	0	0	0	0	0	0
5	6	4	0	0	0	0	0	0	0	0	0
8	9	10	12	13	7	0	0	0	0	0	0
5	0	0	0	0	0	0	0	0	0	0	0
6	0	0	0	0	0	0	0	0	0	0	0
12	13	8	0	0	0	0	0	0	0	0	0
9	0	0	0	0	0	0	0	0	0	0	0
10	0	0	0	0	0	0	0	0	0	0	0
12	0	0	0	0	0	0	0	0	0	0	0
13	0	0	0	0	0	0	0	0	0	0	0

6.5.1.3 Development of the path-array

The path-array records the path for each load current. The path describes the route through which the load current passes. The column number of the D-array, which contains various system branches between the load node and the voltage supply node, identifies this route. Keeping track of each route for different load currents enables the probabilistic power flow program to determine the total first moments and the total second moments of the branch voltage drops at each node with the supply node as the reference.

Suppose the path of the load current at node 13 is of interest. This node appears in the 12th column of the D-array. According to fig. 6.3, the path of the load current will be through the branches 13-8, 8-7, 7-3, 3-2 and 2-1. From the D-array, these branches are identified in terms of the column numbers as 12, 8, 5, 2 and 1. These column numbers appear in the 12th row of the path-array as shown in table 6.4. The route for the load current described by the column number Q6 in the D-array will appear in the Q6th row of the path-array. The entire path-array for the network system shown in fig. 6.3 will appear as shown in table 6.4.

Table 6.4: The path-array as formulated from the input data.

1	0	0	0	0
2	1	0	0	0
3	1	0	0	0
4	2	1	0	0
5	2	1	0	0
6	4	2	1	0
7	4	2	1	0
8	5	2	1	0
9	5	2	1	0
10	5	2	1	0
11	8	5	2	0
12	8	5	2	1

6.5.1.4 Development of the wx-array

The wx-array contains the total number of load currents flowing through any branch of the system. Each node of the system is treated as a load node. The entire wx-array will appear as shown in table 6.5.

Table 6.5: The wx-array as formulated from the input data.

12	10	1	3	6	1	1	3	1	1	1	1
----	----	---	---	---	---	---	---	---	---	---	---

Referring to fig. 6.3, consider again branch 3-7, which appears in the 5th column of the D-array. The load currents flowing through the mentioned branch are 7, 9, 10, 8, 12 and 13. There are six currents in total and this total number appears in the 5th column of the wx-array. Thus, if the branch appears in the Q7th column of the D-array then, the total number of load currents through the branch in question will appear in the Q7th column of the wx-array.

6.5.1.5 Development of the x2-array

The x2-array contains the total number of paths from any node of the network system to the supply node. As mentioned previously, the path is the route taken by the individual load current from the load node towards the supply node. The system branches connected between the node in consideration and the supply node define this route. The entire x2-array will appear as shown in table 6.6.

Table 6.6: The x2-array as formulated from the input data.

1	2	2	3	3	4	4	4	4	4	5	5
---	---	---	---	---	---	---	---	---	---	---	---

Suppose the path for the current at node 12 is of interest. From fig. 6.3, the route will be through branches 12-8, 8-7, 7-3, 3-2 and 2-1. There are a total number of five paths. The total number of paths in this case appears in the 11th column of the x2-array as shown in table 6.6. The x2-array stores the total number of paths in its column number corresponding to the column number of the D-array that defines the load current.

6.5.1.6 Development of the Z1-array

The variable for the line impedance in ohms is assigned a variable Z. If the network has equal branch impedances of IMP ohms per km, the input branch impedance data to be specified according to fig. 6.3 should be as follows:

$$\begin{aligned}
 &Z(1,2)=IMP; \quad Z(2,11)=IMP; \quad Z(2,3)=IMP; \quad Z(3,4)=IMP; \quad Z(3,7)=IMP; \quad Z(4,5)=IMP; \\
 &Z(4,6)=IMP; \\
 &Z(7,9)=IMP; \quad Z(7,10)=IMP; \quad Z(7,8)=IMP; \quad Z(8,12)=IMP; \quad Z(8,13)=IMP;
 \end{aligned}$$

The Z1-array, which is the column matrix, stores the values of the system branch impedance. Each column of the Z1-array stores the system branch impedance values as shown in the D-array. By considering that each branch has impedance of Z_k , k associated with the column number in the D-array, it follows that, the entire Z1-array will appear as shown in table 6.7.

Table 6.7: The Z1-array as formulated from the input data.

Z_1	Z_2	Z_3	Z_4	Z_5	Z_6	Z_7	Z_8	Z_9	Z_{10}	Z_{11}	Z_{12}
-------	-------	-------	-------	-------	-------	-------	-------	-------	----------	----------	----------

6.5.1.7 Development of the R1-array

The R1-array, which is a column matrix, stores the values of the system branch resistance. Each column of the R1-array stores the system branch resistance values as shown in the D-array. These are obtained by taking the real component of the branch impedance shown in table 6.7. By considering that each branch has resistance R_k , k associated with the column number in the D-array, it follows that, the entire R1-array will appear as shown in table 6.8.

Table 6.8: The R1-array as formulated from the input data.

R_1	R_2	R_3	R_4	R_5	R_6	R_7	R_8	R_9	R_{10}	R_{11}	R_{12}
-------	-------	-------	-------	-------	-------	-------	-------	-------	----------	----------	----------

6.5.1.8 Development of X1-array

The X1-array, which is a column matrix, stores the values of the system branch inductive reactance. Each column of the X1-array stores the system branch inductive reactance values as shown in the D-array. These are obtained by taking the imaginary component of the branch impedance shown in table 6.7. By considering that each branch has inductive reactance X_k , k associated with the column number in the D-array, it follows that, the entire X1-array will appear as shown in table 6.9.

Table 6.9: The X1-array as formulated from the input data.

X_1	X_2	X_3	X_4	X_5	X_6	X_7	X_8	X_9	X_{10}	X_{11}	X_{12}
-------	-------	-------	-------	-------	-------	-------	-------	-------	----------	----------	----------

6.5.2 The development of the arrays for three-phase distribution systems

When dealing with a simplified conventional 22kV ESKOM, three-phase distribution system as shown in fig. 6.4, the individual phases should be clearly defined. This is very important so that, the consumer voltage values can be evaluated. The single-phase systems and SWER systems through isolating transformers are connected between two phases of the three-phase delta-delta connected distribution systems. In this context, the SWER systems are regarded as single-phase systems (phase to phase connection) by nature of their connection to the three-phase backbone feeder. As the result of such connection, the system line-to-line voltage value becomes the phase voltage for the single-phase loads. The line input impedance data to be specified should distinguish the different phases. If the three-phase system is symmetrical, meaning that all loads are three phase loads fed from the three-phase network then, the common D-array as described in the single-phase distribution systems is adequate. But as long as single-phase loads are present, the common D-array will no longer be adequate. Therefore, each phase should be defined by separate arrays. In this present work, three arrays are employed called D21-array, D32-array and D13-array to describe the system network for the phase ba , cb and ac respectively. It should be understood that, the entire calculation up to the evaluation of the total real and the total imaginary component of the branch voltage drops at any node of the network system is done by employing the common D-array. Essentially, the D-array describes the one line diagram of the three-phase network system. From this stage the D21-array, D32-array and D13-array are applied to get the overall consumer voltages for each phase respectively. To enable the computer program

to evaluate the consumer voltages and the power losses of the three-phase distribution system in the form described in fig. 6.4, the line input data should be provided in five categories as given below.

Category 1: data to define the common D-array. It is similar to the one shown for the single-phase network. In the case of fig. 6.4, the following data should be specified:

$$m(1,2)=LI; m(2,3)=LI; m(2,5)=LI; m(2,6)=LI; m(3,4)=LI; m(3,7)=LI; m(3,8)=LI; \\ m(4,9)=LI; m(4,10)=LI;$$

The largest number in this category is assigned a variable nt, i.e. nt=10.

Category 2: data to define the line branch impedance. For line 1, the branch impedance between the nodes is given a value Z1. For line 2, the branch impedance is given a value Z2 while for line 3 is given a value Z3. According to fig. 6.4, the following data should be specified.

$$Z1(1,2)=Z1; Z1(2,3)=Z1; Z1(2,5)=Z1; Z1(2,6)=Z1; Z1(3,4)=Z1; Z1(3,7)=Z1; Z1(3,8)=Z1; Z1(4,10)=Z1;$$

$$Z2(1,2)=Z2; Z2(2,3)=Z2; Z2(2,5)=Z2; Z2(2,6)=Z2; Z2(3,4)=Z2; Z2(3,7)=Z2; Z2(3,8)=Z2; Z2(4,9)=Z2;$$

$$Z3(1,2)=Z3; Z3(2,3)=Z3; Z3(2,5)=Z3; Z3(3,4)=Z3; Z3(3,7)=Z3; Z3(3,8)=Z3; Z3(4,9)=Z3; Z3(4,10)=Z3;$$

Note: The arrays similar to those described in section 6.5.1.6-6.5.1.8 should be formulated using the above data for each line.

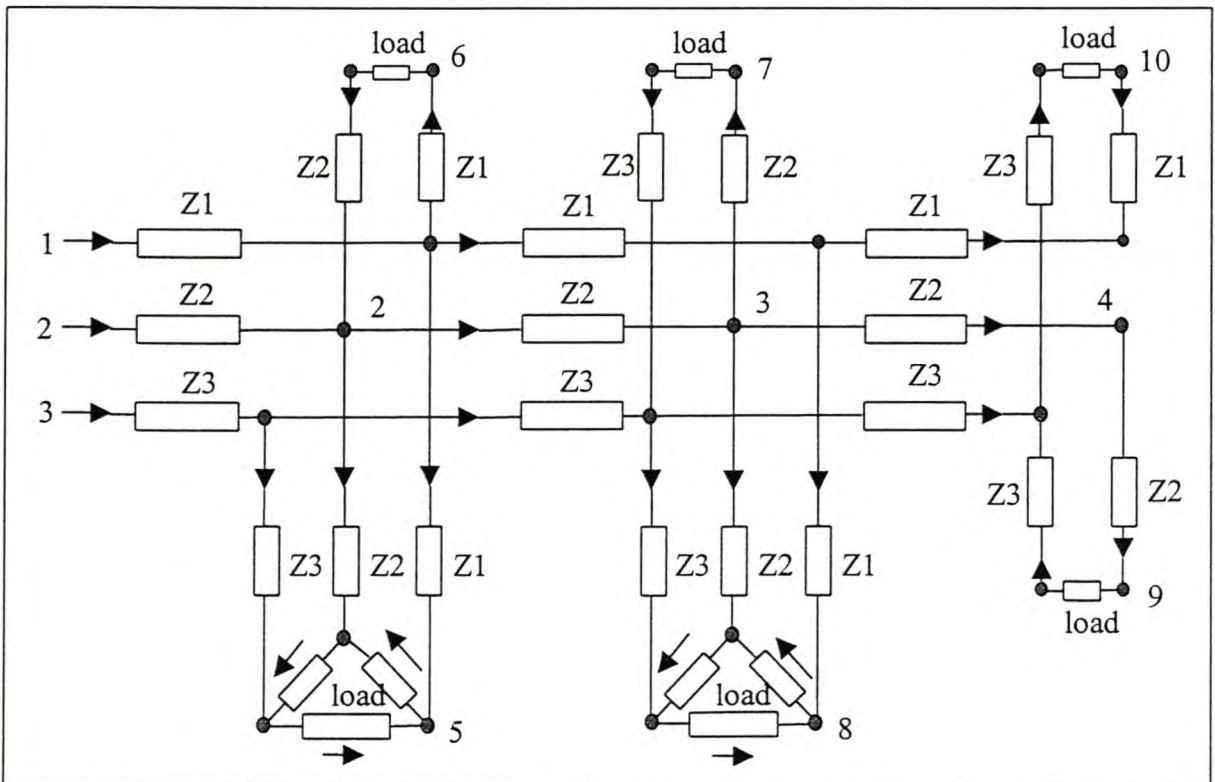


Fig. 6.4: A simplified conventional 22kV ESKOM three-phase distribution system with the conventional direction of the system currents as defined in section 4.1.1

If the feeder voltage control is to be achieved by means of step-voltage regulator, the system impedance should also be specified by using another variable as explained in section 6.4.1. Therefore, by adopting the variables ‘ZW1’, ‘ZW2’ and ‘ZW3’ for line 1, 2 and 3 respectively, the line impedances can also be represented as shown below:

$ZW1(1,2)=Z1$; $ZW1(2,3)=Z1$; $ZW1(2,5)=Z1$; $ZW1(2,6)=Z1$; $ZW1(3,4)=Z1$; $ZW1(3,8)=Z1$; $ZW1(4,10)=Z1$;

$ZW2(1,2)=Z2$; $ZW2(2,3)=Z2$; $ZW2(2,5)=Z2$; $ZW2(2,6)=Z2$; $ZW2(3,4)=Z2$; $ZW2(3,7)=Z2$; $ZW2(3,8)=Z2$; $ZW2(4,9)=Z2$;

$ZW3(1,2)=Z3$; $ZW3(2,3)=Z3$; $ZW3(2,5)=Z3$; $ZW3(3,4)=Z3$; $ZW3(3,7)=Z3$; $ZW3(3,8)=Z3$; $ZW3(4,9)=Z3$; $ZW3(4,10)=Z3$;

Note: The arrays similar to those described in section 6.5.1.6-6.5.1.8 should also be formulated using the above data for each line.

Category 3: data to define the D21-array

$Z21(1,2)=4$; $Z21(2,3)=4$; $Z21(2,5)=4$; $Z21(2,6)=4$; $Z21(3,4)=4$; $Z21(3,8)=4$;

The largest number in this category is assigned a variable nt1, i.e. nt1=9.

Category 4: data to define the D32-array

$Z32(1,2)=4$; $Z32(2,3)=4$; $Z32(2,5)=4$; $Z32(3,4)=4$; $Z32(3,7)=4$; $Z32(3,8)=4$; $Z32(4,9)=4$;

The largest number in this category is assigned a variable nt2, i.e. nt2=9

Category 5: data to define the D13-array

$Z13(1,2)=4$; $Z13(2,3)=4$; $Z13(2,5)=4$; $Z13(3,4)=4$; $Z13(3,8)=4$; $Z13(4,10)=4$;

The largest number in this category is assigned a variable nt3, i.e. nt3=10.

Note: The impedance value assigned to the elements of the individual phase impedance array is a numeric number 4. Any numeric number is acceptable with the exception of a zero value.

After specifying the above input data, the arrays are determined automatically by the program and will appear as shown in table 6.10-6.13.

Table 6.10: The D-array as formulated from the input data

1	2	2	2	3	3	3	4	4
2	3	5	6	4	7	8	9	10

Table 6.11: The D21-array as formulated from the input data

1	2	2	2	3	3
2	3	5	6	4	8

Table 6.12: The D32-array as formulated from the input data

1	2	2	3	3	3	4
2	3	5	4	7	8	9

Table 6.13: The D13-array as formulated from the input data

1	2	2	3	3	4
2	3	5	4	8	10

The path-array, b-array, wx-array and x2-array are formulated by the use of the common D-array as explained previously in this chapter. Other arrays such as R-array, X-array and Z-array are defined for each line. The arrays have the same format to those described when dealing with single-phase systems. But their values are obtained by referring to the data that defines **category2**. That means, for describing line 1 impedance network, the impedances to be applied are those coded Z1. For describing line 2, the impedances to be applied are those coded Z2. The same applies to line 3, the impedances to be applied are those are coded Z3.

The numbering of the nodes in three-phase radial distribution systems should adhere to the following protocol:

- number 1 is assigned to the supply node
- jumping of the numeric sequence order is not allowed
- numbering of the nodes should follow the direction of the current flow, that means, the current must always flow from the smaller number towards the bigger number
- The individual phase network should be monitored to make sure that the biggest node number for each phase network is connected to the node that is the biggest in relation to other nodes of the same phase network that are connected, as can clearly be seen in fig. 6.4.

6.5.3 The computer program syntax for creating arrays in single and three-phase distribution systems

The computer program syntax for creating the arrays mentioned in this chapter is presented in the following sections. It is very important to observe the rules given when the data is specified. The variable 'awy' in the computer program syntax is automatically assigned a value zero if there is no step-voltage regulator or else it is assigned a numeric value equal to the number of the step-voltage regulators. If step-voltage regulators are employed on the single-phase distribution system, the network system should be modified to reflect the arrangement of the network system due to the introduction of the artificial nodes. But if voltage control by step-voltage regulator is required on the three-phase network, apart from the modification of the system due to the introduction of artificial nodes, another network impedance coded 'ZW' has to be used in order to implement the procedure described in section 6.4.1.1.

6.5.3.1 The computer syntax for creating the D-array, Z1-array, R1-array and X1-array

The computer program flow-chart for the above-mentioned arrays in single-phase systems is shown in Appendix 6-A. They are similar to the ones developed for each line in three-phase systems. The computer program syntax written in MATLAB for the implementation of the above-mentioned arrays is given below.

```
% to create the D-array and the system branch impedance

qq=0; % initialize the count
for s=1:nt+awy % search for system line parameters
for r=1:nt+awy % search for system line parameters
if qq==nt+awy-1 % condition for procedure termination
break % terminate the procedure
else if m(s,r)~=0 % set a condition for creating the arrays
qq=qq+1; % increase the count
D(1,qq)=s;D(2,qq)=r; % create D-array
mm(qq)=m(s,r); % create line array
Z(s,r)=Z(s,r)*mm(qq); % create line impedance array
Z1(qq)=Z(s,r); % create line impedance array
R1(qq)=real(Z1(qq)); % create line resistance array
X1(qq)=imag(Z1(qq)); % create line reactance array
else
ta=50;
end
end
end
end
```

Note: The final value of 'qq' gives the total number of the system branches, which is equal to the total number of columns in the D-array.

6.5.3.2 The computer syntax for creating b-array and wx-array

The computer program flow-chart for the above-mentioned array is shown in Appendix 6-B. The computer program syntax written in MATLAB for the implementation of the above-mentioned two arrays is given below.

```
% algorithm for determining the branch currents

for s = 1:nt+awy-1 % keep track the branch under investigation
ac = 0; % initialise a count of nodes connected to the previous node
wx(s) = 0; % initialise the count for recording total no. of branch currents
for s1 = 1:nt+awy-1 % this deals with the nodes connected to node 2 of the system
if D(2,s) == D(1,s1) % set a condition for recording the load currents
ac = ac+1;wx(s) = wx(s)+1; % increase the respective counts
b(s,ac) = D(2,s1); % store the nodes connected to the previous node
end
end
at = 0;Q = 60;ad = ac;
while Q == 60 % set a condition for ending the search for currents through a branch
```



```

an = 0;      % reset for the count that track no. of nodes scanned in the second row
if ac>=1    % set a condition for further search of node connected to the node
            % under consideration
    for t = 1:ac % search for all nodes to be evaluated
        at = at+1; % keeps track on the nodes to be scanned in the first row
        for s1=1:nt+awy-1 % search for all nodes making branches with the node
            % under consideration
                if b(s,at) == D(1,s1) % set condition for recording the currents
                    ad = ad+1; an = an+1; wx(s) = wx(s)+1; % increase the respective counts
                    b(s,ad) = D(2,s1); % records the currents through the respective branches
                end
            end
        end
    end
    ac=an; % keeps track on the nodes to be evaluated
    else
        Q=100 % ends the search if no more scanned nodes in the second row
    end
end
end
end
for s=1:nt+awy-1 % the procedure to complete the creation of b-array
    wx(s)=wx(s)+1;
    b(s,wx(s))=D(2,s);
end

```

6.5.3.3 The computer syntax for creating the path-array and x2-array

The computer program flow-chart for the above-mentioned arrays is shown in Appendix 6-C. The computer program syntax written in MATLAB for the implementation of the two arrays is given below.

% algorithm for locating the path of load currents to the supply node

```

bt = 100;p = 0;x2(1) = 0;
while bt == 100 % set a condition to end the search
    p = p+1; % keeps track for the node under investigation
    ak = 0; % reset the counting
    y2=0; % set a condition to search the path for particular node
    if p == 1 % a condition to track node 2 of the system
        y2 = 1; % set value to end a search for node 2
        ak == ak+1; % increase the count
        x2(p) = x2(p)+1; % records the no. of path for current at node 2
        path(p,ak) = 1; % store the path
        ak = 0; % reset the count
    end
    if y2 == 0 % set a condition to continue with a search
        x2(p) = 0; % reset the count for load current total paths evaluation
        for p1 = 1:nt+awy-1
            p2 = nt+awy-p1; % keeps track on the branch where p2=p scanning towards
            %supply
            if p2 == p % set a condition to track the branch under investigation
                ak = ak+1; x2(p) = x2(p)+1; % increase the count for paths for the load
                % current under consideration
            end
        end
    end
end

```

```

y2 =1;          % set value to end a search for all nodes except node2
node(ak) = D(1,p2); % assign a variable to a node connected to the node
                    % under investigation tracking towards the supply node
path(p,ak) = p;   % store the identified branches
end
end
for p1=1:nt+awy-1 % search for the path
for p2=1:nt+awy-1; % search for the path
if D(2,p2) == node(ak) % track the previous identified node
ak = ak+1; x2(p) = x2(p)+1; % increase the respective counts
node(ak) = D(1,p2); % assign to a variable the node connected to the
                    % node under investigation
path(p,ak)=p2;     % store the identified branches
end
end
end
end
if p == nt+awy-1 % if all the nodes are scanned terminate the procedure
bt=500;         % assigned a value to terminate the scanning process
end
end
end

```

6.5.3.4 The computer program syntax for creating the D21-array, D32-array and D13-array

The computer program syntaxes for developing the arrays responsible for the identification of the individual phases in three-phase distribution systems described in fig. 6.4 are presented. The description of the arrays is found in section 6.5.2. The final values of 'qq1', 'qq2' and 'qq3' are the total number of branches in phase *ba*, *cb* and *ac* respectively. Their associated computer program flow charts are shown in appendix 6-D, 6-E and 6-F.

% the computer program syntax for the D21-array

```

qq1= 0;          % initialise the count
for s =1:nt1    % scan for the system impedance for the phase ba
for r =1:nt1    % scan for the system impedance for the phase ba
if qq1 ~ = 0    % set a condition to make sure the D21-array is accessible
if nt1 == D21(2,qq1) % condition for procedure termination
break          % terminate the procedure
end
end
if abs(Z21(s,r)) ~ =0
qq1 = qq1+1;   % increase the count
D21(1,qq1) = s; D21(2,qq1) = r; % create the D21-array
end
end
end
end

```

% the computer program syntax for the D32-array

```

qq2 = 0;          % initialise the count
for s = 1:nt2    % scan for the system impedance for the phase cb

```

```

for r = 1:nt2 % scan for the system impedance for the phase cb
  if qq2 ~ = 0 % set a condition to make sure the D32-array is accessible
    if nt2 == D32(2,qq2) % condition for procedure termination
      break % terminate the procedure
    end
  end
end
• end
  if abs(Z32(s,r)) ~ = 0
    qq2 = qq2+1; % increase the count
    D32(1,qq2) = s; D32(2,qq2) = r; % create the D32-array
  end
end
end
end

```

% the computer program syntax for the D13-array

```

qq3 = 0; % initialise the count
for s = 1:nt3 % scan for the system impedance for the phase ac
  for r = 1:nt3 % scan for the system impedance for the phase ac
    if qq3 ~ = 0 % set a condition to make sure the D32-array is accessible
      if nt3 == D13(2,qq3) % condition for procedure termination
        break % terminate the procedure
      end
    end
    if abs(Z13(s,r)) ~ = 0
      qq3 = qq3+1; % increase the count
      D13(1,qq3) = s; D13(2,qq3) = r; % create the D13-array
    end
  end
end
end
end

```

6.5.3.5 The computer syntax for formulating DD21-array and the impedance system mapping

% to convert the D-array to DD21-array for NR-algorithm

```

DD21(1,1) = 1; % assign the element in the first row first column the supply node
for s = 1:qq
  DD21(2,s) = s+1; % assign the second row of the DD21-array ascending numeric no's
  % from 2 upwards
end

for s = 1:qq
  for r = 1:qq
    if D(2,s) == D(1,r)
      DD21(1,r) = DD21(2,s); % to formulate the DD21-array
    end
  end
end
end

```

```
% system impedance mapping
```

```
for s = 1:qq
ZZ33(DD21(1,s),DD21(2,s))=Z1(s): % system impedance mapping
end
```

6.5.3.6 The computer syntax for implementing line capacitance node values

```
% assign node line capacitance to the new system node arrangement
```

```
for s = 1:qq
C1(DD21(2,s)) = C2(D(2,s))
end
```

```
% assign line capacitive currents to the actual node after the convergence of the NR-
algorithm
```

```
for s = 1:qq
IC2(D(2,s)) = IC1(DD21(2,s))
end
```

6.6 Significance of the developed arrays

The arrays mentioned in this chapter are significant when evaluating any electrical parameter of interest on the MV radial distribution systems. The D-array as mentioned in section 6.5.1.1, describes the one line diagram of the distribution network, while the path-array defines the path for the individual load current to the supply node. The column numbers of the D-array identifies this path. The b-array records all load currents that pass through any branch of the system. These load currents are merely the defined system nodes without distinguishing whether the load is connected to it or not. The wx-array and x2-array record the total number of load currents through any branch and the total number of paths for each load current respectively. The arrays coded with the first letter 'R', 'X' and 'Z' describe the branch resistance, branch inductive reactance and the branch impedance. All the above-mentioned arrays have strong link to the D-array in which the entire network system is represented as one line diagram. For the column matrix arrays such as R-array, X-array, Z-array, wx-array and x2-array, the data needed for the branch identified by the column number in the D-array is obtained from the same column number of the respective array. For the path-array and the b-array, the data needed for the branch identified by the D-array is obtained from the row number corresponding to the column number in the D-array. The way to apply these arrays will depend on the problem at hand to be evaluated.

6.6.1 Evaluation of a single value

Suppose the voltage drop across the branch 3-7 in fig. 6.3 is to be evaluated. In the first place the load currents through the mentioned branch must be known. These load currents can be found in the b-array row number, which corresponds to the column number that contains the branch 3-7 in the D-array. As can be seen in table 6.1, the branch is found in the fifth column and therefore, the required load currents should be located in the fifth row of the b-array. These load currents are: 8, 9, 10, 12, 13, and 7. In writing a computer program to solve the voltage across the branch 3-7, six currents should be scanned with the help of wx-array. The value to be used for this purpose must be found in the fifth column of the wx-array. The branch impedance required is found in the fifth column in the Z1-array. If the load currents

are identified by the variable 'IP(k)', k being the node number, the computer program syntax should be as follows:

```
% to calculate the voltage drop across the branch 3-7 of fig. 6.3

    Q1 = 0;                                % initialise the summation of the voltage drop
for s = 1:wx(5)                             % scan for the total number of branch currents
    Q1=Q1+IP(b(5,s))*Z1(5)                 % summing the voltage drops
end
```

6.6.2 Evaluation of two or more values

Suppose the total voltage drop between node 12 and supply node as shown in fig. 6.3 is to be evaluated. This is a practical case and the universal algorithm was developed mainly to solve this kind of a problem. The x2-array plays a significant role in the solution because the total number of branches connecting node 12 and the supply node must be known in advance. As can be seen in fig. 6.3, there are a total number of five branches. According to the D-array, node 12 is in the 11th column as shown in table 6.1. The total number of five paths is found in the 11th column of the x2-array. To solve the problem of this nature, the total number of five paths must be scanned. Each path is to be scanned by the help of the x2-array. The total number of load currents that flow through each of these paths has to be identified. The wx-array is employed to identify the total number of load currents in each path. The individual load current through each path has to be identified. These individual load currents are retrieved from the b-array. The branch impedance for each path should be identified. The data can be found in the Z1-array.

Therefore, to write a computer program for this particular case, it must be able to perform four procedures. The first procedure is to scan for the total number of paths and the second one is to scan for the total number of load currents for each path. The third procedure is to retrieve all load currents that passes through each path and the fourth procedure is to be able to track the branch impedance for each path. It should be understood that, the data concerned about the path is retrieved from the path-array. For this particular case, the 11th row in the path array is to be applied. The computer program syntax should be as follows:

```
% to calculate the total voltage drop between node 12 and the supply node of fig.6.3

    Q1 = 0;                                % initialise the summation
for s = 1:x2(11)                             % scan for the no. of paths
    for s3 = 1:wx(path(11,s))                % scan for the currents in each path
        Q1 = Q1 + IP(b(path(11,s),s3)) * (Z1(path(11,s)));% summing the branch voltage drops
    end
end
```

6.7 Development of the probabilistic power flow program

The probabilistic power flow program utilises the equations developed in chapter 5. The general expressions for the consumer voltages and the total line power losses were developed from distribution systems without branches. But in practice they are usually branched systems. With the aid of the universal algorithm, at each node point i , the system is treated as if it is not a branched system. From equation (5.33), the expected value of the normalised consumer voltage $E[V_{scn_i}^{\#}]$ at node i , can be expressed as:

$$E[V^{\#}_{scon_i}] = 1 - \frac{E[\Delta V_{ireal_total}]}{V_S} + 0.501 \frac{E[\Delta V^2_{iimag_total}]}{V_S^2} + 0.448 \frac{E[\Delta V_{real_total}]E[\Delta V^2_{iimag_total}]}{V_S^3} + 0.829 \frac{E[\Delta V^2_{ireal_total}]E[\Delta V^2_{iimag_total}]}{V_S^4} \quad (6.20)$$

Also, referring to equation (5.34), the second moment of the normalised consumer voltage $E[V^{\#2}_{scon_i}]$ at node i , can be expressed as:

$$E[V^{\#2}_{scon_i}] = 1 - 2 \frac{E[\Delta V_{ireal_total}]}{V_S} + \frac{E[\Delta V^2_{ireal_total}]}{V_S^2} + \frac{E[\Delta V^2_{iimag_total}]}{V_S^2} \quad (6.21)$$

The equations (6.20) and (6.21) are general expressions that can be applied for both single and three-phase distribution networks. As can be seen from these two equations, the moments of the total real and the total imaginary components of the branch voltage drops at each node as mentioned in chapter 5 are required. These values for the single and three-phase distribution systems have to be evaluated and substituted in the above equations. The statistical parameters for the consumer voltages are then evaluated as shown in equation (5.31) and (5.32) and then, the percentile values of the consumer voltages are obtained by using equation (5.35) and (5.36). If non-statistical currents are present, the principle of superposition is applied as discussed in chapter 5 in order to calculate the overall consumer voltages. The probabilistic computer program flow charts for the single and three-phase distribution systems are presented in appendix 6-G, 6-H and appendix 6-I, 6-J respectively. The general expressions responsible for the evaluation of equation (6.20) and (6.21) are revisited for convenience.

For the single-phase systems:

$E[\Delta V_{ireal_total}]$ refer equation (5.19)

$E[\Delta V^2_{ireal_total}]$ refer equation (5.21)

$E[\Delta V^2_{iimag_total}]$ refer equation (5.22)

For the three-phase systems:

- phase ba

$E[\Delta V_{ireal_total}]$ refer equation (5.23)

$E[\Delta V^2_{ireal_total}]$ refer equation (5.24) + (5.26)

$E[\Delta V^2_{iimag_total}]$ refer equation (5.25) + (5.27)

6.8 Demonstration of the application of the universal algorithm

This section demonstrates how the universal algorithm can be applied when evaluating the total real and the total imaginary components of the branch voltage drops due to statistical

and non-statistical node currents in single-phase distribution systems as discussed in chapter 4.

6.8.1 The computer program syntax for non-statistical currents

The presence of the step-voltage regulators for feeder voltage control is manifested by the value of the variable 'awy' as previously mentioned in this chapter. The node current variable is denoted 'IPP1(k)', k being the node number. The computer program syntax caters for any system configuration. The calculation is done on a per unit basis but the total real and the total imaginary component of the branch voltage drops at each node are evaluated as actual values by multiplying with the system voltage base value 'V1'.

```
% evaluate the total real and the total imaginary component of branch voltage drops at
each node

for p4 = 1:nt+awy-1 % identification of the node in consideration
    Q1 = 0; % initialise the summation
    for s = 1:x2(p4) % scan for the no. of paths
        for s3 = 1:wx(path(p4,s)) % scan for the currents in each path
            Q1 = Q1 + IPP1(b(path(p4,s),s3)) * (Z11(path(p4,s))); % summing the branch voltage
                                                                    % drops
        end
    end
end
delta_V21(D(2,p4)) = Q1; % store the total branch voltage drop at each node
rre2(D(2,p4)) = real(delta_V21(D(2,p4))) * V1; % determine the total real component of
                                                                    % the branch voltage drops at each node
iim2(D(2,p4)) = imag(delta_V21(D(2,p4))) * V1; % determine the total imaginary
                                                                    % component of the branch voltage drops at each node
end
```

6.8.2 The computer program syntax for statistical currents

As stated in chapter 4, the branch voltage drops due to statistical currents are evaluated by firstly converting the consumer voltage percentile values into phasors. For this purpose, two arrays denoted 'array1' and 'array2' are employed to store the real and the imaginary component of branch voltage drops. By utilising the data contained in the path-array, the real and the imaginary component of the branch voltage drop can be summed to obtain the total real and the total imaginary components of the branch voltage drops at each node of the system. The percentile value of the consumer voltage at a specified level of risk is given a variable 'Vcon' and its phase angle, which is deterministically evaluated, is given a variable 'Av'.

```
% evaluate the real and the imaginary component of branch voltage drops at each node

Vcon(D(1,1)) = Vs; Av(D(1,1))=0; % assign values for the supply voltage

for p4 = 1:qq % specify each branch in the D-array

array1(p4) = real(Vcon(D(1,p4))*(cos(Av(D(1,p4)))+j*sin(Av(D(1,p4)))))-
(Vcon(D(2,p4))*(cos(Av(D(2,p4)))+j*sin(Av(D(2,p4)))))); % determine the
                                                                    % real component of the branch voltage drop
```

```

array2(p4) = imag(Vcon(D(1,p4))*(cos(Av(D(1,p4)))+j*sin(Av(D(1,p4))))-
                (Vcon(D(2,p4))*(cos(Av(D(2,p4)))+j*sin(Av(D(2,p4))))));%determine the
                % imaginary component of the branch voltage drop
end

% evaluate the total real and the total imaginary component of branch voltage drops at
% each node

for p4 = 1:nt+awy-1 % identify the required node
    ak1 = 0; ak2 = 0; % initialise the counts
    for p8 = 1:nt+awy-1 % scan for the elements in the path-array
        if path(p4,p8)>1 % set a condition to terminate the summation of the branch
            % voltage drops
            ak1 = ak1+array1(path(p4,p8)); % sum the real component of the branch voltage
            % drops
            ak2 = ak2+array2(path(p4,p8)); % sum the imaginary component of the branch
            % voltage drops
        else
            ak1 = ak1+array1(path(p4,p8)); % sum the real component of the branch voltage
            % drops
            ak2 = ak2+array2(path(p4,p8)); % sum the imaginary component of the branch
            % voltage drops
        end
        break % terminate summation for the node in consideration
    end
end
rre1(D(2,p4)) = ak1; % store the total real component of the branch voltage drops at
% each node
iim1(D(2,p4)) = ak2; % store the total imaginary component of the branch voltage
% drops at each node

end

```

6.8.3 The computer program syntax superposition of voltage drops

The superposition of the components of the voltage drops at each node of the system can easily be implemented. The syntax to evaluate the total real and the total imaginary component of the branch voltage drops at each node due to statistical and non-statistical node currents will be as follows:

```

for p4 = 1:qq % identify the required node
    realtotal(D(2,p4)) = rre1(D(2,p4)) + rre2(D(2,p4)); % calculate the total real component
    % at each node
    imagtotal(D(2,p4)) = iim1(D(2,p4)) + iim2(D(2,p4)); % calculate the total imaginary
    % component at each node
end

```

6.9 Summary

The computer programs developed in this present work have been described. The obvious thing to note is the development of the universal algorithm. This enables the general expressions developed for the network systems without branches to be evaluated when

applied to a practical MV distribution network. This proved to be a vital tool to solve such a complex problem. In chapter 7, the algorithms adopted in previous chapters will be verified.

VERIFICATION OF THE DEVELOPED ALGORITHMS

7.1 Introduction

In this chapter, the analytical results are compared with results from Monte Carlo simulations. The consumer voltages are evaluated by considering the two different loading systems as mentioned in the previous chapters. These loading systems are:

- beta distributed load currents at the interval of system maximum demand
- constant P-Q load currents

If the feeder voltage regulation needs improvement, the feeder voltage control is achieved by the application of capacitors or step-voltage regulators. Also, the evaluation of the total line power losses due to load currents modelled as signals in single and three-phase MV power distribution systems will be presented.

7.2 Single-phase MV distribution systems

The consumer voltage percentile values are evaluated using the methods mentioned in chapter 5 based on the one line diagram depicted in appendix 7-A. To assess the suitability of the proposed algorithms presented in previous chapters, the “fox” conductor is specified when dealing with the evaluation of the consumer voltages. This type of conductor, despite being the most recommended conductor in MV distribution systems by ESKOM, also gives a line inductive reactance value that is close to half the line resistance value. These line parameters are suitable to test the accuracy of equation 4.48. Monte Carlo simulation of consumer voltages is executed by generating random currents from the beta distributed load currents. A flow chart for the simulation procedure from beta distributed load currents and constant P-Q loads incorporating feeder voltage regulators is shown in appendix 7-B.

The simulation for the total line power losses is derived from the load data based on the one line diagram depicted in appendix 7-C, which was supplied by ESKOM, the utility company in South Africa. The line data used is shown in table 7.1.

Table 7.1: Feeder impedance per km.

Conductor	R (ohm)	single-phase X (ohm)	three-phase X (ohm)
Bantam	4.802	0.437	0.437
fox	0.78	0.3702	0.3848
Magpie	2.7	0.3876	0.4021

7.2.1 Comparison between calculated and simulated results for consumer voltages

The comparison of the consumer voltages as depicted in appendix 7-A is conducted by assuming different line length intervals and loads that will give different consumer voltages. This will enable the evaluation of voltage drops up to 35 % (for USE application) and above in order to justify the accuracy of the proposed algorithm on single-phase distribution systems. The “fox” conductor is used with impedance line value given in table 7.1. The line interval in km is given a variable LI . In order to simplify the procedure, the same statistical parameters of the load currents are applied which are $\alpha = 0.76$, $\beta = 9.51$ and the scaling

factor $SF = 60$. These are typical values for lower income communities in South Africa. This type of load gives ADMD equal to 1.02 kVA . The number of consumers at the load point is given by the variable NC . The constant P-Q loads are represented by the variable S in kVA and the power factor pf lagging. The number of simulations employed for each case is 15000 in order to achieve a reasonable accuracy in evaluating the consumer voltage.

In calculating the % difference volt-drop as shown in the table of results, the MC simulated results are treated as benchmark values. The sample calculation adopted is as follows:

Suppose the consumer voltage values evaluated from MC simulation and an analytical method are given variables V_{mc} and V_{an} respectively, it follows that:

The % voltage drop due to MC simulation ΔV_{mc} will be:

$$\Delta V_{mc} = \frac{V_{op} - V_{mc}}{V_{op}} * 100 \tag{7.1}$$

Similarly, the % voltage drop due to analytical method ΔV_{an} will be:

$$\Delta V_{an} = \frac{V_{op} - V_{an}}{V_{op}} * 100 \tag{7.2}$$

Therefore,

$$\text{The \% difference volt-drop} = \frac{\Delta V_{mc} - \Delta V_{an}}{\Delta V_{mc}} * 100 \tag{7.3}$$

where

V_{op} is the operating system voltage and in this case is 22000 Volts

Table 7.2: The comparison of consumer voltages for $LI = 90$ and $NC = 40$.

Node No:	Risk=10%			Risk=20%		
	Analytical (Volts)	MC simulation (Volts)	% difference volt-drop	Analytical (volts)	MC simulation (Volts)	% difference volt-drop
2	19442	19453	-0.43188	19518	19522	-0.16142
3	16931	16950	-0.37624	17077	17084	-0.14239
4	16152	16178	-0.44658	16322	16334	-0.21179
5	15755	15783	-0.45038	15941	15953	-0.19845
6	15755	15782	-0.43422	15941	15958	-0.28136
7	15214	15250	-0.53333	15414	15433	-0.28933
8	14312	14375	-0.82623	14550	14583	-0.44492
9	14793	14843	-0.69862	15010	15033	-0.33013
10	14793	14840	-0.65642	15010	15029	-0.27256
11	13853	13938	-1.05433	14113	14160	-0.59949
12	13853	13941	-1.09195	14113	14159	-0.58666

Note that the simulated MV voltage of 13941 represents a transmission line voltage regulation of 36.6%. While this excessive voltage drop would be intolerable in normal distribution practice, it is the kind of level that could be compensated for with a “USE” device.

Table 7.3: The comparison of consumer voltages for $LI = 45$, $NC = 40$, $S = 40$ and $pf = 0.95$.

Node No:	Risk=10%			Risk=20%		
	Analytical (Volts)	MC simulation (Volts)	% difference volt-drop	Analytical (Volts)	MC simulation (Volts)	% difference volt-drop
2	19495	19498	-0.11990	19533	19537	-0.16240
3	17006	17014	-0.16045	17082	17090	-0.16293
4	16232	16239	-0.12151	16320	16326	-0.10575
5	15843	15850	-0.11382	15938	15943	-0.08255
6	15843	15849	-0.09755	15938	15941	-0.04951
7	15310	15315	-0.07479	15413	15420	-0.10638
8	14438	14441	-0.03969	14556	14561	-0.06721
9	14900	14900	0.00000	15010	15015	-0.07158
10	14900	14904	-0.05637	15010	15017	-0.10024
11	14001	14001	0.00000	14128	14132	-0.05084
12	14001	14005	-0.05003	14128	14133	-0.06356

Table 7.4: The comparison for consumer voltages for $LI = 87.5$, $NC = 20$, $S = 20$ and $pf = 0.9$. Step-voltage regulators are employed with transformation ratio 1.1 at node 2, 3 and 7.

Node No:	Risk=10%			Step-voltage regulator voltage control at node 2, 3 and 7 Risk=10%		
	Analytical (Volts)	MC simulation (Volts)	% difference volt-drop	Analytical (Volts)	MC simulation (Volts)	% difference volt-drop
2	19592	19594	-0.08313	21321	21318	0.43988
3	17192	17199	-0.14580	20921	20910	1.00917
4	16435	16442	-0.12594	20306	20297	0.52848
5	16052	16058	-0.10098	19995	19988	0.34791
6	16052	16061	-0.15154	19995	19988	0.34791
7	15548	15560	-0.18634	21501	21484	3.29457
8	14699	14713	-0.19212	20905	20886	1.70557
9	15147	15160	-0.19006	21211	21194	2.10918
10	15147	15160	-0.19006	21211	21196	1.86567
11	14271	14287	-0.20744	20604	20584	1.41243
12	14271	14284	-0.16848	20604	20585	1.34276

Table 7.5: The comparison of consumer voltages for $LI = 20$, $NC = 40$, $S = 40$ and $pf = 0.95$. Capacitor voltage control is employed at node 7 with a rating of 500 $kVAr$ s.

Node No:	Risk=10%			Capacitor voltage control at node 7 Risk=10%		
	Analytical (Volts)	MC simulation (Volts)	% difference volt-drop	Analytical (Volts)	MC simulation (Volts)	% difference volt-drop
2	21154	21154	0.00000	21439	21439	0.00000
3	20310	20311	-0.05921	20919	20916	0.27675
4	20031	20034	-0.15259	20653	20651	0.14826
5	19891	19894	-0.14245	20520	20517	0.20229
6	19891	19893	-0.09492	20520	20516	0.26954
7	19742	19746	-0.17746	20700	20694	0.45942
8	19455	19460	-0.19685	20435	20427	0.50858
9	19600	19605	-0.20877	20569	20562	0.48679
10	19600	19604	-0.16694	20569	20562	0.48679
11	19310	19316	-0.22355	20301	20293	0.46866
12	19310	19316	-0.22355	20301	20293	0.46866

Table 7.6: The comparison of consumer voltages for $LI = 50$, $NC = 40$. Capacitor voltage control is employed at nodes 4, 7 and 8 with ratings of 100, 100 and 150 $kVAr$ s respectively.

Node No:	Risk=10%			Capacitor voltage control at node 4, 7 & 8 Risk=10%		
	Analytical (Volts)	MC simulation (Volts)	% difference volt-drop	Analytical (Volts)	MC simulation (Volts)	% difference volt-drop
2	20884	20888	-0.35971	21319	21321	-0.29455
3	19775	19787	-0.54225	20772	20781	-0.73831
4	19413	19426	-0.50505	20609	20621	-0.87020
5	19229	19242	-0.47136	20446	20460	-0.90909
6	19229	19241	-0.43494	20446	20458	-0.77821
7	19032	19048	-0.54201	20497	20511	-0.94023
8	18655	18674	-0.57126	20419	20435	-1.02236
9	18847	18865	-0.57416	20338	20355	-1.03343
10	18847	18864	-0.54209	20338	20354	-0.97205
11	18464	18483	-0.54023	20260	20276	-0.92807
12	18464	18483	-0.54023	20260	20279	-1.10401

Table 7.7: The comparison of consumer voltages for $LI = 30$, $NC = 40$, $S = 40$ and $pf = 0.95$. Capacitor voltage control is employed at nodes 4, 7 and 8 having ratings of 100, 100 and 200 $kVAr$ s respectively.

Node No:	Risk=10%			Capacitor control at node 4, 7 & 8 Risk=10%		
	Analytical (Volts)	MC simulation (Volts)	% difference volt-drop	Analytical (Volts)	MC simulation (Volts)	% difference volt-drop
2	20625	20626	-0.07278	20963	20962	0.09634
3	19253	19259	-0.21890	19989	19983	0.29747
4	18808	18816	-0.25126	19664	19656	0.34130
5	18584	18591	-0.20534	19455	19445	0.39139
6	18584	18592	-0.23474	19455	19445	0.39139
7	18329	18337	-0.21840	19395	19380	0.57252
8	17859	17868	-0.21781	19152	19127	0.87017
9	18100	18109	-0.23130	19185	19168	0.60028
10	18100	18109	-0.23130	19185	19170	0.53004
11	17623	17631	-0.18311	18940	18915	0.81037
12	17623	17631	-0.18311	18940	18914	0.84251

Table 7.8: The comparison of consumer voltages for $LI = 65$ and $NC = 40$. Capacitor voltage control is employed at nodes 4 and 8 each of rating of 400 $kVAr$ s.

Node No:	Risk=10%			Capacitor voltage control at node 4 & 8 Risk=10%		
	Analytical (Volts)	MC simulation (Volts)	% difference volt-drop	Analytical (Volts)	MC simulation (Volts)	% difference volt-drop
2	20445	20448	-0.19330	20742	20747	-0.39904
3	18907	18915	-0.25932	20456	20465	-0.58632
4	18414	18423	-0.25161	20956	20966	-0.96712
5	18163	18173	-0.26130	20797	20806	-0.75377
6	18163	18172	-0.23511	20797	20806	-0.75377
7	17877	17886	-0.21877	20433	20440	-0.44872
8	17351	17360	-0.19397	20983	20984	-0.09843
9	17622	17634	-0.27485	20273	20281	-0.46539
10	17622	17632	-0.22894	20273	20280	-0.40698
11	17086	17094	-0.16307	20843	20844	-0.08651
12	17086	17098	-0.24480	20843	20844	-0.08651

Table 7.9: The comparison of consumer voltages for $LI = 65$ and $NC = 40$. Step-voltage regulators are employed with transformation ratio 1.1 at node 3 and 7.

Node No:	Risk=10%			Step-voltage regulator voltage control at node 3 and 7 Risk=10%		
	Analytical (Volts)	MC simulation (Volts)	% difference volt-drop	Analytical (Volts)	MC simulation (Volts)	% difference volt-drop
2	20445	20448	-0.19330	20451	20455	-0.25890
3	18907	18915	-0.25932	20752	20776	-1.96078
4	18414	18423	-0.25161	20306	20328	-1.31579
5	18163	18173	-0.26130	20079	20100	-1.10526
6	18163	18172	-0.23511	20079	20099	-1.05208
7	17877	17886	-0.21877	21858	21859	-0.70922
8	17351	17360	-0.19397	21443	21435	1.41593
9	17622	17634	-0.27485	21655	21649	1.70940
10	17622	17632	-0.22894	21655	21651	1.14613
11	17086	17094	-0.16307	21232	21223	1.15830
12	17086	17098	-0.24480	21232	21221	1.41207

7.2.2 Comparison between calculated and simulated results for system power losses in single-phase distribution systems

The line power losses in single-phase systems based on the one line diagram depicted in appendix 7-C is evaluated using the methods given in chapter 5. To assess the suitability of the proposed algorithms, the “fox” and “bantam” conductors are specified when evaluating the power losses. The reason for adopting these conductors is to be able to evaluate a variety of system line power losses from the system provided by ESKOM. In simulating the line power losses, the Monte Carlo simulation is executed directly from the load data. A flow chart for simulating from the load data is shown in appendix 7-D.

In the tables of results shown in this section, the sampled average total line power losses are evaluated from two different numbers of samples namely 1000 and 20,000 for 60 consumers at each load point. The reason of applying different numbers of samples is to demonstrate the effect of number of samples has on the results. It is evident that, the accuracy of the results depends largely on the number of samples taken in Monte Carlo simulations. If the number of samples is increased, the accuracy of the results increases.

In calculating the % difference for the average total power losses as shown in the tables of results, the sample calculation adopted is as follows:

Suppose the total line average power losses evaluated from MC simulation and an analytical method are given variables P_{mc} and P_{an} respectively, it follows that:

The % difference on average total power losses ΔP_{ave} will be:

$$\Delta P_{ave} = \frac{P_{mc} - P_{an}}{P_{mc}} * 100 \tag{7.4}$$

The symbols used in section 7.2.1 for the line interval and numbers of consumers at each load point are also applied in this section.

The data used to produce the results shown in table 7.10 and table 7.11 are as follows: $LI = 7.5$ and $NC = 60$

Table 8.10: Results using “fox” conductor with 1000 samples.

Repetitions	Monte Carlo simulations		Analytical	% difference on average total loss
	loss standard deviation (W)	Average total loss(W)	Average total loss (W)	
10	1.376	187.139	182.952	2.237
20	2.425	186.648	182.952	1.980
30	2.364	186.713	182.952	2.014
40	2.425	186.371	182.952	1.834

Table 7.11: Results using “bantam” conductor with 1000 samples with $LI = 7.5$, $NC = 60$.

Repetitions	Monte Carlo simulations		Analytical	% difference on average total loss
	loss standard deviation (W)	Average total loss (W)	Average total loss(W)	
10	17.352	1189.400	1171.300	1.522
20	16.190	1192.500	1171.300	1.778
30	15.168	1195.000	1171.300	1.983
40	14.831	1193.400	1171.300	1.852

The data used to produce the results shown in table 7.12 and table 7.13 are as follows: $LI = 15$ and $NC = 60$.

Table 7.12: Results using “bantam” conductor with 1000 samples with $LI = 15$; $NC = 60$.

Repetitions	Monte Carlo simulations		Analytical	% difference on average total loss
	loss standard deviation (W)	Average total loss (W)	Average total loss (W)	
10	25.578	2537.700	2463.400	2.928
20	29.109	2494.200	2463.400	1.235
30	29.454	2494.800	2463.400	1.259
40	30.000	2510.400	2463.400	1.872

Table 7.13: Results using bantam conductor with 20,000 samples.

Repetitions	Monte Carlo simulations		Analytical	% difference on average total loss
	loss standard deviation (W)	Average total loss (W)	Average total loss (W)	
10	9.048	2515.600	2463.400	2.075
20	8.147	2513.700	2463.400	2.001
30	7.406	2515.600	2463.400	2.075
40	7.517	2512.400	2463.400	1.950

Note: Number of repetitions represents the number of sampled values

7.3 Three-phase MV distribution systems

The consumer voltage percentile values are evaluated using the methods given in chapters 4 and 5 based on the one line diagram depicted in fig. 7.1. To assess the suitability of the proposed algorithms presented in previous chapter, the “fox” conductor is also applied when dealing with the evaluation of the consumer voltages as mentioned in section 7.2. In the case of the simulation for the consumer voltages, the Monte Carlo simulation is executed by generating random currents from the beta distributed load currents. A flow chart for simulation from beta distributed load currents and constant P-Q loads incorporating feeder voltage regulators for three-phase system is shown in appendix 7-E.

The simulation for the total line power losses on three-phase distribution system is derived from the load data based on the one line diagram depicted in Appendix 7-C, which was supplied by ESKOM.

7.3.1 The comparison between calculated and simulated consumer voltages

The comparison of the consumer voltages for the system depicted in fig. 7.1 is conducted by assuming different line length intervals that will give different consumer voltages. This will enable the evaluation of voltage drops of up to 35 % (for USE application) and above in order to justify the accuracy of the proposed algorithm on three-phase distribution systems. The conductor impedance is calculated as $0.78 + j 0.3848$ per km. The line interval in km is given a variable LI . In order to simplify the procedure, the same statistical parameters for the load currents are applied which are $\alpha = 0.76$, $\beta = 9.51$ and the scaling factor $SF = 60$. This type of load gives ADMD equal to 1.02 kVA as mentioned previously.

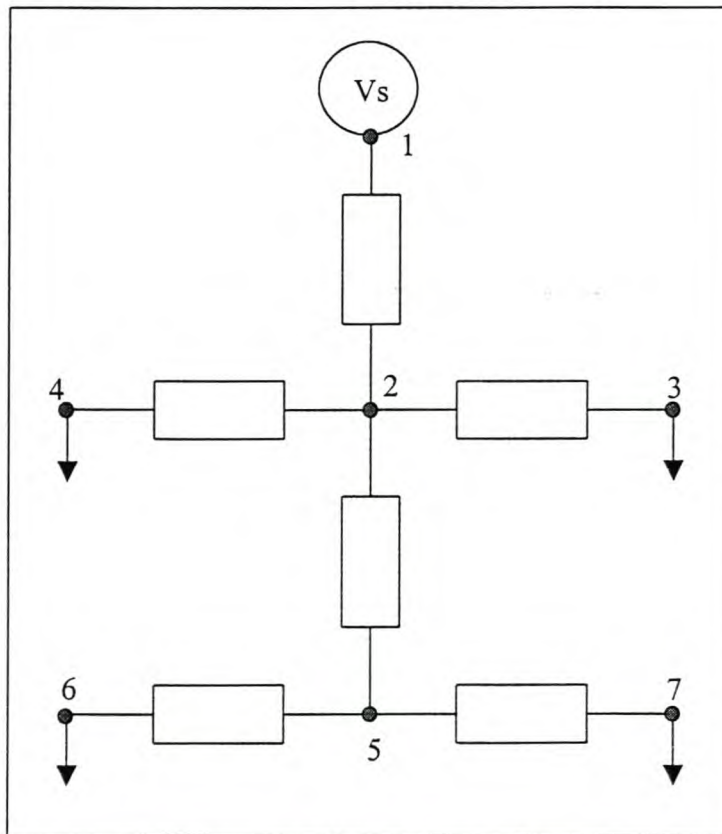


Fig 7.1: One line diagram for simulating the consumer voltage percentile values in three-phase distribution systems

The number of consumers at the load point per phase is given by the variables NC_{ba} , NC_{cb} and NC_{ac} respectively. The constant P-Q loads applied per phase, are represented by the variable S_{ba} , S_{cb} and S_{ac} in kVA for phases ba , cb and ac respectively with the same power factor pf lagging. The number of simulation employed for each case is 15000 in order to achieve an acceptable accuracy in evaluating the consumer voltages as mentioned in section 7.2.1. If capacitor voltage control is employed, it will refer to a three-phase bank capacitor in delta connection.

For step-voltage regulator voltage control, the transformation ratio 1.1 signifies the adoption of two single regulators in open delta configuration, while with ratio 1.15 signifies three regulators in closed delta configuration. The sample calculation per phase for the % difference volt-drop as shown in the table of results is similar to the one described in section 7.2.1.

Table 7.14: The comparison of consumer voltages for $LI = 312$, $NC_{ba} = 20$, $NC_{cb} = 20$ and $NC_{ac} = 20$.

Node No:	Risk=10%								
	Analytical (volts)			MC simulation (volts)			% difference volt-drop		
	Vba	Vcb	Vac	Vba	Vcb	Vac	Vba	Vcb	Vac
2	17724	17724	17724	17735	17745	17733	-0.258	-0.494	-0.211
3	16742	16742	16742	16747	16760	16749	-0.095	-0.344	-0.133
4	16742	16742	16742	16752	16770	16750	-0.191	-0.535	-0.152
5	15434	15434	15434	15461	15465	15447	-0.413	-0.474	-0.198
6	14268	14268	14268	14311	14317	14307	-0.559	-0.638	-0.507
7	14268	14268	14268	14317	14330	14297	-0.638	-0.808	-0.376
Node No:	Risk=20%								
	Analytical (volts)			MC simulation (volts)			% difference volt-drop		
	Vba	Vcb	Vac	Vba	Vcb	Vac	Vba	Vcb	Vac
2	17878	17878	17878	17884	17879	17881	-0.146	-0.024	-0.073
3	16936	16936	16936	16945	16937	16943	-0.178	-0.020	-0.138
4	16936	16936	16936	16940	16939	16940	-0.079	-0.059	-0.079
5	15683	15683	15683	15702	15696	15690	-0.302	-0.206	-0.111
6	14578	14578	14578	14611	14606	14600	-0.447	-0.379	-0.297
7	14578	14578	14578	14614	14616	14607	-0.487	-0.515	-0.392

Table 7.15: Comparison of consumer voltages for $LI = 160$, $NC_{ba} = 20$, $NC_{cb} = 20$, $NC_{ac} = 20$, $S_{ba} = 20$, $S_{cb} = 20$, $S_{ac} = 20$ and $pf = 0.95$.

Node No:	Risk=10%								
	Analytical (volts)			MC simulation (volts)			% difference volt-drop		
	Vba	Vcb	Vac	Vba	Vcb	Vac	Vba	Vcb	Vac
2	17630	17630	17630	17658	17663	17661	-0.645	-0.761	-0.714
3	16627	16627	16627	16662	16668	16669	-0.656	-0.769	-0.788
4	16627	16627	16627	16662	16668	16665	-0.656	-0.769	-0.712
5	15279	15279	15279	15328	15338	15335	-0.734	-0.886	-0.840
6	14106	14106	14106	14169	14179	14178	-0.804	-0.933	-0.920
7	14106	14106	14106	14163	14179	14178	-0.727	-0.933	-0.920
Node No:	Risk=20%								
	Analytical (volts)			MC simulation (volts)			% difference volt-drop		
	Vba	Vcb	Vac	Vba	Vcb	Vac	Vba	Vcb	Vac
2	17713	17713	17713	17745	17746	17742	-0.752	-0.776	-0.681
3	16732	16732	16732	16772	16775	16772	-0.765	-0.823	-0.765
4	16732	16732	16732	16774	16773	16769	-0.804	-0.784	-0.707
5	15414	15414	15414	15470	15476	15471	-0.858	-0.950	-0.873
6	14272	14272	14272	14337	14350	14342	-0.848	-1.020	-0.914
7	14272	14272	14272	14343	14349	14342	-0.927	-1.006	-0.914

Table 7.16: Comparison of consumer voltages for $LI = 110$, $NC_{ba} = 20$, $NC_{cb} = 20$, $NC_{ac} = 20$, $S_{ba} = 20$, $S_{cb} = 20$, $S_{ac} = 20$ and $pf = 0.95$.

Node No:	Risk=10%								
	Analytical (volts)			MC simulation (volts)			% difference volt-drop		
	Vba	Vcb	Vac	Vba	Vcb	Vac	Vba	Vcb	Vac
2	19458	19458	19458	19460	19463	19461	-0.079	-0.197	-0.118
3	18842	18842	18842	18844	18849	18848	-0.063	-0.222	-0.190
4	18842	18842	18842	18844	18846	18846	-0.063	-0.127	-0.127
5	18136	18136	18136	18138	18141	18142	-0.052	-0.130	-0.156
6	17471	17471	17471	17472	17478	17476	-0.022	-0.155	-0.111
7	17471	17471	17471	17472	17472	17478	-0.022	-0.022	-0.155
Node No:	Risk=20%								
	Analytical (volts)			MC simulation (volts)			% difference volt-drop		
	Vba	Vcb	Vac	Vba	Vcb	Vac	Vba	Vcb	Vac
2	19506	19506	19506	19507	19507	19508	-0.040	-0.040	-0.080
3	18905	18905	18905	18907	18904	18907	-0.065	0.032	-0.065
4	18905	18905	18905	18907	18905	18908	-0.065	0.000	-0.097
5	18214	18214	18214	18216	18215	18219	-0.053	-0.026	-0.132
6	17566	17566	17566	17567	17562	17570	-0.023	0.090	-0.090
7	17566	17566	17566	17569	17567	17571	-0.068	-0.023	-0.113

The data used to produce the results for **unbalanced three-phase loads** shown in table 7.17 is as follows: $LI = 140$, $NC_{ba} = 30$, $NC_{cb} = 20$, $NC_{ac} = 10$, $S_{ba} = 30$, $S_{cb} = 20$, $S_{ac} = 10$ and $pf = 0.95$.

Table 7.17: Comparison of consumer voltages.

Node No:	Risk=10%								
	Analytical (volts)			MC simulation (volts)			% difference volt-drop		
	Vba	Vcb	Vac	Vba	Vcb	Vac	Vba	Vcb	Vac
2	17533	18223	19313	17535	18216	19309	-0.045	0.185	0.149
3	16523	17322	18705	16519	17306	18694	0.073	0.341	0.333
4	16523	17322	18705	16517	17309	18695	0.109	0.277	0.303
5	15203	16228	17900	15171	16205	17876	0.469	0.397	0.582
6	14071	15224	17206	14003	15183	17168	0.850	0.601	0.786
7	14071	15224	17206	14002	15187	17165	0.863	0.543	0.848
Node No:	Risk=20%								
	Analytical (volts)			MC simulation (volts)			% difference volt-drop		
	Vba	Vcb	Vac	Vba	Vcb	Vac	Vba	Vcb	Vac
2	17619	18290	19365	17613	18282	19361	0.137	0.215	0.152
3	16632	17409	18772	16616	17397	18761	0.297	0.261	0.340
4	16632	17409	18772	16615	17396	18762	0.316	0.282	0.309
5	15342	16337	17984	15302	16315	17962	0.597	0.387	0.545
6	14240	15259	17309	14164	15324	17271	0.970	-0.974	0.804
7	14240	15359	17309	14161	15322	17270	1.008	0.554	0.825

Table 7.18: Comparison of consumer voltages for $LI = 80$, $NC_{ba} = 20$, $NC_{cb} = 20$, $NC_{ac} = 20$, $S_{ba} = 20$, $S_{cb} = 20$, $S_{ac} = 20$ and $pf = 0.95$.

Node No:	Risk=10%								
	Analytical (volts)			MC simulation (volts)			% difference volt-drop		
	Vba	Vcb	Vac	Vba	Vcb	Vac	Vba	Vcb	Vac
2	20269	20269	20269	20270	20269	20271	-0.058	0.000	-0.116
3	19842	19842	19842	19845	19843	19845	-0.139	-0.046	-0.139
4	19842	19842	19842	19844	19843	19844	-0.093	-0.046	-0.093
5	19378	19378	19378	19382	19379	19381	-0.153	-0.038	-0.115
6	18928	18928	18928	18934	18930	18932	-0.196	-0.065	-0.130
7	18928	18928	18928	18932	18930	18933	-0.130	-0.065	-0.163

Table 7.19: Comparison of consumer voltages for $LI = 80$, $NC_{ba} = 20$, $NC_{cb} = 20$, $NC_{ac} = 20$, $S_{ba} = 20$, $S_{cb} = 20$, $S_{ac} = 20$ and $pf = 0.95$. Capacitor voltage control is employed at node 5 of a rating of 200 $kVAr$ s.

Node No:	Risk=10%								
	Analytical (volts)			MC simulation (volts)			% difference volt-drop		
	Vba	Vcb	Vac	Vba	Vcb	Vac	Vba	Vcb	Vac
2	20951	20951	20951	20943	20943	20944	0.757	0.757	0.663
3	20548	20548	20548	20540	20539	20939	0.548	0.616	0.616
4	20548	20548	20548	20540	20539	20538	0.548	0.616	0.684
5	20904	20904	20904	20878	20878	20878	2.317	2.317	2.317
6	20511	20511	20511	20478	20477	20480	2.168	2.232	2.039
7	20511	20511	20511	20480	20479	20477	2.039	2.104	2.232

Table 7.20: Comparison of consumer voltages for $LI = 220$, $NC_{ba} = 20$, $NC_{cb} = 20$ and $NC_{ac} = 20$.

Node No:	Risk=10%								
	Analytical (volts)			MC simulation (volts)			% difference volt-drop		
	Vba,	Vcb	Vac	Vba	Vcb	Vac	Vba	Vcb	Vac
2	19400	19400	19400	19411	19405	19413	-0.425	-0.193	-0.503
3	18770	18770	18770	18785	18779	18785	-0.467	-0.279	-0.467
4	18770	18770	18770	18783	18778	18782	-0.404	-0.248	-0.373
5	18051	18051	18051	18067	18057	18064	-0.407	-0.152	-0.330
6	17369	17369	17369	17384	17375	17380	-0.325	-0.130	-0.238
7	17369	17369	17369	17378	17374	17382	-0.195	-0.108	-0.282

Table 7.21: Comparison of consumer voltages for $LI = 220$, $NC_{ba} = 20$, $NC_{cb} = 20$ and $NC_{ac} = 20$. Capacitor voltage control is employed at node 5 of a rating of 150 $kVAr$ s.

Node No:	Risk=10%								
	Analytical (volts)			MC simulation (volts)			% difference volt-drop		
	Vba	Vcb	Vac	Vba	Vcb	Vac	Vba	Vcb	Vac
2	20355	20355	20355	20360	20361	20362	-0.305	-0.366	-0.427
3	19802	19802	19802	19814	19810	19813	-0.549	-0.365	-0.503
4	19802	19802	19802	19808	19809	19813	-0.274	-0.319	-0.503
5	20771	20771	20771	20759	20755	20759	0.967	1.285	0.967
6	20299	20299	20299	20278	20273	20283	1.220	1.506	0.932
7	20299	20299	20299	20282	20280	20281	0.990	1.105	1.047

Table 7.22: Comparison of consumer voltages for $LI = 250$, $NC_{ba} = 20$, $NC_{cb} = 20$ and $NC_{ac} = 20$.

Node No:	Risk=10%								
	Analytical (volts)			MC simulation (volts)			% difference volt-drop		
	Vba	Vcb	Vac	Vba	Vcb	Vac	Vba	Vcb	Vac
2	18926	18926	18926	18935	18937	18938	-0.294	-0.359	-0.392
3	18192	18192	18192	18198	18202	18204	-0.158	-0.263	-0.316
4	18192	18192	18192	18199	18203	18203	-0.184	-0.290	-0.290
5	17321	17321	17321	17334	17330	17329	-0.279	-0.193	-0.171
6	16510	16510	16510	16526	16527	16521	-0.292	-0.311	-0.201
7	16510	16510	16510	16520	16520	16519	-0.182	-0.182	-0.164

Table 7.23: Comparison of consumer voltages for $LI = 250$, $NC_{ba} = 20$, $NC_{cb} = 20$ and $NC_{ac} = 20$. Step-voltage regulators are employed to control the voltage at node 2 and 5 each having transformation ratio 1.1.

Node No:	Risk=10%								
	Analytical (volts)			MC simulation (volts)			% difference volt-drop		
	Vba	Vcb	Vac	Vba	Vcb	Vac	Vba	Vcb	Vac
2	20891	20891	20891	20908	20909	20907	-1.557	-1.650	-1.464
3	20205	20205	20205	20220	20225	20223	-0.843	-1.127	-1.013
4	20205	20205	20205	20219	20223	20225	-0.786	-1.013	-1.127
5	21417	21417	21417	21429	21434	21429	-2.102	-3.004	-2.102
6	20721	20721	20721	20731	20737	20727	-0.788	-1.267	-0.471
7	20721	20721	20721	20733	20729	20730	-0.947	-0.629	-0.709

Table 7.24: Comparison of consumer voltages for $LI = 160$, $NC_{ba} = 20$, $NC_{cb} = 20$, $NC_{ac} = 20$, $S_{ba} = 20$, $S_{cb} = 20$, $S_{ac} = 20$ and $pf = 0.9$.

Node No:	Risk=10%								
	Analytical (volts)			MC simulation (volts)			% difference volt-drop		
	Vba	Vcb	Vac	Vba	Vcb	Vac	Vba	Vcb	Vac
2	17638	17638	17638	17648	17646	17643	-0.230	-0.184	-0.115
3	16628	16628	16628	16643	16638	16640	-0.280	-0.186	-0.224
4	16628	16628	16628	16643	16638	16630	-0.280	-0.186	-0.037
5	15279	15279	15279	15294	15287	15287	-0.224	-0.119	-0.119
6	14093	14093	14093	14106	14099	14099	-0.165	-0.076	-0.076
7	14093	14093	14093	14113	14102	14106	-0.254	-0.114	-0.165

Table 7.25: Comparison of consumer voltages for $LI = 160$, $NC_{ba} = 20$, $NC_{cb} = 20$ and $NC_{ac} = 20$, $S_{ba} = 20$, $S_{cb} = 20$, $S_{ac} = 20$ and $pf = 0.9$. Step-voltage regulators are employed to control the voltage at node 2, 3, 4 and 5 with transformation ratio of 1.15, 1.1, 1.1 and 1.15 respectively.

Node No:	Risk=10%								
	Analytical (volts)			MC simulation (volts)			% difference volt-drop		
	Vba	Vcb	Vac	Vba	Vcb	Vac	Vba	Vcb	Vac
2	20259	20259	20259	20263	20262	20261	-0.230	-0.173	-0.115
3	21271	21271	21271	21277	21277	21272	-0.830	-0.830	-0.137
4	21271	21271	21271	21276	21275	21277	-0.691	-0.552	-0.830
5	20901	20901	20901	20900	20900	20901	0.091	0.091	0.000
6	19947	19947	19947	19944	19946	19943	0.146	0.049	0.194
7	19947	19947	19947	19945	19942	19946	0.097	0.243	0.049

7.3.2 The comparison between calculated and simulated results for system power losses in three-phase system

The line power losses on three-phase distribution systems is evaluated as mentioned in chapter 5 based on the one line diagram depicted in appendix 7-C. To assess for the suitability of the proposed algorithm, the fox and bantam conductors are also applied in this

case. In simulating the line power losses, the Monte Carlo simulation is executed directly from the load data. A flow chart for simulating from the load data is shown in appendix 7-F.

In the tables of results shown in this section, the sampled average total line power losses are evaluated from two different numbers of samples namely 1000, 3000 and 20,000 for 60 consumers at each load point. The reason for using different number of samples is already mentioned in section 7.2.2. In calculating the % difference for the average total power losses as shown in the table of results, the sample calculation adopted is mentioned in section 7.2.2. The symbols used in section 7.2.1 are also applicable in this section.

The data used to produce the results shown in table 7.26, table 7.27, table 7.28 and table 7.29 is as follows: $LI = 15$ and $NC = 60$.

Table 7.26: Results using “fox” conductor with 1000 samples.

Repetitions	Monte Carlo simulations		Analytical	% difference on average total loss
	Loss standard Deviation (W)	Average total loss (W)	Average total loss (W)	
10	16.740	1669.900	1638.200	1.898
20	14.804	1672.800	1638.200	2.068
30	13.972	1671.700	1638.200	2.004
40	15.070	1672.900	1638.200	2.074

Table 7.27: Results using “fox” conductor with 20,000 samples.

Repetitions	Monte Carlo simulations		Analytical	% difference on average total loss
	loss standard deviation (W)	Average total loss (W)	Average total loss (W)	
10	2.790	1670.300	1638.200	1.922
20	2.918	1670.000	1638.200	1.904
30	3.183	1670.300	1638.200	1.922
40	3.234	1670.900	1638.200	1.957

Table 7.28: Results “magpie” conductor with 1000 samples.

Repetitions	Monte Carlo simulations		Analytical	% difference on average total loss
	loss standard deviation (W)	Average total loss (W)	Average total loss (W)	
10	66.061	6132.200	6011.300	1.972
20	60.998	6135.400	6011.300	2.023
30	51.717	6132.200	6011.300	1.972
40	46.677	6133.300	6011.300	1.989

Table 7.29: Results “bantam” conductor with 3000 samples.

Repetitions	Monte Carlo simulations		Analytical	% difference on average total loss
	loss standard deviation (W)	Average total loss (W)	Average total loss (W)	
10	49.560	11713.00	11478.00	2.006
20	53.214	11704.00	11478.00	1.931
30	54.506	11713.00	11478.00	2.006
40	50.294	11694.00	11478.00	1.847

Note: Number of repetitions represents the number of sampled values

7.4 Comment on the results

This section is divided into two parts. The first one deals with the comparison of the consumer voltage percentiles while the second one deals with the comparison of the total line power loss values between analytical and MC simulation results in single and three-phase distribution systems.

7.4.1 Comparison of consumer voltage percentile values

The results obtained for the consumer voltage percentile values for single and three-phase systems without employing voltage regulator compare very well. The algorithm demonstrates that, combination of statistical and non-statistical load currents can be applied with acceptable accuracy when evaluating consumer voltage percentile values in the range of up to 65% of the operating voltage. With the application of voltage regulators, two scenarios are of interest. The first scenario is the results due to the application of step-voltage regulators. Referring to table 7.4 and table 7.23, the results do not compare very well to one node of the system if the consumer voltages are regulated to nearly the operating voltage. But in table 7.9 and table 7.25, the results compared very well. From the results, the over-all errors as $mean_{error\%} \pm \sigma_{error\%}$ for single and three-phase systems are presented in table 7.30.

Table 7.30: Over-all errors for consumer voltage percentile values.

topology	$mean_{error\%} \pm \sigma_{error\%}$
single-phase	-0.018 ± 0.840
three-phase	-0.128 ± 0.693

In general it can be concluded that, the results demonstrate the ability of the proposed algorithm being able to handle step-voltage regulators when regulating single and three-phase distribution systems that are experiencing voltage drops well below 35 % to within 10% of the operating voltage.

The second scenario is the application of capacitors for controlling the feeder voltage profile. As pointed in chapter 4, the treatment of the voltage phase angles is somewhat in contrary to the norms. This phenomenon can be due to the leading power factor angle. From this fact, the 10 % level of risk for the consumer voltage percentile values due to statistical load currents or in combination with the non-statistical load currents, may exceed the deterministic value. This of course will depend on the capacitor rating applied. Results shown in table 7.8 and table 7.21 compare very well between analytical and simulation results despite the fact that, the 10 % level of risk values exceeds that of the deterministic values. By observing the trend of the results obtained during the simulations, it came apparent that there should a criterion to be observed when capacitors are employed for feeder voltage control if beta distributed load currents are present in the system. The following were deduced from the analysis:

- for obtaining accurate results when the combination of statistical and non-statistical load currents are considered, the 10 % level of risk value for any consumer voltage percentile value should not exceed the deterministic value
- if only statistical load currents are applied, the above condition does not apply. That means, any values to be evaluated shall have an acceptable accuracy

7.4.2 Comparison of total line power losses

The analytical and simulated average power loss results at each load point in single and three-phase distribution systems compare well. The % difference on the average power total loss of an approximately value of 2 can be regarded as satisfactory result taking into consideration up to a value of 11.478 kW was evaluated. The standard deviations of the sampled average values differ greatly when different number of simulations is applied. It is evident that, if number of simulations is increased far beyond 20,000, the standard deviation of the sampled mean could approach to zero. This is consistent with the central limit theorem. To put things in perspective, the time required to produce the results shown in table 7.27 was approximately 192 hrs. From the results, the over-all errors as $mean_{error\%} \pm \sigma_{error\%}$ for single and three-phase systems are presented in table 7.31.

There is clear evidence that, the result shows the calculation of the average values of the total line power losses proves adequate. The issue of having large dispersion on the line total power losses in MV distribution systems when the load currents are treated as signals is not evident in this case.

Table 7.31: Over-all errors for the average total loss values.

topology	$mean_{error\%} \pm \sigma_{error\%}$
Single-phase	1.192 ± 0.390
Three-phase	1.968 ± 0.062

7.5 Summary

The proposed algorithm in this present work has been verified. When beta distributed load currents are considered, the presence of capacitors in the MV distribution systems requires a special treatment as previously mentioned.

FINANCIAL ANALYSIS ON MV DISTRIBUTION SYSTEMS

8.1 Introduction

The financial aspects of meeting the requirements of implementing electrification projects are discussed in this chapter. As mentioned in chapter 1, the evaluation of the cost of the MV distribution systems falls into three categories namely capital, operating and maintenance costs. The cost can be minimised if the project is properly designed. This is not an easy task, but with financial assessment of different alternatives, an engineering decision can be reached. It is unwise to over-emphasise capital cost, as operating costs and maintenance costs for the anticipated number of years in service of the project should also be included in the financial assessment. The aim of this chapter is not to design new distribution systems, but to apply the developed algorithms in this thesis to assess the financial requirements of MV distribution networks and to provide a criterion for the appropriate application of the USE concept.

8.2 Illustrative example on existing MV distribution system**8.2.1 Selection of parameters**

To illustrate the application of the present work, the existing ESKOM distribution system depicted in the appendix 7-C is investigated. Cost assessment will be done on SWER, single-phase (phase-phase) connection and three-phase topologies using USE devices and step-voltage regulators for system voltage regulation. The MV line cost per km data for different topologies and the cost for an isolating transformer in SWER systems were supplied by ESKOM [8.1]. The cost of USE devices per kVA is estimated at 1000 Rands [8.2] and the total cost for installing a pole mounted 200A, 22 kV open delta connected step-voltage regulator is estimated at 345,954 Rands. For single-phase step-voltage regulators, the total costs are estimated to be half of the open delta connected step-voltage regulators. The load data used is from Sweetwaters 96 community with load current parameters of $E[\mu] = 1.04$, $E[\rho] = 0.24$ and $E[\sigma] = 1.58$ [8.3]. The operating costs due to line power losses are charged at 28 cents per kW-hr while the maintenance costs are assumed to be 20% of the unit cost distributed evenly throughout the anticipated number of 25 years in service. The total cost is evaluated in terms of the present worth value (PWV) using a worth factor of 0.9. The World Bank recommends a net discount value of 8% to 10% [8.4].

The results are not intended to compare different topologies but rather to show the difference in costs between the USE concept and conventional methods. It should be borne in mind that the results are dependent on the data applied. With capacitor voltage control, the regulation achieved depends mainly on the reactance of the system, and a useful increase in voltage will be obtained only if the reactance is substantial [8.5]. In this particular case the capacitor control was not effective for system voltage regulation and therefore was not considered. In all cases investigated, the line conductor current ratings were higher than the magnitude of line currents at the source.

8.2.2 Approach adopted

For the specified load parameters, the line conductor is chosen to cause voltage drop in excess of 30% at the furthest node from the source. This will illustrate the application of USE devices. In the case of conventional methods, different alternatives will be investigated based on the selected system data.

8.2.2.1 Analysis of a SWER network

The number of consumers at each load point is considered to be 40 while the constant P-Q loads are assumed to be 10 kVA at a 0.9 power factor lagging. The statistical load current parameters are $\alpha = 0.76$, $\beta = 9.51$ and scaling factor of 60. The total line length is 132 km. The results in table 8.1 show the use of the “bantam” conductor for the USE concept while the “magpie” and “squirrel” conductors are applied for the conventional method. The “squirrel” conductor satisfies the voltage conditions but “magpie” conductor requires a step-voltage regulator at node 5 for voltage regulation.

Table 8.1: PWV for indicated number of years in service in thousand Rands

SWER network, appendix 7-C , 40 consumers, P-Q loads 10kVA, pf=0.9 lagging at each load point, total line length 132 km			
no. of years in service	USE	conventional method	
	“bantam”	“squirrel”	“magpie” with step-voltage regulator at node 5
5	1251.2	922.4731	953.9268
10	1262.9	923.3808	958.7202
15	1269.9	923.9167	961.5507
20	1274.0	924.2332	963.2221
25	1276.4	924.4201	964.2090

8.2.2.2 Analysis of a single-phase (phase-phase) network

The number of consumers at each load point is considered to be 45 while the constant P-Q loads are assumed to be 15 kVA at a 0.9 power factor lagging.

Table 8.2: PWV for indicated number of years in service in thousand Rands

single-phase network, appendix 7-C , 45 consumers, P-Q loads 15kVA, pf=0.9 lagging at each load point, total line length 132 km			
no. of years in service	USE	conventional method	
	“magpie”	“fox”	“squirrel” with step-voltage regulator at node 5
5	2039.7	1651.0	1630.1
10	2053.4	1651.8	1634.7
15	2061.5	1652.3	1637.4
20	2066.3	1652.6	1638.9
25	2069.1	1652.8	1639.9

The statistical load current parameters are $\alpha = 0.76$, $\beta = 9.51$ and scaling factor of 60. The total line length is 132 km. The results in table 8.2 show the application of “magpie” conductor for the USE concept while the “fox” and “squirrel” conductors are applied for the

conventional method. The “fox” conductor satisfies the voltage conditions but “squirrel” conductor requires a step-voltage regulator at node 5 for voltage regulation.

8.2.2.3 Analysis of a three-phase network

The number of consumers at each load point is considered to be 30 while the constant P-Q loads are assumed to be 10 kVA at a 0.9 power factor lagging per phase. The statistical load current parameters are $\alpha = 0.76$, $\beta = 9.51$ and scaling factor of 60. The total line length is 210 km. The result in table 8.3 shows the application of “magpie” conductor for the USE concept while the “fox” and “squirrel” conductors are applied for the conventional method. The “fox” conductor satisfies the voltage conditions but “squirrel” conductor requires an open delta connected step-voltage regulators at node 5 for voltage regulation.

Table 8.3: PWV for indicated number of years in service in thousand Rands

three-phase network, appendix 7-C , 30 consumers, P-Q loads 10kVA, pf=0.9 lagging per phase at each load point, total line length 210 km			
no. of years in service	USE	conventional method	
	“magpie”	“fox”	“squirrel” with step-voltage regulator at node 5
5	4462.3	3954.0	3634.3
10	4483.9	3954.2	3640.7
15	4496.7	3954.4	3644.5
20	4504.2	3954.4	3646.7
25	4508.7	3954.5	3648.0

The above results indicate that, the USE concept is a more expensive option compared with conventional method. The USE devices are applied at any load point that is experiencing a voltage magnitude drop greater than 10% of the operating voltage. This condition does not favour the USE concept. In section 8.3, the criterion for the application of the USE concept is provided.

8.3 Criteria for the application of the USE concept

In section 8.2, the costs of distribution networks are presented. The cost due to the application of USE concept is greater than that of the conventional method. It should be understood that, the USE devices perform the voltage regulation at the low voltage distribution networks. In relation to MV distribution networks, the devices control the voltage at only one point, i.e., at the distribution transformer. The ability to compensate for the voltage drops of the order of 35% should be exploited when trying to find the best criteria for the application of the USE devices. But the operating costs due to line power losses will have a great repercussion on the total project cost for the anticipated number of years in service if the line resistance per km is large.

In contrast, step-voltage regulators improve the voltage regulation at the point of connection and downstream node points on the MV distribution networks. While capacitors improve the voltage profile on any part of the MV distribution although in a limited magnitude depending on the nature of the system. In this section, a typical distribution network configuration will be examined that favours the application of the USE concept. In order that, the USE concept be more economical, the load points that requires the application of the USE devices should experience a voltage drop of the order of 35%. For increased line lengths, the USE concept stands a chance of becoming more economical compared with

conventional methods. This is due to the fact that, the difference in total line costs between the conductor to be used for the USE concept and the next conductor size for achieving good voltage regulation without voltage regulators can exceed the cost of USE devices. This is the prerequisite for the USE concept to be able to compete with conventional methods.

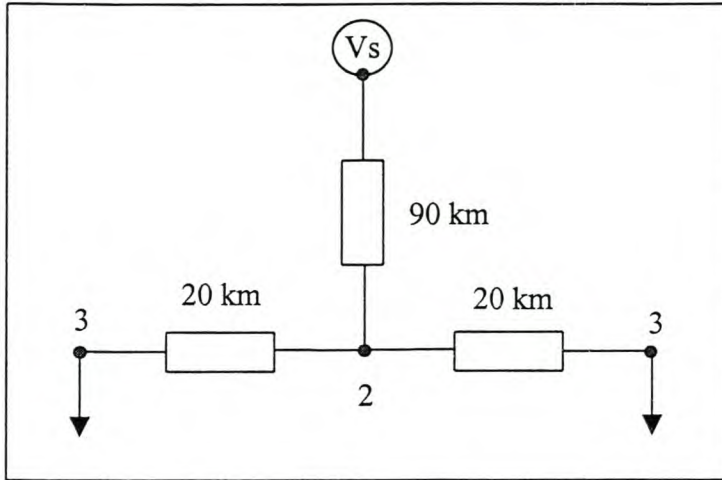


Fig. 8.1: One line diagram for application of the USE concept

Preliminary assessment done on SWER, single-phase (phase-phase) connection and three-phase networks, shows the prospect of USE concept if the network configuration feeds load points that are experiencing a voltage drop of around 35% with the total line length of the network exceeding 100 km. The results obtained from the network depicted in fig. 8.1 indicate that the USE concept is more economical than the conventional method. The results for SWER, single phase and three-phase networks are shown in table 8.4, 8.5 and 8.6 respectively. The costs of capacitors are given in appendix 8-B. For single-phase applications, the value provided is divided by 3.

Table 8.4: PWV for indicated number of years in service in thousand Rands

SWER network, fig. 8.1, 80 consumers at node 3 and 4, total line length 130 km			
no. of years in service	USE	conventional method	
	“bantam”	“squirrel”	“magpie” with step-voltage regulator at node 2
5	872.3823	888.8586	922.1237
10	877.3696	889.5191	926.4146
15	880.3146	889.9091	928.9483
20	882.0535	890.1394	930.4445
25	883.0804	890.2754	931.3275

Table 8.5: PWV for indicated number of years in service in thousand Rands

single-phase network , fig. 8.1, 95 consumers at node 3 and 4, total line length 130 km				
no. of years in service	USE	conventional method		
	“magpie”	“fox”	“squirrel” with step-voltage regulator at node 2	“squirrel” with capacitor control 350kVAr at node 2
5	1401.2	1625.8	1607.7	1450.1
10	1403.7	1626.4	1611.9	1451.7
15	1405.2	1626.8	1614.4	1452.6
20	1406.1	1627.1	1615.9	1453.1
25	1406.6	1627.7	1616.2	1453.5

Table 8.6: PWV for indicated number of years in service in thousand Rands

three-phase network , fig. 8.1, 64 consumers per phase at node 3 and 4, 1 line length 130 km				
no. of years in service	USE	conventional method		
	“magpie”	“fox”	“squirrel” with step-voltage regulator at node 2	“squirrel” with capacitor control 200kVAr at node 2
5	2000.0	2447.8	2385.5	2088.1
10	2000.5	2447.9	2391.8	2089.4
15	2000.8	2448.0	2395.5	2090.1
20	2001.0	2448.0	2397.7	2090.5
25	2001.1	2448.1	2399.0	2090.8

The USE concept in this particular case shows that it can compete with the conventional method. The major factor is the total length in km of the distribution network and the number of load points present that are experiencing a voltage drop of the order of 35%. This simple case demonstrates the viability of the USE concept and with a new distribution network the above-mentioned criteria could be used to indicate the feasibility of the USE concept. Then, the cost assessment can be performed to verify the suitability of the USE concept.

8.4 Comment on the field performance for the USE devices

The performance of the USE devices in the field has been very satisfactory. It is envisaged that the devices can be of great importance to deep-rural areas as demonstrated in section 8.3.

8.5 Summary

In this chapter, the algorithms developed in this thesis were used to perform cost assessment on MV distribution networks. The criterion for the application of the USE concept is briefly outlined. The engineering decision on whether the USE concept is the best-recommended option could be reached after the cost assessment is performed based on the above-mentioned criteria using the analytical tools developed in this thesis. The prospects for the USE concept for deep-rural areas are promising as demonstrated in this chapter. In assessing the convergence rate for the NR-algorithm and back and forward sweep algorithm for the deterministic load flow in single-phase networks due to statistical and non-statistical

currents, it was observed that, the back and forward sweep algorithm requires approximately twice the number of iterations to achieve the same accuracy.

CONCLUSION

9.1 Introduction

The work described in this thesis, uses models of combined beta-distributed and constant $P-Q$ loads for evaluating consumer voltages. Loads modelled as current signals are used for evaluating line power losses. The analysis is performed on single and three-phase ($\Delta-\Delta$) connected MV distribution networks with or without voltage regulators. In previous work, beta-distributed loads and loads treated as current signals were used on LV networks for evaluating consumer voltage percentile values and line power losses respectively. Typical topologies analysed were three-phase four wire and bi-phase networks.

9.2 Previous research work**9.2.1 Evaluation of the consumer voltages**

In reference [9.1], the authors describe a probabilistic load-flow currently known as the Herman Beta method. The Herman Beta method of calculating voltage drops in LV feeders was developed for three-phase, four-wire, bi-phase and single-phase topologies using the Beta pdf description for the load currents. This method uses the principle of manipulating random variables of load currents into voltage drop random variables. Statistical parameters of the consumer voltages are then evaluated from their first and second statistical moments. The first and the second moments of the consumer voltages are expressed in terms of the first and the second moments of the branch voltage drops. A percentile value of the consumer voltage variable is obtained by assigning a risk level or conversely, a confidence level. Heunis et al. applied a principle of superposition to calculate the random variable for the total feeder voltage drop [9.2].

The voltage drop random variable is expressed as the sum of the random variables of each source. The authors developed general expressions for the first and the second moments of the real and imaginary components of the total voltage drop for each load current at any node of the system. By applying the principle of superposition, the individual results are summed to produce the final result.

Hitherto the analysis neglects the effect of the line inductive reactance, consumer voltage phase angles and the loads are assumed to be constant current at unity power factor at the time of the maximum demand. On MV distribution systems, such assumptions are not valid and therefore the analysis was modified to take into consideration the line inductive reactance and the consumer voltage phase-angles. Using the Taylor series approximation in evaluating the first moment of the consumer voltages in the previous work is adequate for LV networks. On MV networks experiencing excessive voltage drops of the order of 35%, the number of terms and coefficients of Taylor series approximation must be extended and modified to ensure accurate results.

9.2.2 Evaluation of line power losses

The treatment of loads as current signals is a concept that describes individual consumer load currents over a given period of time using their mean and standard deviation [9.3]. The research conducted by Heunis in different communities in South Africa reveals that the consumer load currents treated as signals are correlated.

9.3 Contribution of present research work

9.3.1 Evaluation of the consumer voltages

The present work deals with MV (i.e. 11kV and higher) distribution networks for rural electrification. In rural areas two different load types may be present. Such loads are domestic loads, which are beta- distributed loads and pump loads that may be modelled as constant $P-Q$ loads. An analytical tool for computing voltage regulation on MV distribution networks for rural areas feeding the mentioned loads is therefore required. The approach adopted in this present work is as follows:

- beta-distributed load currents are modified and the Herman beta method is applied to a new set of general expressions developed for the system without branches. The modification of the beta-distributed load currents is based on the concept of treating the deterministic component of the beta-distributed loads as constant real power loads with or without voltage regulating devices. This type of load modelling is suitable for MV distribution systems when evaluating up to 35% voltage drop
- consumer voltage angles, current due to the modelling of voltage regulators and system line capacitance are assumed to be deterministic parameters
- employ the first three terms of the expanded Taylor series using a search engine imbedded in the probabilistic load flow to facilitate satisfactory results when evaluating voltage drops of up to 35% when voltage regulating devices such as the USE concept are used
- evaluation of the consumer voltages at the various nodes due to statistical and non-statistical load currents is done using the principle of superposition
- formulation of a routine for the inclusion of step-voltage regulators in open-delta and closed-delta configuration in three-phase ($\Delta - \Delta$) connected networks

9.3.2 Evaluation of line power losses

The product between the line resistance and the square of the line current determines the system line power losses. Since the line currents in MV distribution networks are to be treated as phasors, the square of the branch current can be determined as the sum of the squares of its real and imaginary components. This enables the development of general expressions of the total power loss in single and three-phase MV radial distribution networks without branches.

To apply the load current signals on the MV distribution line, the individual load current signals are transformed. The transformation ratio is evaluated from the distribution transformer turns ratio and the average value of the current signal treated as a constant real power load.

9.4 Development of the universal algorithm

The main objective for developing the so-called “universal algorithm” was to enable the developed general expressions from the networks without branches as stated in section 9.3.1 and 9.3.2 to be applied to practical MV distribution networks. The algorithm is very flexible in its application and it can accommodate step-voltage regulators. The computer program

generates various numbers of arrays automatically when supplied with the input data. The vital array is the D-array which describes the one line diagram for single and three-phase networks. Upon application of step-voltage regulators, the D-array is automatically generated to accommodate the new network arrangement, as a result of the introduction of artificial nodes.

9.5 Development of the computer programs

The probabilistic load flows in single and three-phase distribution networks were developed based on the algorithms stated in section 9.3 and 9.4. The programs are divided into nine parts as follows:

- specification of the input data
- universal algorithm
- deterministic load flow for evaluating the scaling factors and load current phase angles due to current modeled as signals
- evaluation of the line power losses due to current signals
- deterministic load flow due to the combination of the deterministic component of the beta-distributed and constant $P-Q$ loads (If line capacitances and voltage regulators are present they take part in the solution).
- evaluation of consumer voltage percentile values at a specified level of risk due to beta-distributed loads
- evaluation of the consumer voltages due to statistical and non-statistical currents
- an algorithm for including of voltage regulators
- cost assessment of a distribution network in terms of the present worth value

9.6 Observations

In the course of comparing analytical and Monte Carlo simulation results for algorithm verification, the under-mentioned were noted for assuring correct analytical results in evaluating the consumer voltages.

- the voltage angles are valid if line capacitance is neglected and the voltage regulation is not done through the application of capacitors
- if voltage regulation is done using capacitors or line capacitance is not neglected, the deterministic voltage angles prior to the inclusion of voltage regulating capacitors or line capacitance should be used in the probabilistic load flow as well as when the percentile values at any risk are to be converted to phasors
- for non-statistical currents, their phasors at any system condition are valid, this includes currents due to constant $P-Q$ loads, line capacitance and voltage regulators (step-voltage regulators or capacitors)

- for obtaining accurate results when the combination of statistical and non-statistical load currents are considered when voltage regulation is done using capacitors, the 10 % level of risk value for any consumer voltage percentile value should not exceed the deterministic value
- if only statistical load currents are applied, the above condition does not apply. That means, any values to be evaluated shall have an acceptable accuracy

9.7 Significance of the present work

The work presented in this thesis has a wide range of application in the field of Electrical Engineering. The new contributions and their significances are as follows:

9.7.1 Development of the probabilistic load flows

The developed single and three-phase probabilistic load flows in this thesis is a new contribution to MV distribution networks. The evaluation of consumer voltages is due to the combination of beta-distributed and constant $P-Q$ loads with or without voltage regulators. Also presented is the evaluation of line power losses due to load current signals. At each load point on the MV distribution network, different load parameters can be specified. Finally, cost assessment is performed in terms of present worth value.

9.7.2 Modelling of step-voltage regulators on the three-phase ($\Delta-\Delta$) connected network

Application of step-voltage regulators in single and three-phase star-connected systems can be implemented by adopting the single-phase regulator model directly [9.4]. On the three-phase ($\Delta-\Delta$) connected network, the modeling cannot be applied directly. To be able to model the open delta and closed delta configuration in such a network, a procedure has been devised in this thesis to accomplish the task. This is a new contribution taking also into consideration that, beta-distributed and constant $P-Q$ loads are specified as input data.

9.7.3 Derivation of a general expression of line power losses in MV distribution networks

Developed general expressions of line power losses in single and three-phase ($\Delta-\Delta$) connected network in this thesis are significant especially in computer programming. It is now possible to evaluate line power losses in unbalanced three-phase radial distribution ($\Delta-\Delta$) connected networks. Despite the fact that, these general expressions are derived from the network without branches, their practical applications are realised through the use of the so-called “universal algorithm” presented in the thesis.

9.7.4 Development of the universal algorithm

The universal algorithm is a tool that can be used to translate any general expressions developed on an electrical network without branches into branched networks. In other words, the developed universal algorithm can process the existing algorithms for power load flow analysis that do not employ the system Y-bus or Z-bus matrices. The arrays developed are used in such a way to suit the specific algorithm. The algorithm can further assist the following:

- calculation of short circuit currents
- evaluation of the magnitude of line currents for design purposes
- calculation of line power losses in distribution radial networks

9.8 Future research work

In the light of the findings in this thesis, some interesting research work in the future can be pursued in the following topics:

- influence of system capacitance on beta distributed load currents
- electrical modeling of the open delta and closed delta connected step-voltage regulators on three-phase networks and the application of the algorithm presented in this thesis
- investigation of the distribution of the nodal voltage phase angles

REFERENCES

CHAPTER 1

- [1.1] S.G. Menon, B.B.V.R. Rao, "Planning of Distribution Systems in Developing Countries", IEE Proceedings, Vol. 133, No. 7. November 1986, pp. 384-388.
- [1.2] S. Sabharwal, "Rural Electrification Cost Including Transmission and Distribution Losses and Investment", IEEE Transactions on Energy Conversion, Vol. 5, No.3, September 1990, pp. 493-501.
- [1.3] J.J. Burke, "Power Distribution Engineering", MARCEL DEKKER, ICL., 1994 pg. 76-83.
- [1.4] ESKOM Electrification Tool Box, "SWER Single Wire Earth Return Systems", January 1997.
- [1.5] P. Shiel, "Evaluation of Rural Distribution Network Performance", UPEC, 1994, pp. 530-533.
- [1.6] J.A.K. Douglas, "Ranking of design Criteria to Improve Rural Network Performance", Reliability of Transmission and Distribution Equipment, Conference Publication NO. 406, March 1995, pp. 145-150.
- [1.7] R.E. Macey, "The influence of regulators, capacitors and reclosers on rural electrification system design", Electron, July, 1989, pp. 27-31.
- [1.8] D. Povh, M. Wienhold, "Development of FACTS for Distribution Systems", EPRI Future of Power Delivery Conference, Washington D.C., 1996.
- [1.9] S. Thiel, "Investigating the USE Concept for Rural Electrification Applications", M. Eng. Thesis, University of Stellenbosch, December 1997, pg. 31.
- [1.10] Y.G. Paithankar, Transmission Network Protection, Theory and Practice, Marcel Dekker, Inc., 1998, pg. 3.
- [1.11] R. Herman, J.S. Maritz, J.H.R. Enslin, "The analysis of voltage regulation in residential distribution networks using the beta distribution model", Electric Power Systems Research 29 (1994) pp 213-216.
- [1.12] S.W. Heunis, "The Analysis and Quantification of Uncertainty in Least Life-Cost Electrical Low Voltage Distribution Design", Ph.D. thesis, University of Stellenbosch, December 2000.

CHAPTER 2

- [2.1] IEEE Task Force on Load Representation for Dynamic Performance, 'Bibliography on load models for power flow and dynamic performance simulation', IEEE Transactions on Power Systems, Vol. 10, No. 1, February 1995, pp 523-538.

- [2.2] W.C. Brice, "Voltage –Drop Calculations and Power-Flow Studies for Rural Electric Distribution Lines" IEEE Transactions on Industry Applications, Vol. 28, No.4, July/August 1992, pp 774-781.
- [2.3] G.J. Berg, A.K. Kar, "Model representation of power system loads," PICA conf., Proc., 1997, pp. 153-162.
- [2.4] R. Herman, J.J. Kritzinger, "The statistical description of grouped domestic electrical load currents," Electric Power Research, 27, 1993, pp. 43-48.
- [2.5] R. Herman, C.T. Gaunt, S.W. Heunis, "Benchmark Tests and Results for the Evaluation of L.V. Distribution Voltage Drop Calculation Procedures" The Transactions of the S.A. Institute of Electrical Engineers, June 1999, pp. 54-60.
- [2.6] R. Herman, "Voltage regulation analysis for the design of low voltage networks feeding stochastic domestic electrical loads", Ph.D. thesis, University of Stellenbosch, November 1993, pg. 3.4-3.5
- [2.7] D. Das, D.P. Kothari, A. Kalam, "Simple and Efficient Method for Load Flow Solution of Radial Distribution Networks", Electrical Power & Energy Systems, Vol. 17, No. 5, 1995, pp. 335-346.
- [2.8] G.X. Luo, A. Semlyen, "Efficient Load Flow for Large Weakly Meshed Networks", IEEE Transactions on Power Systems, Vol. 5, No. 4, November 1990, pp. 1309-1316.
- [2.9] S.C. Tripathy, G.G. Prasad, O.P. Malik, G.S. Hope, "Load-Flow Solutions for Ill-Conditioned Power Systems by a Newton-Like Method", IEEE Transactions on Power Apparatus and Systems, Vol. PAS-101, No. 10, October 1982, pp. 3648-3657.
- [2.10] D. Rajicic, A. Bose, "A Modification to the Fast De-coupled Power Flow for Networks with High R/X Ratios," IEEE Transactions on Power Systems, Vol. 3, No. 2, May 1988, pp. 743-746
- [2.11] M.E. Baran, E.A. Staton, "Distribution Transformer Models for Branch Current Based Feeder Analysis", IEEE Transactions on Power Systems, Vol. 12, No. 2, May 1997, pp. 698-703.
- [2.12] C.S. Cheng, D. Shirmohammadi, "A three-phase Power Flow Method for Real-Time Distribution System Analysis", IEEE Transactions on Power Systems, May 1995, pp. 671-679.
- [2.13] T.H. Chen, et al., "Distribution System Power Flow Analysis – A Rigid Approach", IEEE Transactions on Power Delivery, Vol. 6, No. 3, July 1991, pp. 1146-1152.
- [2.14] R.D. Zimmerman, H.D. Chiang, "Fast Decoupled Power Flow for Unbalanced Radial Distribution Systems", IEEE Transactions on Power Systems, Vol. 10, No. 4, November 1995, pp. 2045-2052.
- [2.15] D. Shirmohammadi, H.W. Hong, A. Semlyen, G.X. Luo, "A Compensation-Based Power Flow Method for Weakly Meshed Distribution and Transmission Networks", IEEE Transactions on Power Systems, Vol. 3, No. 2, January 1988, pp. 753-762.

- [2.16] W.F. Tinney, C.E. Hart, "Power Flow Solution by Newton's Method", IEEE Transactions on Power Apparatus and Systems, Vol. PAS-86, No. 11, November 1967, pp. 1449-1460.
- [2.17] P. Caramia, G. Carpinelli, P. Varilone, P. Verde, "Probabilistic three-phase load flow", Electrical Power and Energy Systems 21 (1999), pp. 55-69.
- [2.18] R. Herman, J.S. Maritz, J.H.R. Enslin, "The analysis of voltage regulation in residential distribution networks using the beta distribution model", Electric Power Systems Research 29 (1994) pp 213-216.
- [2.19] R. Herman, S.W. Heunis, "General probabilistic voltage drop calculation method for LV distribution networks based on a beta p.d.f. load model, Electric Power Systems Research 46 (1998) pp 45-49.
- [2.20] R.E. Macey, "The influence of regulators, capacitors and reclosers on rural electrification system design", Electron, July, 1989, pp. 27-31.
- [2.21] W.H. Kersting, W.H. Phillips, "Modelling and analysis of rural electric distribution feeders", IEEE Transactions on Industry Application, Vol. 28, No. 4, July 1992, pp. 767-772.
- [2.22] S. Thiel, C. Mostert, J.H.R. Enslin, "Universal power electronic solution to low-cost rural electrification", Electron, Nov/Dec, 1996, pp. 9-12.
- [2.23] J.J. Burke, "Power Distribution Engineering", Marcel Dekker, Inc., 1994 pg. 76-83.
- [2.24] Y. Baghzouz, "Effect of non-linear loads on optimal capacitor placement on radial feeders", IEEE Transactions on Power Delivery, Vol. 6, No. 1, January 1991, pp. 245-251.
- [2.25] J.J. Burke, "Power Distribution Engineering", Marcel Dekker, Inc., 1994 pg. 58.
- [2.26] ESKOM, Distribution Standard, Pat 4: Medium Voltage Reticulation, Section 0: General Information and Requirements for Overhead Lines up to 33Kv with Conductors up to Hare, September 2001.
- [2.27] J. J. Grainger, W.D. Stevenson, Jr., "Power System Analysis", McGraw Hill, Inc., 1994, pg. 361-363.
- [2.28] S. Thiel, "Investigating the USE Concept for Rural Electrification Applications", M. Eng. Thesis, University of Stellenbosch, December 1997, pg. 31.
- [2.29] C. Mostert, S. Thiel, J.H.R. Enslin, R. Herman, R. Stephen, "Investigating the Different combinations of uFacts Devices in Low Cost Rural Electrification", Cigre Study Committee 14 International Colloquium on HVDC and Facts, September 1997.
- [2.30] S.W. Heunis, "The Analysis and Quantification of Uncertainty in Least Life-Cost Electrical Low Voltage Distribution Design", Ph.D. thesis, University of Stellenbosch, December 2000.

Chapter 3

- [3.1] R. Herman, Voltage regulation analysis for the design of low voltage networks feeding stochastic domestic electrical loads, Ph.D. thesis, University of Stellenbosch, November 1993.

Chapter 4

- [4.1] R. Herman, Voltage regulation analysis for the design of low voltage networks feeding stochastic domestic electrical loads, Ph.D. thesis, University of Stellenbosch, November 1993.
- [4.2] Thiel, S, Mostert, C, Enslin, J.H.R., Stephen,R., “Universal power electronic solution to low-cost rural electrification”, Electron, Nov/Dec 1996, pp. 9-12.
- [4.3] R. Herman, J.S. Maritz, “Voltage regulation algorithm for a bi-phase distribution system feeding residential using a Beta p.d.f. load model”, Electric Power Systems Research 43, 1997, pp. 77-80.
- [4.4] Stagg and EL-Abiad, Computer Methods in Power System Analysis, McGRAW-HILL, ICN. Pg. 292-299, 1968.
- [4.5] Grainger, J. J., Stevenson , W.D., Jr., Power System Analysis, McGraw-Hill, Inc., 1994,pg. 170.

Chapter 5

- [5.1] Herman, R., Heunis, S.W., “ General probabilistic voltage drop calculation method for LV distribution networks based on a beta p.d.f. load model”, Electric Power Systems Research 46 (1998) pp 45-49.
- [5.2] Herman, R., Gaunt, C.T., Heunis, S.W., “Benchmark Tests and Results for the Evaluation of LV Distribution Voltage Drop Calculation Procedures”, The Transactions of the S.A. Institute of Electrical Engineers, June 1999, pp. 54-60.
- [5.3] Herman, R., Maritz, J.S., Enslin, J.H.R., “ The analysis of voltage regulation in residential distribution networks using the beta distribution model”, Electric Power Systems Research 29 (1994) pp 213-216.
- [5.4] N. I. Johnson and S. Kotz, Continuous univariate distribution – 2, Houghton Mifflin, pg. 40, 1970.
- [5.5] R. Herman, Voltage regulation analysis for the design of low voltage networks feeding stochastic domestic electrical loads, Ph.D. thesis, University of Stellenbosch, November 1993.
- [5.6] S.W. Heunis, “The Analysis and Quantification of Uncertainty in Least Life-Cost Electrical Low Voltage Distribution Design”, Ph.D. thesis, University of Stellenbosch, December 2000.

- [5.7] Scheaffer, R.L., McClave, J.T., Statistical for Engineers, PWS Publishers, 1982, pg.46, pg. 51.
- [5.8] NRS Load Research database, project manager Marcus Dekenah of Marcus Dekenah Consulting company, mdekenah@pixie.co.za.
- [5.9] Davies, O.L., Goldsmith, P.L., Statistical methods in research and production, Oliver and Boyd Tweeddale Court, Edinburgh, 1972, pg.231.

Chapter 6

- [6.1] Grainger, J. J., Stevenson , W.D., Jr., Power System Analysis, McGraw-Hill, Inc., 1994,pg. 361-364.
- [6.2] Stagg and EL-Abiad, Computer Methods in Power System Analysis, McGraw Hill, Inc., pg. 270-273, 1968.
- [6.3] M.E. Baran, E.A. Staton, “Distribution Transformer Models for Branch Current Based Feeder Analysis”, IEEE Transactions on Power Systems, Vol. 12, No. 2, May 1997, pp. 698-703.

Chapter 8

- [8.1] H.J. Geldenhuys, Project Leader for Electrification Cost Estimator, ESKOM, 1998.
- [8.2] H.J. Beukes, W. Swiegers, J.H.R. Enslin, G. Lee, C. Mostert, S. Thiel, “Development of a 45 kVA Universal Semiconductor Electrification Device”, EPRI, 8th International Power Quality Applications Conference, 9-11 November 1998, Cape Town, South Africa.
- [8.3] S.W. Heunis, “The Analysis and Quantification of Uncertainty in Least Life-Cost Electrical Low Voltage Distribution Design”, Ph.D. thesis, University of Stellenbosch, December 2000.
- [8.4] NRS, Rationalized User Specification, Guidelines for the Provision of Electrical Distribution Networks in Residential Areas, Part 1: Planning and Design of Distribution Systems, NRS O34-1: 1997.
- [8.5] The Electricity Council, Power System Protection, Peter Peregrinus Ltd., Stevenage, UK and New York, Vol. 3, Application, Reprinted 1990, pg. 219.

Chapter 9

- [9.1] R. Herman, J.S. Maritz, J.H.R. Enslin, “The analysis of voltage regulation in residential distribution networks using the beta distribution model”, Electric Power Systems Research 29 (1994) pp 213-216.
- [9.2] R. Herman, S.W. Heunis, “General probabilistic voltage drop calculation method for LV distribution networks based on a beta p.d.f. load model, Electric Power Systems Research 46 (1998) pp 45-49.

- [9.3] S.W. Heunis, "The Analysis and Quantification of Uncertainty in Least Life-Cost Electrical Low Voltage Distribution Design", Ph.D. thesis, University of Stellenbosch, December 2000.
- [9.4] Grainger, J. J., Stevenson , W.D., Jr., Power System Analysis, McGraw-Hill, Inc., 1994,pg. 361-364.

Modified Herman Beta Method

The summary of the developed general expressions in the three-phase four-wire system for LV distribution networks is presented below.

The network system input data is defined as:

$$R_{pi} = \sum_{s=1}^i R_s \quad (2-A1)$$

$$K_i = \frac{\sum_{s=1}^i R_s}{\sum_{t=1}^i R_t} \quad (2-A2)$$

R_s and R_t being the phase conductor resistance and neutral conductor resistance respectively between node $i-1$ and i with ma_i , mb_i and mc_i being the total number of customers connected to the phases a , b and c at node i respectively. The beta parameters of the load current of individual consumer are given as α and β with CB as the circuit breaker rating.

The general expressions developed are as follows:

The first statistical moment or expected value of the total real component of the voltage drop at node i , $E[\Delta V_{re-itotal}]$ is given as:

$$E[\Delta V_{re-itotal}] = \sum_{i=1}^N E[\Delta V_{re-i}] \quad (2-A3)$$

given

$$E[V_{re-i}] = C_{mkli} R_{pi} CB \frac{\alpha}{\alpha + \beta} \quad (2-A4)$$

where

$$C_{mkli} = (1 + K_i)ma_i - K_i(mb_i + mc_i) / 2$$

The second statistical moment of the total real component of the voltage drop at node i , $E[\Delta V_{re-itotal}^2]$ is given as:

$$E[\Delta V_{re-itotal}^2] = \sum_{i=1}^N E[\Delta V_{re-i}^2] + \sum_{m=1}^N \sum_{\substack{p=1 \\ p \neq m}}^N E[\Delta V_{re-p}] \quad (2-A5)$$

given

$$E[\Delta V_{re-i}^2] = R_{pi}^2 CB^2 \left\{ C_{mk2i} \frac{\alpha(\alpha + 1)}{(\alpha + \beta)(\alpha + \beta + 1)} + C_{mk3i} \frac{\alpha^2}{(\alpha + \beta)^2} \right\} \quad (2-A6)$$

where

$$C_{mk2i} = K_i^2 \{ (ma_i + 0.25mb_i + 0.25mc_i) + (2k_i + 1)ma_i \}$$

$$C_{mk3i} = \psi_{1i} K_i^2 + \psi_{2i} K_i + \psi_{3i}$$

$$\psi_{1i} = ma_i(ma_i - 1) - ma_i(mb_i + mc_i) + 0.25(mb_i + mc_i - 1)(mb_i + mc_i)$$

$$\Psi_{2i} = ma_i(2ma_i - mb_i - mc_i - 2)$$

$$\Psi_{3i} = ma_i(ma_i - 1)$$

The first statistical moment or expected value of the total imaginary component of the voltage drop at node i , $E[\Delta V_{im-total}]$ is given as:

$$E[\Delta V_{im-total}] = \sum_{i=1}^N E[\Delta V_{im-i}] \quad (2-A7)$$

given

$$E[\Delta V_{im-i}] = C_{mk6i} R_{pi} CB \frac{\alpha}{\alpha + \beta} \quad (2-A8)$$

where

$$C_{mk6i} = \frac{\sqrt{3}}{2} K_i (mb_i - mc_i)$$

The second statistical moment of the total imaginary component of the voltage drop at node i , $E[\Delta V_{im-total}^2]$ is given as:

$$E[\Delta V_{im-total}^2] = \sum_{i=1}^N E[\Delta V_{im-i}^2] + \sum_{m=1}^N \sum_{\substack{p=1 \\ p \neq m}}^N E[\Delta V_{im-p}] \quad (2-A9)$$

given

$$E[\Delta V_{im-i}^2] = R_{pi}^2 CB^2 \left\{ C_{mk4i} \frac{\alpha(\alpha + 1)}{(\alpha + \beta)(\alpha + \beta + 1)} + C_{mk5i} \frac{\alpha^2}{(\alpha + \beta)^2} \right\} \quad (2-A10)$$

where

$$C_{mk4i} = \frac{3}{4} K_i^2 (mb_i + mc_i)$$

$$C_{mk5i} = \frac{3}{4} K_i^2 (mb_i + mc_i)^2 - (mb_i + mc_i)$$

To evaluate for the consumer voltages at a specified level of risk, the normalised first moment and the second moment for each consumer voltage should be evaluated so that their statistical parameters can be obtained.

By applying the Taylor expansion approximation, the first moment for the consumer voltage at node i , $E[V_{con-total}]$ is expressed as:

$$E[V_{con-total}] = V_S \left\{ 1 - \frac{E[\Delta V_{re-total}]}{V_S} + \frac{1}{2} E\left[\frac{\Delta V_{im-total}^2}{V_S^2}\right] \right\} \quad (2-A11)$$

The second moment for the consumer voltage at node i , $E[V_{con-total}^2]$ can be expressed as:

$$E[V_{con-total}^2] = V_S^2 - 2V_S E[\Delta V_{re-total}] + E[\Delta V_{re-total}^2] + E[\Delta V_{im-total}^2] \quad (2-A12)$$

Derivation of the real component of the branch voltage drops

According to fig. 3.1 and equation (3.4), the voltage drop $\Delta\bar{V}_2$ across the branch impedance \bar{Z}_2 will be:

$$\begin{aligned} \Delta\bar{V}_2 &= (R_2 + jX_2)(\bar{I}_2 + \bar{I}_3 + \bar{I}_4 + \bar{I}_5 + \dots + \bar{I}_{m-1} + \bar{I}_m) \\ &= (R_2 + jX_2)\{I_2(\cos\alpha_2 + j\sin\alpha_2) + I_3(\cos\alpha_3 + j\sin\alpha_3) + \dots + I_m(\cos\alpha_m + j\sin\alpha_m)\} \\ &= I_2(R_2\cos\alpha_2 + jR_2\sin\alpha_2 + jX_2\cos\alpha_2 - X_2\sin\alpha_2) + I_3(R_2\cos\alpha_3 + jR_2\sin\alpha_3 \\ &\quad + jX_2\cos\alpha_3 - X_2\sin\alpha_3) + \dots + I_m(R_2\cos\alpha_m + jR_2\sin\alpha_m + jX_2\cos\alpha_m - X_2\sin\alpha_m) \end{aligned}$$

The real component of the voltage drop ΔV_{2real} across the branch impedance \bar{Z}_2 can be expressed as:

$$\Delta V_{2real} = I_2(R_2\cos\alpha_2 - X_2\sin\alpha_2) + I_3(R_2\cos\alpha_3 - X_2\sin\alpha_3) + \dots + I_m(R_2\cos\alpha_m - X_2\sin\alpha_m)$$

The voltage drop $\Delta\bar{V}_3$ across the branch impedance \bar{Z}_3 will be:

$$\begin{aligned} \Delta\bar{V}_3 &= (R_3 + jX_3)(\bar{I}_3 + \bar{I}_4 + \bar{I}_5 + \dots + \bar{I}_{m-1} + \bar{I}_m) \\ &= (R_3 + jX_3)\{I_3(\cos\alpha_3 + j\sin\alpha_3) + I_4(\cos\alpha_4 + j\sin\alpha_4) + \dots + I_m(\cos\alpha_m + j\sin\alpha_m)\} \\ &= I_3(R_3\cos\alpha_3 + jR_3\sin\alpha_3 + jX_3\cos\alpha_3 - X_3\sin\alpha_3) + I_4(R_3\cos\alpha_4 + jR_3\sin\alpha_4 + jX_3\cos\alpha_4 \\ &\quad - X_3\sin\alpha_3) + \dots + I_m(R_3\cos\alpha_m + jR_3\sin\alpha_m + jX_3\cos\alpha_m - X_3\sin\alpha_m) \end{aligned}$$

The real component of the voltage drop ΔV_{3real} across the branch impedance \bar{Z}_3 can be expressed as:

$$\Delta V_{3real} = I_3(R_3\cos\alpha_3 - X_3\sin\alpha_3) + I_4(R_3\cos\alpha_4 - X_3\sin\alpha_4) + \dots + I_m(R_3\cos\alpha_m - X_3\sin\alpha_m)$$

Also, the voltage drop $\Delta\bar{V}_m$ across the branch impedance \bar{Z}_m will be:

$$\begin{aligned} \Delta\bar{V}_m &= (R_m + jX_m)\bar{I}_m \\ &= (R_m + jX_m)\{I_m(\cos\alpha_m + j\sin\alpha_m)\} \\ &= I_m(R_m\cos\alpha_m + jR_m\sin\alpha_m + jX_m\cos\alpha_m - X_m\sin\alpha_m) \end{aligned}$$

The real component of the voltage drop ΔV_{mreal} across the branch impedance \bar{Z}_m can be expressed as:

$$\Delta V_{mreal} = I_m (R_m \cos \alpha_m - X_m \sin \alpha_m)$$

Examining the above expressions of the real component of the branch voltage drops, it can be concluded that, the general expression for the real component of the voltage drop ΔV_{ireal} across the branch impedance \bar{Z}_i can be expressed as:

$$\Delta V_{ireal} = \sum_{k=i}^m I_k (R_k \cos \alpha_k - X_k \sin \alpha_k)$$

APPENDIX 3-B

Derivation of the square of the real component of the branch voltage drops

The general expression for the real component of the voltage drop ΔV_{ireal} across the impedance \bar{Z}_i is given as (Appendix 3-A):

$$\Delta V_{ireal} = \sum_{k=i}^m I_k (R_k \cos \alpha_k - X_k \sin \alpha_k)$$

The square of the real component of the voltage drop ΔV^2_{2real} across the impedance \bar{Z}_2 will be:

$$\Delta V^2_{2real} = \{I_2(R_2 \cos \alpha_2 - X_2 \sin \alpha_2) + \dots + I_m(R_m \cos \alpha_m - X_m \sin \alpha_m)\}^2$$

Let $A_2 = I_2(R_2 \cos \alpha_2 - X_2 \sin \alpha_2)$, $A_3 = I_3(R_3 \cos \alpha_3 - X_3 \sin \alpha_3)$,

$$A_m = I_m(R_m \cos \alpha_m - X_m \sin \alpha_m)$$

Thus, $\Delta V^2_{2real} = (A_2 + A_3 + \dots + A_m)^2$

$$= A_2^2 + A_3^2 + \dots + A_m^2 + A_2 A_3 + \dots + A_2 A_m + A_3 A_2 + \dots + A_3 A_m + A_{m-1} A_2 + A_{m-1} A_3 + \dots + A_{m-1} A_m$$

If the other branches are considered, therefore in general, the square of the real component of the voltage drops across the branch impedance \bar{Z}_i , can be expressed as:

$$\sum_{k=i}^m A_k^2 + 2 \sum_{k=i}^{m-1} \sum_{n=k+1}^m A_k A_n$$

From the above:

$$A_2^2 = I_2^2 (R_2^2 \cos^2 \alpha_2 + X_2^2 \sin^2 \alpha_2 - 2R_2 X_2 \cos \alpha_2 \sin \alpha_2)$$

$$A_3^2 = I_3^2 (R_3^2 \cos^2 \alpha_3 + X_3^2 \sin^2 \alpha_3 - 2R_3 X_3 \cos \alpha_3 \sin \alpha_3)$$

$$A_m^2 = I_m^2 (R_m^2 \cos^2 \alpha_m + X_m^2 \sin^2 \alpha_m - 2R_m X_m \cos \alpha_m \sin \alpha_m)$$

$$\begin{aligned} 2A_2A_3 &= 2I_2I_3(R_2 \cos \alpha_2 - X_2 \sin \alpha_2)(R_2 \cos \alpha_3 - X_2 \sin \alpha_3) \\ &= 2I_2I_3(R_2^2 \cos \alpha_2 \cos \alpha_3 - R_2X_2 \cos \alpha_2 \sin \alpha_3 - R_2X_2 \sin \alpha_2 \cos \alpha_3 + X_2^2 \sin \alpha_2 \sin \alpha_3) \\ &= 2I_2I_3(R_2^2 \cos \alpha_2 \cos \alpha_3 + X_2^2 \sin \alpha_2 \sin \alpha_3 - R_2X_2 \sin(\alpha_2 + \alpha_3)) \end{aligned}$$

$$\begin{aligned} 2A_2A_m &= 2I_2I_m(R_2 \cos \alpha_2 - X_2 \sin \alpha_2)(R_2 \cos \alpha_m - X_2 \sin \alpha_m) \\ &= 2I_2I_m(R_2^2 \cos \alpha_2 \cos \alpha_m + X_2^2 \sin \alpha_2 \sin \alpha_m - R_2X_2 \sin(\alpha_2 + \alpha_m)) \end{aligned}$$

$$\begin{aligned} 2A_3A_m &= 2I_3I_m(R_2 \cos \alpha_3 - X_2 \sin \alpha_3)(R_2 \cos \alpha_m - X_2 \sin \alpha_m) \\ &= 2I_3I_m(R_2^2 \cos \alpha_3 \cos \alpha_m + X_2^2 \sin \alpha_3 \sin \alpha_m - R_2X_2 \sin(\alpha_3 + \alpha_m)) \end{aligned}$$

If the same procedure is performed for all branches, the result shows that, the expression for the square of the real component of the voltage drop ΔV_{ireal}^2 across the impedance \bar{Z}_i can be given as:

$$\begin{aligned} \Delta V_{ireal}^2 &= \sum_{Z=i}^m I_Z^2 (R_i^2 \cos^2 \alpha_Z + X_i^2 \sin^2 \alpha_Z - 2R_iX_i \cos \alpha_Z \sin \alpha_Z) \\ &\quad + 2 \sum_{k=i}^{m-1} \sum_{n=k+1}^m I_k I_n \{R_i^2 \cos \alpha_k \cos \alpha_n + X_i^2 \sin \alpha_k \sin \alpha_n - R_iX_i \sin(\alpha_k + \alpha_n)\} \end{aligned}$$

APPENDIX 3-C

Derivation of the imaginary component of the branch voltage drops

According to fig. 3.1 and equation (3.4), the voltage drop $\Delta \bar{V}_2$ across the branch impedance \bar{Z}_2 will be:

$$\begin{aligned} \Delta \bar{V}_2 &= (R_2 + jX_2)(\bar{I}_2 + \bar{I}_3 + \bar{I}_4 + \bar{I}_5 + \dots + \bar{I}_{m-1} + \bar{I}_m) \\ &= (R_2 + jX_2)\{I_2(\cos \alpha_2 + j \sin \alpha_2) + I_3(\cos \alpha_3 + j \sin \alpha_3) + \dots + I_m(\cos \alpha_m + j \sin \alpha_m)\} \\ &= I_2(R_2 \cos \alpha_2 + jR_2 \sin \alpha_2 + jX_2 \cos \alpha_2 - X_2 \sin \alpha_2) + I_3(R_2 \cos \alpha_3 + jR_2 \sin \alpha_3 + jX_2 \cos \alpha_3 \\ &\quad - X_2 \sin \alpha_3) + \dots + I_m(R_2 \cos \alpha_m + jR_2 \sin \alpha_m + jX_2 \cos \alpha_m - X_2 \sin \alpha_m) \end{aligned}$$

The imaginary component of the voltage drop ΔV_{2imag} across the branch impedance \bar{Z}_2 can be expressed as:

$$\Delta V_{2imag} = I_2(R_2 \sin \alpha_2 + X_2 \cos \alpha_2) + I_3(R_2 \sin \alpha_3 + X_2 \cos \alpha_3) + \dots + I_m(R_2 \sin \alpha_m + X_2 \cos \alpha_m)$$

The voltage drop $\Delta \bar{V}_3$ across the branch impedance \bar{Z}_3 will be:

$$\Delta \bar{V}_3 = (R_3 + jX_3)(\bar{I}_3 + \bar{I}_4 + \bar{I}_5 + \dots + \bar{I}_{m-1} + \bar{I}_m)$$

$$\begin{aligned}
 &= (R_3 + jX_3)\{I_3(\cos\alpha_3 + j\sin\alpha_3) + I_4(\cos\alpha_4 + j\sin\alpha_4) + \dots + I_m(\cos\alpha_m + j\sin\alpha_m)\} \\
 &= I_3(R_3 \cos\alpha_3 + jR_3 \sin\alpha_3 + jX_3 \cos\alpha_3 - X_3 \sin\alpha_3) + I_4(R_3 \cos\alpha_4 + jR_3 \sin\alpha_4 + jX_3 \cos\alpha_4 \\
 &\quad - X_3 \sin\alpha_3) + \dots + I_m(R_3 \cos\alpha_m + jR_3 \sin\alpha_m + jX_3 \cos\alpha_m - X_3 \sin\alpha_m)
 \end{aligned}$$

The imaginary component of the voltage drop ΔV_{3imag} across the branch impedance \bar{Z}_3 can be expressed as:

$$\Delta V_{3imag} = I_3(R_3 \sin\alpha_3 + X_3 \cos\alpha_3) + I_4(R_3 \sin\alpha_4 + X_3 \cos\alpha_4) + \dots + I_m(R_3 \sin\alpha_m + X_3 \cos\alpha_m)$$

Also, the voltage drop $\Delta \bar{V}_m$ across the branch impedance \bar{Z}_m will be:

$$\begin{aligned}
 \Delta V_m &= (R_m + jX_m)I_m \\
 &= (R_m + jX_m)\{I_m(\cos\alpha_m + j\sin\alpha_m)\} \\
 &= I_m(R_m \cos\alpha_m + jR_m \sin\alpha_m + jX_m \cos\alpha_m - X_m \sin\alpha_m)
 \end{aligned}$$

The imaginary component of the voltage drop ΔV_{mimag} across the branch impedance \bar{Z}_m can be expressed as:

$$\Delta V_{mimag} = I_m(R_m \sin\alpha_m + X_m \cos\alpha_m)$$

Examining the above expressions of the imaginary component of the branch voltage drops, it can be concluded that, the general expression for the imaginary component of the voltage drop ΔV_{iimag} across the branch impedance \bar{Z}_i can be expressed as:

$$\Delta V_{iimag} = \sum_{k=i}^m I_k (R_i \sin\alpha_k + X_i \cos\alpha_k)$$

APPENDIX 3-D

Derivation of the square of the imaginary component of the branch voltage drops

The general expression for the imaginary component of the voltage drop ΔV_{iimag} across the impedance \bar{Z}_i is given as (Appendix 3-C):

$$\Delta V_{iimag} = \sum_{k=i}^m I_k (R_i \sin\alpha_k + X_i \cos\alpha_k)$$

The square of the imaginary component of the voltage drop ΔV_{2imag}^2 across the impedance \bar{Z}_2 will be:

$$\Delta V^2_{2imag} = \{I_2(R_2 \sin \alpha_2 + X_2 \cos \alpha_2) + \dots + I_m(R_2 \sin \alpha_m + X_2 \cos \alpha_m)\}^2$$

$$\text{Let } B_2 = I_2(R_2 \sin \alpha_2 + X_2 \cos \alpha_2), B_3 = I_3(R_2 \sin \alpha_3 + X_2 \cos \alpha_3),$$

$$B_m = I_2(R_2 \sin \alpha_m + X_2 \cos \alpha_m)$$

$$\text{Thus, } (\Delta V^2_{2imag})^2 = (B_2 + B_3 + \dots + B_m)^2$$

$$= B_2^2 + B_3^2 + \dots + B_m^2 + B_2B_3 + \dots + B_2B_m + B_3B_2 + \dots + B_3B_m + B_{m-1}B_2 + B_{m-1}B_3 + \dots + B_{m-1}B_m$$

If the other branches are considered, therefore in general, the square of the imaginary component of the voltage drops across the branch impedance \bar{Z}_i , can be expressed as:

$$\sum_{k=i}^m B_k^2 + 2 \sum_{k=i}^{m-1} \sum_{n=k+1}^m B_k B_n$$

From the above:

$$B_2^2 = I_2^2 (R_2^2 \sin^2 \alpha_2 + X_2^2 \cos^2 \alpha_2 + 2R_2X_2 \sin \alpha_2 \cos \alpha_2)$$

$$B_3^2 = I_3^2 (R_2^2 \sin^2 \alpha_3 + X_2^2 \cos^2 \alpha_3 + 2R_2X_2 \sin \alpha_3 \cos \alpha_3)$$

$$B_m^2 = I_2^2 (R_2^2 \sin^2 \alpha_m + X_2^2 \cos^2 \alpha_m + 2R_2X_2 \sin \alpha_m \cos \alpha_m)$$

$$\begin{aligned} 2B_2B_3 &= 2I_2I_3(R_2 \sin \alpha_2 + X_2 \cos \alpha_2)(R_2 \sin \alpha_3 + X_2 \cos \alpha_3) \\ &= 2I_2I_3(R_2^2 \sin \alpha_2 \sin \alpha_3 + R_2X_2 \sin \alpha_2 \cos \alpha_3 + R_2X_2 \cos \alpha_2 \sin \alpha_3 + X_2^2 \cos \alpha_2 \cos \alpha_3) \\ &= 2I_2I_3(R_2^2 \sin \alpha_2 \sin \alpha_3 + X_2^2 \cos \alpha_2 \cos \alpha_3 + R_2X_2 \sin(\alpha_2 + \alpha_3)) \end{aligned}$$

$$\begin{aligned} 2B_2B_m &= 2I_2I_m(R_2 \sin \alpha_2 + X_2 \cos \alpha_2)(R_2 \sin \alpha_m + X_2 \cos \alpha_m) \\ &= 2I_2I_m(R_2^2 \sin \alpha_2 \sin \alpha_m + X_2^2 \cos \alpha_2 \cos \alpha_m + R_2X_2 \sin(\alpha_2 + \alpha_m)) \end{aligned}$$

$$\begin{aligned} 2B_3B_m &= 2I_3I_m(R_2 \sin \alpha_3 + X_2 \cos \alpha_3)(R_2 \sin \alpha_m + X_2 \cos \alpha_m) \\ &= 2I_3I_m(R_2^2 \sin \alpha_3 \sin \alpha_m + X_2^2 \cos \alpha_3 \cos \alpha_m + R_2X_2 \sin(\alpha_3 + \alpha_m)) \end{aligned}$$

If the same procedure is performed for all branches, the result shows that, the expression for the square of the imaginary component of the voltage drop ΔV^2_{iimag} across the impedance \bar{Z}_i can be given as:

$$\begin{aligned} \Delta V^2_{iimag} &= \sum_{Z=i}^m I_Z^2 (R_i^2 \sin^2 \alpha_Z + X_i^2 \cos^2 \alpha_Z + 2R_iX_i \sin \alpha_Z \cos \alpha_Z) \\ &\quad + 2 \sum_{k=i}^{m-1} \sum_{n=k+1}^m I_k I_n \{R_i^2 \sin \alpha_k \sin \alpha_n + X_i^2 \cos \alpha_k \cos \alpha_n + R_iX_i \sin(\alpha_k + \alpha_n)\} \end{aligned}$$

Derivation of the square of the total real component of the branch voltage drops

The total real component of the branch voltage drops ΔV_{ireal_total} at node i can be expressed as (see appendix 3-A):

$$\begin{aligned}\Delta V_{ireal_total} &= \sum_{y=2}^i \Delta V_{yreal} \\ &= \sum_{y=2}^i \sum_{k=y}^m I_k (R_y \cos \alpha_k - X_y \sin \alpha_k)\end{aligned}$$

If $i = 2$, $\Delta V_{ireal_total} = \Delta V_{ireal}$

$$\text{But if } i = 3, \Delta V_{ireal_total} = \sum_{y=2}^3 \sum_{k=y}^m I_k (R_y \cos \alpha_k - X_y \sin \alpha_k)$$

$$\text{In case of } i = m, \quad \Delta V_{ireal_total} = \sum_{y=2}^m \sum_{k=y}^m I_k (R_y \cos \alpha_k - X_y \sin \alpha_k)$$

The square of the total real component of the branch voltage drops at any node can be determined by squaring the above expressions.

The procedure is very demanding and cannot be repeated here due to space limitation. But in general, the square of the total real component of the branch voltage drops $\Delta V_{ireal_total}^2$ at node i can be expressed as:

$$\begin{aligned}\Delta V_{ireal_total}^2 &= \left(\sum_{y=2}^i \sum_{k=y}^m I_k (R_y \cos \alpha_k - X_y \sin \alpha_k) \right)^2 \\ &= \sum_{y=2}^i \sum_{Z=y}^m I_Z^2 (R_y^2 \cos^2 \alpha_Z + X_y^2 \sin^2 \alpha_Z - 2R_y X_y \cos \alpha_Z \sin \alpha_Z) \\ &+ 2 \sum_{y=2}^i \sum_{f=y+1}^i \sum_{g=f}^m I_g^2 \{ R_y R_f \cos^2 \alpha_g + X_y X_f \sin^2 \alpha_g - \cos \alpha_g \sin \alpha_g (R_y X_f - R_f X_y) \} \\ &+ 2 \sum_{y=2}^i \sum_{k=y}^{m-1} \sum_{n=k+1}^m I_k I_n \{ R_y^2 \cos \alpha_k \cos \alpha_n + X_y^2 \sin \alpha_k \sin \alpha_n - R_y X_y \sin(\alpha_k + \alpha_n) \} \\ &+ 2 \sum_{y=2}^i \sum_A^i \sum_B^{m-1} \sum_C^m I_r I_t (R_y R_p \cos \alpha_r \cos \alpha_t + X_y X_p \sin \alpha_r \sin \alpha_t \\ &\quad - R_y X_p \cos \alpha_r \sin \alpha_t - X_y R_p \sin \alpha_r \cos \alpha_t)\end{aligned}$$

where A stands for $p = 2, p \neq y$

B stands for $r = 2, r \geq y$

C stands for $t = 2, t > r, t > y, t \geq p$

The above expression was tested for its accuracy through programming. The procedure adopted was to square the expression $\Delta V_{ireal_total} = \sum_{y=2}^i \sum_{k=y}^m I_k (R_y \cos \alpha_k - X_y \sin \alpha_k)$ at each node i and compared it with the above expression $\Delta V^2_{ireal_total}$. The two gave the same results.

Unfortunately, the developed universal algorithm as described in chapter 6 when dealing with single-phase and three-phase branched systems cannot easily adopt the above expression $\Delta V^2_{ireal_total}$.

Referring to fig. 3.2, at node m , the total branch voltage drops $\Delta \bar{V}_{m_total}$ can be given as:

$$\Delta \bar{V}_{m_total} = \Delta \bar{V}_2 + \Delta \bar{V}_3 + \Delta \bar{V}_4 + \dots + \Delta \bar{V}_{m-1} + \Delta \bar{V}_m$$

$$\Delta \bar{V}^2_{m_total} = (\Delta \bar{V}_2 + \Delta \bar{V}_3 + \Delta \bar{V}_4 + \dots + \Delta \bar{V}_{m-1} + \Delta \bar{V}_m)^2$$

$$= \Delta \bar{V}^2_2 + \Delta \bar{V}^2_3 + \Delta \bar{V}^2_4 + \dots + \Delta \bar{V}^2_{m-1} + \Delta \bar{V}^2_m + \Delta \bar{V}_2 \cdot \Delta \bar{V}_3 + \dots + \Delta \bar{V}_2 \cdot \Delta \bar{V}_m + \Delta \bar{V}_3 \cdot \Delta \bar{V}_2 + \dots + \Delta \bar{V}_3 \cdot \Delta \bar{V}_m + \dots + \Delta \bar{V}_{m-1} \cdot \Delta \bar{V}_2 + \dots + \Delta \bar{V}_{m-1} \cdot \Delta \bar{V}_m + \Delta \bar{V}_m \cdot \Delta \bar{V}_2 + \dots + \Delta \bar{V}_m \cdot \Delta \bar{V}_{m-1}$$

It can be concluded that, at node i , the square of the total real component of the branch voltage drops $\Delta V^2_{ireal_total}$ can be expressed as:

$$\Delta V^2_{ireal_total} = \sum_{y=2}^i \Delta V^2_{yreal} + 2 \sum_{k=2}^{i-1} \sum_{n=k+1}^i \Delta V_{kreal} \cdot \Delta V_{nreal} \quad (\text{A3-E})$$

According to equation (A3-E):

$\sum_{y=2}^i \Delta V^2_{yreal}$ is the total sum of the square of the real component of the branch voltage drops at node i as described in equation (3.16)

$2 \sum_{k=2}^{i-1} \sum_{n=k+1}^i \Delta V_{kreal} \cdot \Delta V_{nreal}$ is the sum of the product of the real component of the branch voltage

drops at node i

The real component of the branch voltage drops is determined as indicated in appendix 3-A. When determining the second moment of the total real component of the branch voltage drops, it will be difficult to implement the sum of the product of the real component of the branch voltage drops. This is due to the fact that, the identification of the product of load currents and the square of load currents cannot be easily performed.

Derivation of the square of the total imaginary component of the branch voltage drops

The total imaginary component of the branch voltage drops ΔV_{iimag_total} at node i can be expressed as (see appendix 3-C):

$$\begin{aligned}\Delta V_{iimag_total} &= \sum_{y=2}^i \Delta V_{yimag} \\ &= \sum_{y=2}^i \sum_{k=y}^M I_k (R_y \sin \alpha_k + X_y \cos \alpha_k)\end{aligned}$$

If $i = 2$, $\Delta V_{iimag_total} = \Delta V_{iimag}$

But if $i = 3$, $\Delta V_{iimag_total} = \sum_{y=2}^3 \sum_{k=y}^m I_k (R_y \sin \alpha_k + X_y \cos \alpha_k)$

In case of $i = m$, $\Delta V_{iimag_total} = \sum_{y=2}^m \sum_{k=y}^m I_k (R_y \sin \alpha_k + X_y \cos \alpha_k)$

The square of the total imaginary component of the branch voltage drops at any node can be determined by squaring the above expressions.

The procedure is very demanding as previously mentioned in appendix 3-E and cannot be repeated here due to space limitation. But in general, the square of the total imaginary component of the branch voltage drops $\Delta V^2_{iimag_total}$ at node i can be expressed as:

$$\begin{aligned}\Delta V^2_{iimag_total} &= \left(\sum_{y=2}^i \sum_{k=y}^m I_k (R_y \sin \alpha_k + X_y \cos \alpha_k) \right)^2 \\ &= \sum_{y=2}^i \sum_{Z=y}^m I_Z^2 (R_y^2 \sin^2 \alpha_Z + X_y^2 \cos^2 \alpha_Z + 2R_y X_y \cos \alpha_Z \sin \alpha_Z) \\ &+ 2 \sum_{y=2}^i \sum_{f=y+1}^i \sum_{g=f}^m I_g^2 (R_y R_f \sin^2 \alpha_g + X_y X_f \cos^2 \alpha_g + \cos \alpha_g \sin \alpha_g (R_y X_f + R_f X_y)) \\ &+ 2 \sum_{y=2}^i \sum_{k=y}^{m-1} \sum_{n=k+1}^m I_k I_n \{ R_y^2 \sin \alpha_k \sin \alpha_n + X_y^2 \cos \alpha_k \cos \alpha_n + R_y X_y \sin(\alpha_k + \alpha_n) \} \\ &+ 2 \sum_{y=2}^i \sum_A^i \sum_B^m \sum_C^m I_r I_t (R_y R_p \sin \alpha_r \sin \alpha_t + X_y X_p \cos \alpha_r \cos \alpha_t \\ &\quad + R_y X_p \sin \alpha_r \cos \alpha_t + X_y R_p \cos \alpha_r \sin \alpha_t)\end{aligned}$$

where A stands for $p = 2, p \neq y$

B stands for $r = 2, r \geq y$

C stands for $t = 2, t > r, t > y, t \geq p$

The above expression was tested for its accuracy through programming. The procedure adopted was to square the expression $\Delta V_{imag_total} = \sum_{y=2}^i \sum_{k=y}^m I_k (R_y \sin \alpha_k + X_y \cos \alpha_k)$ at each node i and compared it with the above expression $\Delta V^2_{iimag_total}$. The two gave the same results. Unfortunately, the developed universal algorithm as described in chapter 6 when dealing with single-phase and three-phase branched systems cannot easily adopt the above expression $\Delta V^2_{iimag_total}$.

$$\Delta \bar{V}_{m_total} = \Delta \bar{V}_2 + \Delta \bar{V}_3 + \Delta \bar{V}_4 + \dots + \Delta \bar{V}_{m-1} + \Delta \bar{V}_m$$

$$\Delta \bar{V}^2_{m_total} = (\Delta \bar{V}_2 + \Delta \bar{V}_3 + \Delta \bar{V}_4 + \dots + \Delta \bar{V}_{m-1} + \Delta \bar{V}_m)^2$$

$$= \Delta \bar{V}^2_2 + \Delta \bar{V}^2_3 + \Delta \bar{V}^2_4 + \dots + \Delta \bar{V}^2_{m-1} + \Delta \bar{V}^2_m + \Delta \bar{V}_2 \cdot \Delta \bar{V}_3 + \dots + \Delta \bar{V}_2 \cdot \Delta \bar{V}_m + \Delta \bar{V}_3 \cdot \Delta \bar{V}_2 + \dots + \Delta \bar{V}_3 \cdot \Delta \bar{V}_m + \dots + \Delta \bar{V}_{m-1} \cdot \Delta \bar{V}_2 + \dots + \Delta \bar{V}_{m-1} \cdot \Delta \bar{V}_m + \Delta \bar{V}_m \cdot \Delta \bar{V}_2 + \dots + \Delta \bar{V}_m \cdot \Delta \bar{V}_{m-1}$$

It can be concluded that, at node i , the square of the total real component of the branch voltage drops $\Delta V^2_{iimag_total}$ can be expressed as:

$$\Delta V^2_{iimag_total} = \sum_{y=2}^i \Delta V^2_{yimag} + 2 \sum_{k=2}^{i-1} \sum_{n=k+1}^i \Delta V_{kimag} \cdot \Delta V_{nimag} \tag{A3-F}$$

According to equation (A3-F):

$\sum_{y=2}^i \Delta V^2_{yimag}$ is the total sum of the square of the real component of the branch voltage drops at node i as described in equation (3.17)

$2 \sum_{k=2}^{i-1} \sum_{n=k+1}^i \Delta V_{kimag} \cdot \Delta V_{nimag}$ is the sum of the product of the real component of the branch voltage drops at node i

The imaginary component of the branch voltage drops is determined as indicated in appendix 3-C. When determining the second moment of the total imaginary component of the branch voltage drops, it will be difficult to implement the sum of the product of the imaginary component of the branch voltage drops. This is due to the fact that, the identification of the product of load currents and the square of load currents cannot be easily performed.

APPENDIX 3-G

Derivation of the sum of the product of the real component of the branch voltage drops

It is shown in appendix 3-E that, there is a difficult to be experienced when dealing with the sum of the product of the real component of the branch voltage drops in the determination of the second moment of the total real component of the branch voltage drops. In this appendix,

the expression of the sum of the product of the real component of the branch voltage drops adaptable for the universal algorithm described in chapter 6 is derived based on fig. 3.2.

Let us consider the product of the first two branch voltage drops. Therefore we shall have:

$$\Delta V_{2real} = I_2(R_2 \cos \alpha_2 - X_2 \sin \alpha_2) + I_3(R_2 \cos \alpha_3 - X_2 \sin \alpha_3) + \dots + I_m(R_2 \cos \alpha_m - X_2 \sin \alpha_m)$$

$$\Delta V_{3real} = I_3(R_3 \cos \alpha_2 - X_3 \sin \alpha_2) + I_3(R_3 \cos \alpha_3 - X_3 \sin \alpha_3) + \dots + I_m(R_3 \cos \alpha_m - X_3 \sin \alpha_m)$$

The product of the above voltage drops $\Delta V_{2real} \cdot \Delta V_{3real}$ will be equal to:

$$I_2 I_3 (R_2 R_3 \cos \alpha_2 \cos \alpha_3 + X_2 X_3 \sin \alpha_2 \sin \alpha_3 - R_2 X_3 \cos \alpha_2 \sin \alpha_3 - R_3 X_2 \cos \alpha_3 \sin \alpha_2)$$

$$+ I_2 I_4 (R_2 R_3 \cos \alpha_2 \cos \alpha_4 + X_2 X_3 \sin \alpha_2 \sin \alpha_4 - R_2 X_3 \cos \alpha_2 \sin \alpha_4 - R_3 X_2 \cos \alpha_4 \sin \alpha_2)$$

$$\cdot$$

$$+ I_2 I_m (R_2 R_3 \cos \alpha_2 \cos \alpha_m + X_2 X_3 \sin \alpha_2 \sin \alpha_m - R_2 X_3 \cos \alpha_2 \sin \alpha_m - R_3 X_2 \cos \alpha_m \sin \alpha_2)$$

$$+ I_3^2 (R_2 R_3 \cos \alpha_3 \cos \alpha_3 + X_2 X_3 \sin \alpha_3 \sin \alpha_3 - R_2 X_3 \cos \alpha_3 \sin \alpha_3 - R_3 X_2 \cos \alpha_3 \sin \alpha_3)$$

$$+ I_3 I_4 (R_2 R_3 \cos \alpha_3 \cos \alpha_4 + X_2 X_3 \sin \alpha_3 \sin \alpha_4 - R_2 X_3 \cos \alpha_3 \sin \alpha_4 - R_3 X_2 \cos \alpha_4 \sin \alpha_3)$$

$$\cdot$$

$$+ I_3 I_m (R_2 R_3 \cos \alpha_3 \cos \alpha_m + X_2 X_3 \sin \alpha_3 \sin \alpha_m - R_2 X_3 \cos \alpha_3 \sin \alpha_m - R_3 X_2 \cos \alpha_m \sin \alpha_3)$$

$$+ I_4^2 (R_2 R_3 \cos^2 \alpha_4 + X_2 X_3 \sin^2 \alpha_4 - R_2 X_3 \cos \alpha_4 \sin \alpha_4 - R_3 X_2 \cos \alpha_4 \sin \alpha_4)$$

$$+ I_4 I_3 (R_2 R_3 \cos \alpha_4 \cos \alpha_3 + X_2 X_3 \sin \alpha_4 \sin \alpha_3 - R_2 X_3 \cos \alpha_4 \sin \alpha_3 - R_3 X_2 \cos \alpha_3 \sin \alpha_4)$$

$$\cdot$$

$$+ I_4 I_m (R_2 R_3 \cos \alpha_4 \cos \alpha_m + X_2 X_3 \sin \alpha_4 \sin \alpha_m - R_2 X_3 \cos \alpha_4 \sin \alpha_m - R_3 X_2 \cos \alpha_m \sin \alpha_4)$$

$$+ I_5^2 (R_2 R_3 \cos^2 \alpha_5 + X_2 X_3 \sin^2 \alpha_5 - R_2 X_3 \cos \alpha_5 \sin \alpha_5 - R_3 X_2 \cos \alpha_5 \sin \alpha_5)$$

$$+ I_5 I_3 (R_2 R_3 \cos \alpha_5 \cos \alpha_3 + X_2 X_3 \sin \alpha_5 \sin \alpha_3 - R_2 X_3 \cos \alpha_5 \sin \alpha_3 - R_3 X_2 \cos \alpha_3 \sin \alpha_5)$$

$$\cdot$$

$$+ I_5 I_m (R_2 R_3 \cos \alpha_5 \cos \alpha_m + X_2 X_3 \sin \alpha_5 \sin \alpha_m - R_2 X_3 \cos \alpha_5 \sin \alpha_m - R_3 X_2 \cos \alpha_m \sin \alpha_5)$$

$$+ I_m I_3 (R_2 R_3 \cos \alpha_m \cos \alpha_3 + X_2 X_3 \sin \alpha_m \sin \alpha_3 - R_2 X_3 \cos \alpha_m \sin \alpha_3 - R_3 X_2 \cos \alpha_3 \sin \alpha_m)$$

$$+ I_m^2 (R_2 R_3 \cos^2 \alpha_m + X_2 X_3 \sin^2 \alpha_m - R_2 X_3 \cos \alpha_m \sin \alpha_m - R_3 X_2 \cos \alpha_m \sin \alpha_m)$$

Observing the above expression, it can be said in general, the expression $\Delta V_{ireal} \cdot \Delta V_{kreal}$ will include the following:

- the product of $R_i R_k$ and $X_i X_k$
- the currents at node i and k with the currents downstream respectively
- each current has to be squared, that contributing to the two respective voltage drops
- the currents should form a product with each other

In order to accommodate the four conditions mentioned above, the general expression of the sum of product of the real component of the branch voltage drops should be able to describe four variables. At this point common sense approach is required in order to find its general expression at any node of the system. The logic is as follows:

- e) one of the two variables to control the branch resistance and the branch reactance should range from a value of two and have a limit one less of the node under consideration. The other variable should be controlled by the previous one and should have a limit of the node under consideration. This is to ensure that, the square of the branch resistance and reactance is avoided.
- f) the two variables to control the load currents should have values controlled by the two variables that are controlling the branch resistance and the branch reactance.

Based on the above logic, the sum of the product of the real component of the branch voltage drops $\Delta^* \Delta V_{ireal-sum}$ at node i , can be expressed as:

$$\Delta^* \Delta V_{ireal-sum} = \sum_{t=2}^{i-1} \sum_{r=t+1}^i \sum_{k=t}^m \sum_{n=r}^m I_k I_n \{ R_t R_r \cos \alpha_k \cos \alpha_n + X_t X_r \sin \alpha_k \sin \alpha_n \\ - R_t X_r \cos \alpha_k \sin \alpha_n - X_t R_r \sin \alpha_k \cos \alpha_n \}$$

APPENDIX 3-H

Derivation of the sum product of the imaginary component of the branch voltage drops

It is shown in appendix 3-F that, there is a difficult to be experienced when dealing with the sum of the product of the imaginary component of the branch voltage drops in the determination of the second moment of the total imaginary component of the branch voltage drops. In this appendix the expression of the sum of the product of the imaginary component of the branch voltage drops adaptable for the universal algorithm described in chapter 6 is derived based on fig. 3.2.

Let us consider the product of the first two branch voltage drops. Therefore we shall have:

$$\Delta V_{2imag} = I_2 (R_2 \sin \alpha_2 + X_2 \cos \alpha_2) + I_3 (R_2 \sin \alpha_3 + X_2 \cos \alpha_3) + \dots + I_m (R_2 \sin \alpha_m + X_2 \cos \alpha_m) \\ \Delta V_{3imag} = I_3 (R_3 \sin \alpha_2 + X_3 \cos \alpha_2) + I_3 (R_3 \sin \alpha_3 + X_3 \cos \alpha_3) + \dots + I_m (R_3 \sin \alpha_m + X_3 \cos \alpha_m)$$

The product of the above voltage drops $\Delta V_{2imag} \cdot \Delta V_{3imag}$ will be equal to:

$$I_2 I_3 (R_2 R_3 \sin \alpha_2 \sin \alpha_3 + X_2 X_3 \cos \alpha_2 \cos \alpha_3 + R_2 X_3 \sin \alpha_2 \cos \alpha_3 + R_3 X_2 \sin \alpha_3 \cos \alpha_2) \\ + I_2 I_4 (R_2 R_3 \sin \alpha_2 \sin \alpha_4 + X_2 X_3 \cos \alpha_2 \cos \alpha_4 + R_2 X_3 \sin \alpha_2 \cos \alpha_4 + R_3 X_2 \sin \alpha_4 \cos \alpha_2) \\ \dots \\ + I_2 I_m (R_2 R_3 \sin \alpha_2 \sin \alpha_m + X_2 X_3 \cos \alpha_2 \cos \alpha_m + R_2 X_3 \sin \alpha_2 \cos \alpha_m + R_3 X_2 \sin \alpha_m \cos \alpha_2) \\ + I_3^2 (R_2 R_3 \sin \alpha_3 \sin \alpha_3 + X_2 X_3 \cos \alpha_3 \cos \alpha_3 + R_2 X_3 \sin \alpha_3 \cos \alpha_3 + R_3 X_2 \sin \alpha_3 \cos \alpha_3) \\ + I_3 I_4 (R_2 R_3 \sin \alpha_3 \sin \alpha_4 + X_2 X_3 \cos \alpha_3 \cos \alpha_4 + R_2 X_3 \sin \alpha_3 \cos \alpha_4 + R_3 X_2 \sin \alpha_4 \cos \alpha_3) \\ + I_3 I_m (R_2 R_3 \sin \alpha_3 \sin \alpha_m + X_2 X_3 \cos \alpha_3 \cos \alpha_m + R_2 X_3 \sin \alpha_3 \cos \alpha_m + R_3 X_2 \sin \alpha_m \cos \alpha_3) \\ + I_4^2 (R_2 R_3 \sin^2 \alpha_4 + X_2 X_3 \cos^2 \alpha_4 + R_2 X_3 \sin \alpha_4 \cos \alpha_4 + R_3 X_2 \sin \alpha_4 \cos \alpha_4) \\ + I_4 I_3 (R_2 R_3 \sin \alpha_4 \sin \alpha_3 + X_2 X_3 \cos \alpha_4 \cos \alpha_3 + R_2 X_3 \sin \alpha_4 \cos \alpha_3 + R_3 X_2 \sin \alpha_3 \cos \alpha_4) \\ \dots$$

$$\begin{aligned}
 &+ I_4 I_m (R_2 R_3 \sin \alpha_4 \sin \alpha_m + X_2 X_3 \cos \alpha_4 \cos \alpha_m + R_2 X_3 \sin \alpha_4 \cos \alpha_m + R_3 X_2 \sin \alpha_m \cos \alpha_4) \\
 &+ I_5^2 (R_2 R_3 \sin^2 \alpha_5 + X_2 X_3 \cos^2 \alpha_5 + R_2 X_3 \sin \alpha_5 \cos \alpha_5 + R_3 X_2 \sin \alpha_5 \cos \alpha_5) \\
 &+ I_5 I_3 (R_2 R_3 \sin \alpha_5 \sin \alpha_3 + X_2 X_3 \cos \alpha_5 \cos \alpha_3 + R_2 X_3 \sin \alpha_5 \cos \alpha_3 + R_3 X_2 \sin \alpha_3 \cos \alpha_5) \\
 &\cdot \\
 &+ I_5 I_m (R_2 R_3 \sin \alpha_5 \sin \alpha_m + X_2 X_3 \cos \alpha_5 \cos \alpha_m + R_2 X_3 \sin \alpha_5 \cos \alpha_m + R_3 X_2 \sin \alpha_m \cos \alpha_5) \\
 &+ I_m I_3 (R_2 R_3 \sin \alpha_m \sin \alpha_3 + X_2 X_3 \cos \alpha_m \cos \alpha_3 + R_2 X_3 \sin \alpha_m \cos \alpha_3 + R_3 X_2 \sin \alpha_3 \cos \alpha_m) \\
 &+ I_m^2 (R_2 R_3 \sin^2 \alpha_m + X_2 X_3 \cos^2 \alpha_m + R_2 X_3 \sin \alpha_m \cos \alpha_m + R_3 X_2 \sin \alpha_m \cos \alpha_m)
 \end{aligned}$$

Observing the above expression, it can be said in general, the expression $\Delta V_{iimag} \cdot \Delta V_{kimag}$ will include the following:

- g) the product of $R_i R_k$ and $X_i X_k$
 - h) the currents at node i and k with the currents downstream respectively
 - i) each current has to be squared, that contributing the two respective voltage drops
 - j) the currents should form a product with each other
- k) In order to accommodate the four conditions mentioned above, the general expression of the sum of product of the imaginary component of the branch voltage drops should be able to describe four variables. At this point common sense approach is required as indicated in appendix 3-G.

Based on the above logic, the sum of the product of the imaginary component of the branch voltage drops $\Delta^* \Delta V_{iimag-sum}$ at node i , can be expressed as:

$$\begin{aligned}
 \Delta^* \Delta V_{iimag-sum} &= \sum_{t=2}^{i-1} \sum_{r=t+1}^i \sum_{k=t}^m \sum_{n=r}^m I_k I_n \{ R_t R_r \sin \alpha_k \sin \alpha_n + X_t X_r \cos \alpha_k \cos \alpha_n \\
 &\quad + R_t X_r \cos \alpha_n \sin \alpha_k + X_t R_r \sin \alpha_n \cos \alpha_t \}
 \end{aligned}$$

APPENDIX 3-I

Derivation of the sum of squares of the total real component of the branch voltage drops of two loads at each node

In this appendix, the general expression of the sum of squares of the total real component of the branch voltage drops due to two load currents connected at each node is derived based on fig. 3.3.

The system load currents are: $\bar{I}_2, \bar{I}_3, \bar{I}_4, \dots, \bar{I}_{m-1}, \bar{I}_m$ and $\bar{I}_{22}, \bar{I}_{33}, \bar{I}_{44}, \dots, \bar{I}_{mm-1}, \bar{I}_{mm}$ respectively

The branch voltage drop due to the above system load currents are designated as:

$$\Delta \bar{V}_2, \Delta \bar{V}_3, \Delta \bar{V}_4, \dots, \Delta \bar{V}_{m-1}, \Delta \bar{V}_m \text{ and } \Delta \bar{V}_{22}, \Delta \bar{V}_{33}, \Delta \bar{V}_{44}, \dots, \Delta \bar{V}_{mm-1}, \Delta \bar{V}_{mm} \text{ respectively}$$

Let us consider the square of the real component of the branch voltage drop on the first branch, which in this case will be $(\Delta V_{2real} + \Delta V_{22real})^2$.

According to equation (3.5), the real component of the branch voltage drops are evaluated as:

$$\Delta V_{2real} = I_2(R_2 \cos \alpha_2 - X_2 \sin \alpha_2) + I_3(R_2 \cos \alpha_3 - X_2 \sin \alpha_3) + \dots + I_m(R_2 \cos \alpha_m - X_2 \sin \alpha_m)$$

$$\Delta V_{22real} = I_{22}(R_2 \sin \alpha_{22} - X_2 \sin \alpha_{22}) + \dots + I_{mm}(R_2 \cos \alpha_{mm} - X_2 \sin \alpha_{mm})$$

The square of the real component of the voltage drop $(\Delta V_{2real} + \Delta V_{22real})^2$ across the impedance \bar{Z}_2 will be equal to:

$$\{I_2(R_2 \cos \alpha_2 - X_2 \sin \alpha_2) + I_3(R_2 \cos \alpha_3 - X_2 \sin \alpha_3) + \dots + I_m(R_2 \cos \alpha_m - X_2 \sin \alpha_m) + I_{22}(R_2 \cos \alpha_{22} - X_2 \sin \alpha_{22}) + \dots + I_{mm}(R_2 \cos \alpha_{mm} - X_2 \sin \alpha_{mm})\}^2$$

Assign the above with variables as follows:

$$A_2 = I_2(R_2 \sin \alpha_2 - X_2 \sin \alpha_2), A_3 = I_3(R_2 \cos \alpha_3 - X_2 \sin \alpha_3),$$

$$A_m = I_m(R_2 \cos \alpha_m - X_2 \sin \alpha_m)$$

$$B_2 = I_{22}(R_2 \cos \alpha_{22} - X_2 \sin \alpha_{22}), B_3 = I_{33}(R_2 \cos \alpha_{33} - X_2 \sin \alpha_{33}),$$

$$B_m = I_{mm}(R_2 \cos \alpha_{mm} - X_2 \sin \alpha_{mm})$$

$$\text{Thus, } (\Delta V_{2real} + \Delta V_{22real})^2 = (A_2 + A_3 + \dots + A_m + B_2 + B_3 + \dots + B_m)^2$$

$$= A_2^2 + A_3^2 + \dots + A_m^2 + A_2A_3 + \dots + A_2A_m + A_3A_2 + \dots + A_3A_m + A_{m-1}A_2 + A_{m-1}A_3 + \dots + A_{m-1}A_m$$

$$+ B_2^2 + B_3^2 + \dots + B_m^2 + B_2B_3 + \dots + B_2B_m + B_3B_2 + \dots + B_3B_m + B_{m-1}B_2 + B_{m-1}B_3 + \dots + B_{m-1}B_m$$

$$+ 2A_2B_2 + 2A_2B_3 + \dots + 2A_2B_m + A_3B_2 + 2A_3B_3 + \dots + 2A_3B_m + \dots + 2A_mB_2 + 2A_mB_3 + \dots + 2A_mB_m$$

Recalling the results obtained in the appendix 3-B, the first two lines are known. The last line, which shows the product of the real component of the branch voltage drops due to the two load currents, is to be evaluated. If the other branches are considered, it can be stated that, this product of the real component of the voltage drop across the branch impedance \bar{Z}_i can be expressed as:

$$2 \sum_{k=2}^m \sum_{n=2}^m A_k B_n$$

The product will be as follows:

$$2A_2B_2 = I_2(R_2 \cos \alpha_2 - X_2 \sin \alpha_2) I_{22}(R_2 \cos \alpha_{22} - X_2 \sin \alpha_{22})$$

$$= I_2 I_{22} (R_2^2 \cos \alpha_2 \cos \alpha_{22} + X_2^2 \sin \alpha_2 \sin \alpha_{22} - R_2 X_2 \cos \alpha_2 \sin \alpha_{22} - R_2 X_2 \cos \alpha_{22} \sin \alpha_2)$$

$$= I_2 I_{22} (R_2^2 \cos \alpha_2 \cos \alpha_{22} + X_2^2 \sin \alpha_2 \sin \alpha_{22} - R_2 X_2 \sin(\alpha_2 + \alpha_{22}))$$

$$2A_2B_m = I_2(R_2 \cos \alpha_2 - X_2 \sin \alpha_2) I_{mm}(R_2 \cos \alpha_{mm} - X_2 \sin \alpha_{mm})$$

$$= I_2 I_{mm} (R_2^2 \cos \alpha_2 \cos \alpha_{mm} + X_2^2 \sin \alpha_2 \sin \alpha_{mm} - R_2 X_2 \cos \alpha_2 \sin \alpha_{mm} - R_2 X_2 \cos \alpha_{mm} \sin \alpha_2)$$

$$= I_2 I_{mm} (R_2^2 \cos \alpha_2 \cos \alpha_{mm} + X_2^2 \sin \alpha_2 \sin \alpha_{mm} - R_2 X_2 \sin(\alpha_2 + \alpha_{mm}))$$

$$\begin{aligned}
 2A_3B_m &= I_3(R_2 \cos \alpha_3 - X_2 \sin \alpha_3) \cdot I_{mm}(R_2 \cos \alpha_{mm} - X_2 \sin \alpha_{mm}) \\
 &= I_3 I_{mm} (R_2^2 \cos \alpha_3 \cos \alpha_{mm} + X_2^2 \sin \alpha_3 \sin \alpha_{mm} - R_2 X_2 \sin(\alpha_3 + \alpha_{mm}))
 \end{aligned}$$

$$\begin{aligned}
 2A_mB_m &= I_m(R_2 \cos \alpha_m - X_2 \sin \alpha_m) \cdot I_{mm}(R_2 \cos \alpha_{mm} - X_2 \sin \alpha_{mm}) \\
 &= I_m I_{mm} (R_2^2 \cos \alpha_m \cos \alpha_{mm} + X_2^2 \sin \alpha_m \sin \alpha_{mm} - R_2 X_2 \sin(\alpha_m + \alpha_{mm}))
 \end{aligned}$$

Therefore, the total sum of this product at node i from the source node can be expressed as:

$$\begin{aligned}
 2 \sum_{y=2}^i \sum_{k=y}^m \sum_{n=y}^m A_k B_n &= \\
 2 \sum_{y=2}^i \sum_{k=y}^m \sum_{nn=y}^m I_k I_{nn} (R_y^2 \cos \alpha_k \cos \alpha_{nn} + X_y^2 \sin \alpha_k \sin \alpha_{nn} - R_y X_y \sin(\alpha_k + \alpha_{nn})) &=
 \end{aligned}$$

According to Appendix 3-B, and referring to the above expression, the sum of the squares of the total real component of the branch voltage drops at node i due to two load currents at each node can be expressed as:

$$\begin{aligned}
 \Delta V_{ireal_total_sum}^2 &= \sum_{y=2}^i \sum_{Z=y}^m I_z^2 (R_y^2 \cos^2 \alpha_z + X_y^2 \sin^2 \alpha_z - 2R_y X_y \cos \alpha_z \sin \alpha_z) \\
 &+ \sum_{y=2}^i \sum_{ZZ=y}^m I_{ZZ}^2 (R_y^2 \cos^2 \alpha_{ZZ} + X_y^2 \sin^2 \alpha_{ZZ} - 2R_y X_y \cos \alpha_{ZZ} \sin \alpha_{ZZ}) \\
 &+ 2 \sum_{y=2}^i \sum_{k=y}^{m-1} \sum_{n=k+1}^m I_k I_n \{R_y^2 \cos \alpha_k \cos \alpha_n + X_y^2 \sin \alpha_k \sin \alpha_n - R_y X_y \sin(\alpha_k + \alpha_n)\} \\
 &+ 2 \sum_{y=2}^i \sum_{kk=y}^{m-1} \sum_{nn=kk+1}^m I_{kk} I_{nn} \{R_y^2 \cos \alpha_{kk} \cos \alpha_{nn} + X_y^2 \sin \alpha_{kk} \sin \alpha_{nn} - R_y X_y \sin(\alpha_{kk} + \alpha_{nn})\} \\
 &+ 2 \sum_{y=2}^i \sum_{k=y}^m \sum_{nn=y}^m I_k I_{nn} \{R_y^2 \cos \alpha_k \cos \alpha_{nn} + X_y^2 \sin \alpha_k \sin \alpha_{nn} - R_y X_y \sin(\alpha_k + \alpha_{nn})\}
 \end{aligned}$$

APPENDIX 3-J

Derivation of the sum of squares of the total imaginary component of the branch voltage drops of two loads at each node

In this appendix, the general expression of the sum of squares of the total imaginary component of the branch voltage drops due to two load currents connected at each node is derived based on fig. 3.3.

The system load currents and the branch voltage drop due to above system load current are designated as indicated in the appendix 3-I.

Let us consider the square of the imaginary component of the branch voltage drop on the first branch, which in this case will be $(\Delta V_{2imag} + \Delta V_{22imag})^2$.

According to equation (3.7), the imaginary component of the branch voltage drops are evaluated as:

$$\Delta V_{2imag} = I_2(R_2 \sin \alpha_2 + X_2 \cos \alpha_2) + \dots + I_m(R_2 \sin \alpha_m + X_2 \cos \alpha_m)$$

$$\Delta V_{22imag} = I_{22}(R_2 \sin \alpha_{22} + X_2 \cos \alpha_{22}) + \dots + I_{mm}(R_2 \sin \alpha_{mm} + X_2 \cos \alpha_{mm})$$

The square of the imaginary component of the voltage drop $(\Delta V_{2imag} + \Delta V_{22imag})^2$ across the impedance \bar{Z}_2 will be equal to:

$$\{I_2(R_2 \sin \alpha_2 + X_2 \cos \alpha_2) + I_3(R_2 \sin \alpha_3 + X_2 \cos \alpha_3) + \dots + I_m(R_2 \sin \alpha_m + X_2 \cos \alpha_m) + I_{22}(R_2 \sin \alpha_{22} + X_2 \cos \alpha_{22}) + \dots + I_{mm}(R_2 \sin \alpha_{mm} + X_2 \cos \alpha_{mm})\}^2$$

Assign the above with variables as follows:

$$A_2 = I_2(R_2 \sin \alpha_2 + X_2 \cos \alpha_2), A_3 = I_3(R_2 \sin \alpha_3 + X_2 \cos \alpha_3),$$

$$A_m = I_m(R_2 \sin \alpha_m + X_2 \cos \alpha_m)$$

$$B_2 = I_{22}(R_2 \sin \alpha_{22} + X_2 \cos \alpha_{22}), B_3 = I_{33}(R_2 \sin \alpha_{33} + X_2 \cos \alpha_{33}),$$

$$B_m = I_{mm}(R_2 \sin \alpha_{mm} + X_2 \cos \alpha_{mm})$$

$$\text{Thus, } (\Delta V_{2imag} + \Delta V_{22imag})^2 = (A_2 + A_3 + \dots + A_m + B_2 + B_3 + \dots + B_m)^2$$

$$\begin{aligned} &= A_2^2 + A_3^2 + \dots + A_m^2 + A_2A_3 + \dots + A_2A_m + A_3A_2 + \dots + A_3A_m + \dots + A_mA_2 + A_mA_3 + \dots + A_{m-1}A_m \\ &+ B_2^2 + B_3^2 + \dots + B_m^2 + B_2B_3 + \dots + B_2B_m + B_3B_2 + \dots + B_3B_m + \dots + B_mB_2 + B_mB_3 + \dots + B_{m-1}B_m \\ &+ 2A_2B_2 + 2A_2B_3 + \dots + 2A_2B_m + 2A_3B_2 + 2A_3B_3 + \dots + 2A_3B_m + \dots + 2A_mB_2 + 2A_mB_3 + \dots + 2A_mB_m \end{aligned}$$

Recalling the results obtained in the appendix 3-D, the first two lines are known. The last line, which shows the product of the imaginary component of the branch voltage drops due to the two load currents, is to be evaluated. If the other branches are considered, it can be stated that, the product of the imaginary component of the voltage drops across the branch impedance \bar{Z}_i , can be expressed as:

$$2 \sum_{k=2}^m \sum_{n=2}^m A_k B_n$$

The product will be as follows:

$$\begin{aligned} 2A_2B_2 &= I_2(R_2 \sin \alpha_2 + X_2 \cos \alpha_2) I_{22}(R_2 \sin \alpha_{22} + X_2 \cos \alpha_{22}) \\ &= I_2 I_{22} (R_2^2 \sin \alpha_2 \sin \alpha_{22} + X_2^2 \cos \alpha_2 \cos \alpha_{22} + R_2 X_2 \sin \alpha_2 \cos \alpha_{22} + R_2 X_2 \sin \alpha_{22} \cos \alpha_2) \\ &= I_2 I_{22} (R_2^2 \sin \alpha_2 \sin \alpha_{22} + X_2^2 \cos \alpha_2 \cos \alpha_{22} + R_2 X_2 \sin(\alpha_2 + \alpha_{22})) \end{aligned}$$

$$\begin{aligned} 2A_2B_m &= I_2(R_2 \sin \alpha_2 + X_2 \cos \alpha_2) I_{mm}(R_2 \sin \alpha_{mm} + X_2 \cos \alpha_{mm}) \\ &= I_2 I_{mm} (R_2^2 \sin \alpha_2 \sin \alpha_{mm} + X_2^2 \cos \alpha_2 \cos \alpha_{mm} + R_2 X_2 \sin \alpha_2 \cos \alpha_{mm} + R_2 X_2 \sin \alpha_{mm} \cos \alpha_2) \\ &= I_2 I_{mm} (R_2^2 \sin \alpha_2 \sin \alpha_{mm} + X_2^2 \cos \alpha_2 \cos \alpha_{mm} + R_2 X_2 \sin(\alpha_2 + \alpha_{mm})) \end{aligned}$$

$$\begin{aligned}
 2A_3B_m &= I_3(R_2 \sin \alpha_3 + X_2 \cos \alpha_3) I_{mm}(R_2 \sin \alpha_{mm} + X_2 \cos \alpha_{mm}) \\
 &= I_3 I_{mm}(R_2^2 \sin \alpha_3 \sin \alpha_{mm} + X_2^2 \cos \alpha_3 \cos \alpha_{mm} + R_2 X_2 \sin(\alpha_3 + \alpha_{mm})) \\
 &\cdot \\
 2A_mB_m &= I_m(R_2 \sin \alpha_m + X_2 \cos \alpha_m) I_{mm}(R_2 \sin \alpha_{mm} + X_2 \cos \alpha_{mm}) \\
 I_m I_{mm}(R_2^2 \sin \alpha_m \sin \alpha_{mm} + X_2^2 \cos \alpha_m \cos \alpha_{mm} + R_2 X_2 \sin(\alpha_m + \alpha_{mm}))
 \end{aligned}$$

Therefore, the total sum of this product at node i from the source node can be expressed as:

$$\begin{aligned}
 2 \sum_{y=2}^i \sum_{k=y}^m \sum_{n=y}^m A_k B_n &= \\
 2 \sum_{y=2}^i \sum_{k=y}^m \sum_{nn=y}^m I_k I_{nn} (R_y^2 \sin \alpha_k \sin \alpha_{nn} + X_y^2 \cos \alpha_k \cos \alpha_{nn} + R_y X_y \sin(\alpha_k + \alpha_{nn}))
 \end{aligned}$$

According to Appendix 3-D, and referring to the above expression, the sum of the squares of the total imaginary component of the branch voltage drops at node i due to two load currents at each node can be expressed as:

$$\begin{aligned}
 \Delta V_{iimag_total_sum}^2 &= \sum_{y=2}^i \sum_{Z=y}^m I_z^2 (R_y^2 \sin^2 \alpha_z + X_y^2 \cos^2 \alpha_z + 2R_y X_y \sin \alpha_z \cos \alpha_z) \\
 &+ \sum_{y=2}^i \sum_{ZZ=y}^m I_{ZZ}^2 (R_y^2 \sin^2 \alpha_{ZZ} + X_y^2 \cos^2 \alpha_{ZZ} + 2R_y X_y \sin \alpha_{ZZ} \cos \alpha_{ZZ}) \\
 &+ 2 \sum_{y=2}^i \sum_{k=y}^{m-1} \sum_{n=k+1}^m I_k I_n (R_y^2 \sin \alpha_k \sin \alpha_n + X_y^2 \cos \alpha_k \cos \alpha_n + R_y X_y \sin(\alpha_k + \alpha_n)) \\
 &+ 2 \sum_{y=2}^i \sum_{kk=y}^{m-1} \sum_{nn=kk+1}^m I_{kk} I_{nn} (R_y^2 \sin \alpha_{kk} \sin \alpha_{nn} + X_y^2 \cos \alpha_{kk} \cos \alpha_{nn} + R_y X_y \sin(\alpha_{kk} + \alpha_{nn})) \\
 &+ 2 \sum_{y=2}^i \sum_{k=y}^m \sum_{nn=y}^m I_k I_{nn} (R_y^2 \sin \alpha_k \sin \alpha_{nn} + X_y^2 \cos \alpha_k \cos \alpha_{nn} + R_y X_y \sin(\alpha_k + \alpha_{nn}))
 \end{aligned}$$

APPENDIX 3-K

Derivation of the sum product of the real component of the branch voltage drops

In reference to fig. 3.3, let us consider the product of the first and the second real component of the branch voltage drops i.e. $(\Delta V_{2real} + \Delta V_{22real}) * (\Delta V_{3real} + \Delta V_{33real})$

According to equation 3.5, the real components of the respective branch voltage drops are as follows:

$$\begin{aligned}
 (\Delta V_2 + \Delta V_{22})_{real} &= I_2(R_2 \cos \alpha_2 - X_2 \sin \alpha_2) + \dots + I_m(R_2 \cos \alpha_m - X_2 \sin \alpha_m) \\
 &+ I_{22}(R_2 \cos \alpha_{22} - X_2 \sin \alpha_{22}) + \dots + I_{mm}(R_2 \cos \alpha_{mm} - X_2 \sin \alpha_{mm}) \\
 (\Delta V_3 + \Delta V_{33})_{real} &= I_3(R_3 \cos \alpha_3 - X_3 \sin \alpha_3) + \dots + I_m(R_3 \cos \alpha_m - X_3 \sin \alpha_m)
 \end{aligned}$$

$$+ I_{33}(R_3 \cos \alpha_{33} - X_3 \sin \alpha_{33}) + \dots + I_{mm}(R_3 \cos \alpha_{mm} - X_3 \sin \alpha_{mm})$$

Let assign variables to the above terms as follows:

$$A_2 = I_2(R_2 \cos \alpha_2 - X_2 \sin \alpha_2), A_3 = I_3(R_2 \cos \alpha_3 - X_2 \sin \alpha_3),$$

$$A_m = I_m(R_2 \cos \alpha_m - X_2 \sin \alpha_m)$$

$$B_2 = I_{22}(R_2 \cos \alpha_{22} - X_2 \sin \alpha_{22}), B_3 = I_{33}(R_2 \cos \alpha_{33} - X_2 \sin \alpha_{33}),$$

$$B_m = I_{mm}(R_2 \cos \alpha_{mm} - X_2 \sin \alpha_{mm})$$

$$C_2 = I_3(R_3 \cos \alpha_3 - X_3 \sin \alpha_3), C_3 = I_4(R_3 \cos \alpha_4 - X_3 \sin \alpha_4),$$

$$C_m = I_m(R_3 \cos \alpha_m - X_3 \sin \alpha_m)$$

$$D_2 = I_{33}(R_3 \cos \alpha_{33} - X_3 \sin \alpha_{33}), D_3 = I_{44}(R_3 \cos \alpha_{44} - X_3 \sin \alpha_{44}),$$

$$D_m = I_{mm}(R_3 \cos \alpha_{mm} - X_3 \sin \alpha_{mm})$$

Therefore,

$$(\Delta V_{2real} + \Delta V_{22real}) * (\Delta V_{3real} + \Delta V_{33real}) = (A_2 + \dots + A_m + B_2 + \dots + B_m)(C_2 + \dots C_m + D_2 + \dots + D_m)$$

The product has four groups of interest namely:

$A_2 C_2 + \dots + A_2 C_m$	$B_2 D_2 + \dots + B_2 D_m$
$A_m C_2 + \dots + A_m C_m$	$B_2 D_2 + \dots + B_2 D_m$
$A_2 D_2 + \dots + A_2 D_m$	$B_m C_2 + \dots + B_m C_m$
$A_m D_2 + \dots + A_m D_m$	$B_m C_2 + \dots + B_m C_m$

The two groups in the first row determines the real component of the branch voltage drops due to the currents of the same loading system while the two groups in the second row determines the real component of the branch voltage drops due to the product of the load currents of the different loading system.

Below, the sample is presented that shows the format of the four groups mentioned above.

$$A_2 C_2 = I_2(R_2 \cos \alpha_2 - X_2 \sin \alpha_2).I_3(R_3 \cos \alpha_3 - X_3 \sin \alpha_3)$$

$$= I_2 I_3 (R_2 R_3 \cos \alpha_2 \cos \alpha_3 + X_2 X_3 \sin \alpha_2 \sin \alpha_3 - R_2 X_3 \cos \alpha_2 \sin \alpha_3 - X_2 R_3 \sin \alpha_2 \cos \alpha_3)$$

$$B_2 D_2 = I_{22}(R_2 \cos \alpha_{22} - X_2 \sin \alpha_{22}).I_{33}(R_3 \cos \alpha_{33} - X_3 \sin \alpha_{33})$$

$$= I_{22} I_{33} (R_2 R_3 \cos \alpha_{22} \cos \alpha_{33} + X_2 X_3 \sin \alpha_{22} \sin \alpha_{33} - R_2 X_3 \cos \alpha_{22} \sin \alpha_{33} - X_2 R_3 \sin \alpha_{22} \cos \alpha_{33})$$

$$A_2 D_2 = I_2 (R_2 \cos \alpha_2 - X_2 \sin \alpha_2) I_{33} (R_3 \cos \alpha_{33} - X_3 \sin \alpha_{33})$$

$$= I_2 I_{33} (R_2 R_3 \cos \alpha_2 \cos \alpha_{33} + X_2 X_3 \sin \alpha_2 \sin \alpha_{33} - R_2 X_3 \cos \alpha_2 \sin \alpha_{33} - X_2 R_3 \sin \alpha_2 \cos \alpha_{33})$$

$$B_2 C_2 = I_{22} (R_2 \cos \alpha_{22} - X_2 \sin \alpha_{22}) I_3 (R_3 \cos \alpha_3 - X_3 \sin \alpha_3)$$

$$= I_{22} I_3 (R_2 R_3 \cos \alpha_{22} \cos \alpha_3 + X_2 X_3 \sin \alpha_{22} \sin \alpha_3 - R_2 X_3 \cos \alpha_{22} \sin \alpha_3 - X_2 R_3 \sin \alpha_{22} \cos \alpha_3)$$

If a complete expansion is performed for each group mentioned above, the result for each group will resemble the one appeared in the appendix-G.

Therefore, it can be concluded that, at load point i , the real component of the sum product of the branch voltage drops $\Delta^* \Delta V_{ireal-sum}$ for combined loading is:

$$\Delta^* \Delta V_{ireal-sum} = \sum_{t=2}^{i-1} \sum_{r=t+1}^i \sum_{k=t}^m \sum_{n=r}^m I_k I_n \{R_t R_r \cos \alpha_k \cos \alpha_n + X_t X_r \sin \alpha_k \sin \alpha_n$$

$$- R_t X_r \cos \alpha_k \sin \alpha_n - X_t R_r \sin \alpha_k \cos \alpha_n \}$$

$$+ \sum_{t=2}^{i-1} \sum_{r=t+1}^i \sum_{kk=t}^m \sum_{nn=r}^m I_{kk} I_{nn} \{R_t R_r \cos \alpha_{kk} \cos \alpha_{nn} + X_t X_r \sin \alpha_{kk} \sin \alpha_{nn}$$

$$- R_t X_r \cos \alpha_{kk} \sin \alpha_{nn} - X_t R_r \sin \alpha_{kk} \cos \alpha_{nn} \}$$

$$+ \sum_{t=2}^{i-1} \sum_{r=t+1}^i \sum_{k=t}^m \sum_{nn=r}^m I_k I_{nn} \{R_t R_r \cos \alpha_k \cos \alpha_{nn} + X_t X_r \sin \alpha_k \sin \alpha_{nn}$$

$$- R_t X_r \cos \alpha_k \sin \alpha_{nn} - X_t R_r \sin \alpha_k \cos \alpha_{nn} \}$$

$$+ \sum_{t=2}^{i-1} \sum_{r=t+1}^i \sum_{kk=t}^m \sum_{n=r}^m I_{kk} I_n \{R_t R_r \cos \alpha_{kk} \cos \alpha_n + X_t X_r \sin \alpha_{kk} \sin \alpha_n$$

$$- R_t X_r \cos \alpha_{kk} \sin \alpha_n - X_t R_r \sin \alpha_{kk} \cos \alpha_n \}$$

APPENDIX 3-L

Derivation of the sum product of the imaginary component of the branch voltage drops

In reference to fig. 3.3, let us consider the product of the first and the second imaginary component of the branch voltage drops i.e. $(\Delta V_{2imag} + \Delta V_{22imag})^* (\Delta V_{3imag} + \Delta V_{33imag})$

According to equation 3.7, the imaginary component of the respective branch voltage drops are as follows:

$$(\Delta V_2 + \Delta V_{22})_{imag} = I_2 (R_2 \sin \alpha_2 + X_2 \cos \alpha_2) + \dots + I_m (R_2 \sin \alpha_m + X_2 \cos \alpha_m)$$

$$+ I_{22} (R_2 \sin \alpha_{22} + X_2 \cos \alpha_{22}) + \dots + I_{mm} (R_2 \sin \alpha_{mm} + X_2 \cos \alpha_{mm})$$

$$(\Delta V_3 + \Delta V_{33})_{imag} = I_3(R_3 \sin \alpha_3 + X_3 \cos \alpha_3) + \dots + I_m(R_3 \sin \alpha_m + X_3 \cos \alpha_m) \\ + I_{33}(R_3 \sin \alpha_{33} + X_3 \cos \alpha_{33}) + \dots + I_{mm}(R_3 \sin \alpha_{mm} + X_3 \cos \alpha_{mm})$$

Let assign variables to the above terms as follows:

$$A_2 = I_2(R_2 \sin \alpha_2 + X_2 \cos \alpha_2), A_3 = I_3(R_2 \sin \alpha_3 + X_2 \cos \alpha_3), \\ A_m = I_m(R_2 \sin \alpha_m + X_2 \cos \alpha_m)$$

$$B_2 = I_{22}(R_2 \sin \alpha_{22} + X_2 \cos \alpha_{22}), B_3 = I_{33}(R_2 \sin \alpha_{33} + X_2 \cos \alpha_{33}), \\ B_m = I_{mm}(R_2 \sin \alpha_{mm} + X_2 \cos \alpha_{mm})$$

$$C_2 = I_3(R_3 \sin \alpha_3 + X_3 \cos \alpha_3), C_3 = I_4(R_3 \sin \alpha_4 + X_3 \cos \alpha_4), \\ C_m = I_m(R_3 \sin \alpha_m + X_3 \cos \alpha_m)$$

$$D_2 = I_{33}(R_3 \sin \alpha_{33} + X_3 \cos \alpha_{33}), D_3 = I_{44}(R_3 \sin \alpha_{44} + X_3 \cos \alpha_{44}), \\ D_m = I_{mm}(R_3 \sin \alpha_{mm} + X_3 \cos \alpha_{mm})$$

Therefore,

$$(\Delta V_{2imag} + \Delta V_{22imag}) * (\Delta V_{3imag} + \Delta V_{33imag}) = (A_2 + \dots + A_m + B_2 + \dots + B_m)(C_2 + \dots + C_m + D_2 + \dots + D_m)$$

The product has four groups of interest namely:

$$\begin{array}{ll} A_2 C_2 + \dots + A_2 C_m & B_2 D_2 + \dots + B_2 D_m \\ A_m C_2 + \dots + A_m C_m & B_m D_2 + \dots + B_m D_m \\ A_2 D_2 + \dots + A_2 D_m & B_2 C_2 + \dots + B_2 C_m \\ A_m D_2 + \dots + A_m D_m & B_m C_2 + \dots + B_m C_m \end{array}$$

The two groups in the first row determines the imaginary component of the branch voltage drops due to the currents of the same loading system while the two groups in the second row determines the imaginary component of the branch voltage drops due to the product of the load currents of the different loading systems.

Below, the sample is presented that shows the format of the four groups mentioned above.

$$A_2 C_2 = I_2(R_2 \sin \alpha_2 + X_2 \cos \alpha_2).I_3(R_3 \sin \alpha_3 + X_3 \cos \alpha_3) \\ = I_2 I_3 (R_2 R_3 \sin \alpha_2 \sin \alpha_3 + X_2 X_3 \cos \alpha_2 \cos \alpha_3 + R_2 X_3 \sin \alpha_2 \cos \alpha_3 + X_2 R_3 \cos \alpha_2 \sin \alpha_3)$$

$$B_2 D_2 = I_{22}(R_2 \sin \alpha_{22} + X_2 \cos \alpha_{22}).I_{33}(R_3 \sin \alpha_{33} + X_3 \cos \alpha_{33}) \\ = I_{22} I_{33} (R_2 R_3 \sin \alpha_{22} \sin \alpha_{33} + X_2 X_3 \cos \alpha_{22} \cos \alpha_{33} + R_2 X_3 \sin \alpha_{22} \cos \alpha_{33} \\ + X_2 R_3 \cos \alpha_{22} \sin \alpha_{33})$$

$$A_2 D_2 = I_2 (R_2 \sin \alpha_2 + X_2 \cos \alpha_2) I_{33} (R_3 \sin \alpha_{33} + X_3 \cos \alpha_{33})$$

$$= I_2 I_{33} (R_2 R_3 \sin \alpha_2 \sin \alpha_{33} + X_2 X_3 \cos \alpha_2 \cos \alpha_{33} + R_2 X_3 \sin \alpha_2 \cos \alpha_{33} + X_2 R_3 \cos \alpha_2 \sin \alpha_{33})$$

$$B_2 C_2 = I_{22} (R_2 \sin \alpha_{22} + X_2 \cos \alpha_{22}) I_3 (R_3 \sin \alpha_3 + X_3 \cos \alpha_3)$$

$$= I_{22} I_3 (R_2 R_3 \sin \alpha_{22} \sin \alpha_3 + X_2 X_3 \cos \alpha_{22} \cos \alpha_3 + R_2 X_3 \sin \alpha_{22} \cos \alpha_3 + X_2 R_3 \cos \alpha_{22} \sin \alpha_3)$$

If a complete expansion is performed for each group mentioned above, the result for each group will resemble the one appeared in the appendix-H.

Therefore, it can be concluded that, at load point i , the real component of the sum product of the branch voltage drops $\Delta^* \Delta V_{iimag-sum}$ for combined loading is:

$$\Delta^* \Delta V_{iimag-sum} = \sum_{t=2}^{i-1} \sum_{r=t+1}^i \sum_{k=t}^m \sum_{n=r}^m I_k I_n \{R_t R_r \sin \alpha_k \sin \alpha_n + X_t X_r \cos \alpha_k \cos \alpha_n$$

$$+ R_t X_r \cos \alpha_n \sin \alpha_k + X_t R_r \sin \alpha_n \cos \alpha_k \}$$

$$+ \sum_{t=2}^{i-1} \sum_{r=t+1}^i \sum_{kk=t}^m \sum_{nn=r}^m I_{kk} I_{nn} \{R_t R_r \sin \alpha_{kk} \sin \alpha_{nn} + X_t X_r \cos \alpha_{kk} \cos \alpha_{nn}$$

$$+ R_t X_r \sin \alpha_{kk} \cos \alpha_{nn} + X_t R_r \cos \alpha_{kk} \sin \alpha_{nn} \}$$

$$+ \sum_{t=2}^{i-1} \sum_{r=t+1}^i \sum_{k=t}^m \sum_{nn=r}^m I_k I_{nn} \{R_t R_r \sin \alpha_k \sin \alpha_{nn} + X_t X_r \cos \alpha_k \cos \alpha_{nn}$$

$$+ R_t X_r \sin \alpha_k \cos \alpha_{nn} + X_t R_r \cos \alpha_k \sin \alpha_{nn} \}$$

$$+ \sum_{t=2}^{i-1} \sum_{r=t+1}^i \sum_{kk=t}^m \sum_{n=r}^m I_{kk} I_n \{R_t R_r \sin \alpha_{kk} \sin \alpha_n + X_t X_r \cos \alpha_{kk} \cos \alpha_n$$

$$+ R_t X_r \sin \alpha_{kk} \cos \alpha_n + X_t R_r \cos \alpha_{kk} \sin \alpha_n \}$$

APPENDIX 4-A**Determination of the new scaling factors in order to maintain the same statistical parameters at the MV distribution lines.**

In this appendix, the numerical proof for the determination of the new scaling factors to maintain the same statistical parameters of the beta distributed load current pdf's at the MV level of the distribution lines are discussed. The formulae used are those that evaluate the mean μ and standard deviation σ of a data set. With the original specified scaling factor C_b , the statistical parameters α and β of the beta distributed data are evaluated for two different scenarios. The formulae used are as follows:

$$\mu = \frac{1}{n} \sum_{i=1}^n x_i$$

$$\sigma = \sqrt{\left\{ \frac{1}{n} \sum_{i=1}^n (x_i - \mu)^2 \right\}}$$

$$\alpha = \frac{\mu(\mu C_b - \mu^2 - \sigma^2)}{\sigma^2 C_b}$$

$$\beta = \frac{(C_b - \mu)(C_b \mu - \mu^2 - \sigma^2)}{\sigma^2 C_b}$$

Suppose the original current data are: 10, 12, 8, 4, 20, 6 with scaling factor $C_b = 60$.

The mean μ_0 and variance σ_0^2 original data can be evaluated as:

$$\mu_0 = \frac{10 + 12 + 8 + 4 + 20 + 6}{6} = 10$$

$$\sigma_0^2 = \frac{1}{6} \{ (10-10)^2 + (12-10)^2 + (8-10)^2 + (4-10)^2 + (20-10)^2 + (6-10)^2 \} = \frac{160}{6}$$

$$\text{i.e. } \sigma_0 = \sqrt{\frac{160}{6}}$$

Therefore, the original Beta pdf parameters α_0 and β_0 are evaluated as:

$$\alpha_0 = \frac{10(60 * 10 - 10^2 - \frac{160}{6})}{\frac{160}{6} * 60} = 2.95833333 \quad (4-A1)$$

$$\beta_0 = \frac{(60-10)(60*10-10^2 - \frac{160}{6})}{\frac{160}{6}*60} = 14.79166667 \quad (4-A2)$$

Two conditions are investigated. One is when the data are transformed up by the ratio of 10:1 and the second is when the data is transformed down in the ratio of 0.1. In both cases, the original scaling factor C_b will also be transformed in the same ratio.

1) Data transformed up in the ratio of 10

The new data set will be: 100, 120, 80, 40, 200, 60 and $C_{b10} = 600$

Therefore,

$$\mu_{10} = \frac{100+120+80+40+200+60}{6} = 100$$

$$\text{i.e. } \mu_{10} = n\mu_0 \quad (4-A3)$$

$$\begin{aligned} \sigma_{10}^2 &= \frac{1}{6} \{ (100-100)^2 + (120-100)^2 + (80-100)^2 + (40-100)^2 + (200-100)^2 + (60-100)^2 \} \\ &= \frac{1600}{6} = \frac{160*100}{6} = \frac{160*n^2}{6} \end{aligned}$$

$$\text{i.e. } \sigma_{10} = \sqrt{\frac{160*n^2}{6}} = n\sigma_0 \quad (4-A4)$$

The new statistical parameters are evaluated as:

$$\alpha_{10} = \frac{100(600*100-100^2 - \frac{160000}{6})}{\frac{160000}{6}*600} = 2.95833333 \quad (4-A5)$$

$$\beta_{10} = \frac{(600-100)(600*100-100^2 - \frac{160000}{6})}{\frac{160000}{6}*600} = 14.79166667 \quad (4-A6)$$

From the above, it is clearly shown that, to be able to maintain the original statistical parameters when the data is transformed up, the scaling factor should also be transformed with the same ratio. The other interesting outcome is the relationship between the new mean and the new standard deviation to the original values as given in equation (4-A3) and (4-A4).

2) Data transformed down in the ratio of 0.1

The new data set will be: 1, 1.2, 0.8, 0.4, 2, 0.6 and $C_{b0.1} = 6$

$$\text{Therefore, } \mu_{0.1} = \frac{1+1.2+0.8+0.4+2+0.6}{6} = 1$$

$$\text{i.e. } \mu_{0.1} = n\mu_0 \quad (4-A7)$$

$$\begin{aligned} \sigma_{0.1}^2 &= \frac{1}{6} \{(1-1)^2 + (1.2-1)^2 + (0.8-1)^2 + (0.4-1)^2 + (2-1)^2 + (0.6-1)^2\} = \frac{1.6}{6} \\ &= \frac{160}{6*100} = \frac{160*0.01}{6} = \frac{160}{6} * n^2 \end{aligned}$$

$$\text{i.e. } \sigma_{0.1} = \sqrt{\frac{160*n^2}{6}} = n\sigma_0 \quad (4-A8)$$

Therefore, the new statistical parameters are evaluated as:

$$\alpha_{0.1} = \frac{1(6*1-1^2 - \frac{1.6}{6})}{\frac{1.6}{6}*6} = 2.95833333 \quad (4-A9)$$

$$\beta_{0.1} = \frac{(6-1)(6*1-1^2 - \frac{1.6}{6})}{\frac{1.6}{6}*6} = 14.79166667 \quad (4-A10)$$

From the above, it is clearly shown that, to be able to maintain the original statistical parameters when the data is transformed down, the scaling factor should also be transformed with the same ratio. The other interesting outcome is the relationship between the new mean and the new standard deviation to the original values as given in equation (4-A7) and (4-A8).

NOTE: The relationship between the mean and standard deviation for the two scenarios with the original values is going to be extensively employed in the next chapter when determining the statistical total power loss in single-phase and three-phase MV distribution systems.

APPENDIX 4-B

Determination of the beta distributed consumer voltage expression responsible for the evaluation of its 1st moment

The method using Taylor's expansion for expression (4-B2) is adopted to determine the expression of the beta distributed consumer voltages that can be utilised for the evaluation of its 1st moment. The Taylor series is described as:

$$(1+X)^{\frac{1}{2}} = 1 + \frac{1}{2}X - \frac{1}{8}X^2 + \frac{1}{16}X^3 \dots \dots \dots \quad -1 < X < 1 \quad (4-B1)$$

The consumer voltage V_{scon_i} at node i is given as:

$$\begin{aligned} V_{scon_i} &= \{(V_S - \Delta V_{ireal_total})^2 + (\Delta V_{iimag_total})^2\}^{\frac{1}{2}} \\ &= V_S \left\{ 1 - 2 \frac{\Delta V_{ireal_total}}{V_S} + \frac{\Delta V_{ireal_total}^2}{V_S^2} + \frac{\Delta V_{iimag_total}^2}{V_S^2} \right\}^{\frac{1}{2}} \end{aligned} \quad (4-B2)$$

The normalised consumer voltage V_{n-scon_i} can be expressed as:

$$V_{n-scon_i} = \left\{ 1 - 2 \frac{\Delta V_{ireal_total}}{V_S} + \frac{\Delta V_{ireal_total}^2}{V_S^2} + \frac{\Delta V_{iimag_total}^2}{V_S^2} \right\}^{\frac{1}{2}} \quad (4-B3)$$

According to the above expressions, the parameter X can be described as:

$$X = -\frac{2\Delta V_{ireal_total}}{V_S} + \frac{\Delta V_{ireal_total}^2}{V_S^2} + \frac{\Delta V_{iimag_total}^2}{V_S^2} \quad (4-B4)$$

The term $1 + \frac{1}{2}X - \frac{1}{8}X^2 + \frac{1}{16}X^3$ will be considered in the Taylor's expansion. It follows that,

$$\frac{1}{2}X = -\frac{\Delta V_{ireal_total}}{V_S} + 0.5 \frac{\Delta V_{ireal_total}^2}{V_S^2} + 0.5 \frac{\Delta V_{iimag_total}^2}{V_S^2} \quad (4-B5)$$

$$\begin{aligned} X^2 &= \left\{ -2 \frac{\Delta V_{ireal_total}}{V_S} + \frac{\Delta V_{ireal_total}^2}{V_S^2} + \frac{\Delta V_{iimag_total}^2}{V_S^2} \right\}^2 \\ &= 4 \frac{\Delta V_{ireal_total}^2}{V_S^2} - 2 \frac{\Delta V_{ireal_total}^3}{V_S^3} - 2 \frac{\Delta V_{ireal_total} \Delta V_{iimag_total}^2}{V_S^3} - 2 \frac{\Delta V_{ireal_total}^3}{V_S^3} \\ &\quad + \frac{\Delta V_{ireal_total}^4}{V_S^4} + \frac{\Delta V_{ireal_total}^2 \Delta V_{iimag_total}^2}{V_S^4} - 2 \frac{\Delta V_{ireal_total} \Delta V_{iimag_total}^2}{V_S^3} \\ &\quad + \frac{\Delta V_{ireal_total}^2 \Delta V_{iimag_total}^2}{V_S^4} + \frac{\Delta V_{iimag_total}^4}{V_S^4} \end{aligned} \quad (4-B6)$$

According to equation (4-B6), the terms in the expansion for the total component of the branch voltage drops having powers greater than two are discarded due to the fact that, there are difficult to evaluate.

Therefore, the expression of X^2 can be described as:

$$\begin{aligned}
 X^2 &= 4 \frac{\Delta V_{ireal_total}^2}{V_S^2} - 2 \frac{\Delta V_{ireal_total} \Delta V_{iimag_total}^2}{V_S^3} \\
 &+ \frac{\Delta V_{ireal_total}^2 \Delta V_{iimag_total}^2}{V_S^4} - 2 \frac{\Delta V_{ireal_total} \Delta V_{iimag_total}^2}{V_S^3} + \frac{\Delta V_{ireal_total}^2 \Delta V_{iimag_total}^2}{V_S^4} \\
 &= 4 \frac{\Delta V_{ireal_total}^2}{V_S^2} - 4 \frac{\Delta V_{ireal_total} \Delta V_{iimag_total}^2}{V_S^3} + 2 \frac{\Delta V_{ireal_total}^2 \Delta V_{iimag_total}^2}{V_S^4} \quad (4-B7)
 \end{aligned}$$

$$X^3 = \left\{ -\frac{2\Delta V_{ireal_total}}{V_S} + \frac{\Delta V_{ireal_total}^2}{V_S^2} + \frac{\Delta V_{iimag_total}^2}{V_S^2} \right\} X^2 \quad (4-B8)$$

By discarding the terms for the total component of the branch voltage drops having powers greater than two in equation (4-B8), the expression of X^3 can be given as:

$$\begin{aligned}
 X^3 &= 8 \frac{\Delta V_{ireal_total} \Delta V_{iimag_total}^2}{V_S^4} + 4 \frac{\Delta V_{ireal_total}^2 \Delta V_{iimag_total}^2}{V_S^4} \\
 &= 12 \frac{\Delta V_{ireal_total} \Delta V_{iimag_total}^2}{V_S^4} \quad (4-B9)
 \end{aligned}$$

It follows that,

$$\begin{aligned}
 -\frac{1}{8} X^2 &= -0.5 \frac{\Delta V_{ireal_total}^2}{V_S^2} + 0.5 \frac{\Delta V_{ireal_total} \Delta V_{iimag_total}^2}{V_S^3} - 0.25 \frac{\Delta V_{ireal_total}^2 \Delta V_{iimag_total}^2}{V_S^4} \\
 \frac{1}{16} X^3 &= \frac{12}{16} \frac{\Delta V_{ireal_total} \Delta V_{iimag_total}^2}{V_S^4}
 \end{aligned}$$

Adding the three terms $1 + \frac{1}{2}X - \frac{1}{8}X^2 + \frac{1}{16}X^3$, the final expression of the normalised consumer voltage will be:

$$\begin{aligned}
 1 - \frac{\Delta V_{ireal_total}}{V_S} + 0.5 \frac{\Delta V_{iimag_total}^2}{V_S^2} + 0.5 \frac{\Delta V_{ireal_total} \Delta V_{iimag_total}^2}{V_S^3} \\
 + 0.5 \frac{\Delta V_{ireal_total}^2 \Delta V_{iimag_total}^2}{V_S^4}
 \end{aligned}$$

Therefore, the actual expression of the consumer voltage V_{scon_i} can be approximated as:

$$V_{scon_i} = V_S \left\{ 1 - \frac{\Delta V_{ireal_total}}{V_S} + 0.5 \frac{\Delta V_{iimag_total}^2}{V_S^2} + 0.5 \frac{\Delta V_{ireal_total} \Delta V_{iimag_total}^2}{V_S^3} + 0.5 \frac{\Delta V_{ireal_total}^2 \Delta V_{iimag_total}^2}{V_S^4} \right\} \quad (4-B10)$$

APPENDIX 4-C

Evaluation of the total real and the total imaginary component of the branch voltage drops due to non-statistical nodal currents on the MV distribution lines.

In this appendix, the general expressions of the total real and the total imaginary components of the branch voltage drops due to non-statistical are derived based on the one line diagram depicted in fig. 4.4. The total voltage drop $\Delta \bar{V}_{2-total}$ at node 2 can be expressed as:

$$\Delta \bar{V}_{2-total} = \bar{Z}_2 (\bar{I}_2 + \bar{I}_3 + \bar{I}_4 + \dots + \bar{I}_m)$$

The total voltage drop $\Delta \bar{V}_{3-total}$ at node 3 can be expressed as:

$$\Delta \bar{V}_{3-total} = \bar{Z}_2 (\bar{I}_2 + \bar{I}_3 + \bar{I}_4 + \dots + \bar{I}_m) + \bar{Z}_3 (\bar{I}_3 + \bar{I}_4 + \dots + \bar{I}_m)$$

The total voltage drop $\Delta \bar{V}_{m-1-total}$ at node $m-1$ can be expressed as:

$$\Delta \bar{V}_{m-1-total} = \bar{Z}_2 (\bar{I}_2 + \bar{I}_3 + \bar{I}_4 + \dots + \bar{I}_m) + \bar{Z}_3 (\bar{I}_3 + \bar{I}_4 + \dots + \bar{I}_m) + \dots + \bar{Z}_{m-1} (\bar{I}_{m-1} + \bar{I}_m)$$

The total voltage drop $\Delta \bar{V}_{m-total}$ at node m can be expressed as:

$$\Delta \bar{V}_{m-total} = \bar{Z}_2 (\bar{I}_2 + \bar{I}_3 + \bar{I}_4 + \dots + \bar{I}_m) + \bar{Z}_3 (\bar{I}_3 + \bar{I}_4 + \dots + \bar{I}_m) + \dots + \bar{Z}_{m-1} (\bar{I}_{m-1} + \bar{I}_m) + \bar{Z}_m \bar{I}_m$$

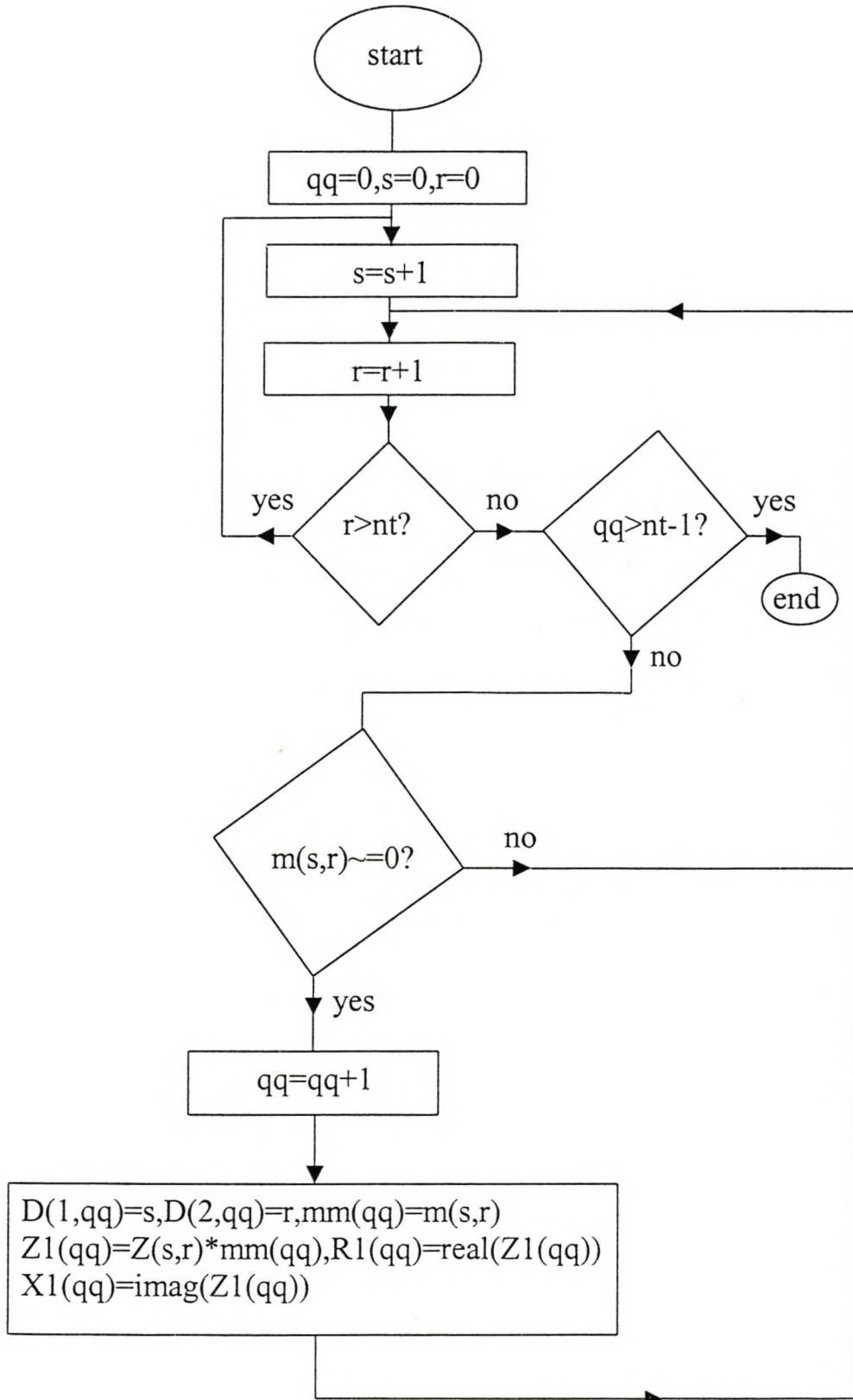
According to the above expressions, the total real $\Delta V_{i-real-total}$ and the total imaginary $\Delta V_{i-imag-total}$ components of the branch voltage drops at node i can be given as:

$$\Delta V_{i-real-total} = \text{real} \left(\sum_{k=2}^i \sum_{n=k}^m \bar{Z}_k \bar{I}_n \right)$$

$$\Delta V_{i-imag-total} = \text{imag} \left(\sum_{k=2}^i \sum_{n=k}^m \bar{Z}_k \bar{I}_n \right)$$

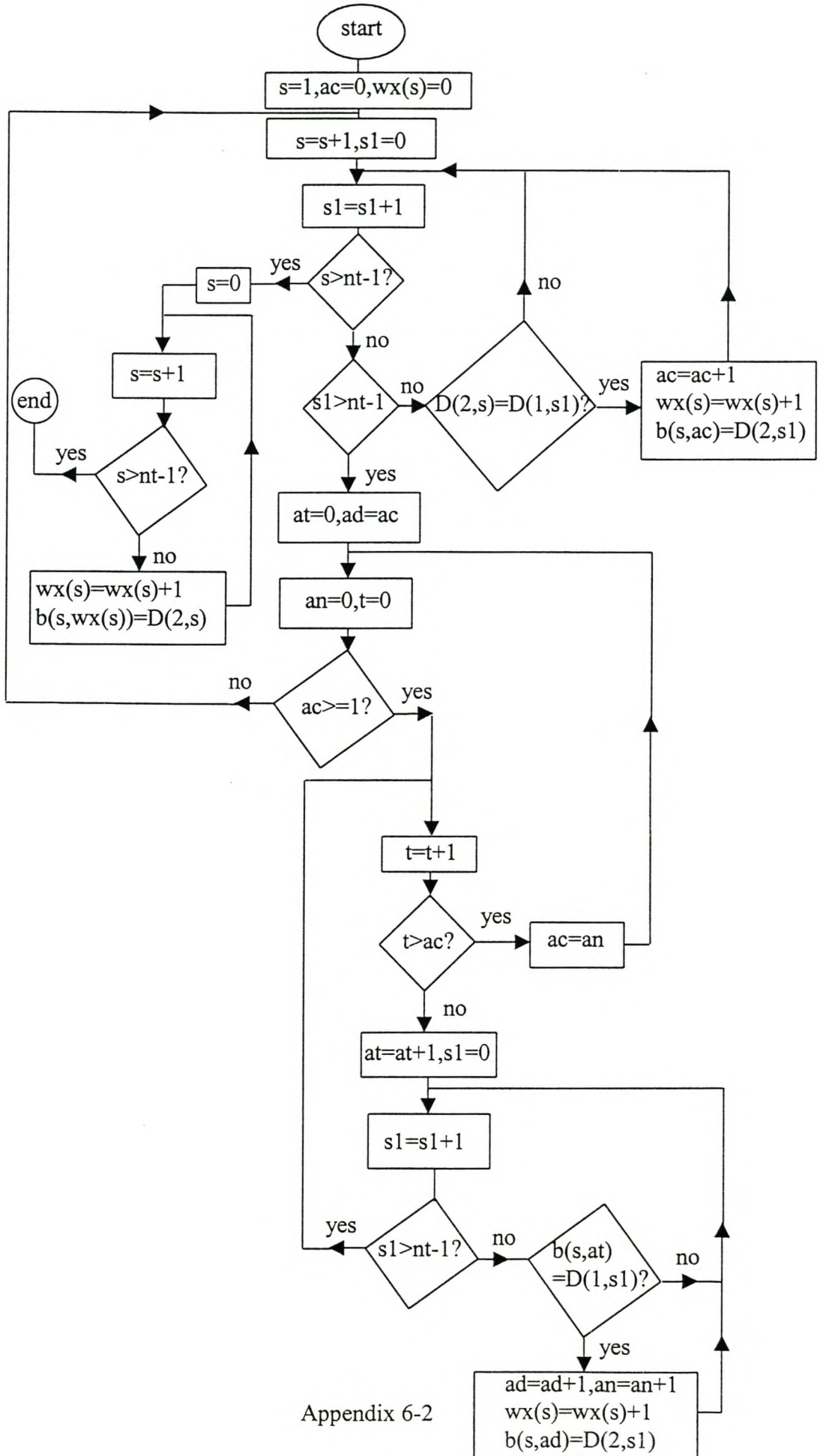
Appendix 6-A

The computer program flow chart for creating the D-array, Z1-array, R1-array and X1-array in single-phase distribution systems



Appendix 6-B:

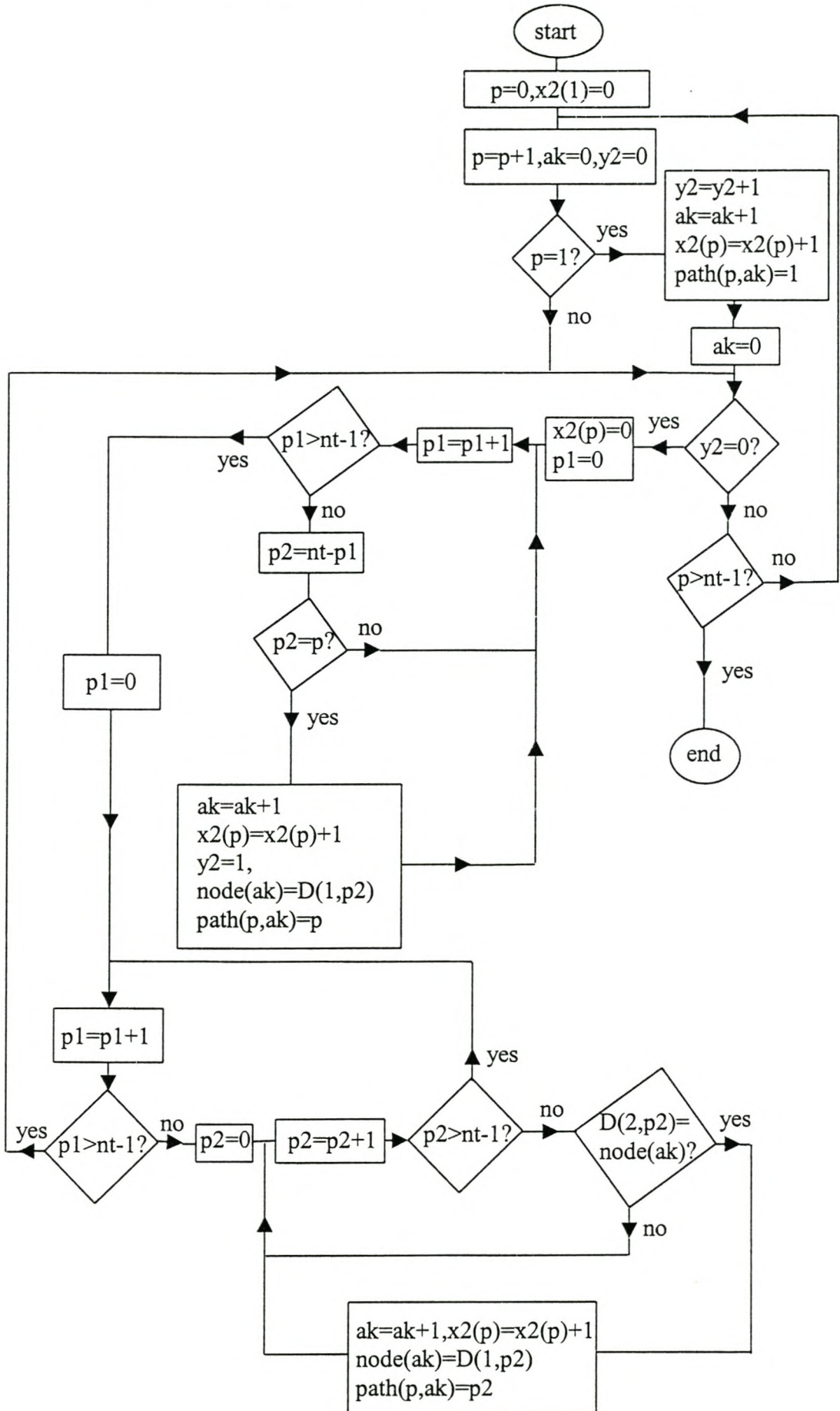
The computer flow chart for creating the b-array and wx-array



Appendix 6-2

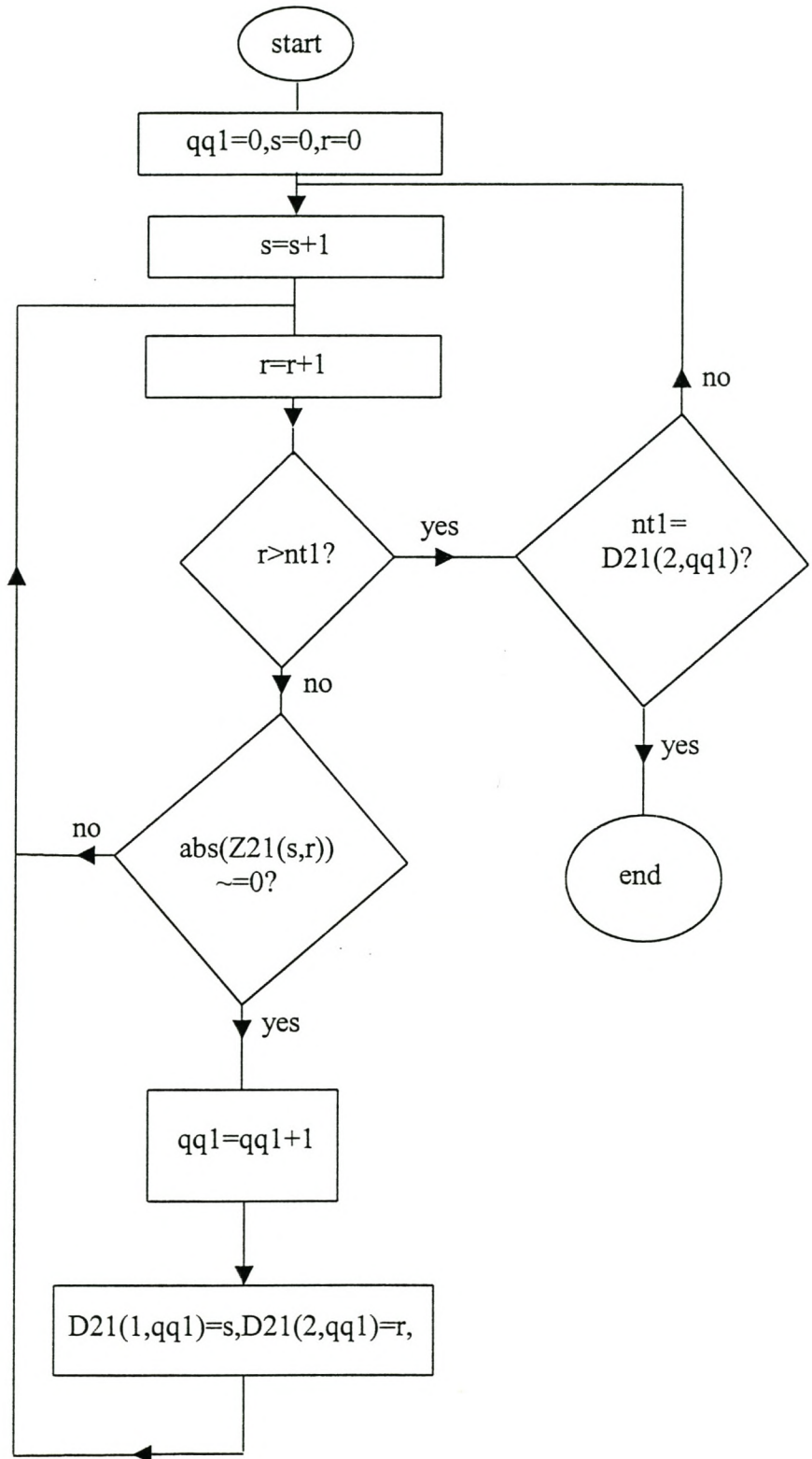
Appendix 6-C

The computer program flow chart for creating the path-array and x2-array



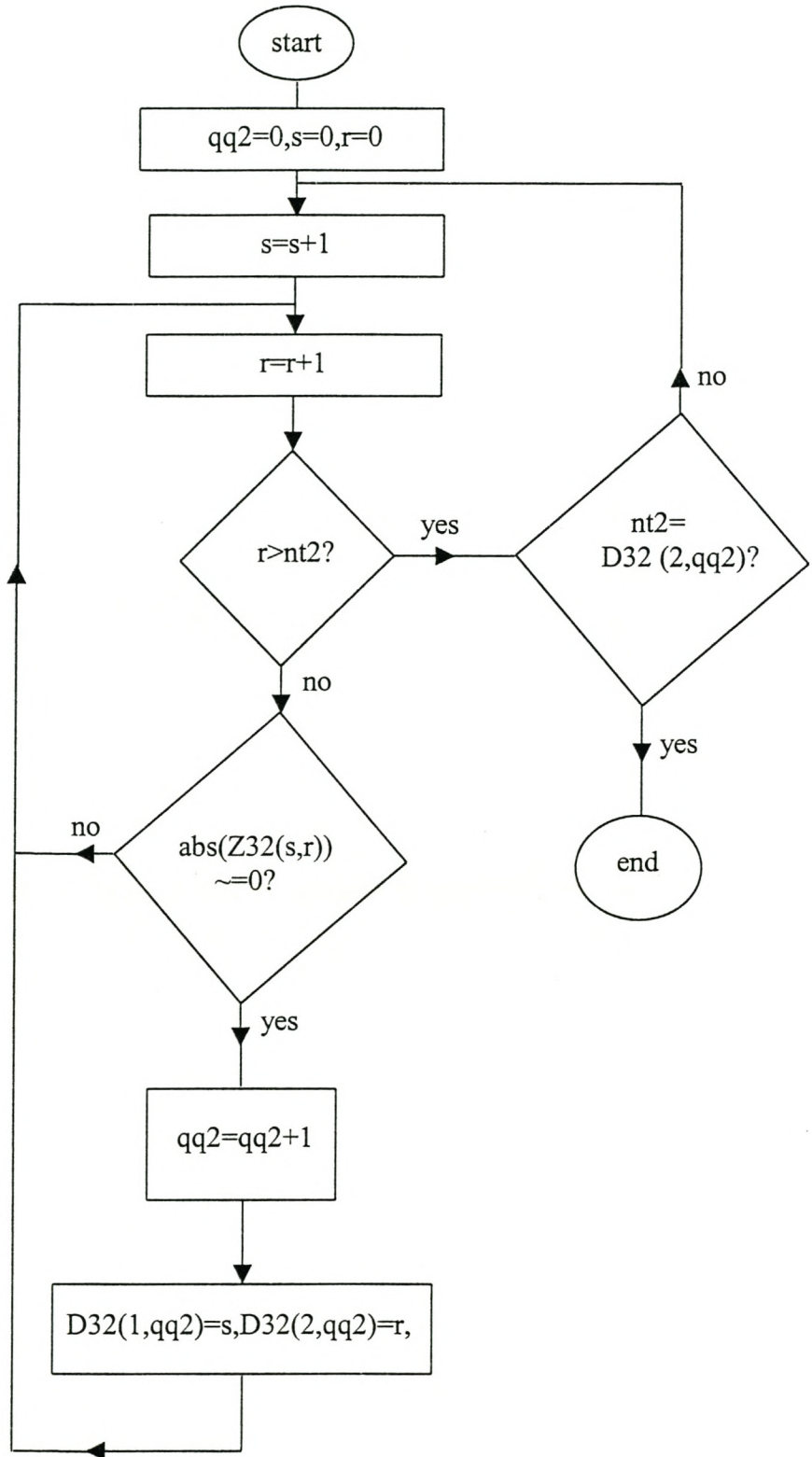
Appendix 6-D

The computer program flow chart for creating the D21-array



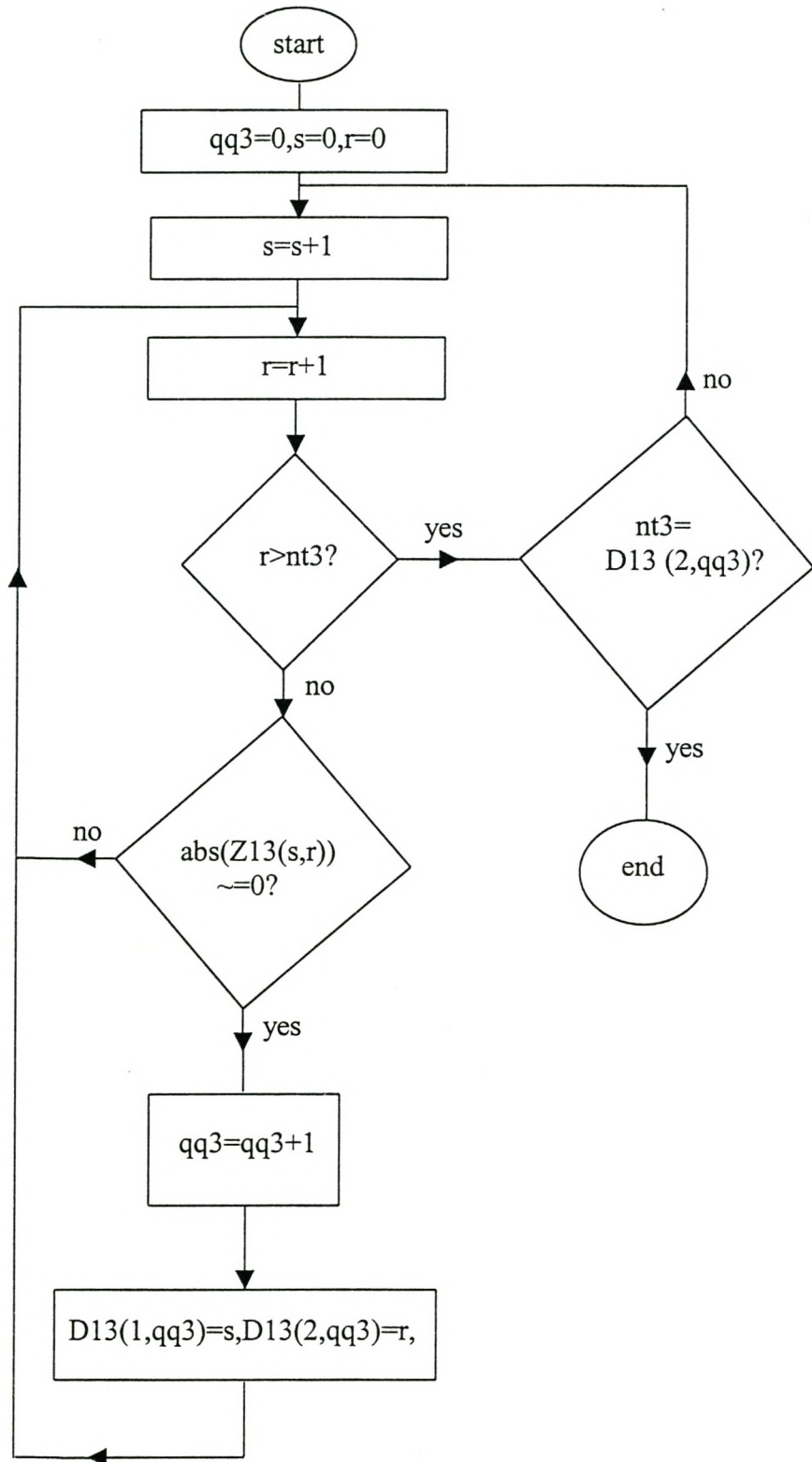
Appendix 6-E

The computer program flow chart for creating the D32-array



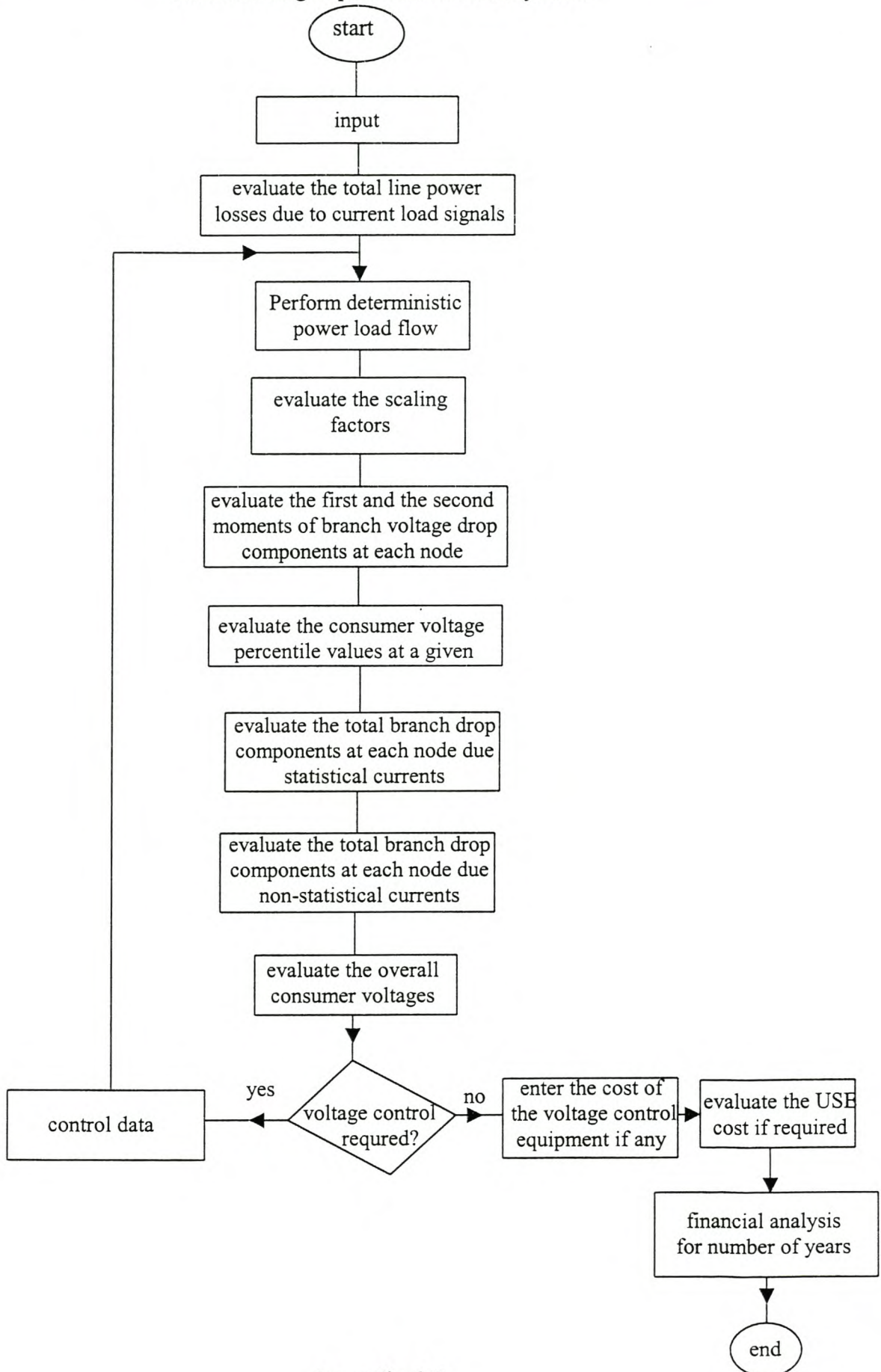
Appendix 6-F

The computer program flow chart for creating the D13- array



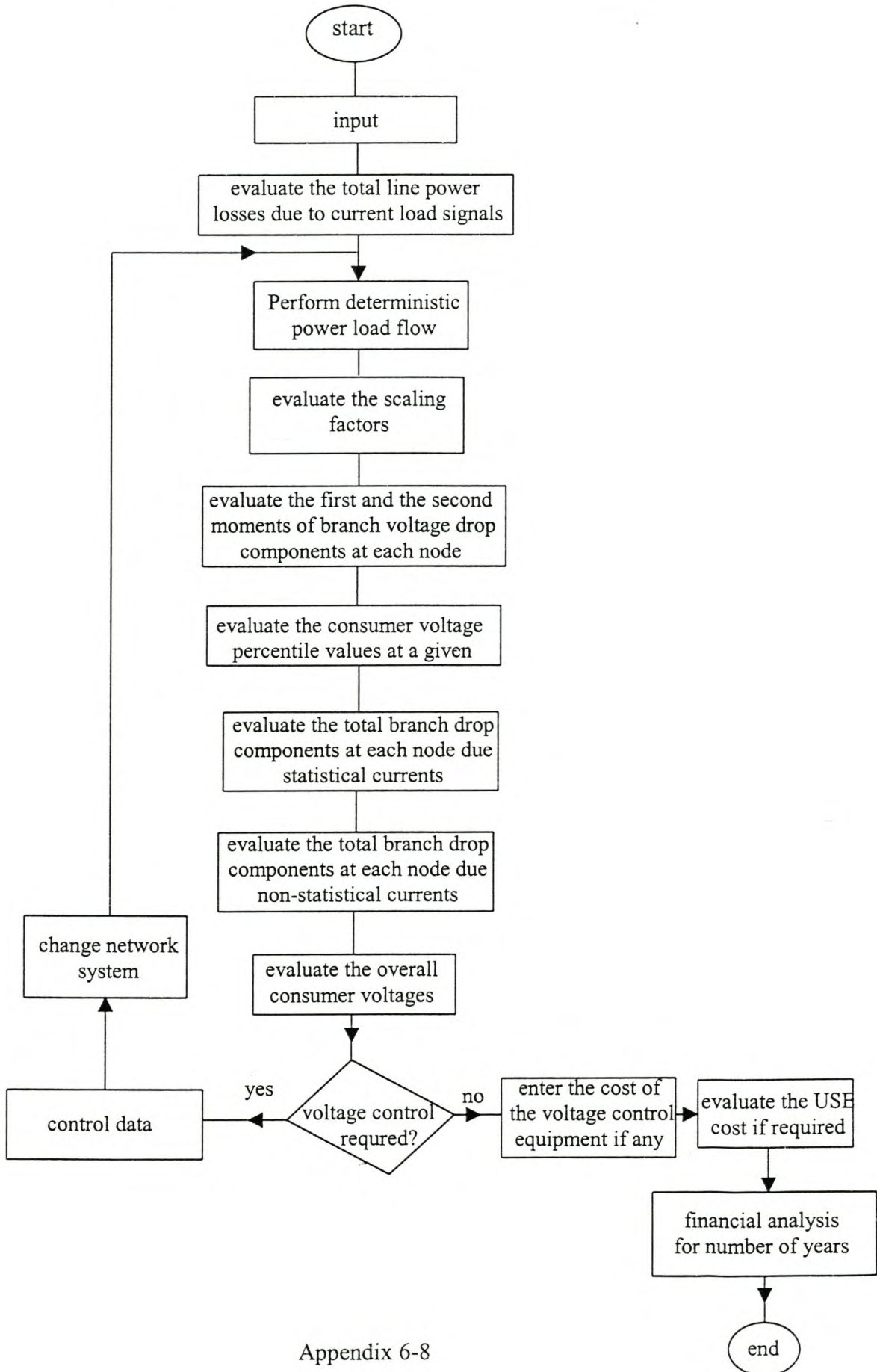
Appendix 6-G:

The computer program flow chart for the probabilistic power load flow with capacitor feeder voltage control in single- phase distribution systems



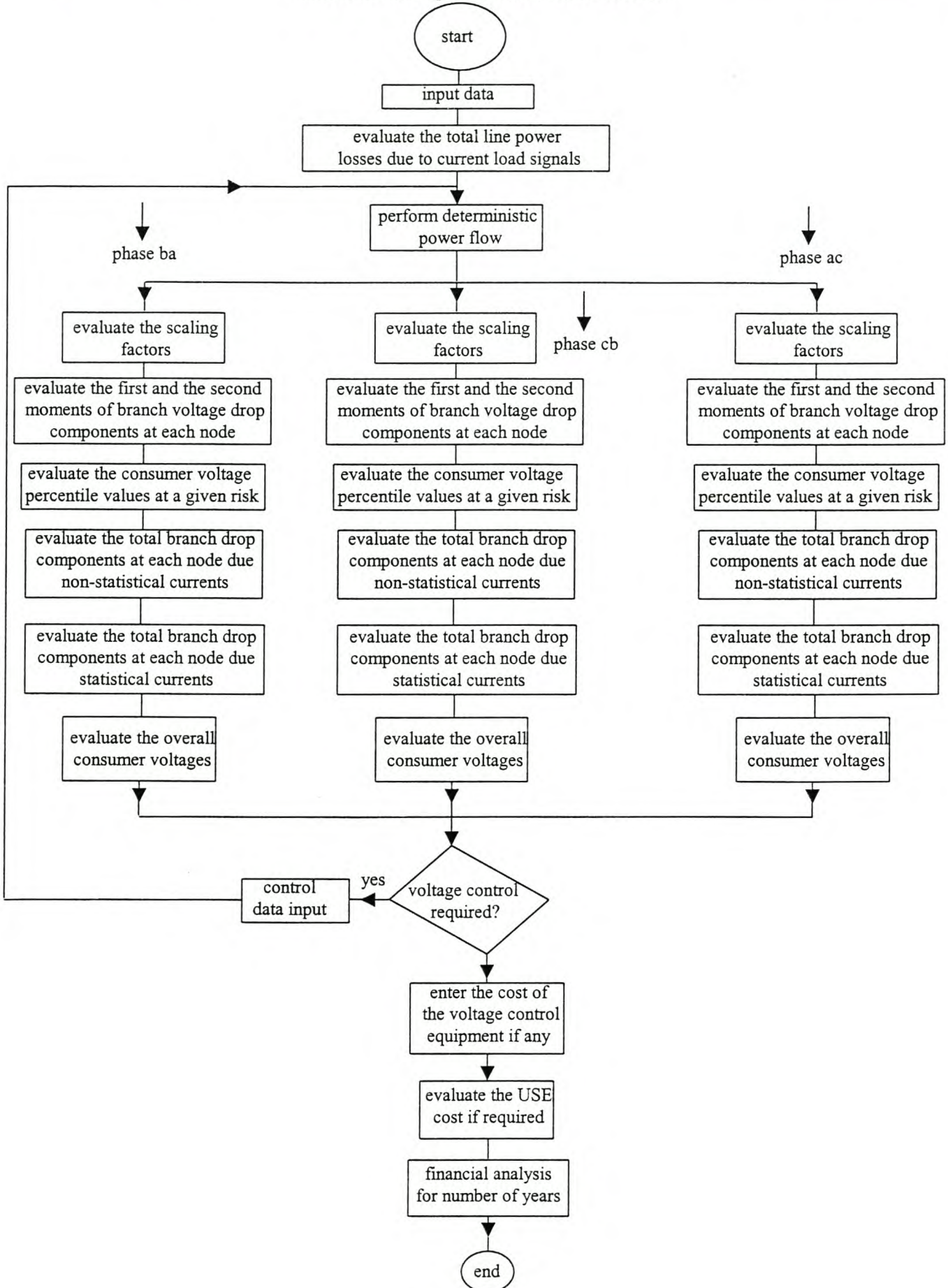
Appendix 6-H:

The computer program flow chart for the probabilistic power load flow with transformer tape-changer feeder voltage control in single-phase distribution systems



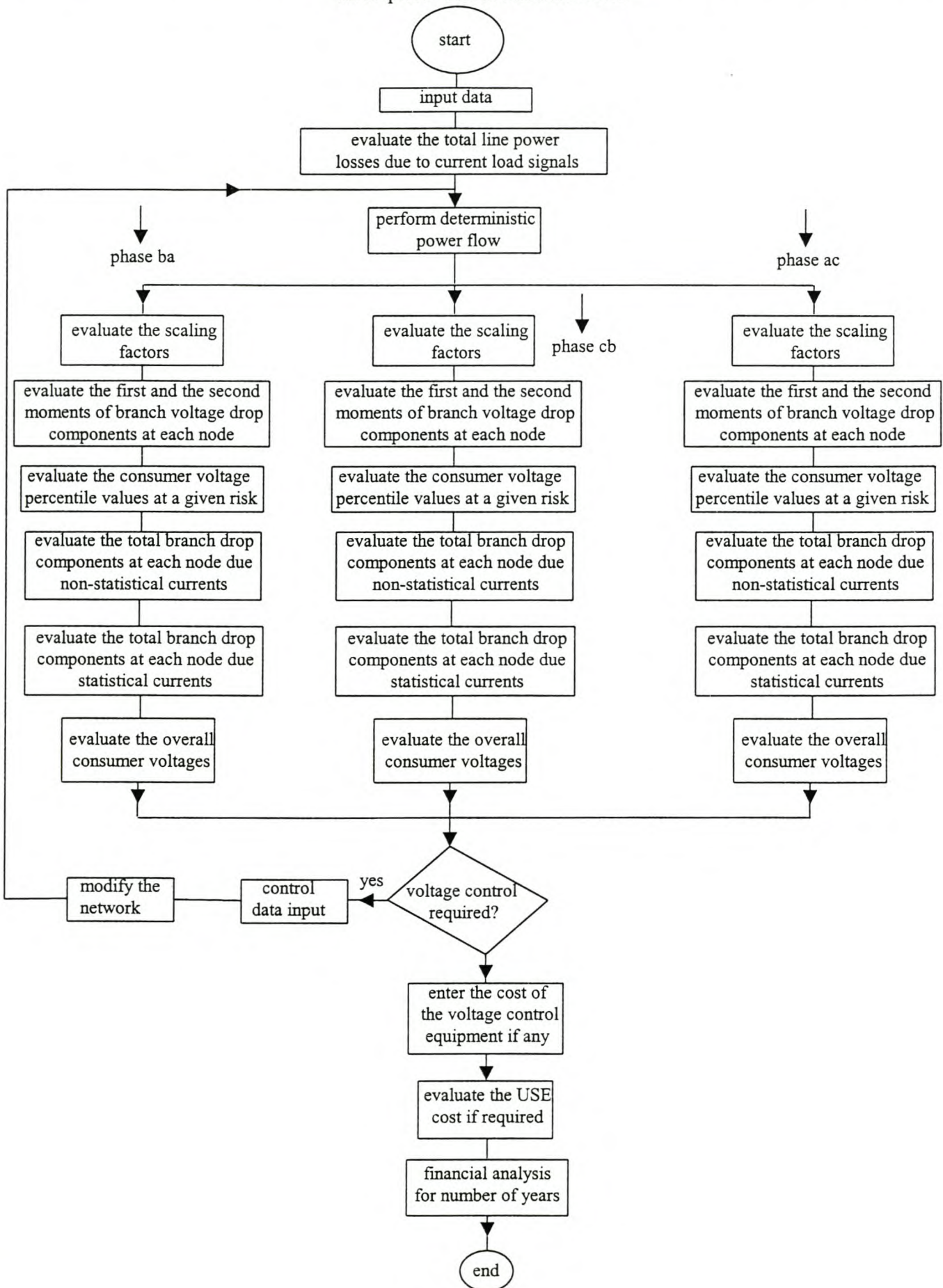
Appendix 6-I:

The computer program flow chart for the probabilistic power load flow with capacitor feeder voltage control in three-phase distribution network



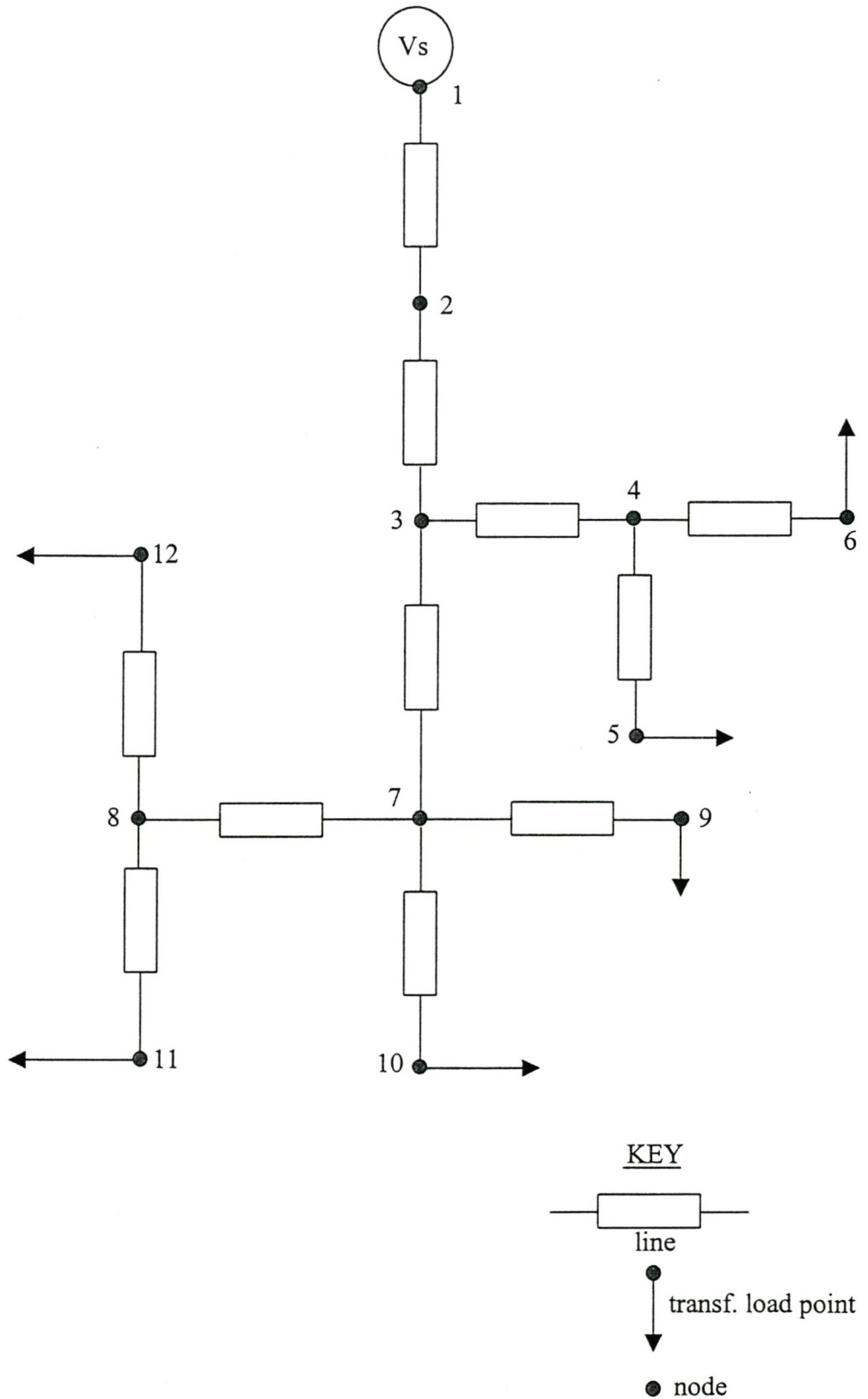
Appendix 6-J:

The computer program flow chart for the probabilistic power load flow with step-voltage regulators in three-phase distribution network



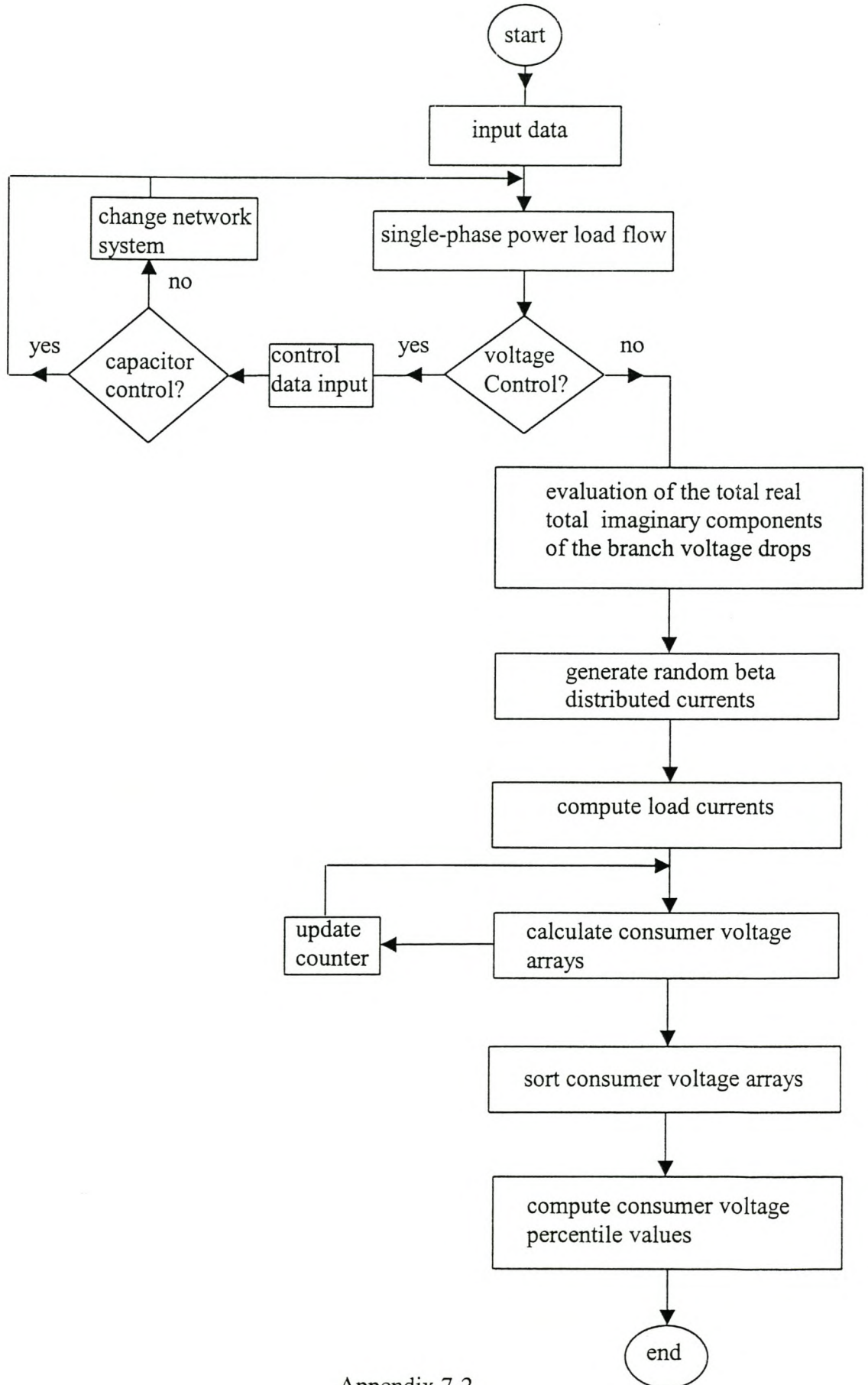
APPENDIX 7-A

One line diagram for comparing the analytical and MC simulation result for consumer voltage percentile values



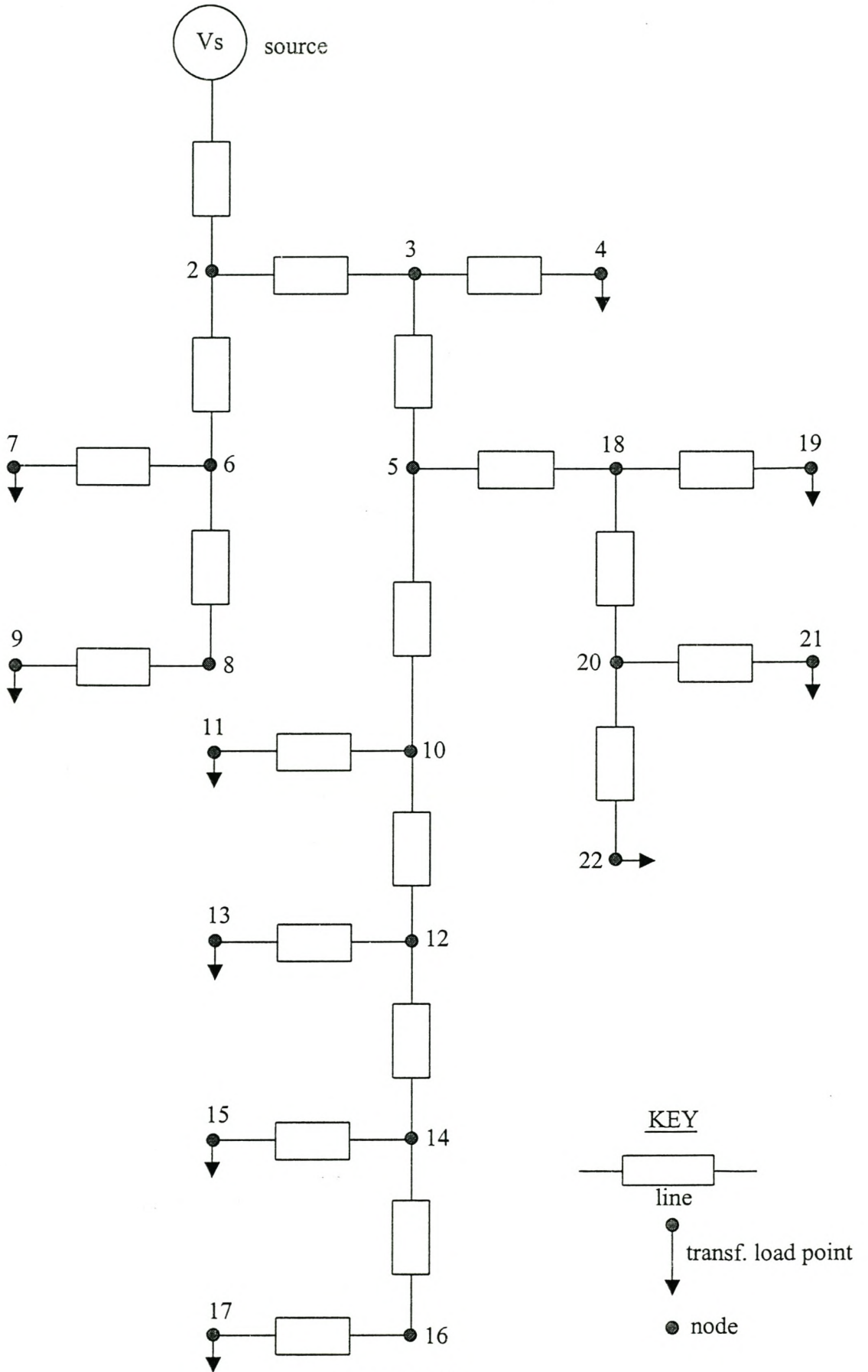
APPENDIX 7-B

A computer flow chart for MC simulations of the consumer voltages incorporating voltage regulators in single-phase distribution systems



APPENDIX 7-C

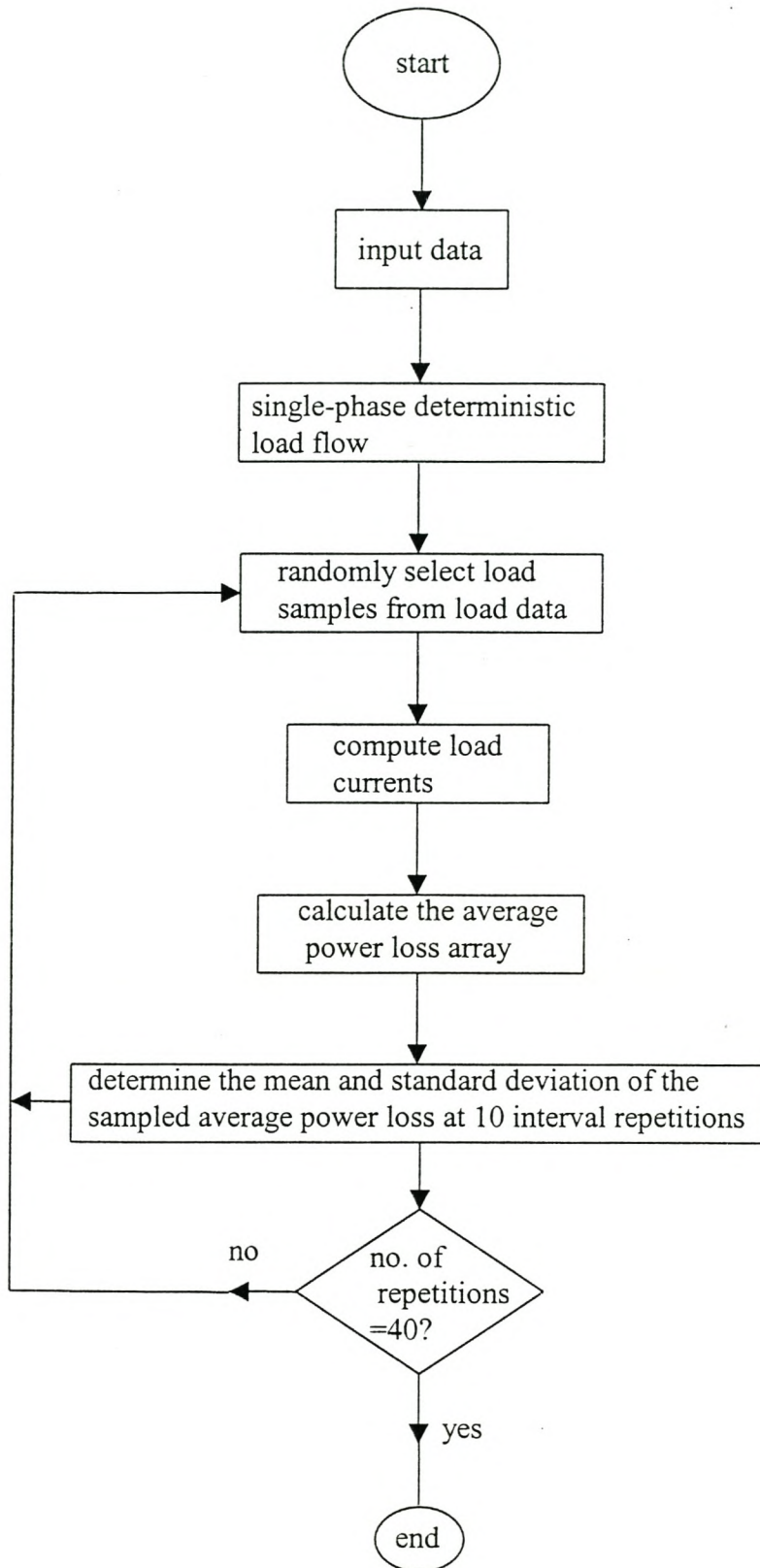
One line diagram for comparing the analytical and MC simulation results for line power losses in single and three-phase distribution systems



Appendix 7-3

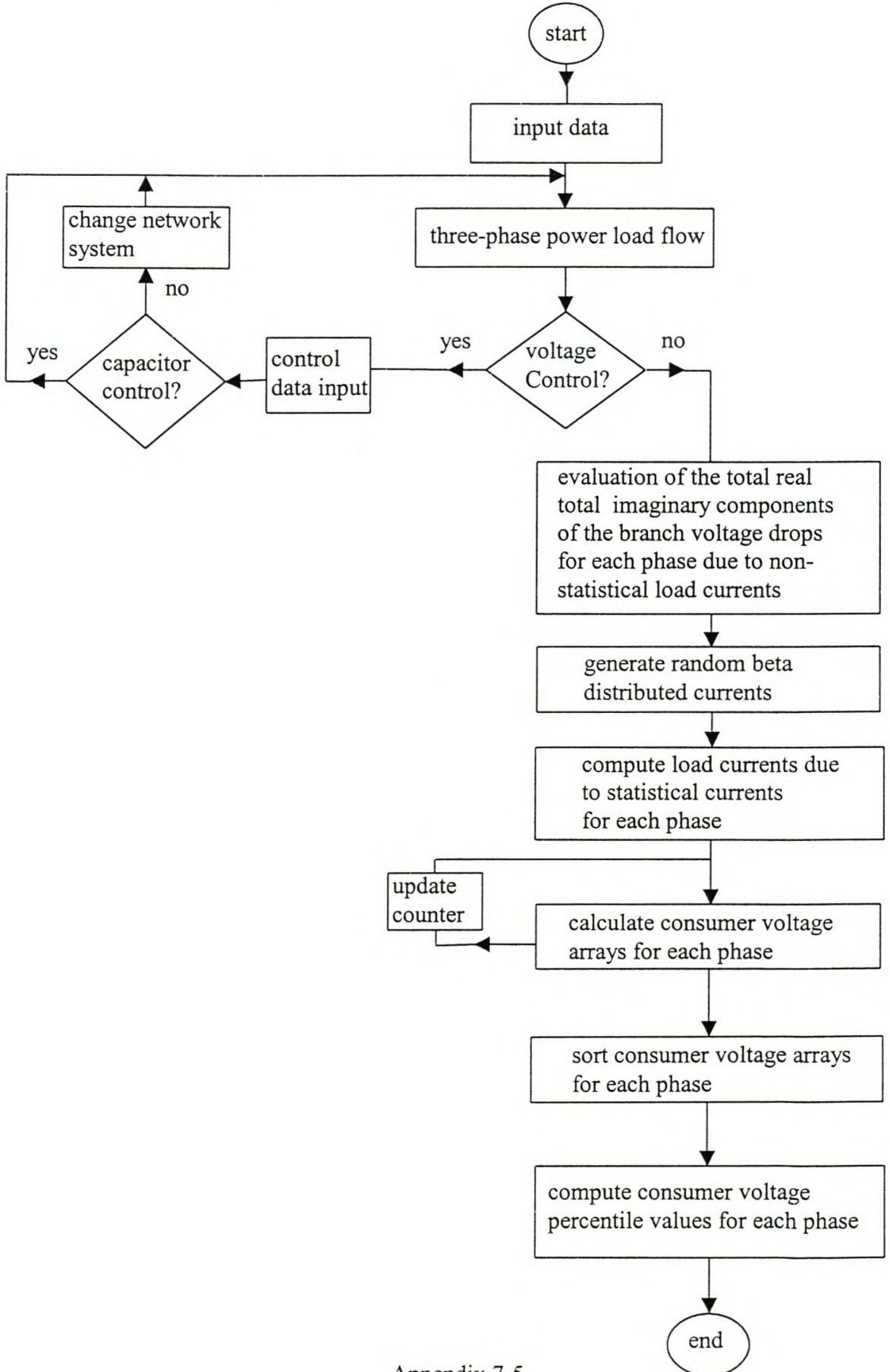
Appendix 7-D

A computer flow chart for MC simulations of the power loss executed directly from the load data in single-phase networks



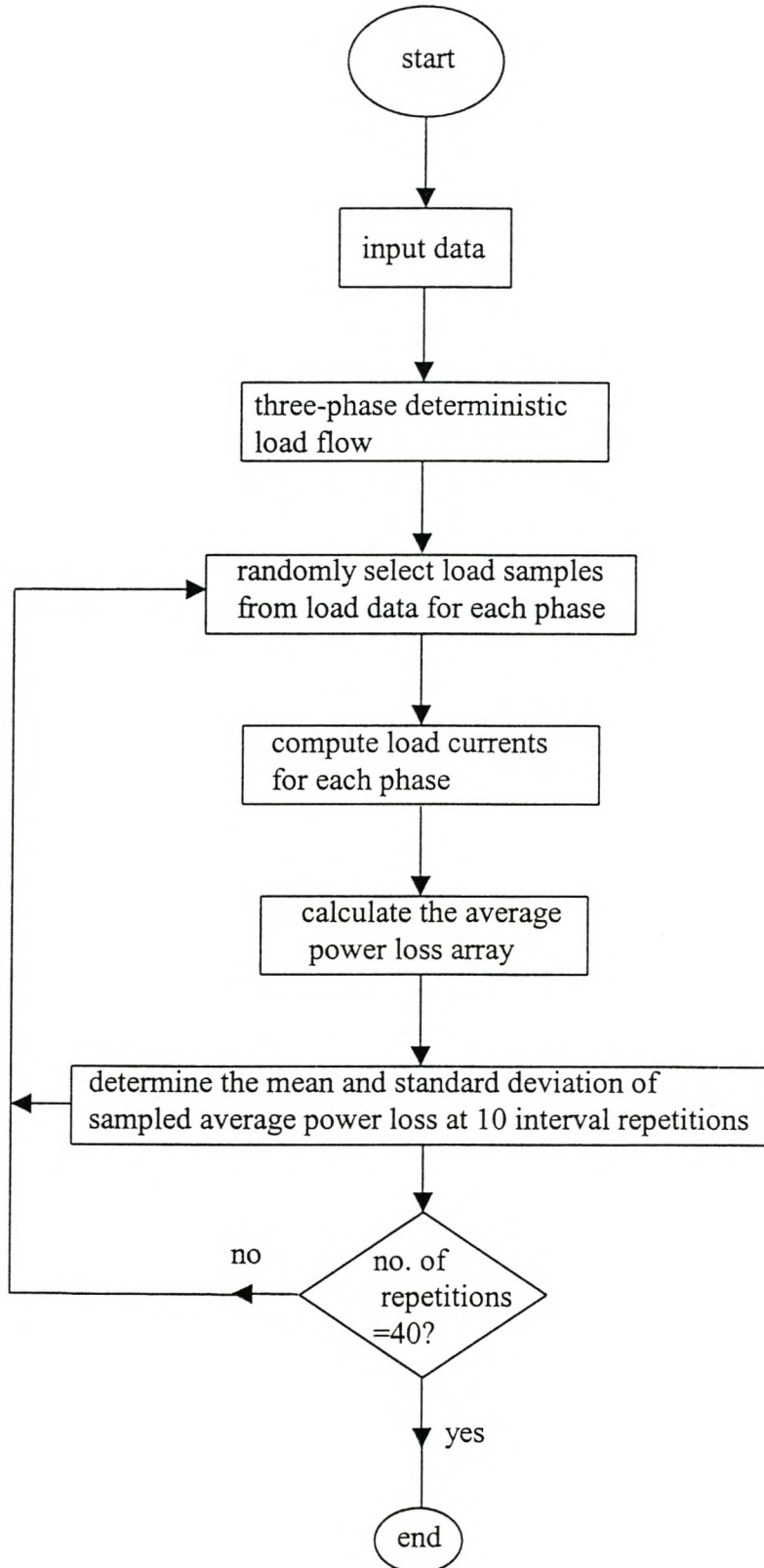
APPENDIX 7-E

A computer flow chart for MC simulations of the consumer voltages incorporating voltage regulators on three-phase distribution systems



Appendix 7-F

A computer flow chart for MC simulations of the power loss executed directly from the load data in three-phase networks



Appendix 8-A

The cost of capacitors

3 phase units		Capacitor cans only	Supplier A		Supplier B	
			Fixed	Switched	Fixed	Switched
100	kVAr	R8,515	R21,630	R55,585		
125	kVAr	R8,790	R21,905	R55,860		
150	kVAr	R9,150	R22,265	R56,220		
175	kVAr	R9,580	R22,695	R56,650		
200	kVAr	R10,005	R23,120	R57,075		
225	kVAr	R10,430	R23,545	R57,500		
250	kVAr	R10850	R23,965	R57,920		
275	kVAr	R11,275	R24,390	R58,345		
300	kVAr	R11,700	R24,815	R58,770	R26,935	R66,422
325	kVAr	R12,125	R25,240	R59,195		
350	kVAr	R12,705	R25,820	R59,775		
375	kVAr	R13,285	R26,400	R60,355		
400	kVAr	R13,865	R26,980	R60,935		
425	kVAr	R14,445	R27,560	R61,515		
450	kVAr	R15,025	R28,140	R62,095		
3 x single phase units						
500	kVAr	R28,745	R41,860	R75,815		
600	kVAr	R30,015	R43,130	R77,085	R37,350	R76,837
750	kVAr	R32,560	R45,675	R79,630		
900	kVAr	R35,100	R48,215	R82,170	R47,765	R87,252
1000	kVAr	R38,115	R51,230	R85,185		
1250	kVAr	R43,330	R56,445	R90,400	R60,980	R100,467
1500	kVAr	R68,200	R81,315	R115,270	R71,394	R110,881
1750	kVAr	R70,200	R83,315	R117,270		
2000	kVAr	R76,225	R89,340	R123,295		